

# **Retention and stabilization of organic matter in forest subsoils**

Von der Naturwissenschaftlichen Fakultät der  
Gottfried Wilhelm Leibniz Universität Hannover

zur Erlangung des Grades  
Doktor der Naturwissenschaften  
(Dr. rer. nat.)

genehmigte Dissertation

von

Patrick Liebmann, M. Sc.

[2021]

Referent: Prof. Dr. rer. nat. Georg Guggenberger

Korreferent: Prof. Dr. rer. nat. Karsten Kalbitz

Korreferent: Dr. Frank Hagedorn

Tag der Promotion: 08.07.2021

Zwei Dinge sind zu unserer Arbeit nötig: Unermüdliche Ausdauer und die Bereitschaft, etwas, in das man viel Zeit und Arbeit gesteckt hat, wieder wegzuwerfen.

Albert Einstein

### Abstract

Soils represent a major terrestrial carbon (C) reservoir and are herewith an important constituent of global climate change. They can act either as C sinks or as C sources, depending on the respective environmental conditions and management practices. At present, global forest ecosystems, including temperate European forests, are considered as C sinks. Whereas mineral topsoils under forest were found to be close to C saturation, it is assumed that especially subsoils provide large capacities for additional C storage in future. This is related to a high availability of sorption sites on mineral surfaces for organic matter compounds, which is frequently observed in laboratory experiments. However, sources of subsoil C are still under discussion and the potentials of mineral subsoils for C stabilization were not sufficiently investigated under field conditions so far. The crucial question remains, if forest subsoils can effectively retain and stabilize additional C inputs under the current environmental conditions, and thus contribute to mitigate global climate change. Therefore, this thesis aimed at evaluating (1) the role of the recent litter layer as a source for soil organic carbon (SOC), (2) at investigating dissolved organic carbon (DOC) dynamics as a controlling factor for organic C (OC) translocation in soils, and (3) the capability of subsoil to retain and stabilize fresh OC inputs.

The objectives were addressed by conducting different  $^{13}\text{C}$  manipulation experiments in central European beech forests (Lower Saxony, Germany). This included (i) a  $^{13}\text{C}$  litter manipulation combined with DOC and  $\text{CO}_2$  monitoring at the Grunderwald subsoil observatories, (ii) injection of  $\text{DO}^{13}\text{C}$  solution into three forest top- and subsoils, and (iii) burial and subsequent field incubation of  $^{13}\text{C}$ -coated minerals. Field approaches were complemented by (iv) laboratory sorption and desorption experiments. The field approaches comprised soil samplings down to the deep subsoil of  $> 100$  cm and included recurring samplings for assessing the stability of the translocated OC. The soils in this thesis included Cambisols and Luvisols and the parent materials ranged from Pleistocene glacio-fluvial sand and Triassic upper red sandstone to Weichselian loess.

Litter manipulation revealed that carbon inputs originating from the recent litter layer facilitated the actively cycling C pool in the mineral topsoil, but were not a major source of subsoil OC. Main acceptors of the litter-derived inputs in the soil were mineral surfaces, thereby forming mineral-associated organic carbon (MAOC). Migration of OC from the soil surface to the subsoil followed a sequence of sorption, microbial processing, and desorption cycles, resulting in a time offset until significant inputs reached the subsoil via DOC in the leaching soil solution. Bypassing this cascade of cycles in preferential flow paths caused a fast translocation into the subsoil, but DOC and  $\text{CO}_2$  monitoring suggest that these inputs were prone to microbial decomposition.

Undersaturation of sorption capacities for OC binding in the forest subsoil, obtained in laboratory experiments, was not replicated under field conditions, since the injection of a 200 ppm DOC solution into subsoils did not result in additional C accumulation three months later. This suggests that under natural conditions, the stability of retained OC is more decisive for C accumulation in subsoils than the potential free sorption capacities based on laboratory experiments. But at a scale of years, the majority of fresh inputs of OC to top- and subsoils were not effectively preserved, neither in particulate form, nor in association with soil minerals. Accumulation of organic matter (OM) on mineral surfaces may even stimulate the activity of the microbial community due to an increased availability of easily accessible OM substrate, thus promoting decomposition and mobilization instead of stabilization.

At present, the temperate forest top- and subsoils are neither sinks nor sources of C since they are situated in an equilibrium state of C inputs and C outputs, thereby maintaining their current C level

## Abstract

---

through processes including sorption, microbial processing, and desorption. Additional C inputs likely promote mineralization and mobilization of fresh and also older SOC and thus cannot be effectively stabilized in forest subsoils. Hence it can be expected that the potential free capacities of forest subsoils for additional C uptake are not exploitable under the current environmental conditions and eventually, forest (sub)soils will not notably contribute to climate change mitigation. Upcoming investigations of subsoils and estimations of their OM stabilization potential should not rely on laboratory studies only, but rather integrate both laboratory and field approaches to obtain more precise insights into subsoil C dynamics.

**Keywords:** Forest soils, subsoils, soil organic matter, carbon stabilization, climate change mitigation

## Zusammenfassung

Böden stellen ein großes terrestrisches Kohlenstoff (C)-Reservoir dar und sind damit ein wichtiger Wirkungsfaktor beim globalen Klimawandel. Sie können entweder als C-Senken oder als C-Quellen fungieren, abhängig von den jeweiligen Umweltbedingungen und ihrer Bewirtschaftung. Gegenwärtig werden die globalen Waldökosysteme, einschließlich der gemäßigten europäischen Wälder, als C-Senken angesehen. Während die mineralischen Oberböden unter Wald nahezu C-gesättigt sind, wird angenommen, dass insbesondere die Unterböden große Kapazitäten für eine zusätzliche C-Speicherung in der Zukunft bieten. Dies hängt mit einer hohen Verfügbarkeit von Sorptionsplätzen an mineralischen Oberflächen für Komponenten der organischen Substanz zusammen, die in Laborexperimenten häufig beobachtet wird. Die Quellen des Unterboden-Cs werden jedoch noch diskutiert, und die Potenziale mineralischer Unterböden zur C-Stabilisierung wurden bisher unter Feldbedingungen nicht ausreichend untersucht. Die entscheidende Frage bleibt, ob Waldböden unter den derzeitigen Umweltbedingungen zusätzliche C-Einträge effektiv zurückhalten und stabilisieren können und damit einen Beitrag zur Abschwächung des globalen Klimawandels leisten können. Daher zielte diese Arbeit darauf ab, (1) die Rolle der rezenten Streuschicht als Quelle für organischen Kohlenstoff (SOC) im Boden zu untersuchen, (2) die Dynamik des gelösten organischen Kohlenstoffs (DOC) als kontrollierenden Faktor für die Verlagerung von organischem Kohlenstoff (OC) in Böden zu untersuchen und (3) die Fähigkeit des Unterbodens zu bewerten, frische OC-Einträge zurückzuhalten und zu stabilisieren.

Die Ziele wurden durch die Durchführung verschiedener  $^{13}\text{C}$ -Manipulationsexperimente in mitteleuropäischen Buchenwäldern (Niedersachsen, Deutschland) verfolgt. Dazu gehörten (i) eine  $^{13}\text{C}$ -Streu-Manipulation in Kombination mit DOC- und  $\text{CO}_2$ -Messungen in den Grunderwald-Unterboden-Observatorien, (ii) die Injektion von  $\text{DO}^{13}\text{C}$ -Lösung in drei Ober- und -Unterböden unter Wald, und (iii) das Vergraben mit anschließender Feldinkubation von  $^{13}\text{C}$ -belegten Mineralen. Die Feldansätze wurden ergänzt durch (iv) Sorptions- und Desorptionsexperimente im Labor. Die Feldansätze umfassten Probenahmen bis in den tiefen Unterboden von  $> 100$  cm und beinhalteten wiederkehrende Beprobungen zur Beurteilung der Stabilität des verlagerten OCs. Die Böden in dieser Arbeit umfassten Braunerden und Parabraunerden und die Ausgangsmaterialien reichten von pleistozänen glazi-fluviatilen Sand und triassischem Buntsandstein bis hin zu weichselzeitlichem Löss.

Die Streu-Manipulation ergab, dass Kohlenstoffeinträge aus der rezenten Streuschicht den aktiv zirkulierenden C-Pool im mineralischen Oberboden unterstützten, aber keine wesentliche Quelle für OC im Unterboden darstellten. Die Hauptempfänger der Streu-bürtigen Einträge in den Boden waren mineralische Oberflächen, wodurch mineral-assoziiertes organisches Kohlenstoff (MAOC) gebildet wurde. Die Migration von OC von der Bodenoberfläche in den Unterboden folgte einer Abfolge von Sorptions-, mikrobiellen Verarbeitungs- und Desorptionszyklen, was zu einer zeitlichen Verschiebung führte, bis signifikante Einträge den Unterboden, über DOC in der Bodenlösung, erreichten. Präferentieller Fluss umging diese Kaskade von Zyklen und führte zu einer schnellen Verlagerung in den Unterboden. Die DOC- und  $\text{CO}_2$ -Messungen deuten aber darauf hin, dass diese Einträge anfällig für mikrobiellen Abbau waren.

Die in Laborexperimenten ermittelte Untersättigung der Sorptionskapazitäten für die Bindung von OC in Waldunterböden konnte unter Feldbedingungen nicht repliziert werden, denn die Injektion einer 200 ppm DOC-Lösung in Unterböden führte drei Monate später nicht zu einer zusätzlichen C-Akkumulation. Dies deutet darauf hin, dass unter natürlichen Bedingungen die Stabilität des gebundenen OC in Unterböden entscheidender für die C-Akkumulation ist als die potenziellen freien

## Zusammenfassung

---

Sorptionskapazitäten, die auf Laborexperimenten basieren. Auf einer Skala von Jahren wurde der Großteil der frischen Einträge von OC in Ober- und Unterböden jedoch nicht effektiv konserviert, weder in partikulärer Form noch in Verbindung mit Bodenmineralen. Die Akkumulation von organischer Substanz (OM) auf mineralischen Oberflächen könnte sogar die Aktivität der mikrobiellen Gemeinschaft aufgrund einer erhöhten Verfügbarkeit von leicht zugänglichem OM-Substrat stimulieren und so Zersetzung und Mobilisierung statt Stabilisierung fördern.

Gegenwärtig sind die Ober- und Unterböden gemäßiger Wälder weder Senken noch Quellen für C, da sie sich in einem Gleichgewichtszustand von C-Einträgen und C-Austrägen befinden und somit ihr aktuelles C-Niveau durch Prozesse wie Sorption, mikrobielle Verarbeitung und Desorption aufrechterhalten. Voraussichtlich fördern zusätzliche C-Einträge eher die Mineralisierung und Mobilisierung von frischem und auch älterem SOC und können daher im Waldunterboden nicht effektiv stabilisiert werden. Folglich ist anzunehmen, dass die potenziellen freien Kapazitäten von Waldunterböden für eine zusätzliche C-Aufnahme unter den gegenwärtigen Umweltbedingungen nicht ausgenutzt werden können und Wald(unter)böden letztlich keinen nennenswerten Beitrag zur Abschwächung des Klimawandels leisten werden. Zukünftige Untersuchungen von Unterböden und Abschätzungen ihres OM-Stabilisierungspotenzials sollten sich nicht nur auf Laborstudien stützen, sondern sowohl Labor- als auch Feldansätze integrieren, um genauere Erkenntnisse über die C-Dynamik im Unterboden zu erhalten.

**Stichwörter:** Waldboden, Unterboden, organische Bodensubstanz, Kohlenstoffstabilisierung, Klimawandelabschwächung

# Table of contents

---

## Table of contents

Zitat .....	I
Abstract .....	II
Zusammenfassung .....	IV
Table of contents .....	VI
List of Tables .....	VII
List of Figures .....	IX
Abbreviations .....	XVII
1. General Introduction.....	1
1.1. Soils in times of global climate change.....	1
1.2. Subsoils – the neglected part in soil science .....	2
1.3. Soil organic matter as a heterogeneous carbon pool .....	2
1.4. Organic matter dynamics – A cascade of input, transformation, and output .....	4
1.5. Preservation and persistence of soil organic matter .....	7
1.6. Importance of forest ecosystems as carbon sinks.....	8
1.7. Rationale and objectives.....	9
1.8. Hypotheses .....	10
1.9. References General Introduction.....	12
2. Study I .....	20
Study I – Supplementary material .....	50
3. Study II.....	56
Study II – Supplementary material.....	86
4. Study III.....	91
Study III – Supplementary material .....	106
5. Synthesis.....	145
5.1. Aboveground litter translocation.....	145
5.2. Pathways of dissolved organic matter within the mineral soil .....	151
5.3. Retention of organic matter in subsoils .....	153
5.4. Stability of organic matter in subsoils.....	155
6. Conclusion and outlook.....	158
References Synthesis & Conclusion and outlook.....	161
Acknowledgements .....	166
CV .....	167
Publications .....	168



## List of Tables

### Study I

**Table 1** Selected soil properties given as the mean of all three sites (n = 3) and standard deviation in brackets (data adapted from Leinemann et al. (2016)). 25

**Table 2** Mean OC stocks in bulk soil of different soil compartments down to 180 cm presented as absolute values and as a percent of total soil OC stock (n = 12; standard deviation is given in brackets). 32

**Table 3** Mean contents of labeled litter-derived OM in different soil fractions of all depth increments used for density fractionation (0-50 cm, 100-140 cm) 22 months (November 2016) and 40 months (May 2018) after labeled litter application (n = 3; standard deviation is given in brackets). The percentage loss over 18 months was calculated based on differences in C contents in OM fractions at both samplings. Overall, 36-40 % of the initially applied litter was lost by respiration during 22 months of field exposure (Wordell-Dietrich, unpublished). 36

**Supplementary Table S1** Relevant standard substances included in the EA-IRMS measurements for calibration, correction, and quality control 51

**Supplementary Table S2** Contents of dithionite- and oxalate-extractable Fe ( $Fe_d$  resp.  $Fe_o$ ) and oxalate-extractable Al ( $Al_o$ ) and Mn ( $Mn_o$ ). Extractions were conducted for the samples from the first sampling in November 2016. Data show the mean (n = 6) with the standard deviation in brackets. 51

### Study II

**Table 1** Soil properties for the top 20 cm below the different injection depths. Values represent means and standard deviations of the DOC injection plots for a 20 cm depth increment (n = 9).  $Fe_o$  and  $Al_o$  represents the amount of poorly crystalline aluminosilicates and Fe hydroxides,  $Fe_d$  the amount of poorly crystalline as well as crystalline iron oxides and BD is the bulk density of the fine soil. 64

**Table 2** Recovered C from the injected DOC over the first meter below injection depth for all plots at the three sites. 71

**Table 3** Cumulative respiration after 103 days of incubation normalised to bulk SOC and to the retained amount of injected DOC with standard errors. 73

## List of Tables

---

<b>Supplementary Table A1</b> Qualitative results from a GCMS pyrolysis for the freeze-dried DOC samples. The samples (approx. 300 µg) were pyrolyzed at 600°C for 6 s using a Multi-Shot Pyrolyzer EGA/PY-3030D (Frontier Laboratories Ltd.; Fukushima, Japan) connected to an Agilent 7890B gas chromatograph (Agilent Technologies, Inc.; Santa Clara, CA, USA). The pyrolysis products were separated on a HP-5 ms column (30 m length, 0.25 mm inner diameter, 0.25 µm film thickness) with 5.0 He as carrier gas. Inlet temperature of the GC was set to 320°C. A split ratio of 1:20 was applied. The GC column was connected to an Agilent 5977 MSD (Agilent Technologies, Inc.; Santa Clara, CA, USA) and scanned from 50 to 600 m/z. The raw data files were exported from the proprietary instrument software (Agilent Masshunter GC MS Acquisition B.07.00) and processed in MassLab version 1.2.7 using the NIST library.	89
 <u>Study III</u>	
<b>Supplementary Table S1</b> Mean dissolved organic carbon (DOC) concentrations, annual water and DOC and fluxes and mean specific UV absorbance at 280 nm (SUVA <sub>280</sub> ) values during the experiment runtime February 2015 – November 2016. Values in brackets represent the standard deviation. This table is an extension to the data published by Leinemann et al. <sup>5</sup>	119
<b>Supplementary Table S2</b> Basic parameters of the C-coated goethite and vermiculite (G0, V0) and the buried goethite and vermiculite in the respective depths (G/V-10, 50, 150 cm). Data of the buried mineral samples are given as the mean of three replicates with the standard deviation in brackets, while the other samples show single values.	120
<b>Supplementary Table S3</b> Selected soil parameters as the mean of the three subsoil observatories with the standard deviation in brackets (adopted from Liebmann et al. <sup>12</sup> ).	121
<b>Supplementary Table S4</b> Number of soil solutions sampled and their proportion of the theoretical possible number per observatory and depth.	122
<b>Supplementary Table S5</b> qPCR primers and conditions.	123
<b>Supplementary Table S6</b> Parameters of the sorption isotherm solutions and the stock solution, including the target dissolved organic carbon (DOC) level, the actual DOC concentration, dissolved total nitrogen (DTN), pH, and the specific UV absorbance at 280 nm (SUVA <sub>280</sub> ).	124
<b>Supplementary Table S7</b> Basic parameters of soils used for the sorption isotherms, and sorption and desorption experiments.	125

**List of Figures**

General Introduction

**Fig. 1.1** Framework and connecting processes of atmosphere, hydrosphere, lithosphere, biosphere, and pedosphere within the ecosphere, modified from Lal et al. (1997), is shown in (a). Carbon cycling and connecting processes within the ecosphere, modified from Lal (2014), is shown in (b).

1

**Fig. 1.2** Schematic illustration of sources, inputs, and translocation of organic matter (OM) in individual functional OM fractions in the soil profile during downward cycling with inspirations from Kaiser and Kalbitz (2012), Mikutta et al. (2019), Sokol et al. (2019), and Lehmann et al. (2020). Several processes are included in OM cycling in soil. Litter-derived OM predominantly enters the soil via particulate organic matter (POM) bioturbations (1) and dissolved organic matter (DOM) leaching (2). In soil, the free POM particles (fPOM) can be occluded by soil particles (oPOM; 3). Belowground OM sources are roots, which contribute either to the POM fractions by decay of dead roots (4) or to DOM due to root exudation (5). Dissolved OM in the soil solution is continuously interacting with the mineral matrix. Those interactions include sorption of DOM compounds to mineral surfaces – potentially by exchange/displacement of older inherent soil OM (SOM; 6), microbial processing of sorbed SOM and DOM (7), and consequently desorption and dissolution of microbial metabolites and altered SOM (8). Organic matter undergoes multiple sorption, microbial processing, desorption cycles while migrating down the soil profile (Kaiser and Kalbitz, 2012). Such interactions affect the amount and the composition of DOM with increasing soil depth, from a plant-derived signature ( $DOM_{\text{plant}}$ ) in the upper parts of the soil profile towards a microbial-derived signature ( $DOM_{\text{micro}}$ ) in the deeper parts of the soil profile (right hand side of the figure). Small DOM fluxes in the deep subsoil including mainly processed, microbial-derived organic compounds leaves it uncertain to which extent stable mineral-associated OM (MAOM) formation (9) is taking place under natural conditions.

5

Study I

**Figure 1** Mean bulk OC contents of both sampling times (November 2016 and May 2018) (a) and calculated OC stocks as the mean of both sampling times (b). Apparent re-increasing OC stocks below 100 cm are the result of doubling the thickness of the analyzed depth increments (i.e., 5 cm increments from 0 to 10 cm, 10 cm increments from 10 to 100 cm, and 20 cm increments from 100 to 180 cm). Data show the mean of 12 samples, and error bars depict the standard deviation.

31

**Figure 2** Soil OC (SOC) distribution in the Dystric Cambisol at the Grinderwald site as a function of soil depth: C in mineral-associated OM ( $C_{\text{MAOM}}$ ), occluded particulate OM ( $C_{\text{oPOM}}$ ), and free particulate OM ( $C_{\text{fPOM}}$ ); C mobilized by sodium polytungstate during density fractionation ( $C_{\text{SPT}}$ ). All data are given as mean of both samplings ( $n = 12$ ; standard deviation varied for  $C_{\text{MAOM}}$  between 7 and 19 %, for  $C_{\text{oPOM}}$  between 2 and 5 %, for  $C_{\text{fPOM}}$  between 7 and 19 %, and for  $C_{\text{SPT}}$  between 0.3 and 5 %). Note that the  $C_{\text{MAOM}}$  fraction was corrected for the C loss during washing (see material and method section).

32

**Figure 3** Mean OC contents in the heavy fraction (HF) (a) and mean C/N ratios (b) of the mineral-associated organic matter fraction (MAOM) from both sampling times, 22 months and 40 months after labeled litter application ( $n = 6$ ; error bars represent the standard deviation). Nitrogen contents in the HF were corrected for extractable nitrate and ammonium contents; N contents in samples below 100 cm were unreliable, and C/N ratios are therefore marked in grey.

33

## List of Figures

---

**Figure 4** Mean proportion of water-extractable-OC ( $C_{WEOM}$ ) per depth increment given in percentage of the total soil OC in bulk soil for both sampling times, 22 months and 40 months after labeled litter application ( $n = 6$ ; error bars represent the standard deviation) is shown in (a). Specific UV absorbance at 280 nm (b) and humification index deduced from fluorescence spectra (c) of the water extracts are given as the mean ( $n = 6$ ) of the first sampling in November 2016. Error bars represent the standard error. 33

**Figure 5.** Mean  $\delta^{13}C$  values of the bulk soil (a), mineral-associated OM ( $C_{MAOM}$ ) (b), and water-extractable OM ( $C_{WEOM}$ ) (c). The graphs show labeled samples of both sampling times, 22 months and 40 months after labeled litter application in colored symbols, compared to the respective unlabeled background distribution in white symbols. Labeled samples represent the mean of three replicates per sampling time, while the control represents the mean of both sampling times ( $n = 6$ ). Please note that the  $x$  axis in (c) has a different scale. 35

**Figure 6.** Mean labeled litter-derived  $^{13}C$  recovered in different OM fractions: C in mineral-associated OM ( $C_{MAOM}$ ), occluded particulate OM ( $C_{oPOM}$ ), and free particulate OM ( $C_{fPOM}$ ); C mobilized by sodium polytungstate during density fractionation ( $C_{SPT}$ ). The upper  $x$  axis shows the recovered  $^{13}C$  in  $g\ m^{-2}$  and the lower  $x$  axis shows the percentage recovery of initially added labeled litter after 22 months (a) and 40 months following labeled litter application (b). Bars show the sum of all fractions per depth increment, while the different colors represent the respective contribution of each fraction to the total recovery ( $n = 3$ ). According to ANOVA tests there were no significant changes in  $^{13}C$  recovery for each fraction with depth per sampling, due to high standard deviations in the range of 0.02–0.53 for  $C_{MAOM}$ , 0.01–0.75 for  $C_{oPOM}$ , 0.02–4.9 for  $C_{fPOM}$ , and 0.01–0.13 for  $C_{SPT}$ . 36

**Figure 7.** Mean proportion of litter-derived C in water extractable organic OM (WEOM) in percentage of the initial label input for both sampling times, 22 months and 40 months after labeled litter application, with soil depth ( $n = 3$ ; error bars represent the standard deviation). According to ANOVA tests, significant changes between both samplings were only present in the 0-5 cm and 10-20 cm increments ( $p < 0.05$ ). Significant differences between soil increments were only present for the topsoil increments compared to all subsoil increments for each sampling time. 37

**Supplementary Figure S1** Mean C/N ratio of the bulk soil from both sampling times, 22 months and 40 months after labeled litter application. Data show the mean of 6 samples and error bars show the standard deviation. The y-axis shows the mean depth of each soil increment. Nitrogen contents of the MAOM fraction were corrected for extractable nitrate and ammonium contents. Nitrogen contents in samples below 100 cm were increasingly below the detection limit and not reliable, therefore C/N ratios are marked in grey. 52

**Supplementary Figure S2** Mean mass recovery and fraction distribution of the soil density fractions heavy fraction (HF), occluded particulate organic matter (oPOM), and free particulate organic matter (fPOM) as the mean of both sampling times (November 2016 and May 2018). The y-axis shows the mean depth of each soil increment. Bars show the mean of 12 samples, the standard deviation varied for HF between 0.3-15 %, for oPOM between 0.1-1.6 %, and for fPOM between 0.1-18 %. Please note that for better visibility, both axes have breaks. 52

**Supplementary Figure S3** Mean  $^{13}C$  recovered at each sampling time, 22 months and 40 months after labeled litter application, in % of the initial label input ( $n = 3$ ). Bars show the sum of all fractions per depth increments, error bars depict the standard deviation. According to ANOVA analysis, there were no significant differences ( $p > 0.05$ ) in the total recovered  $^{13}C$  per depth increment between both sampling times, except of the depth 30-40 cm ( $p = 0.004$ ). Please note

## List of Figures

---

that for better visibility, both axes have breaks. 53

**Supplementary Figure S4** Correlation of the  $^{13}\text{C}$  abundance of the mineral-associated organic matter ( $C_{\text{MAOM}}$ ) in the unlabeled control samples on the Y-axis and the corresponding C/N ratio on the X-axis from both sampling times, 22 months and 40 months after labeled litter application. Data show the mean of three replicates, error bars depict the standard deviation. Spearman correlation resulted in a significant negative correlation for both variables for the first sampling in November 2016 ( $r = -0.677$ ,  $p < 0.05$ ) and the second sampling in May 2018 ( $r = -0.883$ ,  $p < 0.05$ ). 53

**Supplementary Figure S5** Contents of selected elements on the heavy fraction (HF) mineral surface layer according to XPS analysis. Bars show the mean of three spots measured per sample per plot and depth increment, error bars represent the standard deviation. Please note that the X-axis have different scales. Please note, element contents were highly correlated as a function of soil depth. Negative correlations were observed for example for Fe-C ( $r^2 = 0.82$ ,  $p = 0.0021$ ) and Al-C ( $r^2 = 0.58$ ,  $p = 0.0295$ ). Positive correlations were observed for example for Fe-Al ( $r^2 = 0.85$ ,  $p = 0.0012$ ) and C-N ( $r^2 = 0.90$ ,  $p = 0.0004$ ). 54

### Study II

**Fig. 1** Injection of DOC at 10 cm depth at the Red Sandstone site (left) and in 50 and 100 cm depth at the Loess site (right). Note that on the right site, the injection at 100 cm depth is shown. The injection at 50 cm depth was conducted on the opposite site. The injection area was designed for three possible samplings. 65

**Fig. 2** Concept of the sampling design for each of the three sites. The plots were approximately 50 m apart from each other. First sampling was conducted in August 2017, resulting in nine cores from the injection sites plus three respective control cores. Second sampling was conducted in October 2018. The water control ( $\text{CaCl}_2$ ) was completely sampled after 3 months. 65

**Fig. 3** Summarised recovered labelled material over the first meter below injection depth after 3 (white boxes) and 17 months (grey boxes). Columns represent mean values from the three plots. Error bars represent standard errors. 70

**Fig. 4** Depth distribution of retained DOC after three and after seventeen months. Values represent mean values of retained DOC ( $n = 3$ ) and their respective standard errors. Dashed lines represent respective injection depths. 72

**Fig. 5** Cumulative bulk SOC-normalised (upper panel) and labelled SOC-normalised (lower panel) respiration in a 103 days laboratory incubation experiment. Values for SOC and labelled SOC-normalised respiration represent mean values from samples 0-5, 5-10 and 10-20 cm depth below injection with three repetitions per substrate ( $n = 9$ ). Error bars represent standard errors. Different letters indicate significant differences ( $P < 0.05$ ) for cumulative respiration after 103 days of incubation. Because only samples with positive recovery values were taken into account for labelled SOC-normalised respiration, number of observations strongly differs (loess: 5-6, red sandstone: 3-5, sand: 2-3). 73

**Supplementary Fig. A1** Bulk SOC content after 3 (upper panels) and 17 months (lower panels) of injection. Values represent mean values derived from the different plots ( $n = 3$ ) and the respective standard deviations 86

## List of Figures

---

- Supplementary Fig. A2** Amount of retained DOC after 3 (upper panels) and 17 months (lower panels) in relation to bulk SOC content. Values represent mean values derived from the different plots (n = 3) and the respective standard deviations. 86
- Supplementary Fig. A3** Comparison of cumulative respiration normalised to bulk SOC respiration for the samples with labelled substrate and control samples. Values represent mean values derived from the different plots and injection depths (n = 9) and the respective standard deviations 87
- Supplementary Fig. A4** Cumulative respiration normalised to the bulk soil. Values represent mean values from samples 0-5, 5-10 and 10-20 cm depth below injection with three repetitions per substrate (n = 9). Error bars represent standard errors. Different letters indicate significant differences ( $p < 0.05$ ) for cumulative respiration after 103 days of incubation. 87
- Supplementary Fig. A5** Possible influence of the water added with the DOC injection on bulk SOC investigated with the injection of water (CaCl<sub>2</sub> solution). Values represent mean values for samples 3 months after injection. For the Red Sandstone site only one sample per injection depth was taken. 88
- Supplementary Fig. A6** Possible influence of the water added with the DOC injection on  $\delta^{13}\text{C}$  values investigated with the injection of water (CaCl<sub>2</sub> solution). Values represent mean values for samples 3 months after injection. For the Red Sandstone site only one sample per injection depth was taken. 88

### Study III

**Fig. 1** Recovery of litter-derived C into different C pools in topsoil (10 cm), upper subsoil (50 cm), and deeper subsoil (150 cm) over the course of 22 months in a Dystric Cambisol located in a temperate European beech forest in Germany. Values are given in percent of the initially applied labelled litter. Evaluated C pools included the CO<sub>2</sub> production at the soil surface and in the depth increments 10-50 and 50-90 cm (white), leachates of dissolved organic C (DOC) in 10, 50, and 150 cm soil depth (blue), and incorporation of litter material in the depth increments 0-10, 10-50, and 50-150 cm, due to bioturbations as C in particulate organic matter (POC; green) and due to sorption to mineral surfaces thereby forming mineral-associated organic C (MAOC; brown). Residual litter after the field exposure was quantified and is given in the litter layer. The complete C balance revealed a recovery of initially applied litter of about 85 %. CO<sub>2</sub> data were adapted from Wordell-Dietrich et al.<sup>32</sup>, and MAOC/POC differentiation was adapted from Liebmann et al.<sup>30</sup>. The latter authors did not analyse the MAOC in the depth increment 50-100 cm, but reported an interpolation of 0.03 % which we added here. 96

**Fig. 2** Dissolved organic C (DOC) sorption isotherms of soil from 10, 50, and 150 cm soil depth of a Dystric Cambisol located in a temperate European beech forest in Germany. Both x-axes show the DOC added to the soil, on the bottom x-axis normalised to soil mass, on the top x-axis as concentration. Sorption isotherms (yellow circles and red line) show the released or sorbed DOC after the experiment (left y-axis, n = 3) as a function of added DOC. Black bars show the quantified DOC sorption (right y-axis, n = 3), estimated for one m<sup>2</sup> and a soil thickness of 10 cm (since soil samples for the sorption experiments were taken as composite samples of a 10-cm increment; 10-20, 50-60, 100-110 cm). The blue-marked areas represent typical DOC concentrations (top x-axis) in the respective soil depths measured at this study site (see Supplementary Table S1). Concentrations were calculated as the mean of all samples taken during

## List of Figures

---

the timeframe February 2015 to November 2016, and amounted to  $51.5 \pm 22.0$  mg L<sup>-1</sup> in 10 cm (n = 112),  $13.0 \pm 9.0$  in 50 cm (n = 60), and  $8.6 \pm 11.2$  in 150 cm (n = 88). The DOC concentration in 150 cm soil depth was used for the 100-cm variant in this figure. 98

**Fig. 3** Depth-dependent gross C exchange of <sup>13</sup>C-labelled mineral-associated organic C (MAOC) after two-years of field exposure in a Dystric Cambisol located in a temperate European beech forest in Germany. Goethite was chosen as a representative pedogenic Fe oxyhydroxide (left side) and vermiculite as representative 2:1 clay mineral (right side). The net difference in C content before and after the field exposure is given in percent of the initial MAOC content ( $\Delta C$ ). The amount of mobilizable C (MC) during the field exposure is given in percent of initial MAOC as well. The final C content after field exposure was differentiated in pre-existent <sup>13</sup>C-labelled mineral-derived C (MDC) and fresh unlabelled solution-derived C (SDC; yellow color). The soil profile in the center representatively shows a Dystric Cambisol in the Grindewald forest (Germany); left and right figures show scanning electron microscope (SEM) images of the respective C-loaded minerals. 100

**Supplementary Fig. S1** Rates of the litter-derived CO<sub>2</sub> efflux at the soil surface during the 22 months of the labelling at observatory 1 (a), observatory 2 (b), and observatory 3 (c), calculated with the Lloyd-Taylor model<sup>16</sup> in g per m<sup>2</sup> and day. For a better visibility, data points are connected by dotted lines, but do not represent functions or regressions. Data adapted from Wordell-Dietrich et al.<sup>6</sup>. 126

**Supplementary Fig. S2** Contribution of labelled litter-derived DOC to the total DOC flux (DOC<sub>tot</sub>) during the 22 months of the labelling per depth (10, 50, 150 cm) in observatory 1 (a), observatory 2 (b), and observatory 3 (c). Variations in the data quantities and gaps at some time points are the results of insufficient water flow or insignificant DO<sup>13</sup>C enrichment. Please note that only twelve out of 57 sampling campaigns were analysed for DO<sup>13</sup>C, thus the data points in between were calculated by linear interpolations as stated in the supplementary methods section. 127

**Supplementary Fig. S3** Cumulative litter-derived DOC fluxes during the 22 months of the labelling in g DO<sup>13</sup>C per m<sup>2</sup>. Graph (a) shows the 10 cm data of each observatory, (b) data from 50 cm, and (c) data from 150 cm. Please note the different scales for the y-axes. 128

**Supplementary Fig. S4** Cumulated litter-derived CO<sub>2</sub> flux during the 22 months of the labelling at the soil surface (a), in a soil depth of 10 to 50 cm (b), and in a soil depth of 50 to 90 cm (c) during the label experiment for the three observatories, calculated with the Lloyd-Taylor model<sup>16</sup>. Data were generated by multiplying the rates per day with the interval between two sampling dates. Please note the different scales for the y-axes. 129

**Supplementary Fig. S5** Concentrations of individual compounds (hexoses, pentoses, amino acids, proteins, phenols) and the total DOC concentration in the soil solution at different soil depths. Boxplots show the data of four samplings between January and April 2015, with a total sample size of n = 133 for 10 cm, n = 69 for 50 cm, and n = 58 for 150 cm. Boxes represent 50 % of the concentrations, the solid line shows the median. Dotted lines represent the mean and error bars depict the 10 % and 90 % quantiles with black circles as outliers. Please note that the x-axes have different scales. 130

**Supplementary Fig. S6** Mean SOC stocks per depth increment at observatory 1 (a), observatory 2 (b), and observatory 3 (c). Data show the mean of three replicate soil cores, error bars represent the standard deviation. Only soil cores from the labelled plots were used for the analyses. Data were adopted from Liebmann et al.<sup>12</sup>. 131

## List of Figures

---

**Supplementary Fig. S7** X-ray diffraction patterns of oriented clay specimens from three studies sites (a–c) Grinderwald, (d–f) Rüdershausen, and (g–i) Ebergötzen and the depth increments 10–20 cm (left), 30–40/50–60 cm (center), and 60–70/100–110 cm (right). Each sample was analysed in the following four depicted treatments (from top to bottom): Mg-saturated and solvated in ethylene glycol (MgEG), magnesium-saturated (Mg), potassium-saturated and heated to 550°C (K550°C), and potassium-saturated (K). Peaks at 14 Å in the K treatment indicate d(001) reflections of pedogenic chlorite together with a d(003) reflection at 4.7 Å; peaks at 7 Å and 3.5 Å reveal d(001) and d(002) reflections of kaolinite (both signals vanish in the K550°C treatment). The presence of illitic clay is indicated by a d(001) peak at 10 Å in the Mg/MgEG treatments. Increasing intensities at ~14 Å in the Mg/MgEG treatments relative to the K treatment indicate the presence of expandable vermiculite. Broad unresolved signals between ~10–14 Å in the K treatments suggest the presence of hydroxy-interlayered vermiculites with varying degrees of Al hydroxide incorporation. 132

**Supplementary Fig. S8** Sorption isotherms of the Rüdershausen site (left) and Ebergötzen site (right), including three depths according to the initial mass approach by Nodvin et al.<sup>33</sup>. Numbers represent the soil depth. Data show the mean of three replicates and the error bars represent the standard deviation. 135

**Supplementary Fig. S9** Specific UV absorbance (SUVA) at 280 nm of the initial DOC solution before the sorption experiment ( $SUVA_{in}$ , x-axis) and in the solution after the experiment ( $SUVA_s$ , y-axis). The Grinderwald site is on the left, the Rüdershausen site in the middle, and the Ebergötzen site on the right. Numbers represent the soil depth. Data are given as the mean ( $n = 3$ ) with error bars representing the standard deviation. Values above the 1:1 line indicate a net release of aromatic DOM components, while values below indicate a net retention. Colors depict the different DOC concentrations of the sorption experiments. Yellow show the concentrations between 0–10 mg L<sup>-1</sup> (1, 5, 10 mg L<sup>-1</sup>), orange show the concentrations between 11–100 mg L<sup>-1</sup> (25, 50, 100 mg L<sup>-1</sup>), and red show the concentrations between 101–400 mg L<sup>-1</sup> (200 and 400 mg L<sup>-1</sup>). 136

**Supplementary Fig. S10** Soil organic C (SOC) and mobilisable C (MC) in the 9 different soil samples determined before and after batch sorption experiments with (a) “altered” DOM extracted from the field exposed labelled beech litter and with (b) “fresh” DOM extracted from recently fallen un-labelled beech litter. Data show the mean of three replicates and the error bars represent the standard deviation. The Grinderwald site is on the left, the Rüdershausen site in the middle, and the Ebergötzen site on the right. On the x-axis, numbers represent the soil depth. Black and grey bars show the data before the experiment (B), green bars show the data after the DOC sorption experiment (S), and blue bars show the data after the desorption experiment (D). 137

**Supplementary Fig. S11** Distribution of native soil organic C (SOC) and label-derived SOC in topsoil, upper subsoil, and deeper subsoil samples of the three sites in percent of the total SOC ( $SOC_{tot}$ ). Bars show the results of the “altered” DOM approach and include the distribution in the bulk soil (black), which is naturally 100 % native, after the sorption experiment (green), and after the desorption experiment (blue). Bright colored bars represent the label-derived SOC, while dark colored bars depict the native SOC. Bars show the mean of three replicates, error bars show the standard deviation. The Grinderwald site (sandy deposits) is on the left, the Rüdershausen site (loess deposits) in the middle, and the Ebergötzen site (red sandstone) on the right. On the x-axis, numbers represent the soil depth. 138

**Supplementary Fig. S12** Bacterial community composition of the goethite (a) and vermiculite (b), respectively, after 24 months of *in-situ* field exposure in combination with the bulk soil



## List of Figures

---

samples taken above and below each mineral meshbag. Sample names on the y-axes are a combination of the mineral types goethite (G) or vermiculite (V), the soil depth (10, 50, 150 cm), and in case of the bulk samples the suffix above (a) or below (b) the meshbag. Data show the mean of three replicates and the error bars represent the standard deviation. 139

**Supplementary Fig. S13** Microbial community composition of the goethite (a) and vermiculite (b), respectively, after 24 months of *in-situ* field exposure in combination with the bulk soil samples taken above and below each mineral meshbag. Sample names on the y-axes are a combination of the mineral types goethite (G) or vermiculite (V), the soil depth (10, 50, 150 cm), and in case of the bulk samples the suffix above (a) or below (b) the meshbag. Data show the mean of three replicates and the error bars represent the standard deviation. 140

**Supplementary Fig. S14** Schematic illustration of the installations in the Grinderwald subsoil observatories (a) and a top view of the catchment area divided into a  $^{13}\text{C}$ -labelled and un-labelled side (b). Illustrations were adapted and modified from Wordell-Dietrich et al.<sup>6</sup>. Please note that the suction plates were not installed below each other in the soil profile as pictured in this 2D scheme (a). To avoid mutual influences of the plates, they were installed with a horizontal offset. 141

### Synthesis

**Fig. 5.1** Correlation of mean litter-derived DOC in 10 cm ( $n = 3$ ) and mean litter-derived  $\text{CO}_2$  production in the soil increment of 10-50 cm ( $n = 3$ , data from Study III). The red point and the dotted line mark the value from the 20.11.15. The solid line represents the 1:1 line. Due to a better visibility of the general trend, the error bars were excluded in this figure. 149

**Fig. 5.2** Cumulative water flux in 50 cm (a) and 150 cm (b) cm soil depth collected by the segmented suction plates installed in the Grinderwald Observatory 1, next to the cumulative DOC flux in 50 cm (c) and 150 cm (d) from the same installations (Liebmann, unpublished). Colors depict each of the 16 segments per suction plate. Graphs include data from the 10.04.2014 ( $t = 0$  d) until 09.04.2019 ( $t = 1825$  d), covering 5 years of monitoring. 152

**Fig. 5.3** Classification of the C-coated goethite (G-L), the 10 cm buried goethite MAOM (G-10), and the 150 cm buried goethite MAOM (G-150) regions of interest (ROIs) classified according to their  $^{13}\text{C}$  values [at%] measured with the low energy deposit method (Liebmann, unpublished). The classification was done according to Leinemann et al. (2018) by defining three classes, including a low [ $< 1.4$  at%], intermediate [ $> 1.4$  &  $< 2.2$  at%], and high [ $> 2.2$  at%]  $^{13}\text{C}$  enrichment. The  $^{13}\text{C}$  value of each ROI was normalized to the area of all identified ROIs and is given in percent of the total ROI area. 154

### Conclusion and outlook

**Fig. 6.1** Proportions of litter-derived DOC averaged per suction plate in 10, 50, and 150 cm soil depth in OB1 (a), OB2 (b) and OB3 (c). The area marked in dark blue represent the time of labelled litter application from Mai 2015 until November 2016, which is given in Study III (Supplementary Fig. S2). The area marked in light blue represent nearly three years after labelled litter application from November 2016 until June 2019. 159

**Fig. 6.2** Cumulative litter-derived DOC in all three observatories (OB1-3) detected with the segmented suction plates in 10 cm (a), 50 cm (b) and 150 cm (c) soil depth. The area marked in dark blue represent the time of labelled litter application from Mai 2015 until November 2016,

## List of Figures

---

which is given in Study III (Supplementary Fig. S3). The area marked in light blue represent nearly three years after labelled litter application from November 2016 until June 2019.

160

## Abbreviations

---

### Abbreviations

Al <sub>o</sub>	oxalate-extractable aluminum
ANOVA	analysis of variance
C	carbon
C <sub>w</sub>	carbon in heavy fraction washing water
DOC	dissolved organic carbon
DO <sup>13</sup> C	<sup>13</sup> C/ <sup>12</sup> C ratio in dissolved organic carbon
DOM	dissolved organic matter
DOM <sub>Micro</sub>	microbial-derived dissolved organic matter
DOM <sub>Plant</sub>	plant-derived dissolved organic matter
DTN	dissolved total nitrogen
EA-IRMS	elemental analyzer - stable isotope ratio mass spectrometer
Fe <sub>d</sub>	dithionite-extractable iron
Fe <sub>o</sub>	oxalate-extractable iron
fPOM	free particulate organic matter
G	goethite
HF	heavy fraction
HIX	humification index
HOS	high organic sediment
IAEA	International Atomic Energy Agency
IB	ionic background
ICP-OES	inductively coupled plasma – optical emission spectroscopy
LF	light fraction
MAOC	mineral-associated organic carbon
MAOM	mineral-associated organic matter
MC	mobilized carbon
MDC	mineral-derived carbon
Mn <sub>o</sub>	oxalate-extractable manganese
MOM	mineral-associated organic matter
N	nitrogen
N <sub>min</sub>	mineralized nitrogen
NanoSIMS	nano-scale secondary ion mass spectrometry
OB	observatory
OC	organic carbon

## Abbreviations

---

OM	organic matter
oPOM	occluded particulate organic matter
POC	particulate organic carbon
POM	particulate organic matter
ROI	region of interest
SD	standard deviation
SDC	solution-derived carbon
SEM	scanning electron microscope
SOC	soil organic carbon
SO <sup>13</sup> C	<sup>13</sup> C/ <sup>12</sup> C ratio in soil organic carbon
SOM	soil organic matter
SPT	sodium polytungstate
SSA	specific surface area
SUVA <sub>280</sub>	specific ultra violet absorbance at 280 nm
TOC	total organic carbon
TN	total nitrogen
UV	ultraviolet
V	vermiculite
VPDB	Vienna Pee Dee Belemnite
WEOC	water-extractable organic carbon
WEOM	water-extractable organic matter
XPS	X-ray photoelectron spectroscopy
ΔC	net carbon exchange

# 1. General Introduction

## 1.1. Soils in times of global climate change

Soils inhere a key role in the global ecosystem. They are centered in the critical zone, which is defined as the zone from groundwater to the top of the canopy (Brooks et al., 2015; Field et al., 2015). Beyond that, soils serve as a link between atmosphere, hydrosphere, lithosphere, and biosphere (Lal et al., 1997), connected by multiple comprehensive processes as shown in Fig. 1.1a. Globally, they harbor of up to 2500 Pg C as organic C (OC) in the top 3 m of soil (Batjes, 1996; Jobbagy and Jackson, 2000), which is more than the combined pools of vegetation C (~610 Pg) and atmospheric C (750 Pg) (Schimel, 1995) and clearly demonstrates the outstanding function of soils as C reservoirs. Thus, global carbon cycling, with the pedosphere in its center, can be displayed analogously to the ecosphere framework from Fig. 1.1a (Fig. 1.1b; Lal, 2014). The OC in the soil organic layer and the mineral horizons represent up to 50 % of the organic matter (OM) in soil (Blume et al., 2016). While many environmental studies focus on the climate change-relevant and directly measurable OC (e.g. Jobbagy and Jackson, 2000; Paustian et al., 2016), both terms, organic matter and carbon, are used in this thesis for presenting measurement results (OC) and for discussing OM as an entity.

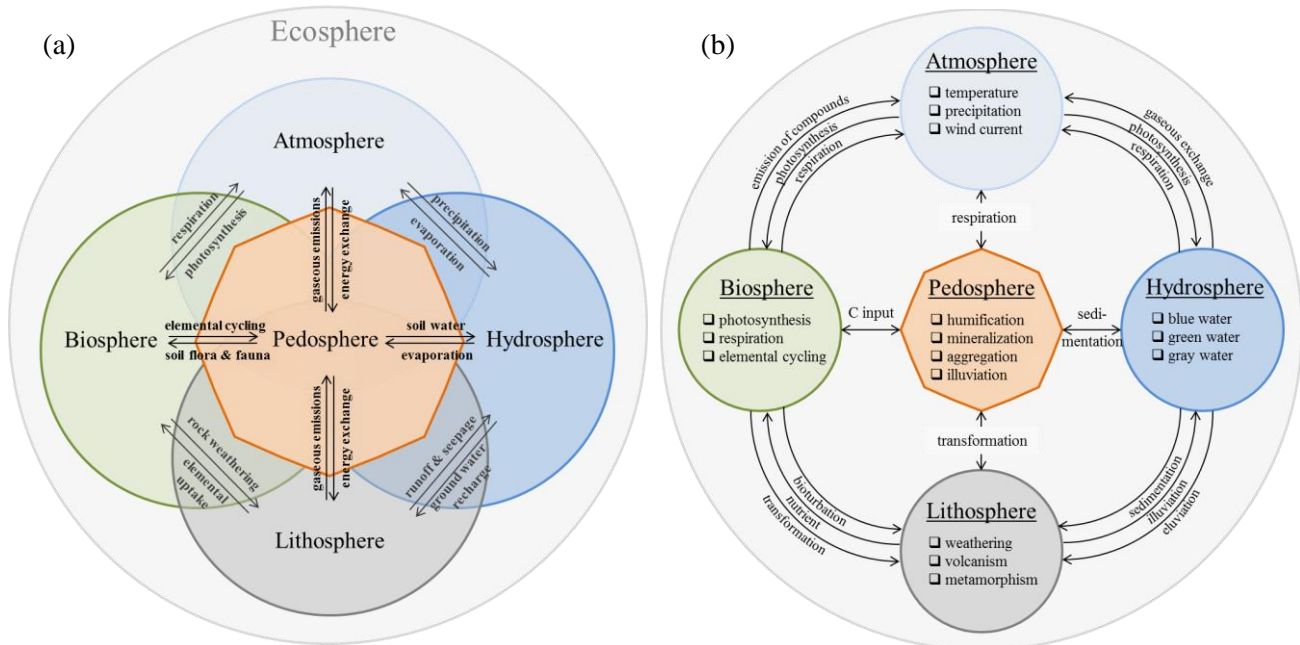


**Fig. 1.1** Framework and connecting processes of atmosphere, hydrosphere, lithosphere, biosphere, and pedosphere within the ecosphere, modified from Lal et al. (1997), is shown in (a). Carbon cycling and connecting processes within the ecosphere, modified from Lal (2014), is shown in (b).

With regard to the omnipresent debates about climate change and greenhouse gas emissions (e.g. Althor et al., 2016; Paustian et al., 2016), interactions between pedosphere, atmosphere, and biosphere appear to be of special interest, either negatively due to the release of greenhouse gases like CO<sub>2</sub> and CH<sub>4</sub> from soils to the atmosphere (respiration, Fig. 1.1b), or positively due to preservation of biologically fixed carbon removed from the atmosphere (C input, Fig. 1.1b; Keenan and Williams, 2018) to name just a few.

### **1.2. Subsoils – the neglected part in soil science**

In past research most studies focused on topsoils in forest and grassland ecosystems (e.g. Baisden et al., 2002; Schöning and Kögel-Knabner, 2006; Crow et al., 2009; Robertson et al., 2019), or down to the ploughing depth in arable soils (e.g. Lugato et al., 2014; Poeplau and Don, 2015). And this is legit as roots, microorganisms, and organic matter are often concentrated in topsoil horizons compared to frequently depleted subsoils (Kandeler et al., 2005; Fontaine et al., 2007; Heinze et al., 2018). However, subsoils exhibit a huge C pool due to their thickness. Considering the upper 200 cm of soils, only about 30 % of OC is located in the top 30 cm (Batjes, 1996), which are typically topsoil horizons depending on the soil type. The other 70 % of OC are present in subsoils, 39 % even in deep mineral subsoils of 100-200 cm depth (Batjes, 1996). Therefore, it is evident that the dynamic and processes affecting subsoil C deserve a similar research attention.

Because OC concentrations are small, sufficient undersaturated mineral surfaces are theoretically available for further retention and stabilization (Guggenberger and Kaiser, 2003). This highlights subsoils as potential future sinks for atmospheric C (Lavania and Lavania, 2009; Lorenz et al., 2011), meeting their C sink function and thus take part in mitigating anthropogenic climate change. But it is not adequately evaluated if these theoretical capacities are exploitable under natural conditions.

### **1.3. Soil organic matter as a heterogeneous carbon pool**

Organic matter in soil is a heterogeneous mixture of all kind of organic molecules, ranging from the simplest sugar or organic acid to the complex structures of lignin and suberin (Kögel-Knabner, 2002). It largely originates from the vegetation and its photosynthesis, but can directly derive from a variety of sources, including litter, root exudates and dead roots, microorganisms, the parent material, or sedimentation (Fig. 1.1b).

Soil organic matter (SOM) can be divided into different fractions, which differ in size, composition, degree of degradation, and their function (Wander, 2004). Fragments of aboveground leaves and branches or belowground roots are summarized as particulate OM (POM; Cerli et al., 2012). Particulate OM is primarily fragmented into small pieces with a low degree of decomposition and thus the composition

## General Introduction

---

resembles its source (Cerli et al., 2012). This type of POM typically exists unattached in the mineral soil matrix and is referred to as free POM (fPOM; Golchin et al., 1994). The fPOM fraction is generally prone to microbial decomposition due to a lack of physical protection, thus representing an easily available substrate for soil microorganisms and is in this context considered rather active (Schrumpf et al., 2013; Lajtha et al., 2014b). A result of this microbial activity is a further fragmentation into much smaller organic particles. Albeit still in a particulate form, they exhibit partial microbial alteration (Golchin et al., 1994). The small size enables this fraction for example to take part in new aggregate formation or to reach the pore space of soil aggregates. Such physical protection makes them temporarily inaccessible for further microbial decomposition (von Lützow et al., 2006). Hence, occluded POM (oPOM) has a longer residence time compared to fPOM (Wagai et al., 2009). However, decomposition will resume after aggregate breakdown.

Apart from particulate fractions, the predominant part of SOM is associated with the mineral phase (Crow et al., 2007; Schrumpf et al., 2013). This fraction is facilitated by dissolved organic compounds, including dissolved organic matter (DOM) like forest floor leachates (Michalzik et al., 2001; Fröberg et al., 2003), microbial residues and metabolites (Kalbitz et al., 2000; Cotrufo et al., 2013; Sokol et al., 2019), and root exudates (Zsolnay et al., 1999). Sorption of these dissolved compounds to mineral surfaces leads to the formation of mineral-associated organic matter (MAOM) in soil (Kaiser and Guggenberger, 2000; Mikutta et al., 2019; Sokol et al., 2019). Organic matter associated with minerals is generally better protected when compared to POM (Schrumpf et al., 2013). Kalbitz and Kaiser (2008) even stated that sorption of OM to reactive minerals like goethite, ferrihydrite, or amorphous Al hydroxides can inhibit mineralization of sorbed OM almost completely. Decomposition of MAOM primarily takes place upon desorption of the mineral protected OM (Mikutta et al., 2007). Thus, the level of protection against desorption and microbial consumption depends on the strength and amount of bonds between OM and mineral surface (Kalbitz et al., 2005; Mikutta et al., 2007). This, in return, is given by the mineral type and the DOM composition (Mikutta et al., 2007).

The three common functional OM fractions can be complemented by a fraction which describes the mobile part of SOM (= DOM). Organic matter in the percolating soil solution may represent the smallest of the four fractions and in the total SOM pool (Chantigny, 2003), but it should be considered as equally important. The mobile fraction connects POM and MAOM fractions through the soil profile, thereby mediating the distribution of OM in the soil profile. For a given site, percolating DOM can be responsible for up to half of the total SOM pool (Kalbitz and Kaiser, 2008). However, while in the soil solution, DOM is exposed to its consumers and a large part is considered to be potentially microbially degradable (Kalbitz et al., 2000; Kalbitz and Kaiser, 2008). Certainly, this is related to the composition of DOM, as especially microbial-derived compounds were found to feature an intrinsic stability towards further degradation (Marschner and Kalbitz, 2003).

### **1.4. Organic matter dynamics – A cascade of input, transformation, and output**

Dividing SOM into fractions with different functionality in soil (section 1.3) provides insights into the dynamic of OM in soil. Pathways of organic matter into soils, especially subsoils, are multifaceted and can be ascribed to four major input paths: (1) bioturbations, (2) root exudation, (3) root biomass, and (4) DOM movement (Rumpel and Kögel-Knabner, 2011; Fig. 1.2). Aboveground inputs derive from the surface litter. Activity of meso- and macrofauna, e.g. burial, translocate POM from the organic layer to the mineral soil (Wilkinson et al., 2009). Such bioturbations (1) translocate particularly plant-derived POM into the upper part of forest soil profiles, where it contributes considerably to SOM (Kaiser et al., 2002; Schrumpf et al., 2013). In greater soil depth, POM mainly derives from necrotic roots (root biomass), but POM contributions to subsoil SOM are only minor (Kaiser et al., 2002; Angst et al., 2018). A number of long-term litter manipulation studies investigated the role of the litter layer for OC inputs to the mineral soil. Despite varying locations and forest stands, the similar approach of plots with doubled litter and exclusion of litter uniformly showed that an increase in litter material did not result in a concomitant increase in SOM whereas exclusion of litter induced significant loss of soil OC (SOC) within decades (e.g. Bowden et al., 2014; Fekete et al., 2014; Lajtha et al., 2014a). Consequently, litter-derived OM can be considered as a source of the actively cycling C in the upper mineral soil (Crow et al., 2009; Bowden et al., 2014; Angst et al., 2016).

The contribution of roots (exudation (2) and biomass (3)) is controversially discussed. On the one side, previous publications give evidence that SOM is to a large extent root-derived due to a slow turnover and effective protection in soil (Rasse et al., 2005; Clemmensen et al., 2013; Angst et al., 2018). But on the other side, rhizosphere priming was found to be able to greatly enhance SOM decomposition (Dijkstra and Cheng, 2007), while root exudation can remove the mineral protection of MAOM thereby enhancing microbial decomposition (Keiluweit et al., 2015). Therefore, it seems evident that a field approach with exclusion of roots had less significant impact on SOC losses in a deciduous forest compared to litter exclusion (Lajtha et al., 2014b).

Movement of DOM (4) illustrates another major input path, which can contribute up to 50 % to the buildup of SOM in forest soils (Kalbitz and Kaiser, 2008). A substantial part of DOM originates from the recent litter layer (Fröberg et al., 2005) but the majority is lost during passage through the organic layer by sorption and mineralization (Fröberg et al., 2005, 2007; Fig. 1.2). Dissolved OM entering the mineral soil largely originate from altered OM of the Oe and Oa horizons (Fröberg et al., 2003; Hagedorn et al., 2004), and is predominantly plant-derived (Fig. 1.2). Dissolved organic carbon (DOC) concentrations in the soil solution entering temperate forest mineral topsoils were reported to vary between 30-80 mg L<sup>-1</sup>, which correspond to fluxes of 10-40 g m<sup>-2</sup> yr<sup>-1</sup> (Fröberg et al., 2006; Michalzik et al., 2001).



# General Introduction

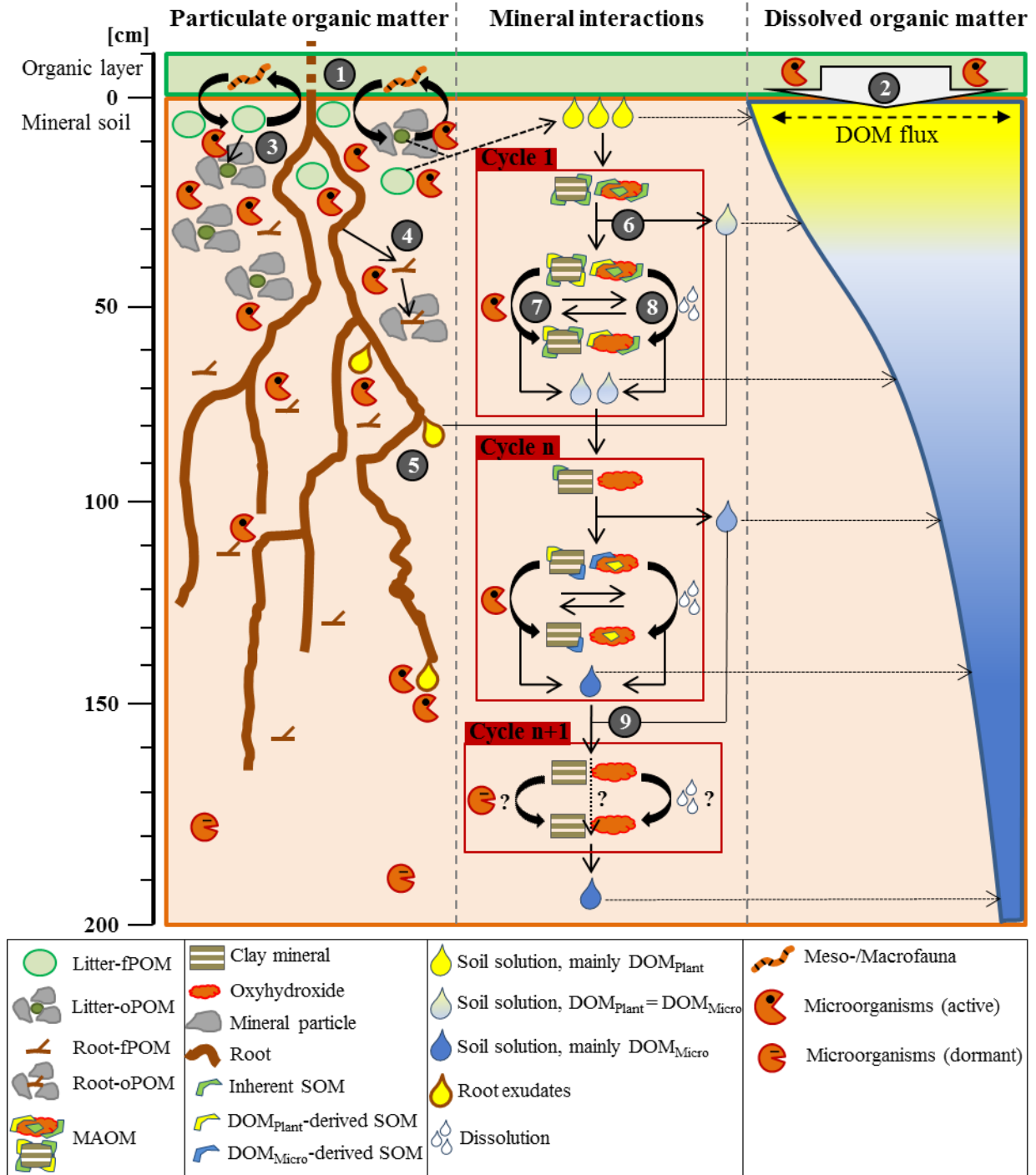


**Fig. 1.2** Schematic illustration of sources, inputs, and translocation of organic matter (OM) in individual functional OM fractions in the soil profile during downward cycling with inspirations from Kaiser and Kalbitz (2012), Mikutta et al. (2019), Sokol et al. (2019), and Lehmann et al. (2020). Several processes are included in OM cycling in soil. Litter-derived OM predominantly enters the soil via particulate organic matter (POM) bioturbations (1) and dissolved organic matter (DOM) leaching (2). In soil, the free POM particles (fPOM) can be occluded by soil particles (oPOM; 3). Belowground OM sources are roots, which contribute either to the POM fractions by decay of dead roots (4) or to DOM due to root exudation (5). Dissolved OM in the soil solution is continuously interacting with the mineral matrix. Those interactions include sorption of DOM compounds to mineral surfaces – potentially by exchange/displacement of older inherent soil OM (SOM; 6), microbial processing of sorbed SOM and DOM (7), and

## General Introduction

---

consequently desorption and dissolution of microbial metabolites and altered SOM (8). Organic matter undergoes multiple sorption, microbial processing, desorption cycles while migrating down the soil profile (Kaiser and Kalbitz, 2012). Such interactions affect the amount and the composition of DOM with increasing soil depth, from a plant-derived signature ( $DOM_{\text{plant}}$ ) in the upper parts of the soil profile towards a microbial-derived signature ( $DOM_{\text{micro}}$ ) in the deeper parts of the soil profile (right hand side of the figure). Small DOM fluxes in the deep subsoil including mainly processed, microbial-derived organic compounds leaves it uncertain to which extent stable mineral-associated OM (MAOM) formation (9) is taking place under natural conditions.

When entering the mineral soil, complex organic compounds, e.g. hydrophobic lignin-derived phenols with a high affinity to mineral surfaces, are strongly retained by the mineral matrix (Kaiser and Guggenberger, 2000; Kaiser et al., 2004). In contrast, the carbohydrate-rich hydrophilic part of DOM remains in solution (Kaiser et al., 2004). Since most mineral surfaces are already occupied in forest topsoils, sorption of high affinity DOM is coupled to displacement of less strongly bound OM (Mikutta et al., 2019). The DOM fraction is frequently affected by abiotic processes like component fractionation during sorption and exchange (“sorptive fractionation”; Kaiser et al., 1996; Mikutta et al., 2007) and hysteresis effects during desorption (Mikutta et al., 2007; Saïdy et al., 2013) while migrating down the soil profile. From the biotic perspective, sorbed OM is better protected against microbial processing compared to OM in solution (Kalbitz and Kaiser, 2008), however microbial mineralization and transformation of MAOM is slowed down but not interrupted completely (Kalbitz et al., 2005). Products of such biodegradation are either directly released to the soil solution or remain mineral-associated but likely more easily desorbable/exchangeable than before (Kaiser and Kalbitz, 2012). Another major product of the microbial consumption is  $CO_2$ , which is released to the atmosphere and thus lost for further stabilization in soil. With increasing soil depth, the soil solution has substantially smaller DOC concentrations, with 0-47  $mg\ L^{-1}$  in the upper subsoil of about 20-50 cm to 0-36  $mg\ L^{-1}$  in the deeper subsoil in 70-150 cm (Michalzik et al., 2001; Kindler et al., 2011; Leinemann et al., 2016) and its composition shifts from a plant-derived signature towards a microbial-derived signature (Kaiser and Kalbitz, 2012; Roth et al., 2019; Fig. 1.2). Carbon fluxes into the upper subsoil of 20-50 cm were recorded to about 0-9  $g\ m^{-2}\ yr^{-1}$ , whereas only 0-3  $g\ m^{-2}\ yr^{-1}$  reaches the deeper subsoil in 90-150 cm soil depth (Michalzik et al., 2001; Leinemann et al., 2016). Since DOM movement has a determining influence on SOM distribution in the whole soil profile, the composition of SOM changes accordingly with increasing soil depth (Kaiser and Kalbitz, 2012). Individual observations of several previous studies suggest that DOM undergoes a sequence of repeating sorption, microbial processing, and desorption cycles, combined in the recently postulated conceptual model or “cascade model” by Kaiser and Kalbitz (2012), albeit comprehensive field evidence is still missing. It should be noted that the model does not cover the transportation of DOM in preferential flow paths (Kaiser and Kalbitz, 2012). Preferential flow in macropores or old root channels (biopores) appears to be much faster than matrix flow, which results in fewer interactions between DOM and mineral surfaces (Hagedorn et al., 2015; Leinemann et al., 2016) and can be of relevance in high leaching forest

ecosystems.  $\text{DO}^{14}\text{C}$  concentrations showed that DOM is much younger than SOM especially in subsoils, contradicting the conceptual model and suggesting that DOM mainly originates from fresh sources (Don and Schulze, 2008). The authors concluded that DOM has little connection to the SOM pool apart from its flow paths. However, preferential flow paths are assumed to be relatively stable and can persist over years (Hagedorn and Bundt, 2002). Consequently, annual DOC fluxes to the subsoil in these flow paths are likely larger and comprise a larger share of complex organic compounds compared to matrix flow DOM, while fluxes and composition particularly depends on the flow velocity.

Cycling of DOM and SOM continues until reaching the aquifer. Export of DOC from temperate forest soils to the groundwater was reported to be in the range of  $2.7\text{-}3.7 \text{ g m}^{-2} \text{ yr}^{-1}$  (Evans et al., 2020). However, the contribution of aboveground C inputs to the C cycling in the deep mineral subsoil remains understudied, thereby the dynamic of preferential and matrix flow deserves more attention.

### **1.5. Preservation and persistence of soil organic matter**

The difference between C inputs and C outputs defines the retention of OC in soils, whereby more inputs than outputs denote a (C) sink and *vice versa* a (C) source. Thus, a key factor in the preservation of SOM is the level of stabilization against microbial decomposition, thereby prolonging its turnover. Stabilization of organic matter in soil can be achieved by several mechanisms, including selective preservation (1), spatial inaccessibility (2), and interactions with mineral surfaces (3) (Guggenberger and Kaiser, 2003; von Lützow et al., 2006). But selective preservation in terms of recalcitrance was recently questioned (Mikutta et al., 2006; Marschner et al., 2008), with reference to the formation of MAOM as the most important mechanism. Spatial inaccessibility refers to occlusion of OM in larger aggregates, which was found to considerably prolong the turnover (von Lützow et al., 2006; Schrumpf et al., 2013). However, the majority of SOM is in most cases found in the MAOM fraction (Crow et al., 2009; Schrumpf et al., 2013). It is estimated that currently about a quarter of the global SOC is retained by reactive Fe- and Al-bearing minerals alone (Kramer and Chadwick, 2018).

Most efficient ways of OM stabilization combine multiple mechanisms. For example, sorptive fractionation (see section 1.4.) connects selective preservation (in terms of selective sorption not recalcitrance) to the interactions with mineral surfaces (Mikutta et al., 2006). Sorption of OM into small pores or at the mouth of micropores (Kaiser and Guggenberger, 2003) connects mineral fixation to spatial inaccessibility for microorganisms, and likely also include selective preservation due to a preferential sorption of compounds able to form multiple attachments (Kaiser and Guggenberger, 2003). It was estimated that SOM stabilized as MAOM has an up to 10 times larger mean residence time in soils compared to “free” SOM with no mineral association (Tipping et al., 2012).

At present, forest soils are assumed to be close to an equilibrium state of OM inputs and outputs (Guggenberger and Kaiser, 2003), thereby maintaining their current C reservoir. Topsoils were attested to be close to C saturation (Wiesmeier et al., 2014; Mikutta et al., 2019). Hence, continuous OM inputs into the topsoil and a passing of comparably small outputs to the subsoil require a highly dynamic cycling and a fast turnover of topsoil OM (Tipping et al., 2012; Schrumpf et al., 2013). Young/modern ages further illustrate short residence times of topsoil SOM (Rumpel et al., 2012). There is a strong correlation between the age of organic matter and soil depth (Rumpel et al., 2012), which can be explained by OM passing through multiple sorption, microbial processing, desorption cycles until reaching a certain soil depth (Kaiser and Kalbitz, 2012). Accordingly, high  $^{14}\text{C}$  ages up to millennia were observed for subsoil SOM (Fontaine et al., 2007; Rumpel et al., 2012). The compositional change with depth may further benefit the prolonged turnover in subsoils. Cotrufo et al. (2013) introduced the MEMS framework, suggesting that microbial decomposition converts labile plant-derived OM into stable microbial-derived SOM. For example, plant-derived carbohydrates in DOM are easily available for microorganisms, whereas microbial-derived carbohydrates in DOM can be relatively stable (Kalbitz and Kaiser, 2008). In addition, subsoil SOM often exists spatially separated from its decomposers (Schmidt et al., 2011; Lehmann et al., 2020), concentrating decomposition to microbial hotspots (Kuzyakov and Blagodatskaya, 2015; Leinemann et al., 2018). But until now, dominating processes in subsoil OC preservation are not fully understood, and the question remains if additional C inputs into forest subsoils can persist for decades and centuries.

### **1.6. Importance of forest ecosystems as carbon sinks**

Worldwide, forests cover an area of about 40 million km<sup>2</sup> which account for 30 % of the global terrestrial area (MacDicken et al., 2015). Temperate forests represent the third biggest part, following boreal and tropical/subtropical forests, and are characterized by the second strongest human footprint (Watson et al., 2018). Moreover, OC stored in temperate forest soils is considered as highly sensitive since mineral-retained OC is responsive to changes in effective soil moisture and thus to future climate change (Kramer and Chadwick, 2018). On the other side, it is expected that a climate change induced greening of the vegetation will particularly promote the growth of young forests < 140 yrs (McDowell et al., 2020), thereby positively influencing net primary production and C inputs to soils (Pan et al., 2011; Liu et al., 2015). However, more extreme weather events such as droughts and storms may offset the increasing productivity (Lindner et al., 2010) whilst promoting C inputs to soil through dead biomass as well (Anderegg et al., 2020).

Globally, forest ecosystems are currently considered as C sinks (Luyssaert et al., 2008), in line with findings from European forests (Schils et al., 2008; Luyssaert et al., 2010). Mineral topsoils in German

forests for example showed an average increase of the OC stock of about 0.4 Mg C ha<sup>-1</sup> yr<sup>-1</sup> between 1987/1993 and 2006/2008 (Grüneberg et al., 2014). Nave et al. (2018) further estimated that re-forestation could result in retention of additional 2 Pg of C in US topsoils within a century. Consequences of increasing C inputs into forest soils, either as a natural consequence of climate change (e.g. greening) or as a human induced measure to mitigate climate change by increasing C sequestration in soils (Paustian et al., 2016), are controversially discussed. While some reported on potentials of soils as future C sinks, others observed that OM additions to forest soils increased microbial respiration rates to the same extent (Sulzman et al., 2005; Phillips et al., 2012). Moreover, additions of such labile OM can induce priming in deep subsoil horizons, activating microorganisms to decompose old stabilized OM (Fontaine et al., 2007; Bernal et al., 2016). Hence, more research is needed to evaluate the function of forest soils as sink or source of C under current field conditions and in scenarios of increasing C inputs with particular focus on its fate in the subsoil.

### 1.7. Rationale and objectives

Understanding the global C dynamics require an understanding of the subsoils to the same extent as topsoils (Salomé et al., 2010). But subsoils were largely underrepresented in past research and processes are not well understood (Rumpel and Kögel-Knabner, 2011; Schmidt et al., 2011; Simo et al., 2019).

While sources and paths of OM in subsoils are principally known (Rumpel and Kögel-Knabner, 2011), there is no consensus about their relevance. The conceptual model by Kaiser and Kalbitz (2012) includes the interacting DOM and SOM dynamics from the aboveground litter layer to the aquifer and is supported by laboratory experiments (e.g. Leinemann et al., 2018) and in parts by field approaches (Hagedorn et al., 2015; Roth et al., 2019). Rothstein et al. (2018) determined litter C inputs in a forest subsoil down to 60 cm depth, but they were not able to quantify and differentiate between illuvial DOM and root-derived OM as subsoil C sources and ultimately tracked podsolization in their soil profiles. There is a lack of comprehensive field experiments for the conceptual model with the use of stable isotopes in order to determine sources and fluxes of the translocated OM. Apart from that, there are no field studies available which examine the contribution of aboveground litter to the subsoil C cycling below 50-60 cm soil depth. In addition, the stability of newly formed SOM in subsoils has not been determined by *in-situ* field experiments so far.

Subsoils are generally accepted as an OM stabilizing environment, but reasons for stability of SOM are still under discussion. As emphasized in sections 1.3. to 1.5., this includes Mikutta et al. (2019), Roth et al. (2019), and Lehmann et al. (2020). Additionally, in a recent compilation of > 400 laboratory sorption experiments, Abramoff et al. (2021) reported on a larger global DOC sorption potential of subsoils over topsoils. Nevertheless, soil monitoring approaches showed that there is considerable input of OC into

subsoils (Michalzik et al., 2001; Leinemann et al., 2016), but SOC concentrations are often observed to be relatively small (Schöning and Kögel-Knabner, 2006; Bowden et al., 2014). This seems contradictory, since considerable capacities for OM sorption were attested to subsoils in the past (Lorenz et al., 2011). In this context, the assumption of stabilizing additional OM in subsoils needs to be critically reviewed.

The overarching goal of this thesis was therefore to evaluate the fate of aboveground litter and its contribution to the formation of SOM in temperate forest soils and specifically to subsoils. Hence, a first objective was to quantify the inputs of litter-derived C to top- and subsoil OC stocks. Further emphasis was on the stability of such newly formed SOM in different functional OM fractions, particularly translocated via the DOC pathway and associated with reactive soil minerals. Moreover, this thesis aimed at providing field insights for the role of forest subsoils as potential contributor to climate change mitigation.

### 1.8. Hypotheses

To achieve these objectives, the following hypotheses were tested, addressing the fate of litter-derived C inputs during downward cycling:

- H1** The majority of aboveground inputs does not reach the subsoil due to retention in the topsoil alongside microbial utilization, thus only a small share of aboveground inputs enters deeper parts of the soil profile after a considerable time lag as a succession of passing through several cascade cycles before. With the translocation of organic matter through the soil profile and its concurrent microbial processing there is a shift in the composition of DOM and SOM from a plant-derived signature to a microbial-derived signature.
- H2** Organic matter inputs and movement through the soil profile is predominantly controlled by DOM flux, enhanced by stable preferential flow paths depending on soil texture.
- H3** The overall capability to retain OM is higher in subsoils due to a high availability of sorption sites compared to topsoils with largely occupied mineral surfaces.
- H4** Organic matter actually retained in subsoils is highly stable, especially when compared to topsoil OM, as a result of more interactions with mineral surfaces and a reduced availability for the microbial community.

In order to verify these hypotheses three studies were conducted to test them in the following way:

### **I Relevance of aboveground litter for soil organic matter formation – a soil profile perspective**

Study I was conducted to quantify the contributions of aboveground litter to the SOM pool in a soil profile down to 180 cm depth, thus testing **H1**. Separation of functionally different OM fractions at two time points was done in order to assess the stability of fresh litter-derived OM inputs depending on their level of protection, thus contributing to **H4**.

In the Grindewald beech forest, the natural litter layer on top of the subsoil observatories (e.g. Leinemann et al., 2016) was exchanged with  $^{13}\text{C}$ -enriched litter. After 22 months of field exposure, residues of  $^{13}\text{C}$ -enriched litter were removed and the natural litter layer was re-established. Soil cores down to 180 cm, taken at re-establishment and 18 months later, were separated into different density fractions (MAOM, fPOM, oPOM) and water-extractable OM and analyzed for litter-derived  $^{13}\text{C}$ .

### **II Fate and stability of dissolved organic carbon in topsoils and subsoils under beech forests**

Study II aimed at evaluating sorption of  $^{13}\text{C}$ -enriched leaf litter leachates (= DOM) in top- and subsoils of undisturbed field profiles at three beech forest locations. Due to variations in parent material, the effects of soil texture and available mineral surfaces on translocation and sorption of percolating DOM was investigated, thus contributing to **H2** and **H3**. Sampling at two time points and subsequent laboratory incubation experiments provided insights into the stability of recently sorbed DOM, thus contributing to **H4**.

Besides the experimental setup of study I and III, another field approach involved the injection of  $^{13}\text{C}$ -enriched DOM solution into undisturbed topsoils (in 10 cm soil depth) and subsoils (in 30/50 cm upper subsoil and 60/100 cm deeper subsoil). Three and 17 months after injection, soil cores were sampled up to 100 cm below the injection depth and samples were analyzed for DOM-derived  $^{13}\text{C}$ . In the laboratory, incubation experiments with a duration of 103 days at 20°C were conducted and mineralization of both, native SOM and fresh DOM-derived SOM, was determined by  $^{13}\text{CO}_2$  measurements at 5 time points.

### **III Biogeochemical constraints limit carbon storage in forest subsoils**

Study III integrated a variety of laboratory and field experiments in order to yield a comprehensive picture of litter-derived C cycling and stabilization by the mineral phase. Since a variety of experiments were incorporated, this study contributes to all hypotheses **H1-4**.

The unique field setup at the Grindewald study site, consisting of three subsoil observatories, made it possible to sample soil solution and soil air down to a depth of 150 cm, thereby

monitoring fluxes of DOC and CO<sub>2</sub> through the soil profile and relate them to C pools. The extensive use of <sup>13</sup>C-enriched leaf litter on top of the observatory areas allowed quantification of litter-derived C fluxes within top- and subsoils. Soil cores taken at re-establishment (see Study I) completed the major C pools. Further, an *in-situ* incubation experiment of <sup>13</sup>C-coated minerals (MAOM burial experiment) specifically examined sorption, exchange, and desorption processes of two major acceptors of OM in soil, clay minerals and Fe oxyhydroxides. Field approaches were complemented by laboratory batch sorption and desorption experiments in order to compare the theoretically possible (laboratory) and the actually occurring (field) interactions between OM and the mineral phase.

### 1.9. References General Introduction

Abramoff, R. Z., Georgiou, K., Guenet, B., Torn, M. S., Huang, Y., Zhang, H., Feng, W., Jagadamma, S., Kaiser, K., Kothawala, D., Mayes, M. A. and Ciais, P.: How much carbon can be added to soil by sorption?, *Biogeochemistry*, <https://doi.org/10.1007/s10533-021-00759-x>, 2021.

Althor, G., Watson, J. E. M. and Fuller, R. A.: Global mismatch between greenhouse gas emissions and the burden of climate change, *Sci. Rep.*, 6(1), 1–6, doi:10.1038/srep20281, 2016.

Anderegg, W. R. L., Trugman, A. T., Badgley, G., Anderson, C. M., Bartuska, A., Ciais, P., Cullenward, D., Field, C. B., Freeman, J., Goetz, S. J., Hicke, J. A., Huntzinger, D., Jackson, R. B., Nickerson, J., Pacala, S. and Randerson, J. T.: Climate-driven risks to the climate mitigation potential of forests, *Science*, 368(6497), doi:10.1126/science.aaz7005, 2020.

Angst, G., John, S., Mueller, C. W., Kögel-Knabner, I. and Rethemeyer, J.: Tracing the sources and spatial distribution of organic carbon in subsoils using a multi-biomarker approach, *Sci. Rep.*, 6(1), doi:10.1038/srep29478, 2016.

Angst, G., Messinger, J., Greiner, M., Häusler, W., Hertel, D., Kirfel, K., Kögel-Knabner, I., Leuschner, C., Rethemeyer, J. and Mueller, C. W.: Soil organic carbon stocks in topsoil and subsoil controlled by parent material, carbon input in the rhizosphere, and microbial-derived compounds, *Soil Biol. Biochem.*, 122, 19–30, doi:10.1016/j.soilbio.2018.03.026, 2018.

Baisden, W. T., Amundson, R., Cook, A. C. and Brenner, D. L.: Turnover and storage of C and N in five density fractions from California annual grassland surface soils, *Glob. Biogeochem. Cycles*, 16(4), 64-1-64-16, doi:10.1029/2001GB001822, 2002.

Batjes, N. H.: Total carbon and nitrogen in the soils of the world, *Eur J Soil Sci*, 47, 151–163, doi:10.1111/ejss.12114\_2, 1996.

Bernal, B., McKinley, D. C., Hungate, B. A., White, P. M., Mozdzer, T. J. and Megonigal, J. P.: Limits to soil carbon stability; Deep, ancient soil carbon decomposition stimulated by new labile organic inputs, *Soil Biol. Biochem.*, 98, 85–94, doi:10.1016/j.soilbio.2016.04.007, 2016.

Blume, H.-P., Brümmer, G. W., Horn, R., Kandeler, E., Kögel-Knabner, I., Kretschmar, R., Stahr, K. and Wilke, B.-M.: Scheffer/Schachtschabel: Lehrbuch der Bodenkunde, Springer-Verlag., 2016.

Bowden, R. D., Deem, L., Plante, A. F., Peltre, C., Nadelhoffer, K. and Lajtha, K.: Litter input controls on



soil carbon in a temperate deciduous forest, *Soil Sci. Soc. Am. J.*, 78(S1), S66–S75, doi:10.2136/sssaj2013.09.0413nafsc, 2014.

Brooks, P. D., Chorover, J., Fan, Y., Godsey, S. E., Maxwell, R. M., McNamara, J. P. and Tague, C.: Hydrological partitioning in the critical zone: Recent advances and opportunities for developing transferable understanding of water cycle dynamics, *Water Resour. Res.*, 51(9), 6973–6987, doi:10.1002/2015WR017039, 2015.

Cerli, C., Celi, L., Kalbitz, K., Guggenberger, G. and Kaiser, K.: Separation of light and heavy organic matter fractions in soil — Testing for proper density cut-off and dispersion level, *Geoderma*, 170, 403–416, doi:10.1016/j.geoderma.2011.10.009, 2012.

Chantigny, M. H.: Dissolved and water-extractable organic matter in soils: A review on the influence of land use and management practices, *Geoderma*, 113(3–4), 357–380, doi:10.1016/S0016-7061(02)00370-1, 2003.

Clemmensen, K. E., Bahr, A., Ovaskainen, O., Dahlberg, A., Ekblad, A., Wallander, H., Stenlid, J., Finlay, R. D., Wardle, D. A. and Lindahl, B. D.: Roots and associated fungi drive long-term carbon sequestration in boreal forest, *Science*, 339(6127), 1615–1618, doi:10.1126/science.1231923, 2013.

Cotrufo, M. F., Wallenstein, M. D., Boot, C. M., Deneff, K. and Paul, E.: The Microbial Efficiency-Matrix Stabilization (MEMS) framework integrates plant litter decomposition with soil organic matter stabilization: Do labile plant inputs form stable soil organic matter?, *Glob. Change Biol.*, 19(4), 988–995, doi:10.1111/gcb.12113, 2013.

Crow, S. E., Swanston, C. W., Lajtha, K., Brooks, J. R. and Keirstead, H.: Density fractionation of forest soils: methodological questions and interpretation of incubation results and turnover time in an ecosystem context, *Biogeochemistry*, 85(1), 69–90, doi:10.1007/s10533-007-9100-8, 2007.

Crow, S. E., Lajtha, K., Filley, T. R., Swanston, C. W., Bowden, R. D. and Caldwell, B. A.: Sources of plant-derived carbon and stability of organic matter in soil: Implications for global change, *Glob. Change Biol.*, 15(8), 2003–2019, doi:10.1111/j.1365-2486.2009.01850.x, 2009.

Dijkstra, F. A. and Cheng, W.: Interactions between soil and tree roots accelerate long-term soil carbon decomposition, *Ecol. Lett.*, 10(11), 1046–1053, doi:10.1111/j.1461-0248.2007.01095.x, 2007.

Don, A. and Schulze, E.-D.: Controls on fluxes and export of dissolved organic carbon in grasslands with contrasting soil types, *Biogeochemistry*, 91(2–3), 117–131, 2008.

Evans, L. R., Pierson, D. and Lajtha, K.: Dissolved organic carbon production and flux under long-term litter manipulations in a Pacific Northwest old-growth forest, *Biogeochemistry*, 149(1), 75–86, doi:10.1007/s10533-020-00667-6, 2020.

Fekete, I., Kotroczó, Z., Varga, C., Nagy, P. T., Várбірó, G., Bowden, R. D., Tóth, J. A. and Lajtha, K.: Alterations in forest detritus inputs influence soil carbon concentration and soil respiration in a Central-European deciduous forest, *Soil Biol. Biochem.*, 74, 106–114, doi:10.1016/j.soilbio.2014.03.006, 2014.

Field, J. P., Breshears, D. D., Law, D. J., Villegas, J. C., López-Hoffman, L., Brooks, P. D., Chorover, J., Barron-Gafford, G. A., Gallery, R. E., Litvak, M. E., Lybrand, R. A., McIntosh, J. C., Meixner, T., Niu, G.-Y., Papuga, S. A., Pelletier, J. D., Rasmussen, C. R. and Troch, P. A.: Critical zone services: Expanding context, constraints, and currency beyond ecosystem services, *Vadose Zone J.*, 14(1), vzj2014.10.0142, doi:10.2136/vzj2014.10.0142, 2015.

Fontaine, S., Barot, S., Barré, P., Bdioui, N., Mary, B. and Rumpel, C.: Stability of organic carbon in deep

soil layers controlled by fresh carbon supply, *Nature*, 450(7167), 277, doi:10.1038/nature06275, 2007.

Fröberg, M., Berggren, D., Bergkvist, B., Bryant, C. and Knicker, H.: Contributions of Oi, Oe and Oa horizons to dissolved organic matter in forest floor leachates, *Geoderma*, 113(3–4), 311–322, doi:10.1016/S0016-7061(02)00367-1, 2003.

Fröberg, M., Kleja, D. B., Bergkvist, B., Tipping, E. and Mulder, J.: Dissolved organic carbon leaching from a coniferous forest floor – a field manipulation experiment, *Biogeochemistry*, 75(2), 271–287, doi:10.1007/s10533-004-7585-y, 2005.

Fröberg, M., Berggren, D., Bergkvist, B., Bryant, C. and Mulder, J.: Concentration and fluxes of dissolved organic carbon (DOC) in three Norway Spruce stands along a climatic gradient in Sweden, *Biogeochemistry*, 77(1), 1–23, doi:10.1007/s10533-004-0564-5, 2006.

Fröberg, M., Berggren, D. and Hagedorn, F.: The contribution of fresh litter to dissolved organic carbon leached from a coniferous forest floor, *Eur. J. Soil Sci.*, 58(1), 108–114, doi:10.1111/j.1365-2389.2006.00812.x, 2007.

Golchin, A., Oades, J. M., Skjemstad, J. O. and Clarke, P.: Study of free and occluded particulate organic matter in soils by Solid state  $^{13}\text{C}$  CP/MAS NMR Spectroscopy and Scanning Electron Microscopy, *Aust. J. Soil Res.*, 32(2), 285–309, 1994.

Grüneberg, E., Ziche, D. and Wellbrock, N.: Organic carbon stocks and sequestration rates of forest soils in Germany, *Glob. Change Biol.*, 20(8), 2644–2662, doi:10.1111/gcb.12558, 2014.

Guggenberger, G. and Kaiser, K.: Dissolved organic matter in soil: Challenging the paradigm of sorptive preservation, *Geoderma*, 113(3–4), 293–310, doi:10.1016/S0016-7061(02)00366-X, 2003.

Hagedorn, F. and Bundt, M.: The age of preferential flow paths, *Geoderma*, 108(1), 119–132, doi:10.1016/S0016-7061(02)00129-5, 2002.

Hagedorn, F., Saurer, M. and Blaser, P.: A  $^{13}\text{C}$  tracer study to identify the origin of dissolved organic carbon in forested mineral soils, *Eur. J. Soil Sci.*, 55(1), 91–100, doi:10.1046/j.1365-2389.2003.00578.x, 2004.

Hagedorn, F., Bruderhofer, N., Ferrari, A. and Niklaus, P. A.: Tracking litter-derived dissolved organic matter along a soil chronosequence using  $^{14}\text{C}$  imaging: Biodegradation, physico-chemical retention or preferential flow?, *Soil Biol. Biochem.*, 88, 333–343, doi:10.1016/j.soilbio.2015.06.014, 2015.

Heinze, S., Ludwig, B., Piepho, H.-P., Mikutta, R., Don, A., Wordell-Dietrich, P., Helfrich, M., Hertel, D., Leuschner, C., Kirfel, K., Kandeler, E., Preusser, S., Guggenberger, G., Leinemann, T. and Marschner, B.: Factors controlling the variability of organic matter in the top- and subsoil of a sandy Dystric Cambisol under beech forest, *Geoderma*, 311, 37–44, doi:10.1016/j.geoderma.2017.09.028, 2018.

Jobbagy, E. G. and Jackson, R. B.: The vertical distribution of soil organic carbon and its relation to climate and vegetation, *Ecol. Appl.*, 10(2), 423–436, doi:10.2307/2641104, 2000.

Kaiser, K. and Guggenberger, G.: The role of DOM sorption to mineral surfaces in the preservation of organic matter in soils, *Org. Geochem.*, 31, 711–725, 2000.

Kaiser, K. and Guggenberger, G.: Mineral surfaces and soil organic matter, *Eur. J. Soil Sci.*, 54(2), 219–236, 2003.

Kaiser, K. and Kalbitz, K.: Cycling downwards – dissolved organic matter in soils, *Soil Biol. Biochem.*, 52, 29–32, doi:10.1016/j.soilbio.2012.04.002, 2012.

Kaiser, K., Guggenberger, G. and Zech, W.: Sorption of DOM and DOM fractions to forest soils, *Geoderma*, 74(3–4), 281–303, 1996.

Kaiser, K., Eusterhues, K., Rumpel, C., Guggenberger, G. and Kögel-Knabner, I.: Stabilization of organic matter by soil minerals — investigations of density and particle-size fractions from two acid forest soils, *J. Plant Nutr. Soil Sci.*, 165(4), 451–459, doi:10.1002/1522-2624(200208)165:4<451::AID-JPLN451>3.0.CO;2-B, 2002.

Kaiser, K., Guggenberger, G. and Haumaier, L.: Changes in dissolved lignin-derived phenols, neutral sugars, uronic acids, and amino sugars with depth in forested Haplic Arenosols and Rendzic Leptosols, *Biogeochemistry*, 70(1), 135–151, 2004.

Kalbitz, K. and Kaiser, K.: Contribution of dissolved organic matter to carbon storage in forest mineral soils, *J. Plant Nutr. Soil Sci.*, 171(1), 52–60, doi:10.1002/jpln.200700043, 2008.

Kalbitz, K., Solinger, S., Park, J.-H., Michalzik, B. and Matzner, E.: Controls on the dynamics of dissolved organic matter in soils: A review, *Soil Sci.*, 165(4), 277–304, 2000.

Kalbitz, K., Schwesig, D., Rethemeyer, J. and Matzner, E.: Stabilization of dissolved organic matter by sorption to the mineral soil, *Soil Biol. Biochem.*, 37(7), 1319–1331, doi:10.1016/j.soilbio.2004.11.028, 2005.

Kandeler, E., Stemmer, M. and Gerzabek, M. H.: Role of microorganisms in carbon cycling in soils, in *Microorganisms in Soils: Roles in Genesis and Functions*, edited by P. D. A. Varma and P. F. Buscot, pp. 139–157, Springer Berlin Heidelberg. [online] Available from: [http://link.springer.com/chapter/10.1007/3-540-26609-7\\_7](http://link.springer.com/chapter/10.1007/3-540-26609-7_7) (Accessed 29 October 2016), 2005.

Keenan, T. F. and Williams, C. A.: The terrestrial carbon sink, *Annu. Rev. Environ. Resour.*, 43, 219–243, 2018.

Keiluweit, M., Bougoure, J. J., Nico, P. S., Pett-Ridge, J., Weber, P. K. and Kleber, M.: Mineral protection of soil carbon counteracted by root exudates, *Nat. Clim. Change*, 5(6), 588–595, doi:10.1038/nclimate2580, 2015.

Kindler, R., Siemens, J., Kaiser, K., Walmsley, D. C., Bernhofer, C., Buchmann, N., Cellier, P., Eugster, W., Gleixner, G., Grünwald, T., Heim, A., Ibrom, A., Jones, S. K., Jones, M., Klumpp, K., Kutsch, W., Larsen, K. S., Lehuger, S., Loubet, B., Mckenzie, R., Moors, E., Osborne, B., Pilegaard, K., Rebmann, C., Saunders, M., Schmidt, M. W. I., Schrupf, M., Seyfferth, J., Skiba, U., Soussana, J.-F., Sutton, M. A., Tefs, C., Vowinkel, B., Zeeman, M. J. and Kaupenjohann, M.: Dissolved carbon leaching from soil is a crucial component of the net ecosystem carbon balance: Dissolved carbon leaching, *Glob. Change Biol.*, 17(2), 1167–1185, doi:10.1111/j.1365-2486.2010.02282.x, 2011.

Kögel-Knabner, I.: The macromolecular organic composition of plant and microbial residues as inputs to soil organic matter, *Soil Biol. Biochem.*, 34(2), 139–162, [https://doi.org/10.1016/S0038-0717\(01\)00158-4](https://doi.org/10.1016/S0038-0717(01)00158-4), 2002.

Kramer, M. G. and Chadwick, O. A.: Climate-driven thresholds in reactive mineral retention of soil carbon at the global scale, *Nat. Clim. Change*, 8(12), 1104–1108, doi:10.1038/s41558-018-0341-4, 2018.

Kuzyakov, Y. and Blagodatskaya, E.: Microbial hotspots and hot moments in soil: Concept & review, *Soil Biol. Biochem.*, 83, 184–199, doi:10.1016/j.soilbio.2015.01.025, 2015.

Lajtha, K., Townsend, K. L., Kramer, M. G., Swanston, C., Bowden, R. D. and Nadelhoffer, K.: Changes to particulate versus mineral-associated soil carbon after 50 years of litter manipulation in forest and

prairie experimental ecosystems, *Biogeochemistry*, 119(1), 341–360, doi:10.1007/s10533-014-9970-5, 2014a.

Lajtha, K., Bowden, R. D. and Nadelhoffer, K.: Litter and root manipulations provide insights into soil organic matter dynamics and stability, *Soil Sci. Soc. Am. J.*, 78(S1), S261–S269, doi:10.2136/sssaj2013.08.0370nafsc, 2014b.

Lal, R.: Soil conservation and ecosystem services, *Int. Soil Water Conserv. Res.*, 2(3), 36–47, doi:10.1016/S2095-6339(15)30021-6, 2014.

Lal, R., Kimble, J. M., Follett, R. F. and Stewart, B. A.: *Soil processes and the carbon cycle*, CRC Press., 1997.

Lavania, U. C. and Lavania, S.: Sequestration of atmospheric carbon into subsoil horizons through deep-rooted grasses - vetiver grass model., *Curr. Sci.*, 97(5), 618–619, 2009.

Lehmann, J., Hansel, C., Kaiser, C., Kleber, M., Maher, K., Manzoni, S., Nunan, N., Reichstein, M., Schimel, J., Torn, M., Wieder, W. and Kögel-Knabner, I.: Persistence of soil organic carbon caused by functional complexity, *Nat. Geosci.*, 1–6, doi:10.1038/s41561-020-0612-3, 2020.

Leinemann, T., Mikutta, R., Kalbitz, K., Schaarschmidt, F. and Guggenberger, G.: Small scale variability of vertical water and dissolved organic matter fluxes in sandy Cambisol subsoils as revealed by segmented suction plates, *Biogeochemistry*, 131(1–2), 1–15, doi:10.1007/s10533-016-0259-8, 2016.

Leinemann, T., Preusser, S., Mikutta, R., Kalbitz, K., Cerli, C., Höschen, C., Mueller, C. W., Kandeler, E. and Guggenberger, G.: Multiple exchange processes on mineral surfaces control the transport of dissolved organic matter through soil profiles, *Soil Biol. Biochem.*, 118, 79–90, 2018.

Lindner, M., Maroschek, M., Netherer, S., Kremer, A., Barbati, A., Garcia-Gonzalo, J., Seidl, R., Delzon, S., Corona, P. and Kolström, M.: Climate change impacts, adaptive capacity, and vulnerability of European forest ecosystems, *For. Ecol. Manag.*, 259(4), 698–709, 2010.

Liu, Y. Y., van Dijk, A. I. J. M., de Jeu, R. A. M., Canadell, J. G., McCabe, M. F., Evans, J. P. and Wang, G.: Recent reversal in loss of global terrestrial biomass, *Nat. Clim. Change*, 5(5), 470–474, doi:10.1038/nclimate2581, 2015.

Lorenz, K., Lal, R. and Shipitalo, M. J.: Stabilized soil organic carbon pools in subsoils under forest are potential sinks for atmospheric CO<sub>2</sub>, *For. Sci.*, 57(1), 19–25, doi:10.1093/forestscience/57.1.19, 2011.

Lugato, E., Bampa, F., Panagos, P., Montanarella, L. and Jones, A.: Potential carbon sequestration of European arable soils estimated by modelling a comprehensive set of management practices, *Glob. Change Biol.*, 20(11), 3557–3567, doi:10.1111/gcb.12551, 2014.

von Lützw, M., Kögel-Knabner, I., Ekschmitt, K., Matzner, E., Guggenberger, G., Marschner, B. and Flessa, H.: Stabilization of organic matter in temperate soils: Mechanisms and their relevance under different soil conditions – a review, *Eur. J. Soil Sci.*, 57(4), 426–445, doi:10.1111/j.1365-2389.2006.00809.x, 2006.

Luyssaert, S., Schulze, E.-D., Börner, A., Knohl, A., Hessenmöller, D., Law, B. E., Ciais, P. and Grace, J.: Old-growth forests as global carbon sinks, *Nature*, 455(7210), 213–215, doi:10.1038/nature07276, 2008.

Luyssaert, S., Ciais, P., Piao, S. L., Schulze, E.-D., Jung, M., Zaehle, S., Schelhaas, M. J., Reichstein, M., Churkina, G., Papale, D., Abril, G., Beer, C., Grace, J., Loustau, D., Matteucci, G., Magnani, F., Nabuurs, G. J., Verbeeck, H., Sulkava, M., Werf, G. R. V. D. and Janssens, I. A.: The European carbon balance. Part 3: forests, *Glob. Change Biol.*, 16(5), 1429–1450, <https://doi.org/https://doi.org/10.1111/j.1365->

2486.2009.02056.x, 2010.

MacDicken, K., Jonsson, Ö., Pina, L., Marklund, L., Maulo, S., Contessa, V., Adikari, Y., Garzuglia, M., Lindquist, E., Reams, G. and D'Annunzio, R.: Global forest resources assessment 2015: How are the world's forests changing?, Food and Agriculture Organization of the United Nations, Rome., 2015.

Marschner, B. and Kalbitz, K.: Controls of bioavailability and biodegradability of dissolved organic matter in soils, *Geoderma*, 113(3–4), 211–235, doi:10.1016/S0016-7061(02)00362-2, 2003.

Marschner, B., Brodowski, S., Dreves, A., Gleixner, G., Gude, A., Grootes, P. M., Hamer, U., Heim, A., Jandl, G., Ji, R., Kaiser, K., Kalbitz, K., Kramer, C., Leinweber, P., Rethemeyer, J., Schäffer, A., Schmidt, M. W. I., Schwark, L. and Wiesenberg, G. L. B.: How relevant is recalcitrance for the stabilization of organic matter in soils?, *J. Plant Nutr. Soil Sci.*, 171(1), 91–110, doi:10.1002/jpln.200700049, 2008.

McDowell, N. G., Allen, C. D., Anderson-Teixeira, K., Aukema, B. H., Bond-Lamberty, B., Chini, L., Clark, J. S., Dietze, M., Grossiord, C., Hanbury-Brown, A., Hurtt, G. C., Jackson, R. B., Johnson, D. J., Kueppers, L., Lichstein, J. W., Ogle, K., Poulter, B., Pugh, T. A. M., Seidl, R., Turner, M. G., Uriarte, M., Walker, A. P. and Xu, C.: Pervasive shifts in forest dynamics in a changing world, *Science*, 368(6494), doi:10.1126/science.aaz9463, 2020.

Michalzik, B., Kalbitz, K., Park, J.-H., Solinger, S. and Matzner, E.: Fluxes and concentrations of dissolved organic carbon and nitrogen—a synthesis for temperate forests, *Biogeochemistry*, 52(2), 173–205, 2001.

Mikutta, R., Kleber, M., Torn, M. S. and Jahn, R.: Stabilization of soil organic matter: Association with minerals or chemical recalcitrance?, *Biogeochemistry*, 77(1), 25–56, doi:10.1007/s10533-005-0712-6, 2006.

Mikutta, R., Mikutta, C., Kalbitz, K., Scheel, T., Kaiser, K. and Jahn, R.: Biodegradation of forest floor organic matter bound to minerals via different binding mechanisms, *Geochim. Cosmochim. Acta*, 71(10), 2569–2590, doi:10.1016/j.gca.2007.03.002, 2007.

Mikutta, R., Turner, S., Schippers, A., Gentsch, N., Meyer-Stüve, S., Condon, L. M., Peltzer, D. A., Richardson, S. J., Eger, A., Hempel, G., Kaiser, K., Klotzbücher, T. and Guggenberger, G.: Microbial and abiotic controls on mineral-associated organic matter in soil profiles along an ecosystem gradient, *Sci. Rep.*, 9(1), 1–9, doi:10.1038/s41598-019-46501-4, 2019.

Nave, L. E., Domke, G. M., Hofmeister, K. L., Mishra, U., Perry, C. H., Walters, B. F. and Swanston, C. W.: Reforestation can sequester two petagrams of carbon in US topsoils in a century, *Proc. Natl. Acad. Sci.*, 115(11), 2776–2781, doi:10.1073/pnas.1719685115, 2018.

Pan, Y., Birdsey, R. A., Fang, J., Houghton, R., Kauppi, P. E., Kurz, W. A., Phillips, O. L., Shvidenko, A., Lewis, S. L., Canadell, J. G., Ciais, P., Jackson, R. B., Pacala, S. W., McGuire, A. D., Piao, S., Rautiainen, A., Sitch, S. and Hayes, D.: A Large and persistent carbon sink in the world's forests, *Science*, 333(6045), 988–993, doi:10.1126/science.1201609, 2011.

Paustian, K., Lehmann, J., Ogle, S., Reay, D., Robertson, G. P. and Smith, P.: Climate-smart soils, *Nature*, 532(7597), 49–57, doi:10.1038/nature17174, 2016.

Phillips, R. P., Meier, I. C., Bernhardt, E. S., Grandy, A. S., Wickings, K. and Finzi, A. C.: Roots and fungi accelerate carbon and nitrogen cycling in forests exposed to elevated CO<sub>2</sub>, *Ecol. Lett.*, 15(9), 1042–1049, doi:10.1111/j.1461-0248.2012.01827.x, 2012.

Poeplau, C. and Don, A.: Carbon sequestration in agricultural soils via cultivation of cover crops – A

meta-analysis, *Agric. Ecosyst. Environ.*, 200, 33–41, doi:10.1016/j.agee.2014.10.024, 2015.

Rasse, D. P., Rumpel, C. and Dignac, M.-F.: Is soil carbon mostly root carbon? Mechanisms for a specific stabilisation, *Plant Soil*, 269(1–2), 341–356, doi:10.1007/s11104-004-0907-y, 2005.

Robertson, A. D., Paustian, K., Ogle, S., Wallenstein, M. D., Lugato, E. and Cotrufo, M. F.: Unifying soil organic matter formation and persistence frameworks: the MEMS model, *Biogeosciences*, 16(6), 1225–1248, doi:https://doi.org/10.5194/bg-16-1225-2019, 2019.

Roth, V.-N., Lange, M., Simon, C., Hertkorn, N., Bucher, S., Goodall, T., Griffiths, R. I., Mellado-Vázquez, P. G., Mommer, L., Oram, N. J., Weigelt, A., Dittmar, T. and Gleixner, G.: Persistence of dissolved organic matter explained by molecular changes during its passage through soil, *Nat. Geosci.*, 12(9), 755–761, doi:10.1038/s41561-019-0417-4, 2019.

Rothstein, D. E., Toosi, E. R., Schaetzl, R. J. and Grandy, A. S.: Translocation of carbon from surface organic horizons to the subsoil in coarse-textured Spodosols: Implications for deep soil C dynamics, *Soil Sci. Soc. Am. J.*, 82(4), 969–982, doi:10.2136/sssaj2018.01.0033, 2018.

Rumpel, C. and Kögel-Knabner, I.: Deep soil organic matter—a key but poorly understood component of terrestrial C cycle, *Plant Soil*, 338(1–2), 143–158, doi:10.1007/s11104-010-0391-5, 2011.

Rumpel, C., Chabbi, A. and Marschner, B.: Carbon storage and sequestration in subsoil horizons: Knowledge, gaps and potentials, in *recarbonization of the biosphere*, edited by R. Lal, K. Lorenz, R. F. Hüttl, B. U. Schneider, and J. von Braun, pp. 445–464, Springer Netherlands, Dordrecht. [online] Available from: [http://www.springerlink.com/index/10.1007/978-94-007-4159-1\\_20](http://www.springerlink.com/index/10.1007/978-94-007-4159-1_20) (Accessed 10 January 2018), 2012.

Saidy, A. R., Smernik, R. J., Baldock, J. A., Kaiser, K. and Sanderman, J.: The sorption of organic carbon onto differing clay minerals in the presence and absence of hydrous iron oxide, *Geoderma*, 209–210, 15–21, doi:10.1016/j.geoderma.2013.05.026, 2013.

Salomé, C., Nunan, N., Pouteau, V., Lerch, T. Z. and Chenu, C.: Carbon dynamics in topsoil and in subsoil may be controlled by different regulatory mechanisms, *Glob. Change Biol.*, 16(1), 416–426, doi:10.1111/j.1365-2486.2009.01884.x, 2010.

Schils, R., Kuikman, P., Liski, J., Van Oijen, M., Smith, P., Webb, J., Alm, J., Somogyi, Z., Van den Akker, J., Billett, M., Emmett, B., Evans, C., Lindner, M., Palosuo, T., Bellamy, P., Jandl, R. and Hiederer, R.: Review of existing information on the interrelations between soil and climate change. (ClimSoil). Final report, Publication - Report. [online] Available from: [http://ec.europa.eu/environment/soil/review\\_en.htm](http://ec.europa.eu/environment/soil/review_en.htm) (Accessed 17 August 2020), 2008.

Schimel, D. S.: Terrestrial ecosystems and the carbon cycle, *Glob. Change Biol.*, 1(1), 77–91, doi:10.1111/j.1365-2486.1995.tb00008.x, 1995.

Schmidt, M. W. I., Torn, M. S., Abiven, S., Dittmar, T., Guggenberger, G., Janssens, I. A., Kleber, M., Kögel-Knabner, I., Lehmann, J., Manning, D. A. C., Nannipieri, P., Rasse, D. P., Weiner, S. and Trumbore, S. E.: Persistence of soil organic matter as an ecosystem property, *Nature*, 478(7367), 49, doi:10.1038/nature10386, 2011.

Schöning, I. and Kögel-Knabner, I.: Chemical composition of young and old carbon pools throughout Cambisol and Luvisol profiles under forests, *Soil Biol. Biochem.*, 38(8), 2411–2424, doi:10.1016/j.soilbio.2006.03.005, 2006.

Schrumpf, M., Kaiser, K., Guggenberger, G., Persson, T., Kögel-Knabner, I. and Schulze, E.-D.: Storage

and stability of organic carbon in soils as related to depth, occlusion within aggregates, and attachment to minerals, *Biogeosciences*, 10(3), 1675–1691, doi:<https://doi.org/10.5194/bg-10-1675-2013>, 2013.

Simo, I., Schulte, R., O’Sullivan, L. and Creamer, R.: Digging deeper: Understanding the contribution of subsoil carbon for climate mitigation, a case study of Ireland, *Environ. Sci. Policy*, 98, 61–69, <https://doi.org/10.1016/j.envsci.2019.05.004>, 2019.

Sokol, N. W., Sanderman, J. and Bradford, M. A.: Pathways of mineral-associated soil organic matter formation: Integrating the role of plant carbon source, chemistry, and point of entry, *Glob. Change Biol.*, 25(1), 12–24, doi:10.1111/gcb.14482, 2019.

Sulzman, E. W., Brant, J. B., Bowden, R. D. and Lajtha, K.: Contribution of aboveground litter, belowground litter, and rhizosphere respiration to total soil CO<sub>2</sub> efflux in an old growth coniferous forest, *Biogeochemistry*, 73(1), 231–256, doi:10.1007/s10533-004-7314-6, 2005.

Tipping, E., Chamberlain, P. M., Fröberg, M., Hanson, P. J. and Jardine, P. M.: Simulation of carbon cycling, including dissolved organic carbon transport, in forest soil locally enriched with <sup>14</sup>C, *Biogeochemistry*, 108(1–3), 91–107, doi:10.1007/s10533-011-9575-1, 2012.

Wagai, R., Mayer, L. M. and Kitayama, K.: Nature of the “occluded” low-density fraction in soil organic matter studies: A critical review, *Soil Sci. Plant Nutr.*, 55(1), 13–25, doi:10.1111/j.1747-0765.2008.00356.x, 2009.

Wander, M.: Soil organic matter fractions and their relevance to soil functions, in *Soil organic matter in sustainable agriculture*, p. 412, CRC Press., 2004.

Watson, J. E. M., Evans, T., Venter, O., Williams, B., Tulloch, A., Stewart, C., Thompson, I., Ray, J. C., Murray, K., Salazar, A., McAlpine, C., Potapov, P., Walston, J., Robinson, J. G., Painter, M., Wilkie, D., Filardi, C., Laurance, W. F., Houghton, R. A., Maxwell, S., Grantham, H., Samper, C., Wang, S., Laestadius, L., Runting, R. K., Silva-Chávez, G. A., Ervin, J. and Lindenmayer, D.: The exceptional value of intact forest ecosystems, *Nat. Ecol. Evol.*, 2(4), 599–610, doi:10.1038/s41559-018-0490-x, 2018.

Wiesmeier, M., Hübner, R., Spörlein, P., Geuß, U., Hangen, E., Reischl, A., Schilling, B., Lützow, M. von and Kögel-Knabner, I.: Carbon sequestration potential of soils in southeast Germany derived from stable soil organic carbon saturation, *Glob. Change Biol.*, 20(2), 653–665, doi:10.1111/gcb.12384, 2014.

Wilkinson, M. T., Richards, P. J. and Humphreys, G. S.: Breaking ground: Pedological, geological, and ecological implications of soil bioturbation, *Earth-Sci. Rev.*, 97(1), 257–272, doi:10.1016/j.earscirev.2009.09.005, 2009.

Zsolnay, A., Baigar, E., Jimenez, M., Steinweg, B. and Saccomandi, F.: Differentiating with fluorescence spectroscopy the sources of dissolved organic matter in soils subjected to drying, *Chemosphere*, 38(1), 45–50, doi:10.1016/S0045-6535(98)00166-0, 1999.

## 2. Study I

### Relevance of aboveground litter for soil organic matter formation – a soil profile perspective

**Contribution:** I was equally involved in the field sampling campaigns, conducted most of the analysis in the laboratory, collected and evaluated the data, compiled the tables and figures, and wrote the manuscript.

**Published in:** *Biogeosciences* 17, 3099-3113, 2020.  
**Paper:** [doi.org/10.5194/bg-17-3099-2020](https://doi.org/10.5194/bg-17-3099-2020)  
**Data repository:** [doi.org/10.20387/bonares-HZGX-GB9S](https://doi.org/10.20387/bonares-HZGX-GB9S) |Site parameter Grinderwald  
[doi.org/10.20387/bonares-69H2-56Q9](https://doi.org/10.20387/bonares-69H2-56Q9) |Bulk data  
[doi.org/10.20387/bonares-DNDW-5T58](https://doi.org/10.20387/bonares-DNDW-5T58) |Fractions data



# **Relevance of aboveground litter for soil organic matter formation – a soil profile perspective**

Patrick Liebmann<sup>1</sup>, Patrick Wordell-Dietrich<sup>2</sup>, Karsten Kalbitz<sup>2</sup>, Robert Mikutta<sup>3</sup>, Fabian Kalks<sup>4</sup>, Axel Don<sup>4</sup>, Susanne K. Woche<sup>1</sup>, Leena R. Dsilva<sup>2</sup>, Georg Guggenberger<sup>1</sup>

<sup>1</sup>Institute of Soil Science, Leibniz Universität Hannover, Herrenhäuser Str. 2, 30419, Hannover, Germany

<sup>2</sup>Institute of Soil Science and Site Ecology, Technische Universität Dresden, Piener Straße 19, 01737 Tharandt, Germany

<sup>3</sup>Soil Science and Soil Protection, Martin Luther University Halle-Wittenberg, Von-Seckendorff-Platz 3, 06210 Halle (Saale), Germany

<sup>4</sup>Thünen Institute of Climate-Smart Agriculture, Bundesallee 65, 38116 Braunschweig, Germany

*Correspondence to:* Patrick Liebmann (liebmann@ifbk.uni-hannover.de)

Received: 27 November 2019 – Discussion started: 2 January 2020

Revised: 17 March 2020 – Accepted: 29 April 2020 – Published: 18 June 2020

**Abstract.** In contrast to mineral topsoils, in subsoils the origin and processes leading to the formation and stabilization of organic matter (OM) are still not well known. This study addresses the fate of litter-derived carbon (C) in whole soil profiles with regard to the conceptual cascade model, which proposes that OM formation in subsoils is linked to sorption-microbial processing-remobilization cycles during the downward migration of dissolved organic carbon (DOC). Our main objectives were to quantify the contribution of recent litter to subsoil C stocks via DOC translocation and to evaluate the stability of litter-derived OM in different functional OM fractions.

A plot-scale stable isotope-labeling experiment was conducted in a temperate beech forest by replacing the natural litter layer with  $^{13}\text{C}$  enriched litter on an area of 20 m<sup>2</sup> above a Dystric Cambisol. After 22 months of field exposure, the labeled litter was replaced again by natural litter and soil cores were drilled down to 180 cm soil depth. Water extraction and density fractionation were combined with stable isotope measurements in order to link the fluxes of recent litter-derived C to its allocation into different functional OM fractions. A second sampling was conducted 18 months later to further account for the stability of translocated young litter-derived C.

Almost no litter-derived particulate OM (POM) entered the subsoil, suggesting root biomass as the major source of subsoil POM. The contribution of aboveground litter to the formation of mineral-associated OM (MAOM) in topsoils (0-10 cm) was  $1.88 \pm 0.83 \text{ g C m}^{-2}$  and decreased to  $0.69 \pm 0.19 \text{ g C m}^{-2}$  in the upper subsoil (10-50 cm) and  $0.01 \pm 0.02 \text{ g C m}^{-2}$  in the deep subsoil > 100 cm soil depth during the 22 months. This finding suggests a subordinate importance of recent litter layer inputs via DOC translocation to subsoil C stocks, and implies that most of the OM in the subsoil is of older age. Smaller losses of litter-derived C within MAOM of about 66 % compared to POM (77–89 %) over 18 months indicate that recent carbon can be stabilized by interaction with mineral surfaces; although the overall stabilization in the sandy study soils is limited. Our isotope-labeling approach supports the concept of OM undergoing a sequence of cycles of sorption, microbial processing, and desorption while migrating down a soil profile, which needs to be considered in models of soil OM formation and subsoil C cycling.

## 1 Introduction

The capability of soils to incorporate and preserve large quantities of organic matter (OM) is a key function in the global carbon (C) cycle (Wiesmeier et al., 2019). While in the past most studies on carbon inventories focused on topsoils, only some of the recent research also expands to subsoil environments (Fontaine et al., 2007; Salomé et al., 2010; Bernal et al., 2016), considering that a significant proportion of soil OM (SOM) is stored in subsoil horizons (Batjes, 1996; Jobbagy and Jackson, 2000). In forest ecosystems, major pathways of OM to enter subsoils are rhizodeposition, root exudation and dissolved organic matter (DOM) leached from the horizons above (Wilkinson et al., 2009; Rumpel and Kögel-Knabner, 2011; Kaiser and Kalbitz, 2012). Dissolved organic matter was estimated to contribute about 19 to 50 % to the total mineral soil C stock in forest soils (Kalbitz and Kaiser, 2008; Sanderman and Amundson, 2008) and is considered a main source of subsoil OM in temperate forest soils (Kaiser and Guggenberger, 2000), next to belowground inputs (Nadelhoffer and Raich, 1992; Majdi, 2001). Further, its high affinity towards reactive mineral phases, thus forming mineral-associated OM (MAOM) makes DOM an important contributor to stabilized SOM (Scheel et al., 2007; Leinemann et al., 2016).

Kaiser and Kalbitz (2012) described the interaction of OM with minerals as a sequence of processes including DOM sorption, microbial processing, and desorption, often referred to as the “cascade model”. This model not only accounts for changes in dissolved organic carbon (DOC) concentration and bioavailability with depth but also considers the depth-dependent changes in the  $^{14}\text{C}$  age of SOM (Trumbore et al., 1992) and in DOM and SOM composition from plant-derived towards microbial-derived OM, as was found in e.g., forest soils (Guggenberger and Zech, 1994; Kaiser et al., 2004). The cascade model also points at a microbial impact on exchange reactions of OM at mineral surfaces, which has been recently confirmed in a laboratory percolation experiment (Leinemann et al., 2018). Modern  $^{14}\text{C}$  ages of MAOM in mineral topsoil horizons, where most sorption sites are likely already occupied, also suggest such exchange of OM (Angst et al., 2018). Increasing OM degradation and transformation with soil depth often result in changes in the stable isotopic composition of SOM. In most soils,  $\delta^{13}\text{C}$  values increase with soil depth, which is related to the isotopic discrimination of the heavier C isotopes during microbial respiration (Nadelhoffer and Fry, 1988; Balesdent et al., 1993; van Dam et al., 1997) or a shift in the fungal to bacterial ratio in favor of the more  $^{13}\text{C}$ -enriched bacteria (Kohl et al., 2015). This depth trend can also reflect a translocation of relatively  $\delta^{13}\text{C}$ -enriched OM to greater depth due to preferential sorption of the  $\delta^{13}\text{C}$ -depleted carboxylated lignin degradation products via multiple sorption-decomposition-desorption steps (Kaiser et al., 2001). On the other hand, Rumpel et al. (2012) questioned the slow turnover of subsoil OM, since DOC and root exudate fluxes can substantially increase the subsoil C pool within decades, a view which is in contrast to the frequently high  $^{14}\text{C}$  ages of subsoil OM.

While the qualitative aspects of subsoil C cycling with respect to possible OM sources and processes are known, e.g., as summarized by Schmidt et al. (2011) and Rumpel et al. (2012), this does not refer to the controlling mechanisms and the turnover of the different subsoil C fractions. Assessment of OM turnover in the subsoil under real conditions still remains a major challenge, as it has to involve analysis of the different C sources (plant-derived versus microbial-derived) and the quantification of respective inputs and outputs. In order to quantify individual C fractions and fluxes, isotope labeling, e.g. using  $^{13}\text{C}$ - or  $^{14}\text{C}$ -enriched litter material, has been proven to be a very powerful tool (Bird et al., 2008; Moore-Kucera and Dick, 2008; Kramer et al., 2010). Extensive retention of DOC in topsoil horizons has been documented for field-exposed mesocosms (Fröberg et al. 2009) or in field approaches (Kammer et al. 2012). Yet, to the best of our knowledge, there are no field studies available that employed stable isotope tracing to estimate the contribution of recent aboveground litter to subsoil C cycling. Additionally, the role of recent litter-derived DOM in the formation of MAOM in the soil profile has not been quantified so far, nor has the biological stability of this newly incorporated OM been determined.

This study therefore addresses the fate of litter-derived C in the subsoil with regard to the conceptual cascade model (Kaiser and Kalbitz, 2012) under field conditions. Specifically, we aim to answer the following questions.

1. Does recent aboveground litter significantly contribute to the accumulation of OM in subsoils?
2. Is OM transferred into the subsoil directly via the DOM pathway or is subsoil OM the result of repeated sorption-microbial processing-desorption cycles?
3. To what extent is recent aboveground litter-derived C sorbed to soil minerals and does this fraction represent a source of stable SOM?

To quantify the contribution of recent litter to subsoil C stocks via DOM movement and evaluate the stability of litter-derived SOM, we carried out a  $^{13}\text{C}$ -labeling experiment, where the natural litter layer on a Dystric Cambisol underneath European beech was replaced by a  $^{13}\text{C}$ -enriched leaf litter. The contribution of litter to subsoil OM was assessed by  $\delta^{13}\text{C}$  analysis in soil cores down to 180 cm soil depth sampled 22 and 40 months after field labeling. The labeled litter was changed back to unlabeled litter before sampling of the first cores, allowing an indication of exchange processes of labeled C in the soil in the subsequent 18 months. Soil density fractionation was used to assess the contribution of young DOM to the formation of MAOM and to differentiate between particulate and dissolved pathways in the contribution of litter-derived C to subsoil OM.

## 2 Materials and methods

### 2.1 Site description

The field experiment was carried out in the Grunderwald beech forest (*Fagus sylvatica*), 40 km north of Hanover, Germany (52°34'22'' N, 9°18'49'' E), comprising a stand age of 103 years. The common soil type in the research area is a Dystric Cambisol (IUSS Working Group WRB, 2014), which developed from periglacial fluvial sandy deposits. The mean annual temperature is 9.7°C, and the mean annual precipitation is 762 mm (Deutscher Wetterdienst, Nienburg, 1981-2010). Selected soil properties of the Grunderwald sites are given in Table 1. More detailed site descriptions can be found in Angst et al. (2016) and Bachmann et al. (2016).

**Table 1** Selected soil properties given as the mean of all three sites (n = 3) and standard deviation in brackets (data adapted from Leinemann et al. (2016)).

Horizon WRB <sup>1</sup> / KA5 <sup>2</sup>	Depth [cm]	OC <sup>3</sup> [mg g <sup>-1</sup> ]	TN <sup>4</sup> [mg g <sup>-1</sup> ]	pH [CaCl <sub>2</sub> ]	Clay -----	Silt [mg g <sup>-1</sup> ]	Sand -----
AE/Ahe	0-10	15.18 (1.72)	0.59 (0.06)	3.2 (0.2)	19 (3)	282 (56)	699 (57)
Bsw/Bsv	10-23	9.59 (2.52)	0.41 (0.09)	3.5 (0.4)	27 (11)	307 (81)	666 (90)
Bw/Bv	23-67	4.65 (1.96)	0.26 (0.04)	3.9 (0.1)	26 (4)	332 (99)	642 (103)
C/Cv	67-99	1.07 (0.46)	0.08 (0.02)	3.9 (0.2)	29 (8)	255 (41)	716 (47)
2C/IICv	99-138	0.34 (0.11)	0.07 (0.09)	4.1 (0.1)	21 (14)	87 (55)	891 (66)
3C/IIICv	138-175	1.05 (0.11)	0.10 (0.11)	4.0 (0.3)	32 (44)	268 (422)	700 (466)
4C/IVCv	175+	0.29 (0.14)	0.03 (0.04)	3.9 (0.2)	19 (6)	58 (8)	923 (14)

<sup>1</sup> according to IUSS Working Group WRB (2014)

<sup>2</sup> according to German soil classification (Ad-hoc-Arbeitsgruppe Boden, 2005)

<sup>3</sup> Organic carbon (OC)

<sup>4</sup> Total nitrogen (TN)

### 2.2 Experimental setup

The study site Grindewald includes three soil observatories on which  $^{13}\text{C}$ -labeled beech litter was applied (Leinemann et al., 2016; Wordell-Dietrich et al., 2019); hereafter referred to as plots 1 to 3. Each plot was divided in two compartments of  $6.57\text{ m}^2$  each. One compartment was labeled with  $^{13}\text{C}$ -enriched litter and the other remained unlabeled as a control. The experiment started in January 2015. For the labeling, the natural litter layer was removed manually and replaced by an equivalent amount of  $275\text{ g }^{13}\text{C}$ -enriched beech litter per square meter representing a typical input of beech litter in Germany (Meier et al., 2005). Labeled litter was prepared as a mixture of highly labeled beech litter (10 atom-% uniformly labeled due to growth under  $^{13}\text{CO}_2$ -enriched atmosphere in a greenhouse, IsoLife, Wageningen, the Netherlands) and beech litter, which resulted in a final  $^{13}\text{C}$ -enrichment of 1241 to 1880 ‰ (Wordell-Dietrich et al., 2019). A net (2 cm mesh size) was installed on top of the litter layer to, first, prevent surface translocation by wind, and, second, avoid dilution of the labeled litter over time by the seasonally fallen litter. The labeled litter stayed in the field for 22 months. In November 2016, the labeled litter was removed manually and amounted to an average of about  $405\text{ g m}^{-2}$  per plot. We thus removed more litter than we initially applied due to incorporation of small leaf debris and beechnut shells during the 22 months. About 25 % of the removed litter were residues of the applied labeled litter. A total of about 36-40 % of the initially applied labeled litter C left as  $\text{CO}_2$  (Wordell-Dietrich, unpublished).

Following the removal of the labeled litter, three soil cores per plot and treatment (labeled versus unlabeled) were taken down to a depth of 200 cm using a machine-driven percussion coring system (Nordmeyer Geotool, Berlin, Germany). Since it was not possible for each soil core to secure the lowest increment of 180-200 cm, this depth was rejected from further processing. The cores were divided into 15 increments, starting with 5 cm increments from 0 to 10 cm, 10 cm increments from 10 to 100 cm, and 20 cm increments from 100 to 180 cm. Depth increments of the soil cores taken from 0 to 5 and 5 to 10 cm are defined as “topsoil”, increments between 10 and 50 cm are defined as “upper subsoil”, those between 50 to 100 cm are defined as “mid subsoil”, and increments below 100 cm are defined as “deep subsoil”. Directly after sampling, an equivalent amount of the natural beech litter of the surrounding area was used for the replacement of the litter that was removed before. A second sampling was conducted 18 months later, in May 2018, in total 40 months after applying the labeled litter on the plots.

Soil samples were oven-dried at  $60^\circ\text{C}$  and sieved to  $< 2\text{ mm}$ . Three replicates per plot and treatment were combined to one composite sample per depth increment on a mass equivalent basis for further processing. Aliquots for water extractions were stored frozen ( $-20^\circ\text{C}$ ) directly after sampling.

### 2.3 Analysis of bulk soil

Bulk samples were analyzed for organic C (OC), total nitrogen (TN) and  $^{13}\text{C}/^{12}\text{C}$  ratio, using a vario ISOPRIME cube (Elementar Analysesysteme GmbH, Hanau, Germany) elemental analyzer coupled to an IsoPrime100 (IsoPrime Ltd, Cheadle Hulme, UK) stable isotope ratio mass spectrometer (EA-IRMS). Carbon isotope values are given in delta notation relative to the Vienna Pee Dee Belemnite standard (VPDB; Hut, 1987). Data were corrected with a variety of standards from the International Atomic Energy Agency (IAEA) and in-house standards (Supplement, Table S1). Pedogenic Fe and Al fractions were analyzed by selective extractions. Oxalate extractions were conducted according to McKeague and Day (1966) by using 0.2 M ammonium oxalate (pH 3) to dissolve poorly crystalline aluminosilicates and Fe hydroxides like ferrihydrite as well as Fe and Al from organic complexes ( $\text{Fe}_o$ ,  $\text{Al}_o$ ). Iron present in organic complexes, poorly crystalline and crystalline Fe oxides ( $\text{Fe}_d$ ) was analyzed by extraction in dithionite-citrate following the method created by Mehra and Jackson (1960) and modified by Sheldrick and McKeague (1975). All extraction solutions were analyzed for dissolved Fe and Al by inductively coupled plasma optical emission spectroscopy (ICP-OES; Varian 725-ES, Palo Alto, California, USA).

Water-extractable OM (WEOM) was used as surrogate of DOM migrating in the soil profile (Corvasce et al., 2006). Prior to the extraction, the frozen samples were thawed for 24 hours at 4°C and thereafter sieved to < 2 mm. Following the procedure of Chantigny et al. (2007), 25 g of fresh, field-moist soil was extracted with 1 mM  $\text{CaCl}_2$  solution at a soil/solution ratio of 1/3. Samples were shaken horizontally for 1 h at a frequency of 3 s<sup>-1</sup> at 4°C. After centrifugation for 30 min at 3,500 g at 4°C, extracts were filtered through 0.45- $\mu\text{m}$  cellulose-nitrate membranes (Sartorius Stedim Biotech GmbH, Göttingen, Germany). Prior to the filtration, filters were pre-rinsed with 250 mL of the 1 mM  $\text{CaCl}_2$  solution. Organic carbon concentrations in the extracts ( $C_{\text{WEOM}}$ ) were measured by high-temperature combustion with a varioTOC elemental analyzer (Elementar, Hanau, Germany). The  $\delta^{13}\text{C}$  values of WEOM were measured with an isoTOC cube coupled to an IRMS vision (Elementar, Hanau, Germany; Leinemann et al., 2018). The ultraviolet (UV) absorbance at 280 nm of WEOC was measured with the Specord 200 UV-VIS spectrometer (Analytic Jena AG, Jena, Germany). Specific ultra violet absorbance at 280 nm (SUVA) was calculated according to Chin et al. (1994) as the ratio of UV absorbance at 280 nm and DOC concentration. Prior to fluorescence measurements, samples, if necessary, were diluted to absorbance values < 0.1 at 280 nm. Thereafter emission spectra from 300 nm to 500 nm were measured at an excitation wavelength of 254 nm (Zsolnay et al., 1999) at a Perkin Elmer LS 50 luminescence spectrometer (Perkin Elmer, Waltham, MA, USA). For all measurements the scan rate was 100 nm min<sup>-1</sup> and the ex-slit/em-slit was 15/10. The stability of the instrument was checked with the Raman peak of deionized water at 350 nm. The fluorescence emission index (HIX) was calculated as the ratio of the area

between 435 and 480 nm and the area between 300 and 345 nm of the emission spectrum (Zsolnay et al., 1999) using FL Winlab Software.

### 2.4 Density fractionation

Samples for density fractionation were selected in order to represent the topsoil (0-5, 5-10 cm), the upper subsoil (10-20, 20-30, 30-40, 40-50 cm), and the deeper subsoil (100-120, 120-140 cm). Density fractionation was conducted according to Golchin et al. (1994a, 1994b), with the following adjustments based on pretests. Aliquots of  $25 \pm 0.05$  g bulk soil were separated into two light fractions (LF), free and occluded particulate OM (fPOM and oPOM), and one heavy fraction (HF) containing MAOM. After adding 125 mL sodium polytungstate (SPT) solution (SPT 0, TC-Tungsten Compounds, Grub am Forst, Germany) with a density of  $1.6 \text{ g cm}^{-3}$  (Kaiser and Guggenberger, 2007; Cerli et al., 2012), the suspensions were manually stirred and allowed to rest for 1 h. Afterwards, the samples were centrifuged at  $4,000 \text{ g}$  and  $17^\circ\text{C}$  for 30 min (Cryofuge 6000, Heraeus Holding GmbH, Hanau, Germany) and the supernatant, containing fPOM material, was filtered through  $0.45\text{-}\mu\text{m}$  polyethersulfone filters (PALL Life Sciences, Ann Arbor, Michigan, USA). The fractionation of the fPOM was repeated once. In a second step, aggregates were destroyed to release oPOM by ultrasonic treatment (Sonopuls HD2200, Bandelin electronic GmbH & Co KG, Berlin, Germany) with an energy input of  $60 \text{ J mL}^{-1}$  (Gentsch et al., 2015; Schiedung et al., 2016). Prior to the treatment, ultrasonic power of the sonotrode was assessed calorimetrically and ultrasound durations were calculated according to North (1976). After centrifugation at  $6,000 \text{ g}$  for 30 min, the supernatant with oPOM material was filtered as well. Both fPOM and oPOM were washed with ultrapure water ( $18.2 \text{ M}\Omega$ ) until the electrical conductivity of the eluate was  $< 5 \mu\text{S cm}^{-1}$  (Angst et al., 2016). The HF was washed three to four times with 200 mL ultrapure water until the conductivity was  $< 50 \mu\text{S cm}^{-1}$ . The water used for washing the HF was collected and measured for dissolved OC ( $C_w$ ). We also measured dissolved OC in all posttreatment SPT solutions. This SPT-mobilized C ( $C_{\text{SPT}}$ ) was taken to represent mobilizable and potentially labile soil OC (Gentsch et al., 2018), derived from POM and MAOM. The dissolved OC concentrations were measured within 2 d after the fractionation by high-temperature combustion with a limit of quantification of  $1 \text{ mg C L}^{-1}$  (Leinemann et al., 2016), using a vario TOC cube (Elementar, Hanau, Germany). Aliquots of both liquid phases were freeze-dried similar to the soil fractions for analysis of OC, TN, and  $^{13}\text{C}/^{12}\text{C}$  ratios by EA-IRMS. Due to negligible amounts of POM material in the deeper subsoil samples (100-140 cm), fPOM and oPOM were no longer differentiated. The mean mass recovery in fPOM, oPOM, and HF after fractionation was  $99.1 \pm 0.9 \%$ . The mean C recovery after fractionation was  $98.3 \pm 26.5 \%$ , including data for the mobilized  $C_w$  and  $C_{\text{SPT}}$ . On average,  $2.0 \pm 2.2 \%$  of the C was mobilized by the fractionation procedure. Nitrate and ammonium were extracted from bulk and HF samples to analyze inorganic N contents ( $N_{\text{min}}$ ). Extraction



was carried out according to Blume et al. (2010) by mixing  $4 \pm 0.01$  g soil with 16 mL 0.0125 M CaCl<sub>2</sub> solution and shaking the mixture for 1 h on an overhead shaker. After sedimentation, the supernatant was filtered through 0.45- $\mu$ m cellulose acetate filters (BerryTec GmbH, Grünwald, Germany) and measured by a segmented flow analyzer (San++ analyzer, Breda, the Netherlands) with a limit of quantification of 0.1 mg N L<sup>-1</sup>. Organic N contents were calculated by subtraction of N<sub>min</sub> from TN. Surfaces of the HF were further investigated by X-ray photoelectron spectroscopy (XPS) with respect to the elemental composition as a function of soil depth. Method description and data are presented in the Supplement.

## 2.5 Calculations and statistics

Soil OC stocks (kg m<sup>-2</sup>) were calculated according to Eq. (1):

$$\text{OC stock} = \text{OC} \times \text{density} \times \text{increment thickness} \times 0.01, \quad (1)$$

with the OC content (mg g<sup>-1</sup>) and bulk density of the fine earth fraction (g cm<sup>-3</sup>) of each soil increment multiplied by the increment thickness (cm). The proportion of each SOM fraction (OC<sub>frac</sub>, in %) in percent of the total recovered OC was calculated based on the sum of all fractions ( $\Sigma$ OC):

$$\text{OC}_{\text{frac}} = \frac{\text{OC}_{\text{frac}}}{\Sigma \text{OC} (C_{\text{IPOM}}, C_{\text{oPOM}}, C_{\text{MAOM}}, C_{\text{SPT}})} \times 100 \%. \quad (2)$$

Water-extractable OC (C<sub>WEOM</sub>) was calculated as the percentage proportion relative to OC in the respective bulk soil sample, according to Eq. (3):

$$C_{\text{WEOM}} = \frac{\text{OC}_{\text{extracted}}}{\text{Bulk OC}} \times 100 \%. \quad (3)$$

As mentioned earlier, all soil fractions released C to the C<sub>SPT</sub> pool, whereas the C<sub>w</sub> fraction solely originated from the MAOM in the HF fraction. Thus, the C<sub>w</sub> fraction was added to the MAOM. Further, the  $\delta^{13}\text{C}$  values of the MAOM (C<sub>MAOM</sub>, in ‰) were corrected for the  $\delta^{13}\text{C}$  values of C<sub>w</sub> by using Eq. (4):

$$\delta^{13}\text{C}_{\text{MAOM}} = \frac{M_{\text{MAOM}} \times \delta^{13}\text{C}_{\text{MAOM}} + M_{\text{Cw}} \times \delta^{13}\text{C}_{\text{w}}}{M_{\text{MAOM}} + M_{\text{Cw}}}, \quad (4)$$

with M<sub>MAOM</sub> as the C mass (mg) of the HF fraction, M<sub>Cw</sub> as the C mass (mg) in the total washing solution, and the  $\delta^{13}\text{C}$  values (‰) of both fractions ( $\delta^{13}\text{C}_{\text{MAOM}}$  and  $\delta^{13}\text{C}_{\text{w}}$ , respectively).

The <sup>13</sup>C-labeled samples were used to calculate the proportion of native SOC (SOC<sub>nat</sub>, in %) and label-derived SOC (SOC<sub>L</sub>, in %) by Eq. (5) and Eq. (6):

$$\text{SOC}_{\text{nat}} = \frac{{}^{13}\text{C}_{\text{L}} - {}^{13}\text{C}_{\text{in}}}{{}^{13}\text{C}_{\text{uL}} - {}^{13}\text{C}_{\text{in}}} \times 100 \%, \quad (5)$$

$$\text{SOC}_L = 100 - \text{SOC}_{\text{nat}}, \quad (6)$$

with  $^{13}\text{C}_L$  as the  $\delta^{13}\text{C}$  value of the labeled sample,  $^{13}\text{C}_{\text{uL}}$  as the  $\delta^{13}\text{C}$  value of the unlabeled control in the same soil depth, and  $^{13}\text{C}_{\text{in}}$  as the  $\delta^{13}\text{C}$  value of the initial labeled litter.

The recovered label-derived SOC was further quantified by calculating the SOC stocks in each respective depth, further calculating the proportion of label-derived SOC, and finally relating the label-derived SOC to the amount of the labeled C in the litter input. The total recovered label was calculated as the sum of the label recovered in all OM fractions and respective soil depth increments and given in g C m<sup>-2</sup>. The potential loss over time was calculated as the relative decrease in recovered label in the 18-month interval between both sampling times.

If not stated differently, data are given as the mean of the three replicates  $\pm$  the standard deviation (SD). Depths refer to the mean depth per depth increment.  $\delta^{13}\text{C}$  values (‰) of the labeled samples and fractions ( $^{13}\text{C}_L$ ) were tested for significant enrichments compared to the natural variations in the control with the upper 90 % quantile limit of the frequency distribution (Nielsen and Wendroth, 2003), using Eq. (7):

$$^{13}\text{C}_L > \bar{X}_{\text{uL}} + (\text{SD}_{\text{uL}} \times t_{\Phi;p}), \quad (7)$$

with  $\bar{X}_{\text{uL}}$  as the mean and  $\text{SD}_{\text{uL}}$  as the standard deviation of the unlabeled control samples of the respective soil increment ( $n = 3$ ). The  $t$  value originated from the Student's  $t$  distribution ( $\Phi = n-1$ ;  $p = 0.9$ ). Only values passing this comparison were used for recovery calculations. Data were tested for normal distribution by using Shapiro-Wilk normality test, prior to linear correlation analyses. Analyses were performed with SigmaPlot 14 (Systat Software GmbH, San Jose, USA) by using Pearson correlations (for normal distributed data,  $p < 0.05$ ) or Spearman rank-order correlations (for not normal distributed data,  $p < 0.05$ ). Label recoveries in density fractions and WEOM were tested for significant changes with depth and between both sampling times by analysis of variance (ANOVA,  $p < 0.05$ ) with the Tukey test as post hoc analysis.

### 3 Results

#### 3.1 Depth distribution and properties of SOC

Soil OC contents decreased strongly from about  $82 \pm 57$  mg g<sup>-1</sup> in the upper topsoil increment (0-5 cm) to  $4 \pm 1$  mg g<sup>-1</sup> in the upper subsoil at 40-50 cm soil depth (Fig. 1a). Within the deeper subsoil, OC content further decreased to about 0.2 mg g<sup>-1</sup> in the deepest increment at 160-180 cm. Organic C stocks in the topsoil (0-10 cm depth) averaged about 5.5 kg C m<sup>-2</sup> at both sampling dates, representing 48 % of the OC

## Study I

stock down to a soil depth of 180 cm (Table 2). Deeper subsoil only accounted for 5 % of the SOC stock (Table 2).

Directly underneath the litter layer, the majority of SOC was present as POM (Fig. 2). With increasing soil depth, the relative contribution of  $C_{\text{POM}}$  to SOC decreased to < 25 %, whereas the contribution of  $C_{\text{MAOM}}$  increased. As for SOC, the  $C_{\text{MAOM}}$  content also declined from about 10 to 22 mg C  $\text{g}^{-1}$  HF in the topsoil to 0.3 to 0.4 mg C  $\text{g}^{-1}$  HF in the deeper subsoil of 100-140 cm soil depth (Fig. 3a). The C/N ratio of the MAOM decreased with depth from about 20 in the topsoil to ~ 5 in the deep subsoil (Fig. 3b), similar to the bulk soil C/N (Fig. S1). Mean ratios from the first sampling in November 2016 were insignificantly (but consistently) higher compared to the second sampling in May 2018. The  $C_{\text{SPT}}$  fraction amounted to 1 to 3 % of the SOC for all soil depths without a consistent trend (Fig. 2). The contribution of  $C_{\text{WEOM}}$  showed an increase with soil depth from 0.2 % of SOC in the topsoil to 0.7 to 1.3 % in the deeper subsoil (Fig. 4a). In addition, water extracts showed a compositional change with increasing soil depth, as SUVA values decreased below 10 cm soil depth until reaching the minimum in the deep subsoil (Fig. 4b). The humification index derived from fluorescence spectra first increased from the topsoil to its maximum in the heavily rooted upper subsoil (Heinze et al., 2018; Wordell-Dietrich et al., 2019). Below this, a constant decrease with increasing soil depth was observed (Fig. 4c).

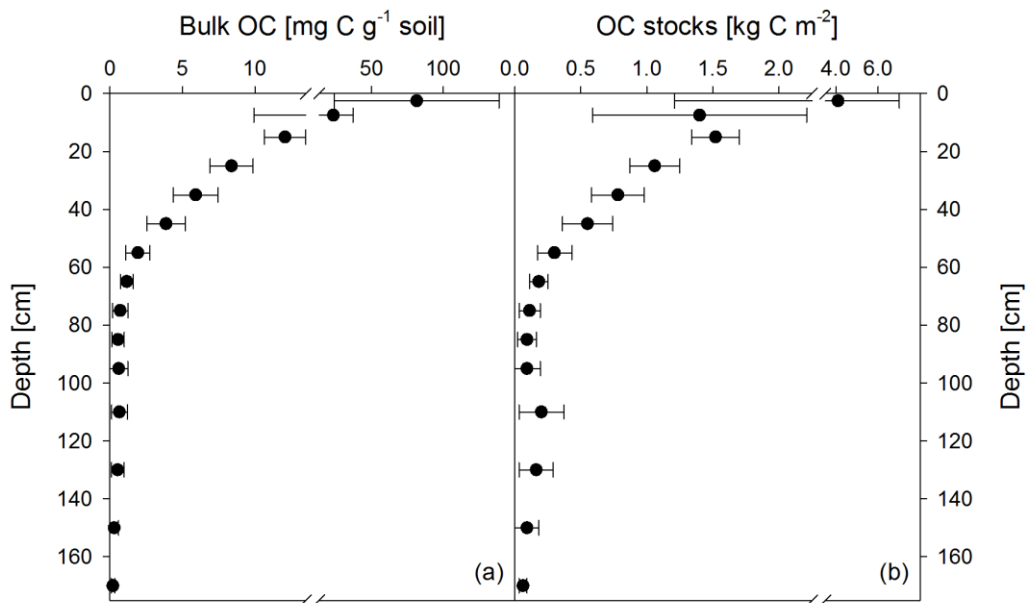


**Figure 1** Mean bulk OC contents of both sampling times (November 2016 and May 2018) (a) and calculated OC stocks as the mean of both sampling times (b). Apparent re-increasing OC stocks below 100 cm are the result of doubling the thickness of the analyzed depth increments (i.e., 5 cm increments from 0 to 10 cm, 10 cm increments from 10 to 100 cm, and 20 cm increments from 100 to 180 cm). Data show the mean of 12 samples, and error bars depict the standard deviation.

## Study I

**Table 2** Mean OC stocks in bulk soil of different soil compartments down to 180 cm presented as absolute values and as a percent of total soil OC stock (n = 12; standard deviation is given in brackets).

Soil compartment	Depth [cm]	Mean OC stock [kg m <sup>-2</sup> ]	% of total OC stock
Topsoil	0-10	5.51 (3.67)	48 (13)
Upper subsoil	10-50	3.91 (0.67)	40 (10)
Mid-subsoil	50-100	0.76 (0.35)	7 (3)
Deeper subsoil	100-180	0.50 (0.33)	5 (3)

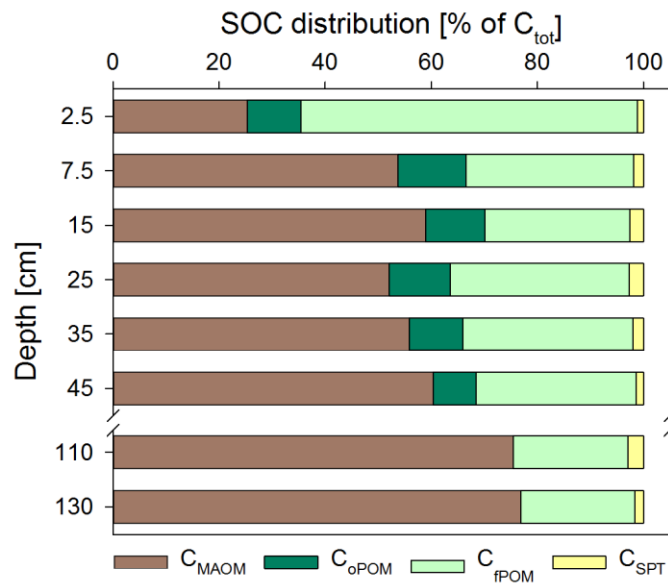


**Figure 2** Soil OC (SOC) distribution in the Dystric Cambisol at the Grinderwald site as a function of soil depth: C in mineral-associated OM (C<sub>MAOM</sub>), occluded particulate OM (C<sub>oPOM</sub>), and free particulate OM (C<sub>fPOM</sub>); C mobilized by sodium polytungstate during density fractionation (C<sub>SPT</sub>). All data are given as mean of both samplings (n = 12; standard deviation varied for C<sub>MAOM</sub> between 7 and 19 %, for C<sub>oPOM</sub> between 2 and 5 %, for C<sub>fPOM</sub> between 7 and 19 %, and for C<sub>SPT</sub> between 0.3 and 5 %). Note that the C<sub>MAOM</sub> fraction was corrected for the C loss during washing (see material and method section).

## Study I

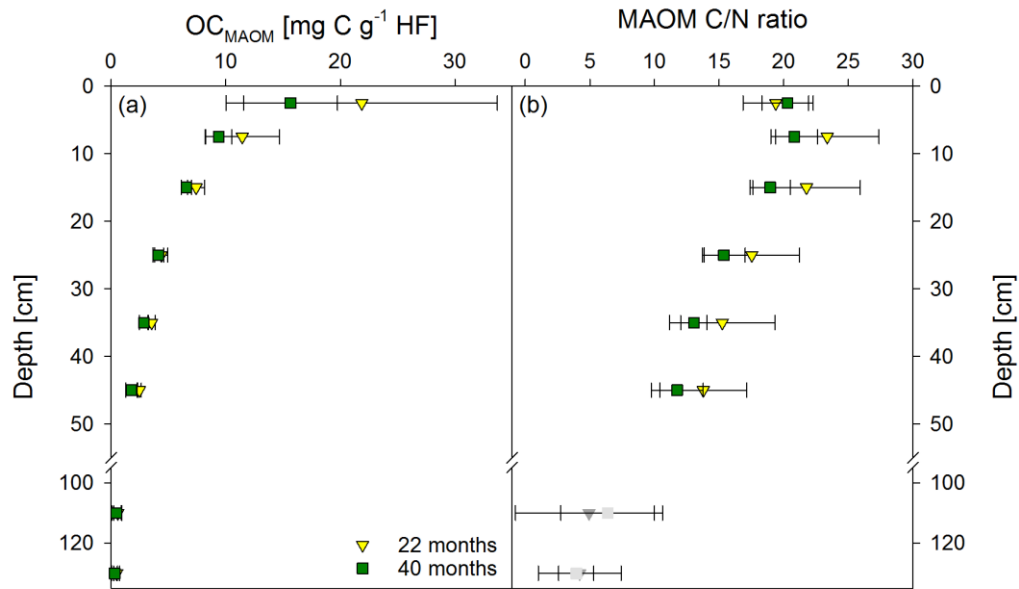


**Figure 3** Mean OC contents in the heavy fraction (HF) (a) and mean C/N ratios (b) of the mineral-associated organic matter fraction (MAOM) from both sampling times, 22 months and 40 months after labeled litter application ( $n = 6$ ; error bars represent the standard deviation). Nitrogen contents in the HF were corrected for extractable nitrate and ammonium contents; N contents in samples below 100 cm were unreliable, and C/N ratios are therefore marked in grey.

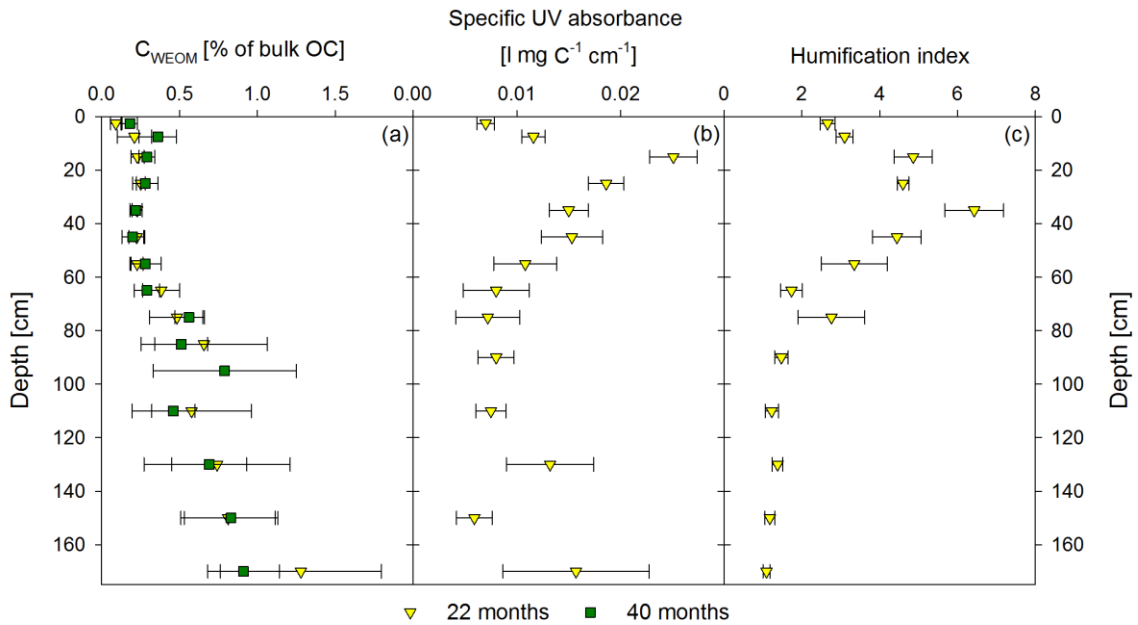


**Figure 4** Mean proportion of water-extractable-OC ( $C_{WEOM}$ ) per depth increment given in percentage of the total soil OC in bulk soil for both sampling times, 22 months and 40 months after labeled litter application ( $n = 6$ ; error bars represent the standard deviation) is shown in (a). Specific UV absorbance at 280 nm (b) and humification index deduced from fluorescence spectra (c) of the water extracts are given as the mean ( $n = 6$ ) of the first sampling in November 2016. Error bars represent the standard error.

### 3.2 Labeled litter-derived C in functional soil OM fractions

Based on  $\delta^{13}\text{C}$  values, bulk OM was more enriched in  $^{13}\text{C}$  from labeled litter than MAOM (Fig. 5a, b). Enrichments in MAOM were significant down to 20 cm soil depth compared to the control. After 40 months, the  $^{13}\text{C}$ -enrichment of MAOM was still significant down to 20 cm, but  $\delta^{13}\text{C}$  values shifted closer towards the background (Fig. 5b). Water-extractable OC showed a significant  $^{13}\text{C}$ -enrichment at greater soil depth (60 cm) compared to the bulk soil and MAOM at both sampling dates (Fig. 5a-c). Below this depth, there was still a noticeable  $^{13}\text{C}$ -enrichment of  $\text{C}_{\text{WEOC}}$  in the labeled plots, albeit not a significant one.

After 22 months, about 11.2 % of the  $^{13}\text{C}$ -labeled litter exposed at the soil surface was recovered in the selected depth increments (0-50, 100-140 cm), with a minor contribution of the deeper depth increments (Fig. 6a, Fig. S3). Considering the  $^{13}\text{C}$  of litter origin at 50-100 cm soil depth by linear interpolation between the increments of 40-50 cm and 100-120 cm, this value would increase by only 0.03 %. The majority of 87 % of the  $^{13}\text{C}$  label was recovered in the first 5 cm of the topsoil, while below 40 cm the recovery was negligible ( $< 0.2$  % of total labeled litter). A total of 18 months later, the recovered labeled  $^{13}\text{C}$  was lower in all depths compared to the first sampling, albeit not significant due to large variations between the plots, with a total recovery of 1.8 %. In the soil increments below 40 cm, the label vanished completely in the density fractions at the second sampling, while minor proportions of label were still recovered within  $\text{C}_{\text{WEOM}}$  (Fig. 5c).

In total, we found that within 22 months about  $8.7 \pm 5.6$  % of the applied labeled litter was incorporated as POM in the mineral topsoil (Fig. 6a). This corresponds to  $9.9 \pm 6.1$  g C m<sup>-2</sup> fPOM and  $1.0 \pm 0.9$  g C m<sup>-2</sup> oPOM, most of it located in the 0-5 cm topsoil increment. Below, the contribution of labeled litter-derived POM decreased strongly. Nevertheless, recovered labeled litter in the oPOM fraction was detected at even greater depth (30-40 cm) after 40 months. Litter-derived  $^{13}\text{C}$  in the MAOM fraction represented 0.7 to 2.0 % of the recovered label in the top 20 cm at both sampling dates (Fig. 6), representing a contribution of litter-derived C to the total  $\text{C}_{\text{MAOM}}$  of only about  $\sim 0.2$  %. Below, contributions were even lower. Additionally, the  $\text{C}_{\text{SPT}}$  fraction, particularly that of the topsoil and upper subsoil of the first sampling date, showed a  $^{13}\text{C}$ -enrichment (Fig. 6a).

However, 18 months after replacing the labeled by unlabeled litter, the proportion of labeled litter-derived C in the SPT solution decreased by 84 % on average (Table 3) and the label was only detectable down to 20 cm soil depth (Fig. 6b).

Proportions of labeled litter-derived C in WEOM illustrated clear depth and temporal trends (Fig. 7). The  $\text{C}_{\text{WEOM}}$  fraction in the topsoil contained more than 1 % of C originally derived from the litter layer at the end of the labeling period in November 2016, with a strong decrease with depth. Below 40 cm,

## Study I

proportions were consistently < 0.2 %. A total of 18 months after litter replacement, the contribution of labeled litter-derived C in WEOM decreased to < 0.3 % in the whole soil profile.

Mean loss of the recovered litter-derived  $^{13}\text{C}$  over the time period of 18 months between the two samplings was 79 %, and all fractions showed a considerable loss of > 65 % (Table 3). The losses followed the sequence: fPOM (89 %) > WEOM (80%) > oPOM (77 %) > MAOM (66 %). The decline of the label from mass-weighted individual OM fractions was similar in magnitude to the loss of labeled litter-derived C in the bulk samples (77 %; data not shown).

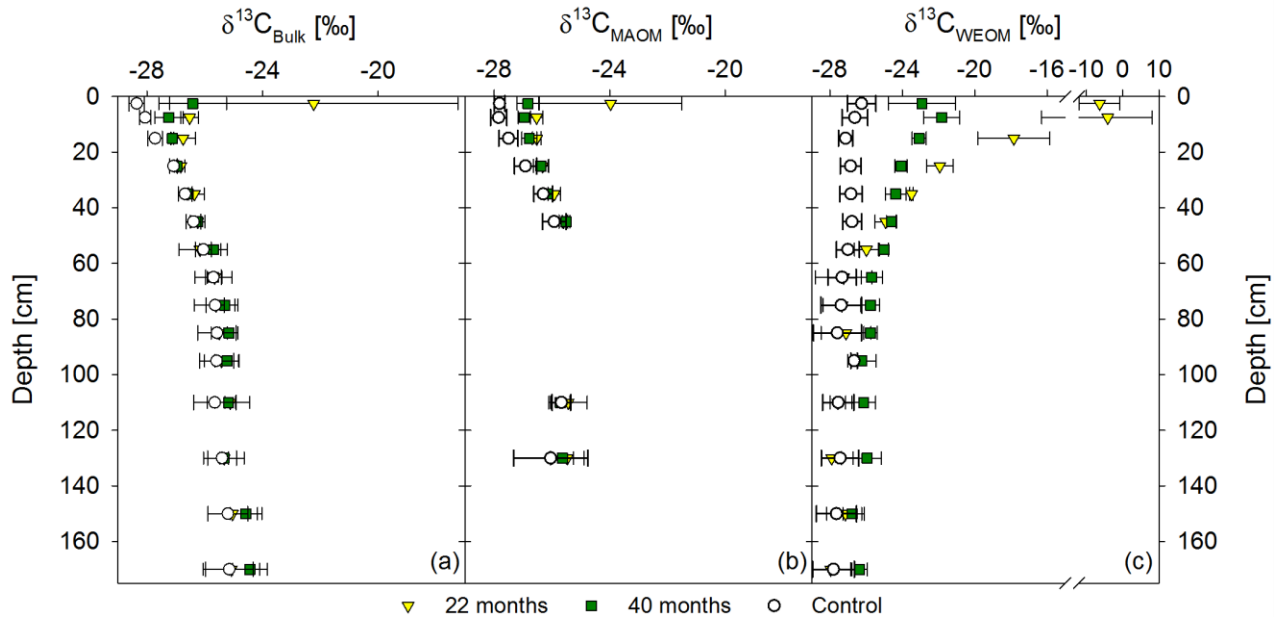


**Figure 5** Mean  $\delta^{13}\text{C}$  values of the bulk soil (a), mineral-associated OM ( $C_{\text{MAOM}}$ ) (b), and water-extractable OM ( $C_{\text{WEOM}}$ ) (c). The graphs show labeled samples of both sampling times, 22 months and 40 months after labeled litter application in colored symbols, compared to the respective unlabeled background distribution in white symbols. Labeled samples represent the mean of three replicates per sampling time, while the control represents the mean of both sampling times ( $n = 6$ ). Please note that the  $x$  axis in (c) has a different scale.

## Study I

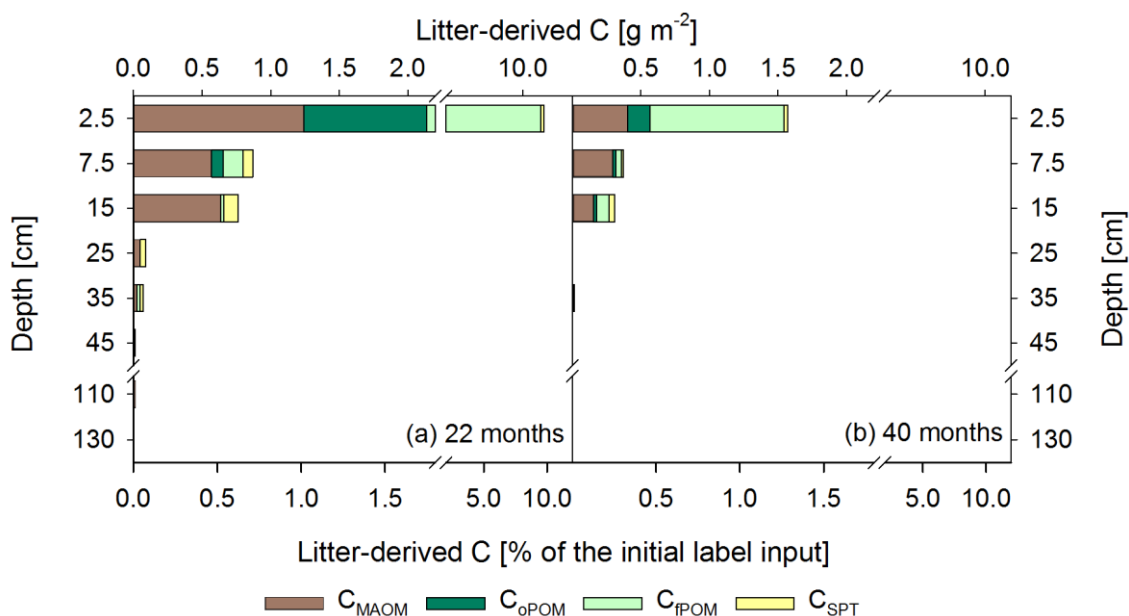


**Figure 6** Mean labeled litter-derived  $^{13}\text{C}$  recovered in different OM fractions: C in mineral-associated OM ( $C_{\text{MAOM}}$ ), occluded particulate OM ( $C_{\text{oPOM}}$ ), and free particulate OM ( $C_{\text{fPOM}}$ ); C mobilized by sodium polytungstate during density fractionation ( $C_{\text{SPT}}$ ). The upper  $x$  axis shows the recovered  $^{13}\text{C}$  in  $\text{g m}^{-2}$  and the lower  $x$  axis shows the percentage recovery of initially added labeled litter after 22 months (a) and 40 months following labeled litter application (b). Bars show the sum of all fractions per depth increment, while the different colors represent the respective contribution of each fraction to the total recovery ( $n = 3$ ). According to ANOVA tests there were no significant changes in  $^{13}\text{C}$  recovery for each fraction with depth per sampling, due to high standard deviations in the range of 0.02–0.53 for  $C_{\text{MAOM}}$ , 0.01–0.75 for  $C_{\text{oPOM}}$ , 0.02–4.9 for  $C_{\text{fPOM}}$ , and 0.01–0.13 for  $C_{\text{SPT}}$ .

**Table 3** Mean contents of labeled litter-derived OM in different soil fractions of all depth increments used for density fractionation (0-50 cm, 100-140 cm) 22 months (November 2016) and 40 months (May 2018) after labeled litter application ( $n = 3$ ; standard deviation is given in brackets). The percentage loss over 18 months was calculated based on differences in C contents in OM fractions at both samplings. Overall, 36-40 % of the initially applied litter was lost by respiration during 22 months of field exposure (Wordell-Dietrich, unpublished).

	Recovered November 2016 [ $\text{g m}^{-2}$ ]	Recovered May 2018 [ $\text{g m}^{-2}$ ]	Loss over time [%]
$C_{\text{MAOM}}^1$	2.54 (0.92)	0.85 (0.52)	66
$C_{\text{fPOM}}^2$	9.89 (6.14)	1.11 (0.96)	89
$C_{\text{oPOM}}^3$	0.98 (0.91)	0.23 (0.24)	77
$C_{\text{SPT}}^4$	0.54 (0.35)	0.08 (0.08)	84
$C_{\text{WEOM}}^5$	0.15 (0.06)	0.03 (0.01)	80

<sup>1</sup> Carbon in mineral-associated OM ( $C_{\text{MAOM}}$ )

<sup>2</sup> Carbon in free particulate OM ( $C_{\text{fPOM}}$ )

<sup>3</sup> Carbon in occluded particulate OM ( $C_{\text{oPOM}}$ )

<sup>4</sup> Sodium polytungstate-mobilizable C ( $C_{\text{SPT}}$ )

<sup>5</sup> Carbon in water-extractable organic matter ( $C_{\text{WEOM}}$ )



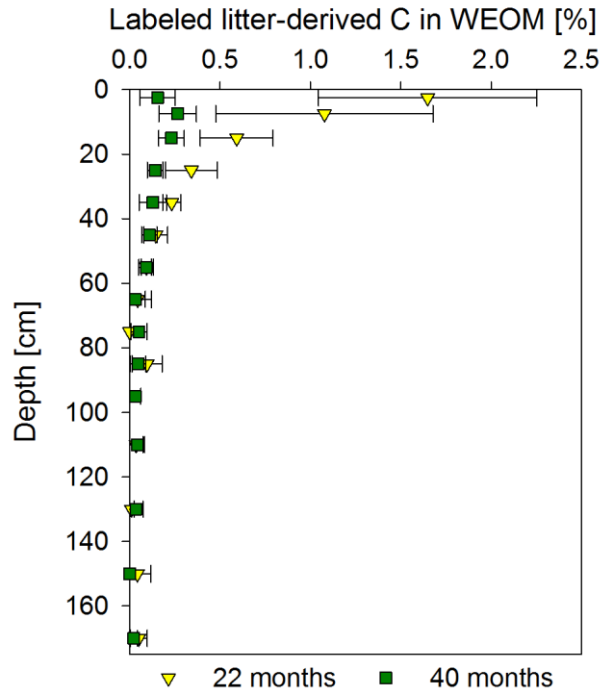


**Figure 7** Mean proportion of litter-derived C in water extractable organic OM (WEOM) in percentage of the initial label input for both sampling times, 22 months and 40 months after labeled litter application, with soil depth ( $n = 3$ ; error bars represent the standard deviation). According to ANOVA tests, significant changes between both samplings were only present in the 0-5 cm and 10-20 cm increments ( $p < 0.05$ ). Significant differences between soil increments were only present for the topsoil increments compared to all subsoil increments for each sampling time.

## 4 Discussion

### 4.1 Particulate OM in the soil profile and contribution of litter-derived POM

Particulate OC contributed  $59 \pm 16$  % to SOC in the Grinderwald topsoil. This high contribution of POM is likely a consequence of translocation by the mesofauna and macrofauna, as bioturbation can drive both inputs and mineralization of SOC (Wilkinson et al., 2009). Results are somewhat higher than findings of Schrumpf et al. (2013) who reported  $25 \pm 16$  % POM contribution to the SOC for several European study sites. Below the topsoil, amounts of POM were only minor (Supplement, Fig. S2). The proportional decrease in POM with soil depth confirms the findings of Kaiser et al. (2002), who reported a similar decrease in the contribution of POM to SOM from about 65 % in the topsoil to 5 % in the subsoil C horizons, illustrating a decreasing role of root input and bioturbation in subsoil horizons (Heinze et al., 2018). Our results suggest that the majority of POM in the topsoil is not directly connected to annual litter inputs as these are very small compared to the total POM pool. Similar to our observations, Lajtha et al. (2014b) reported that a 2-fold increase in litter input did not affect the C concentrations in either the bulk soil, POM, or the HF fraction of the mineral topsoil and upper subsoil within 20 years. They concluded that forest SOC pools are not tightly coupled to changes in aboveground litter inputs in the short term. In

the upper and deeper subsoil, recent litter-derived POM was barely present after 22 months, and completely vanished after 40 months, suggesting that most POM in the subsoil instead derives from root biomass.

In the 18 months between both samplings, we found that 89 % of recent litter-derived fPOM and 77 % of the oPOM material were lost in the soil profile. Consequently, new POM inputs are unstable and prone to decomposition, in line with reported turnover times of < 10 years (Gaudinski et al., 2000; Baisden et al., 2002). Along with that, Crow et al. (2009) described the aboveground litter as the source of the most actively cycling soil C. The smaller C loss from oPOM compared to fPOM within 18 months (77 and 89 %) reflects a better protection of occluded POM compared to free POM—even in this loamy sand soil (Table 1).

### **4.2 Mineral-associated OM and incorporation of litter-derived C via the DOC pathway**

Beside bioturbation and rhizodeposition, translocation and sorption of DOM to the soil matrix are the other prominent processes transferring C to the subsoil (Kaiser and Kalbitz, 2012; Mikutta et al., 2019). The observed strong decrease in the contents of mineral-associated OC with soil depth (Fig. 3a) is in line with smaller root exudation rates (Tückmantel et al., 2017) and DOC fluxes (Leinemann et al., 2016) with increasing soil depth at the Grinderwald site. This also reflects a decrease in available sorption sites with depth due to increasing sand contents (Table 1) and decreasing amounts of poorly crystalline Fe phases (Fe<sub>o</sub> contents; Supplement, Table S2). Leinemann et al. (2016) observed a decrease in SUVA values of DOM with increasing soil depth, indicating a preferential sorption of plant-derived compounds in the upper parts of the soil profile. Specific UV absorbance and the fluorescence indices (HIX) of our water extracts showed a similar decline with soil depth, thus underpinning sorption as a relevant process. Decomposition of roots can substantially contribute to the subsoil SOM pool as well (Rasse et al., 2005). But since root density (Heinze et al., 2018; Wordell-Dietrich et al., 2019) and root exudation (Tückmantel et al., 2017) are low in the Grinderwald subsoil, we assume that the increasing share of MAOM with soil depth instead suggests an increasing importance of DOM as a dominant source of C in this forest subsoil, irrespective of its origin. This depth trend was accompanied by a compositional change of MAOM, as indicated by decreasing C/N ratios and increasing  $\delta^{13}\text{C}$  values. Fresh litter-derived MAOM in the topsoil had typically wide C/N ratios of about 19 to 22 and low natural abundance  $\delta^{13}\text{C}$  values of about -27 to -28 ‰ (Figs. 3b, 5b). Microbial processing (Six et al., 2001; Schmidt et al., 2011) and preferential sorption of  $^{13}\text{C}$ -depleted plant-derived phenols in the topsoil (Guggenberger and Zech, 1994; Kaiser et al., 2001) alter the SOM characteristics with increasing soil depth by narrowing the C/N ratio and increasing the  $^{13}\text{C}$  content. In line with this view, the  $\delta^{13}\text{C}$  of MAOM in the unlabeled control soil showed a consistent increase with decreasing C/N ratio with depth (Supplement, Fig. S4), thus pointing towards an increasing

## Study I

---

contribution of microbially processed MAOM with soil depth, as proposed in the “dynamic exchange” or “cascade model” (Kaiser and Kalbitz, 2012). Gleixner (2005) likewise attributed this trend to a higher contribution of plant and root litter in topsoil horizons, whereas the deeper subsoil horizons are dominated by microbial-derived OM. A change towards microbial-derived OM is further supported by decreasing SUVA and HIX values of WEOM from the upper subsoil downwards, suggesting more aromatic and complex plant-derived OM components like phenols being retained in the topsoil, while more microbial-derived components like carbohydrates are present in the subsoil.

On average  $1.46 \pm 0.67$  % of the fresh litter layer C was associated with minerals in the topsoil ( $0.57 \pm 0.12$  % in the upper subsoil and only  $0.01 \pm 0.02$  % in deeper subsoil compartments) 22 months after adding the labeled beech litter, emphasizing the subordinate importance of recent aboveground litter inputs to soil C stocks in all depths, especially in the deeper subsoil. Lajtha et al. (2014a) also showed that 50 years of doubled litter inputs in a deciduous forest stand did not result in a net accumulation of OC in the topsoil HF, likely as sorption sites in topsoils are already largely occupied by OM (Mikutta et al., 2019). The chemical composition of the HF particle surface layer supports this assumption, as the C and N contents decreased with increasing soil depth (Supplement, Fig. S5). Additionally, a higher content of mineral-borne Al and Fe within the HF surface layer with increasing depth suggests a higher proportion of uncovered mineral surfaces (Supplement, Fig. S5).

For the Dystric Cambisol under European beech, the average annual inputs from the recent litter layer into the HF were estimated as  $0.99 \pm 0.45$  g C m<sup>-2</sup> yr<sup>-1</sup> in the topsoil,  $0.37 \pm 0.10$  g C m<sup>-2</sup> yr<sup>-1</sup> in the upper subsoil, and  $0.01 \pm 0.01$  g C m<sup>-2</sup> yr<sup>-1</sup> in the deeper subsoil. This estimation follows the assumption of a constant input of labeled litter-derived OM during the 22 months, which is a sufficient approximation for this estimate but may not reflect the actual conditions in the field. Fröberg et al. (2007a) reported annual DOC fluxes of about 4-14 g C m<sup>-2</sup> yr<sup>-1</sup> in 15 cm soil depth and 1.5 to 4.5 g C m<sup>-2</sup> yr<sup>-1</sup> in 70 cm soil depth, from which, on average 14 % was derived from recent litter. This corresponds to fluxes of 0.5 to 2 g C m<sup>-2</sup> yr<sup>-1</sup> and 0.2 to 0.6 g C m<sup>-2</sup> yr<sup>-1</sup>, respectively, which is similar in magnitude as the observed <sup>13</sup>C fluxes from the labeled litter into the HF at our study site. Given this similarity, it is reasonable to assume that recent litter-derived C contributes to the MAOM pool in different soil depths mainly by the DOC pathway. The decreasing input and contribution of recent litter-derived C with depth further implies that there is an increasing contribution of older OC to DOC with increasing soil depth, as likewise found when dating <sup>14</sup>C ages of DOC (Don and Schulze, 2008).

There was a substantial decrease in the recovered <sup>13</sup>C label in the MAOM fraction within the 18 months between the first and second sampling. This can be explained either by desorption of litter-derived compounds (either due to microbial degradation or abiotic exchange processes) and/or sorption of fresh unlabeled DOM. We assume that sorption of DOM from the soil solution and the accompanied replacement of litter-derived C from mineral surfaces is the most plausible reason for the observed <sup>13</sup>C

loss. This is because the C content of the HF at both samplings was rather constant (Fig. 3a) and the considerable DOC fluxes of 0.7 to 2.1 g m<sup>-2</sup> yr<sup>-1</sup> in the deep subsoil (Leinemann et al., 2016) ensure sufficient probability for sorption and displacements reactions. In total, 1.69 g m<sup>-2</sup> of initially 2.54 g m<sup>-2</sup> recent litter-derived MAOM were lost throughout the soil profile (66 %) within 18 months. This indicates that young OM associated with minerals, especially in the upper soil, is not effectively stabilized by mineral surfaces (Schrumpf et al., 2013). The minor retention of <sup>13</sup>C by soil minerals and the subsequent remobilization of mineral-bound C in the topsoil are both facilitated by the generally low contents of clay (< 3 %) and pedogenic Fe and Al oxides (Supplement, Table S2). In addition, the clay fraction might be dominated by illite, which is a relatively less sorptive phyllosilicate under acidic conditions (Kaiser et al., 1997).

Despite the fast transformation of recently formed MAOM in the topsoil, this does not result in a significant downward translocation of C within the timeframe of 18 months. This hints to intense microbial processing as desorbed or exchanged recent litter-derived C has a higher bioavailability (Marschner and Kalbitz, 2003). Another reason for explaining the minor <sup>13</sup>C transfer to the subsoil would be the downward translocation of unlabeled litter-derived C (after litter displacement), which could have diluted the tracer with increasing soil depth. On the other hand, at the second sampling, part of the translocated DOM was likely already originating from horizons (O layers and upper mineral soil horizons) already enriched in <sup>13</sup>C, thus potentially counteracting the dilution by new unlabeled DOM to a certain extent.

### **4.3 Mobilizable OM – linking litter inputs and MAOM formation**

The concept of C translocation from topsoil into the subsoil assumes continuous exchange processes at mineral surfaces, leading to partial desorption of microbially altered OM and thus its downward transport (Kaiser and Kalbitz, 2012). Here, WEOM was considered to represent such mobilizable OM, being most susceptible to translocation and, hence, a source for subsoil OM. Accordingly, we found an increasing importance of WEOM with increasing soil depth, as its proportion to SOC was higher in the subsoil than in the topsoil. This implies that the deeper soil compartments were comprised of relatively more soluble OM. A similar depth trend was detected for the mobilization of C during density fractionation, supporting the findings for WEOM. In accordance with Chantigny (2003), WEOM represents only a small part of SOC but was more enriched in litter-derived <sup>13</sup>C than bulk SOC or MAOM (Fig. 5). Despite the higher enrichment, this accounted only for < 1.7 % of total WEOM, suggesting that the majority of mobilizable OC is older than 22 months (for sampling in November 2016) or 40 months (for sampling in May 2018). In line with this, Fröberg et al. (2007b) and Hagedorn et al. (2003) reported that recent litter-derived DOC contributes only minorly to the total DOC leached from the organic layer into the mineral soil.

The high  $\delta^{13}\text{C}$  values of  $C_{\text{WEOM}}$  (Fig. 5c) and the strong decline of litter-derived C in  $C_{\text{WEOM}}$  within the upper 20 cm of the soil profile (Fig. 7) suggest that litter-derived POM is a considerable source of WEOM. For example, the beech litter residues that were removed after 22 months and sieved < 5 mm still contained up to 2 %  $C_{\text{WEOM}}$  (data not shown), which might become liberated in soil. In the subsoil, WEOM likely derives from MAOM and root-derived POM, the latter representing a negligible fraction in the deeper subsoil at the Grindewald site. In a recent soil column experiment, Leinemann et al. (2018) showed that 20 % of the MAOM can be replaced by percolating DOM in samples collected from three depths down to 100 cm soil depth. Most intriguingly, we did not observe a downward migration of the  $^{13}\text{C}$  label within WEOC 18 months later, again pointing to losses of litter-derived C in all soil increments by microbial decomposition. This assumption is supported by findings from Tipping et al. (2012) who showed that the majority of DOM released from the mineral matrix can be lost by mineralization. This also matches well to the fact that subsoil MAOM is only to a minor extent fed by recent litter-derived C sources. In summary, topsoil WEOC at least partly derives from the recent litter layer, whereas this is not the case in the deeper soil. This finding thus supports the view, as proposed in the cascade model, that the downward migration of C involves the mobilization of older SOM components.

### 5 Implications

A prominent concept for the build-up of soil OC stocks not only considers the input of plant residues into soil but also the subsequent fate of OM inputs, where C is assumed to undergo a sequence of cycles including sorptive retention, microbial processing, and desorption on its way down the soil profile (Kaiser and Kalbitz, 2012). This study thus investigated the impact of recent aboveground litter for OC sequestration and the subsequent partitioning of litter-derived C in different soil layers and OM fractions. Annual C inputs from the recent litter layer into the mineral soil were low compared to the C already stored in soil. Most of new litter-derived C is retained in the topsoil, mainly as POM. In fact, we did not find a translocation of considerable amounts of recent litter-derived C into the deep subsoil, indicating that most translocated OM at the study site is of older age. Our field study supports the concept that C accumulation in deeper soil involves several (re)mobilization cycles of OM during its downward migration. The large C losses in the topsoil during a period of 18 months without concomitant increase in subsoil C indicate that the young SOC, especially in the form of POM, represents an actively cycling C pool. Slower turnover of litter-derived C was observed for MAOM compared to both POM fractions, supporting the assumption that accessibility and sorptive stabilization reduces the vulnerability of OM to microbial decomposition. The loss of about 66 % of the C from the HF within 18 months, however, confirms earlier findings (Schrumpf et al., 2013) that part of the MAOM is rather labile, especially in the presence of less reactive minerals such as quartz or illite at our study site.

## Study I

---

In summary, given the highly active C cycling in the topsoil and upper subsoil at the Grinderwald site, only marginal C from a recent litter layer enters the deep mineral subsoil. The build-up of subsoil C stocks is thus not connected to a direct transfer from the litter layer but goes along with repeated sorption and remobilization cycles of OM during downward migration over a much longer period than 3.5 years.

*Data availability.* All compiled data in this study are published in figures and tables. Detailed primary data are saved and published in the BonaRes Repository and available: Liebmann et al. (2020)\_Site\_parameter\_Grinderwald (<https://doi.org/10.20387/bonares-HZGX-GB9S>) (last access: 15 June 2020), Liebmann et al. (2020)\_Bulk\_data (<https://doi.org/10.20387/bonares-69H2-56Q9>) (last access: 15 June 2020), and Liebmann et al. (2020)\_Fractions\_data (<https://doi.org/10.20387/bonares-DNDW-5T58>) (last access: 15 June 2020).

*Supplement.* The supplement related to this article is available online at: <https://doi.org/10.5194/bg-17-3099-2020-supplement>.

*Author contribution.* AD, KK, RM, and GG designed the experiment and PL, FK, and PWD carried it out in the field. PWD, LRD, FK, and PL processed the samples and did the analyses. SKW conducted the XPS measurements. PL took the lead in preparing the manuscript, with contributions from all co-authors.

*Competing interests.* The authors declare that they have no conflict of interest.

*Acknowledgements.* The authors would like to thank Timo Leinemann for all his work in the first SUBSOM phase, including the labeling and sampling for this experiment. We thank Frank Hegewald for support in the field, Manuela Unger for carrying out the  $^{13}\text{C}$  analysis of the water extracts, and all lab teams for assistance in the lab. We also want to thank Leopold Sauheitl for helpful discussions about density fractionation and detection limits and Jürgen Böttcher for helpful discussions about data analysis. We further thank Markus Koch and Moritz Rahlfs for their valuable comments on earlier versions of this manuscript.

We gratefully acknowledge comments from Yolima Carrillo and four anonymous reviewers and a comment from Paul Hanson, which helped to improve the manuscript.

## Study I

---

*Financial support.* This study was performed within the framework of the research unit “The forgotten part of carbon cycling: Organic matter storage and turnover in subsoils (SUBSOM)” (FOR1806). This research has been supported by the Deutsche Forschungsgemeinschaft (DFG) through projects GU 406/28-1,2; KA 1737/10-2; MI 1377/15-2; and DO1734/4-2.

The publication of this article was funded by the open-access fund of Leibniz Universität Hannover.

*Review statement.* This paper was edited by Yakov Kuzyakov and reviewed by Yolima Carrillo and four anonymous referees.

### References

Ad-hoc-Arbeitsgruppe Boden: Bodenkundliche Kartieranleitung KA5, 5th ed., E. Schweizerbart'sche Verlagsbuchhandlung. [online] Available from: <http://www.schweizerbart.de/publications/detail/isbn/9783510959204> (Accessed 1 October 2016), 2005.

Angst, G., Kögel-Knabner, I., Kirfel, K., Hertel, D. and Mueller, C. W.: Spatial distribution and chemical composition of soil organic matter fractions in rhizosphere and non-rhizosphere soil under European beech (*Fagus sylvatica* L.), *Geoderma*, 264, 179–187, doi:10.1016/j.geoderma.2015.10.016, 2016.

Angst, G., Messinger, J., Greiner, M., Häusler, W., Hertel, D., Kirfel, K., Kögel-Knabner, I., Leuschner, C., Rethemeyer, J. and Mueller, C. W.: Soil organic carbon stocks in topsoil and subsoil controlled by parent material, carbon input in the rhizosphere, and microbial-derived compounds, *Soil Biol. Biochem.*, 122, 19–30, doi:10.1016/j.soilbio.2018.03.026, 2018.

Bachmann, J., Krueger, J., Goebel, M.-O. and Heinze, S.: Occurrence and spatial pattern of water repellency in a beech forest subsoil, *J. Hydrol. Hydromech.*, 64, 100-110, doi:10.1515/johh-2016-0005, 2016.

Baisden, W. T., Amundson, R., Cook, A. C. and Brenner, D. L.: Turnover and storage of C and N in five density fractions from California annual grassland surface soils, *Glob. Biogeochem. Cycles*, 16, 117-132, doi:10.1029/2001GB001822, 2002.

Balesdent, J., Girardin, C. and Mariotti, A.: Site-related  $\delta^{13}\text{C}$  of tree leaves and soil organic matter in a temperate forest, *Ecology*, 74(6), 1713–1721, doi:10.2307/1939930, 1993.

Batjes, N. H.: Total carbon and nitrogen in the soils of the world, *Eur. J. Soil Sci.*, 47, 151–163, doi:10.1111/ejss.12114\_2, 1996.

Bernal, B., McKinley, D. C., Hungate, B. A., White, P. M., Mozdzer, T. J. and Megonigal, J. P.: Limits to soil carbon stability; Deep, ancient soil carbon decomposition stimulated by new labile organic inputs, *Soil Biol. Biochem.*, 98, 85–94, doi:10.1016/j.soilbio.2016.04.007, 2016.

## Study I

---

Bird, J. A., Kleber, M. and Torn, M. S.:  $^{13}\text{C}$  and  $^{15}\text{N}$  stabilization dynamics in soil organic matter fractions during needle and fine root decomposition, *Org. Geochem.*, 39(4), 465–477, doi:10.1016/j.orggeochem.2007.12.003, 2008.

Blume, H.-P., Stahr, K. and Leinweber, P.: Laboruntersuchungen, in *Bodenkundliches Praktikum: Eine Einführung in pedologisches Arbeiten für Ökologen, insbesondere Land- und Forstwirte, und für Geowissenschaftler*, edited by H.-P. Blume, K. Stahr, and P. Leinweber, pp. 77–154, Spektrum Akademischer Verlag, Heidelberg., 2010.

Cerli, C., Celi, L., Kalbitz, K., Guggenberger, G. and Kaiser, K.: Separation of light and heavy organic matter fractions in soil — Testing for proper density cut-off and dispersion level, *Geoderma*, 170, 403–416, doi:10.1016/j.geoderma.2011.10.009, 2012.

Chantigny, M. H.: Dissolved and water-extractable organic matter in soils: a review on the influence of land use and management practices, *Geoderma*, 113(3–4), 357–380, doi:10.1016/S0016-7061(02)00370-1, 2003.

Chantigny, M. H., Angers, D. A., Kaiser, K., and Kalbitz, K.: Extraction and Characterization of Dissolved Organic Matter, in *Soil sampling and methods of analysis*, edited by: M. R. Carter and E. G. Gregorich, CRC Press, Boca Raton, USA, 617–635, 2007.

Chin, Y.-Ping., Aiken, George. and O’Loughlin, Edward.: Molecular weight, polydispersity, and spectroscopic properties of aquatic humic substances, *Environ. Sci. Technol.*, 28(11), 1853–1858, doi:10.1021/es00060a015, 1994.

Corvasce, M., Zsolnay, A., D’Orazio, V., Lopez, R. and Miano, T. M.: Characterization of water extractable organic matter in a deep soil profile, *Chemosphere*, 62(10), 1583–1590, doi:10.1016/j.chemosphere.2005.07.065, 2006.

Crow, S. E., Lajtha, K., Filley, T. R., Swanston, C. W., Bowden, R. D. and Caldwell, B. A.: Sources of plant-derived carbon and stability of organic matter in soil: implications for global change, *Glob. Change Biol.*, 15(8), 2003–2019, doi:10.1111/j.1365-2486.2009.01850.x, 2009.

van Dam, D., van Breemen, N. and Veldkamp, E.: Soil organic carbon dynamics: variability with depth in forested and deforested soils under pasture in Costa Rica, *Biogeochemistry*, 39(3), 343–375, doi:10.1023/A:1005880031579, 1997.

Don, A. and Schulze, E.-D.: Controls on fluxes and export of dissolved organic carbon in grasslands with contrasting soil types, *Biogeochemistry*, 91(2), 117–131, doi:10.1007/s10533-008-9263-y, 2008.

Fontaine, S., Barot, S., Barré, P., Bdioui, N., Mary, B. and Rumpel, C.: Stability of organic carbon in deep soil layers controlled by fresh carbon supply, *Nature*, 450(7167), 277–280, doi:10.1038/nature06275, 2007.

Fröberg, M., Jardine, P. M., Hanson, P. J., Swanston, C. W., Todd, D. E., Tarver, J. R. and Garten, C. T.: Low dissolved organic carbon input from fresh litter to deep mineral soils, *Soil Sci. Soc. Am. J.*, 71(2), 347, doi:10.2136/sssaj2006.0188, 2007a.

Fröberg, M., Berggren Kleja, D. and Hagedorn, F.: The contribution of fresh litter to dissolved organic carbon leached from a coniferous forest floor, *Eur. J. Soil Sci.*, 58(1), 108–114, doi:10.1111/j.1365-2389.2006.00812.x, 2007b.



## Study I

---

Fröberg, M., Hanson, P. J., Trumbore, S. E., Swanston, C. W., and Todd, D. E.: Flux of carbon from  $^{14}\text{C}$ -enriched leaf litter throughout a forest soil mesocosm, *Geoderma*, 149, 181–188, doi:10.1016/j.geoderma.2008.11.029, 2009.

Gaudinski, J. B., Trumbore, S. E., Davidson, E. A. and Zheng, S.: Soil carbon cycling in a temperate forest: radiocarbon-based estimates of residence times, sequestration rates and partitioning of fluxes, *Biogeochemistry*, 51(1), 33–69, doi:10.1023/A:1006301010014, 2000.

Gentsch, N., Mikutta, R., Alves, R. J. E., Barta, J., Čapek, P., Gittel, A., Hugelius, G., Kuhry, P., Lashchinskiy, N., Palmtag, J., Richter, A., Šantrůčková, H., Schnecker, J., Shibistova, O., Urich, T., Wild, B. and Guggenberger, G.: Storage and transformation of organic matter fractions in cryoturbated permafrost soils across the Siberian Arctic, *Biogeosciences*, 12(14), 4525–4542, doi:10.5194/bg-12-4525-2015, 2015.

Gentsch, N., Wild, B., Mikutta, R., Čapek, P., Diáková, K., Schrumppf, M., Turner, S., Minnich, C., Schaarschmidt, F., Shibistova, O., Schnecker, J., Urich, T., Gittel, A., Šantrůčková, H., Bárta, J., Lashchinskiy, N., Fuß, R., Richter, A. and Guggenberger, G.: Temperature response of permafrost soil carbon is attenuated by mineral protection, *Glob. Change Biol.*, 24(8), 3401–3415, doi:10.1111/gcb.14316, 2018.

Gleixner, G.: Stable isotope composition of soil organic matter, in Flanagan LB, Ehleringer JR, Pataki DE (eds) *Stable Isotopes and Biosphere-Atmosphere Interactions: Processes and Biological Controls*, pp. 29–46, Elsevier, San Diego., 2005.

Golchin, A., Oades, J. M., Skjemstad, J. O. and Clarke, P.: Soil structure and carbon cycling, *Soil Res.*, 32(5), 1043–1068, doi:10.1071/sr9941043, 1994a.

Golchin, A., Oades, J. M., Skjemstad, J. O. and Clarke, P.: Study of free and occluded particulate organic matter in soils by Solid state  $^{13}\text{C}$  CP/MAS NMR Spectroscopy and Scanning Electron Microscopy, *Aust. J. Soil Res.*, 32(2), 285–309, 1994b.

Guggenberger, G. and Zech, W.: Composition and dynamics of dissolved carbohydrates and lignin-degradation products in two coniferous forests, N.E. Bavaria, Germany, *Soil Biol. Biochem.*, 26(1), 19–27, 1994.

Hagedorn, F., Saurer, M. and Blaser, P.: A  $^{13}\text{C}$  tracer study to identify the origin of dissolved organic carbon in forested mineral soils, *Eur. J. Soil Sci.*, 55(1), 91–100, doi:10.1046/j.1365-2389.2003.00578.x, 2003.

Heinze, S., Ludwig, B., Piepho, H.-P., Mikutta, R., Don, A., Wordell-Dietrich, P., Helfrich, M., Hertel, D., Leuschner, C., Kirfel, K., Kandeler, E., Preusser, S., Guggenberger, G., Leinemann, T. and Marschner, B.: Factors controlling the variability of organic matter in the top- and subsoil of a sandy Dystric Cambisol under beech forest, *Geoderma*, 311, 37–44, doi:10.1016/j.geoderma.2017.09.028, 2018.

Hut, G.: Consultants' group meeting on stable isotope reference samples for geochemical and hydrological investigations, [online] Available from: [http://inis.iaea.org/Search/search.aspx?orig\\_q=RN:18075746](http://inis.iaea.org/Search/search.aspx?orig_q=RN:18075746) (Accessed 13 July 2018), 1987.

IUSS Working Group WRB: World reference base for soil resources 2014. International soil classification system for naming soils and creating legends for soil maps. World Soil Resources Reports No. 106, FAO, Rome, 181pp, 2014.

## Study I

---

Jobbagy, E. G. and Jackson, R. B.: The vertical distribution of soil organic carbon and its relation to climate and vegetation, *Ecol. Appl.*, 10(2), 423–436, doi:10.2307/2641104, 2000.

Kaiser, K. and Guggenberger, G.: The role of DOM sorption to mineral surfaces in the preservation of organic matter in soils, *Org. Geochem.*, 31, 711–725, 2000.

Kaiser, K. and Guggenberger, G.: Distribution of hydrous aluminium and iron over density fractions depends on organic matter load and ultrasonic dispersion, *Geoderma*, 140(1–2), 140–146, doi:10.1016/j.geoderma.2007.03.018, 2007.

Kaiser, K. and Kalbitz, K.: Cycling downwards – dissolved organic matter in soils, *Soil Biol. Biochem.*, 52, 29–32, doi:10.1016/j.soilbio.2012.04.002, 2012.

Kaiser, K., Guggenberger, G., Haumaier, L. and Zech, W.: Dissolved organic matter sorption on subsoils and minerals studied by  $^{13}\text{C}$ -NMR and DRIFT spectroscopy, *Eur. J. Soil Sci.*, 48, 301–310, 1997.

Kaiser, K., Guggenberger, G. and Zech, W.: Isotopic fractionation of dissolved organic carbon in shallow forest soils as affected by sorption, *Eur. J. Soil Sci.*, 52(4), 585–597, doi:10.1046/j.1365-2389.2001.00407.x, 2001.

Kaiser, K., Eusterhues, K., Rumpel, C., Guggenberger, G. and Kögel-Knabner, I.: Stabilization of organic matter by soil minerals — investigations of density and particle-size fractions from two acid forest soils, *J. Plant Nutr. Soil Sci.*, 165(4), 451–459, doi:10.1002/1522-2624(200208)165:4<451::AID-JPLN451>3.0.CO;2-B, 2002.

Kaiser, K., Guggenberger, G. and Haumaier, L.: Changes in dissolved lignin-derived phenols, neutral sugars, uronic acids, and amino sugars with depth in forested Haplic Arenosols and Rendzic Leptosols, *Biogeochemistry*, 70(1), 135–151, 2004.

Kalbitz, K. and Kaiser, K.: Contribution of dissolved organic matter to carbon storage in forest mineral soils, *J. Plant Nutr. Soil Sci.*, 171(1), 52–60, doi:10.1002/jpln.200700043, 2008.

Kohl, L., Laganière, J., Edwards, K. A., Billings, S. A., Morrill, P. L., Van Biesen, G. and Ziegler, S. E.: Distinct fungal and bacterial  $\delta^{13}\text{C}$  signatures as potential drivers of increasing  $\delta^{13}\text{C}$  of soil organic matter with depth, *Biogeochemistry*, 124(1), 13–26, doi:10.1007/s10533-015-0107-2, 2015.

Kramer, C., Trumbore, S., Fröberg, M., Cisneros Dozal, L. M., Zhang, D., Xu, X., Santos, G. M. and Hanson, P. J.: Recent (<4 year old) leaf litter is not a major source of microbial carbon in a temperate forest mineral soil, *Soil Biol. Biochem.*, 42(7), 1028–1037, doi:10.1016/j.soilbio.2010.02.021, 2010.

Lajtha, K., Townsend, K. L., Kramer, M. G., Swanston, C., Bowden, R. D. and Nadelhoffer, K.: Changes to particulate versus mineral-associated soil carbon after 50 years of litter manipulation in forest and prairie experimental ecosystems, *Biogeochemistry*, 119(1), 341–360, doi:10.1007/s10533-014-9970-5, 2014a.

Lajtha, K., Bowden, R. D. and Nadelhoffer, K.: Litter and root manipulations provide insights into soil organic matter dynamics and stability, *Soil Sci. Soc. Am. J.*, 78(S1), S261–S269, doi:10.2136/sssaj2013.08.0370nafsc, 2014b.

Leinemann, T., Mikutta, R., Kalbitz, K., Schaarschmidt, F. and Guggenberger, G.: Small scale variability of vertical water and dissolved organic matter fluxes in sandy Cambisol subsoils as revealed by segmented suction plates, *Biogeochemistry*, 131(1–2), 1–15, doi:10.1007/s10533-016-0259-8, 2016.

## Study I

---

Leinemann, T., Preusser, S., Mikutta, R., Kalbitz, K., Cerli, C., Höschen, C., Mueller, C. W., Kandeler, E. and Guggenberger, G.: Multiple exchange processes on mineral surfaces control the transport of dissolved organic matter through soil profiles, *Soil Biol. Biochem.*, 118, 79–90, doi:10.1016/j.soilbio.2017.12.006, 2018.

Liebmann, P., Wordell-Dietrich, P., Kalbitz, K., Mikutta, R., Kalks, F., Don, A., Woche, S. K., and Guggenberger, G.: Soil profile description from the research site Grunderwald, part of the research unit SubSOM (Version 1.0) (Data set), BonaRes Data Centre (ZALF), <https://doi.org/10.20387/BONARES-HZGX-GB9S>, 2020.

Liebmann, P., Wordell-Dietrich, P., Kalbitz, K., Mikutta, R., Kalks, F., Don, A., Woche, S. K., and Guggenberger, G.: Litter manipulation experiment Grunderwald – Bulk soil data from soil core samples (Version 1.0) (Data set), BonaRes Data Centre (ZALF), <https://doi.org/10.20387/BONARES-69H2-56Q9>, 2020.

Liebmann, P., Wordell-Dietrich, P., Kalbitz, K., Mikutta, R., Kalks, F., Don, A., Woche, S. K., and Guggenberger, G.: Litter manipulation experiment Grunderwald – Density fractionation data from soil core samples (Version 1.0) (Data set), BonaRes Data Centre (ZALF), <https://doi.org/10.20387/BONARES-DNDW-5T58>, 2020.

Majdi, H.: Changes in fine root production and longevity in relation to water and nutrient availability in a Norway spruce stand in northern Sweden, *Tree Physiol.*, 21(14), 1057–1061, doi:10.1093/treephys/21.14.1057, 2001.

Marschner, B. and Kalbitz, K.: Controls of bioavailability and biodegradability of dissolved organic matter in soils, *Geoderma*, 113(3–4), 211–235, doi:10.1016/S0016-7061(02)00362-2, 2003.

McKeague, J. A. and Day, J. H.: Dithionite and oxalate-extractable Fe and Al as aids in differentiating various classes of soils, *Can. J. Soil Sci.*, 46(1), 13–22, doi:10.4141/cjss66-003, 1966.

Mehra, O. P. and Jackson, M. L.: Iron oxide removal from soils and clays by a dithionite-citrate system buffered by sodium bicarbonate, in *Clays and Clay Minerals*, edited by E. Ingerson, pp. 317–327, Pergamon., 1960.

Meier, I. C., Leuschner, Ch. and Hertel, D.: Nutrient return with leaf litter fall in *Fagus sylvatica* forests across a soil fertility gradient, *Plant Ecol.*, 177(1), 99–112, doi:10.1007/s11258-005-2221-z, 2005.

Mikutta, R., Turner, S., Schippers, A., Gentsch, N., Meyer-Stüve, S., Condon, L. M., Peltzer, D. A., Richardson, S. J., Eger, A., Hempel, G., Kaiser, K., Klotzbücher, T. and Guggenberger, G.: Microbial and abiotic controls on mineral-associated organic matter in soil profiles along an ecosystem gradient, *Sci. Rep.*, 9(1), 1–9, doi:10.1038/s41598-019-46501-4, 2019.

Moore-Kucera, J. and Dick, R. P.: Application of <sup>13</sup>C-labeled litter and root materials for in situ decomposition studies using phospholipid fatty acids, *Soil Biol. Biochem.*, 40(10), 2485–2493, doi:10.1016/j.soilbio.2008.06.002, 2008.

Nadelhoffer, K. J. and Fry, B.: Controls on natural nitrogen-15 and carbon-13 abundances in forest soil organic matter, *Soil Sci. Soc. Am. J.*, 52(6), 1633–1640, doi:10.2136/sssaj1988.03615995005200060024x, 1988.

Nadelhoffer, K. J. and Raich, J. W.: Fine root production estimates and belowground carbon allocation in forest ecosystems, *Ecology*, 73(4), 1139–1147, doi:10.2307/1940664, 1992.

## Study I

---

Nielsen, D. R. and Wendroth, O.: Spatial and temporal statistics: sampling field soils and their vegetation., *Spat. Temporal Stat. Sampl. Field Soils Their Veg.* [online] Available from: <https://www.cabdirect.org/cabdirect/abstract/20033041440> (Accessed 20 August 2019), 2003.

North, P. F.: Towards an absolute measurement of soil structural stability using ultrasound, *J. Soil Sci.*, 27(4), 451–459, doi:10.1111/j.1365-2389.1976.tb02014.x, 1976.

Rasse, D. P., Rumpel, C. and Dignac, M.-F.: Is soil carbon mostly root carbon? Mechanisms for a specific stabilisation, *Plant Soil*, 269(1–2), 341–356, doi:10.1007/s11104-004-0907-y, 2005.

Rumpel, C. and Kögel-Knabner, I.: Deep soil organic matter—a key but poorly understood component of terrestrial C cycle, *Plant Soil*, 338(1–2), 143–158, doi:10.1007/s11104-010-0391-5, 2011.

Rumpel, C., Chabbi, A. and Marschner, B.: Carbon storage and sequestration in subsoil horizons: Knowledge, gaps and potentials, in *Recarbonization of the Biosphere*, edited by R. Lal, K. Lorenz, R. F. Hüttl, B. U. Schneider, and J. von Braun, pp. 445–464, Springer Netherlands, Dordrecht., 2012.

Salomé, C., Nunan, N., Pouteau, V., Lerch, T. Z. and Chenu, C.: Carbon dynamics in topsoil and in subsoil may be controlled by different regulatory mechanisms, *Glob. Change Biol.*, 16(1), 416–426, doi:10.1111/j.1365-2486.2009.01884.x, 2010.

Sanderman, J. and Amundson, R.: A comparative study of dissolved organic carbon transport and stabilization in California forest and grassland soils, *Biogeochemistry*, 89(3), 309–327, doi:10.1007/s10533-008-9221-8, 2008.

Scheel, T., Dörfler, C. and Kalbitz, K.: Precipitation of dissolved organic matter by aluminum stabilizes carbon in acidic forest soils, *Soil Sci. Soc. Am. J.*, 71(1), 64–74, 2007.

Schiedung, M., Don, A., Wordell-Dietrich, P., Alcántara, V., Kuner, P. and Guggenberger, G.: Thermal oxidation does not fractionate soil organic carbon with differing biological stabilities, *J. Plant Nutr. Soil Sci.*, 180(1), 18–26, doi:10.1002/jpln.201600172, 2016.

Schmidt, M. W. I., Torn, M. S., Abiven, S., Dittmar, T., Guggenberger, G., Janssens, I. A., Kleber, M., Kögel-Knabner, I., Lehmann, J., Manning, D. A. C., Nannipieri, P., Rasse, D. P., Weiner, S. and Trumbore, S. E.: Persistence of soil organic matter as an ecosystem property, *Nature*, 478(7367), 49–56, doi:10.1038/nature10386, 2011.

Schrumpf, M., Kaiser, K., Guggenberger, G., Persson, T., Kögel-Knabner, I. and Schulze, E.-D.: Storage and stability of organic carbon in soils as related to depth, occlusion within aggregates, and attachment to minerals, *Biogeosciences*, 10(3), 1675–1691, doi:10.5194/bg-10-1675-2013, 2013.

Sheldrick, B. H. and McKeague, J. A.: A comparison of extractable Fe and Al data using methods followed in the USA and Canada, *Can. J. Soil Sci.*, 55(1), 77–78, doi:10.4141/cjss75-012, 1975.

Six, J., Guggenberger, G., Paustian, K., Haumaier, L., Elliott, E. T. and Zech, W.: Sources and composition of soil organic matter fractions between and within soil aggregates, *Eur. J. Soil Sci.*, 52(4), 607–618, doi:10.1046/j.1365-2389.2001.00406.x, 2001.

Tipping, E., Chamberlain, P. M., Fröberg, M., Hanson, P. J. and Jardine, P. M.: Simulation of carbon cycling, including dissolved organic carbon transport, in forest soil locally enriched with <sup>14</sup>C, *Biogeochemistry*, 108(1–3), 91–107, doi:10.1007/s10533-011-9575-1, 2012.

## Study I

---

Trumbore, S. E., Schiff, S. L., Aravena, R. and Elgood, R.: Sources and transformation of dissolved organic carbon in the harp lake forested catchment: The role of soils, *Radiocarbon*, 34(3), 626–635, doi:10.1017/S0033822200063918, 1992.

Tückmantel, T., Leuschner, C., Preusser, S., Kandeler, E., Angst, G., Mueller, C. W. and Meier, I. C.: Root exudation patterns in a beech forest: Dependence on soil depth, root morphology, and environment, *Soil Biol. Biochem.*, 107, 188–197, doi:10.1016/j.soilbio.2017.01.006, 2017.

Wiesmeier, M., Urbanski, L., Hobley, E., Lang, B., von Lützw, M., Marin-Spiotta, E., van Wesemael, B., Rabot, E., Ließ, M., Garcia-Franco, N., Wollschläger, U., Vogel, H.-J. and Kögel-Knabner, I.: Soil organic carbon storage as a key function of soils - A review of drivers and indicators at various scales, *Geoderma*, 333, 149–162, doi:10.1016/j.geoderma.2018.07.026, 2019.

Wilkinson, M. T., Richards, P. J. and Humphreys, G. S.: Breaking ground: Pedological, geological, and ecological implications of soil bioturbation, *Earth-Sci. Rev.*, 97(1), 257–272, doi:10.1016/j.earscirev.2009.09.005, 2009.

Wordell-Dietrich, P., Don, A., Wotte, A., Rethemeyer, J., Bachmann, J., Helfrich, M., Kirfel, K. and Leuschner, C.: Vertical partitioning of CO<sub>2</sub> production in a Dystric Cambisol, *Biogeosciences Discuss.*, 1–27, doi:10.5194/bg-2019-143, 2019.

Zsolnay, A., Baigar, E., Jimenez, M., Steinweg, B. and Saccomandi, F.: Differentiating with fluorescence spectroscopy the sources of dissolved organic matter in soils subjected to drying, *Chemosphere*, 38(1), 45–50, doi:10.1016/S0045-6535(98)00166-0, 1999.

### Study I – Supplementary material

#### S1 Methods

##### S1.1 Surface element analysis

X-ray photoelectron spectroscopy (XPS) analysis was performed with an Axis Ultra DLD instrument (Kratos Analytical, Manchester, UK), using monochromatic AlK $\alpha$  radiation (1486.6 eV), operated at 20 mA and 10 kV. Survey spectra were recorded with a pass energy of 160 eV, a dwell time of 500 ms, and a resolution of 1 eV, while C 1s detail scans were obtained with a pass energy of 20 eV, a dwell time of 259.7 ms, and a resolution of 0.1 eV, with three sweeps per measurement cycle. The take-off angle was 0° and ultra-high vacuum during measurement was  $4 \times 10^{-7}$  Pa. For measurement, the HF was fixed on a sample bar with carbon conductive tape (Agar Scientific Elektron Technology UK Ltd., Stansted, UK) with an area of about 15 mm<sup>2</sup>. Per sample, three spots were measured, comprising an area of 300 × 700  $\mu$ m each in the slot modus. For charge compensation the neutralizer was active during measurement, however, complete compensation was not possible and the survey spectra were corrected relative to the Si 2p peak at a binding energy of 103 eV (Si-O bond, Okada et al., 1998; Woche et al., 2017). Survey spectra were quantified with the software Vision 2 (Kratos Analytical, Manchester, UK), using a linear baseline and the implemented relative sensitivity factors. The content of all detected elements is given in atomic percent (atom-%).

## Study I – Supplementary material

### S2 Tables

**Table S1** Relevant standard substances included in-the EA-IRMS measurements for calibration, correction, and quality control.

Substance	Company	Characteristics*
Quartz sand** (Blank)	In-house standard	
High organic sediment (HOS)	IVA Analysetechnik, Meerbusch, Germany	7.17 % C; 0.57 % N
Cellulose	IAEA***	-24.72 $\delta^{13}\text{C}$ [‰]
Caffeine	IAEA***	-27.77 $\delta^{13}\text{C}$ [‰]
CaCO <sub>3</sub>	In-house standard	-8.17 $\delta^{13}\text{C}$ [‰]
Needle litter	In-house standard	

\*Please note that all data presented in this study were corrected by using the given values only. Excluded properties are not part of this publication.

\*\*Washed with HCl and glowed at 1040°C

\*\*\*International Atomic Energy Agency, Seibersdorf Laboratory, Vienna, Austria

**Table S2** Contents of dithionite- and oxalate-extractable Fe (Fe<sub>d</sub> resp. Fe<sub>o</sub>) and oxalate-extractable Al (Al<sub>o</sub>) and Mn (Mn<sub>o</sub>). Extractions were conducted for the samples from the first sampling in November 2016. Data show the mean (n = 6) with the standard deviation in brackets.

Depth increment [cm]	Fe <sub>d</sub> [mg g <sup>-1</sup> ]	Fe <sub>o</sub> [mg g <sup>-1</sup> ]	Al <sub>o</sub> [mg g <sup>-1</sup> ]	Mn <sub>o</sub> [mg g <sup>-1</sup> ]
0-5	2.38 (0.21)	1.03 (0.22)	0.56 (0.16)	0.29 (0.31)
5-10	2.42 (0.66)	1.13 (0.53)	0.50 (0.10)	0.05 (0.04)
10-20	2.71 (0.33)	1.51 (0.33)	0.64 (0.18)	0.14 (0.20)
20-30	2.42 (0.36)	1.22 (0.22)	1.05 (0.21)	0.38 (0.43)
30-40	2.11 (0.25)	0.95 (0.14)	1.31 (0.23)	0.58 (0.43)
40-50	1.87 (0.21)	0.75 (0.09)	1.08 (0.13)	0.51 (0.37)
50-60	1.70 (0.16)	0.60 (0.11)	0.94 (0.11)	0.53 (0.18)
60-70	1.65 (0.33)	0.51 (0.14)	0.64 (0.11)	0.61 (0.17)
70-80	1.84 (0.89)	0.45 (0.18)	0.48 (0.16)	0.54 (0.16)
80-90	1.68 (0.62)	0.40 (0.20)	0.38 (0.13)	0.70 (0.24)
90-100	1.65 (0.70)	0.40 (0.22)	0.35 (0.13)	0.58 (0.18)
100-120	1.99 (1.14)	0.49 (0.36)	0.40 (0.20)	0.68 (0.33)
120-140	2.47 (1.88)	0.60 (0.51)	0.41 (0.25)	0.57 (0.37)
140-160	2.04 (2.12)	0.42 (0.49)	0.29 (0.26)	0.57 (0.25)
160-180	1.15 (0.83)	0.23 (0.18)	0.16 (0.08)	0.89 (0.24)

S3 Figures

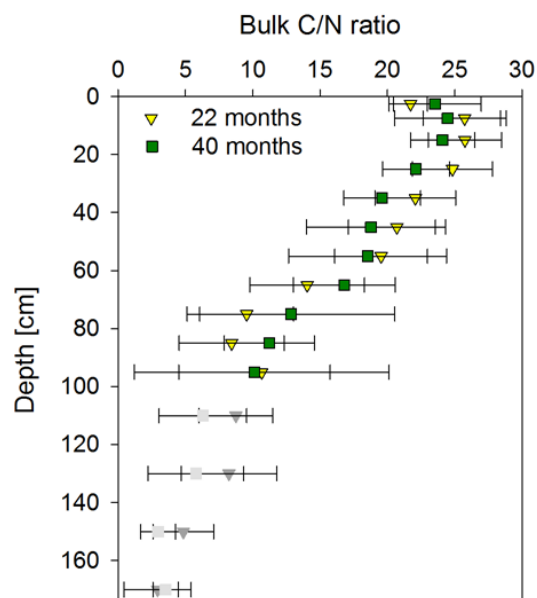


**Figure S1** Mean C/N ratio of the bulk soil from both sampling times, 22 months and 40 months after labeled litter application. Data show the mean of 6 samples and error bars show the standard deviation. The y-axis shows the mean depth of each soil increment. Nitrogen contents of the MAOM fraction were corrected for extractable nitrate and ammonium contents. Nitrogen contents in samples below 100 cm were increasingly below the detection limit and not reliable, therefore C/N ratios are marked in grey.

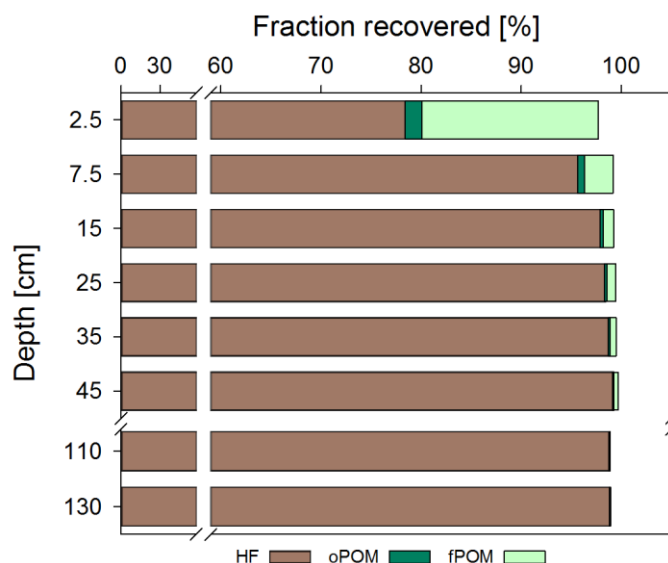


**Figure S2** Mean mass recovery and fraction distribution of the soil density fractions heavy fraction (HF), occluded particulate organic matter (oPOM), and free particulate organic matter (fPOM) as the mean of both sampling times (November 2016 and May 2018). The y-axis shows the mean depth of each soil increment. Bars show the mean of 12 samples, the standard deviation varied for HF between 0.3-15 %, for oPOM between 0.1-1.6 %, and for fPOM between 0.1-18 %. Please note that for better visibility, both axes have breaks.



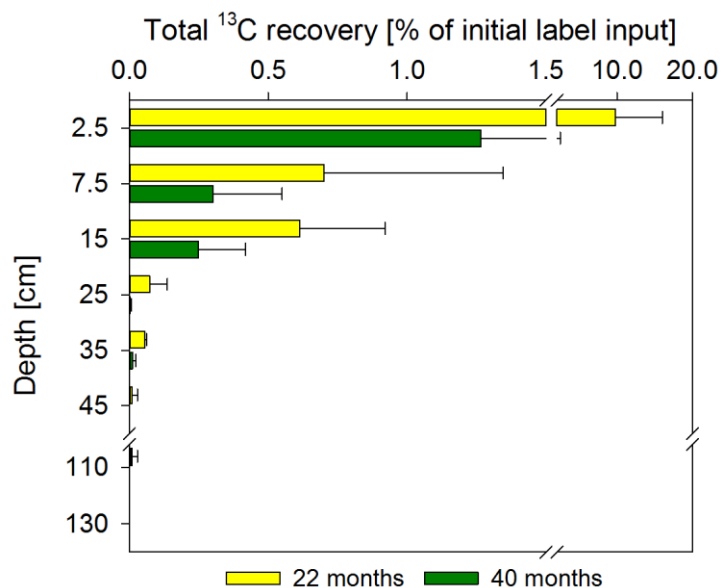


**Figure S3** Mean  $^{13}\text{C}$  recovered at each sampling time, 22 months and 40 months after labeled litter application, in % of the initial label input ( $n = 3$ ). Bars show the sum of all fractions per depth increments, error bars depict the standard deviation. According to ANOVA analysis, there were no significant differences ( $p > 0.05$ ) in the total recovered  $^{13}\text{C}$  per depth increment between both sampling times, except of the depth 30-40 cm ( $p = 0.004$ ). Please note that for better visibility, both axes have breaks.

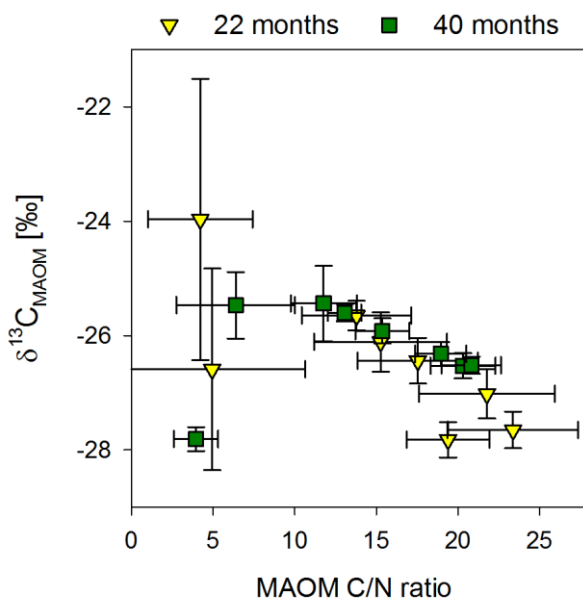


**Figure S4** Correlation of the  $^{13}\text{C}$  abundance of the mineral-associated organic matter ( $C_{\text{MAOM}}$ ) in the unlabeled control samples on the Y-axis and the corresponding C/N ratio on the X-axis from both sampling times, 22 months and 40 months after labeled litter application. Data show the mean of three replicates, error bars depict the standard deviation. Spearman correlation resulted in a significant negative correlation for both variables for the first sampling in November 2016 ( $r = -0.677$ ,  $p < 0.05$ ) and the second sampling in May 2018 ( $r = -0.883$ ,  $p < 0.05$ ).

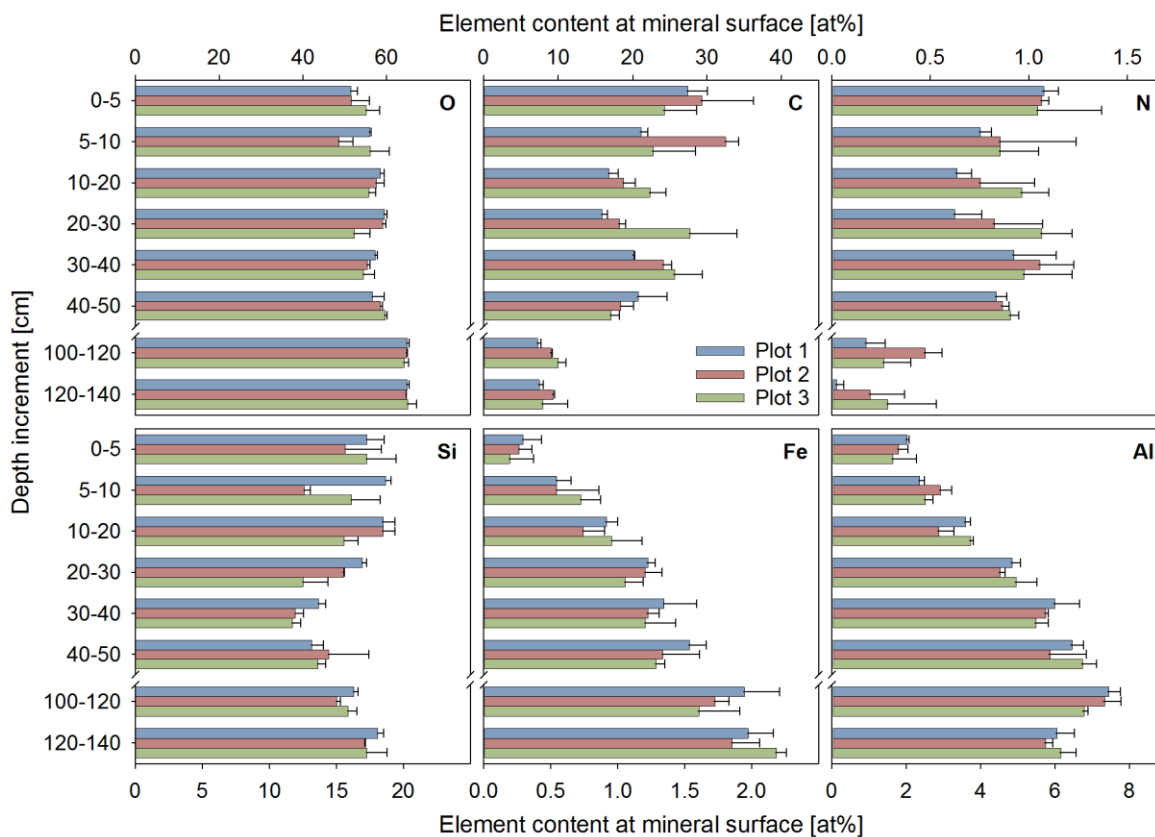


**Figure S5** Contents of selected elements on the heavy fraction (HF) mineral surface layer according to XPS analysis. Bars show the mean of three spots measured per sample per plot and depth increment, error bars represent the standard deviation. Please note that the X-axis have different scales. Please note, element contents were highly correlated as a function of soil depth. Negative correlations were observed for example for Fe-C ( $r^2 = 0.82$ ,  $p = 0.0021$ ) and Al-C ( $r^2 = 0.58$ ,  $p = 0.0295$ ). Positive correlations were observed for example for Fe-Al ( $r^2 = 0.85$ ,  $p = 0.0012$ ) and C-N ( $r^2 = 0.90$ ,  $p = 0.0004$ ).

### S4 References

Okada, K., Kameshima, Y., Yasumori, A., 1998. Chemical shifts of silicon X-ray photoelectron spectra by polymerization structures of silicates. *J. Am. Ceram. Soc.* 81, 1970–1972. <https://doi.org/10.1111/j.1151-2916.1998.tb02579.x>

Woche, S.K., Goebel, M.-O., Mikutta, R., Schurig, C., Kaestner, M., Guggenberger, G., Bachmann, J., 2017. Soil wettability can be explained by the chemical composition of particle interfaces - An XPS study. *Sci. Rep.* 7, 42877. <https://doi.org/10.1038/srep42877>

### 3. Study II

#### **Fate and stability of dissolved organic carbon in topsoils and subsoils under beech forests**

**Contribution:** I was equally involved in the field work and sampling campaigns, conducted parts of the laboratory analysis (including bulk OC, TN, and  $\delta^{13}\text{C}$ , and dithionite- and oxalate-extractable Fe, Al, Mn), and contributed to the manuscript writing.

**Published in:** *Biogeochemistry*, 1-18, 2020.

**Paper:** [doi.org/10.1007/s10533-020-00649-8](https://doi.org/10.1007/s10533-020-00649-8)

# **Fate and stability of dissolved organic carbon in topsoils and subsoils under beech forests**

Fabian Kalks<sup>a\*</sup>, Patrick Liebmann<sup>b</sup>, Patrick Wordell-Dietrich<sup>c</sup>, Georg Guggenberger<sup>b</sup>, Karsten Kalbitz<sup>c</sup>, Robert Mikutta<sup>d</sup>, Mirjam Helfrich<sup>a</sup>, Axel Don<sup>a</sup>

<sup>a</sup>Thünen Institute of Climate-Smart Agriculture, Bundesallee 65, 38116 Braunschweig, Germany

<sup>b</sup>Institute of Soil Science, Leibniz University Hannover, Herrenhäuser Str. 2, 30419 Hannover, Germany

<sup>c</sup>Institute of Soil Science and Site Ecology, Technische Universität Dresden, Piener Straße 19, 01737 Tharandt, Germany

<sup>d</sup>Faculty of Natural Sciences III, Martin-Luther-University Halle-Wittenberg, Von-Seckendorff-Platz 3, 06120 Halle, Germany

\*Corresponding author: [fabian.kalks@thuenen.de](mailto:fabian.kalks@thuenen.de) + 49 531 596 2719

Received: 15 October 2019 / Accepted: 17 February 2020 / Published online: 09 March 2020

## Study II

---

**Abstract.** Dissolved organic carbon (DOC) from Oa horizons has been proposed to be an important contributor for subsoil organic carbon stocks. We investigated the fate of DOC by directly injecting a DOC solution from  $^{13}\text{C}$  labelled litter into three soil depths at beech forest sites. Fate of injected DOC was quantified with deep drilling soil cores down to 2 m depth, 3 and 17 months after the injection.  $27 \pm 26\%$  of the injected DOC was retained after 3 months and  $17 \pm 22\%$  after 17 months. Retained DOC was to 70% found in the first 10 cm below the injection depth and on average higher in the topsoil than in the subsoil. After 17 months DOC in the topsoil was largely lost (- 19%) while DOC in the subsoil did not change much (- 4.4%). Data indicated a high stabilisation of injected DOC in the subsoils with no differences between the sites. Potential mineralisation as revealed by incubation experiments however, was not different between DOC injected in topsoil or subsoils underlining the importance of environmental factors in the subsoil for DOC stabilisation compared to topsoil. We conclude that stability of DOC in subsoil is primary driven by its spatial inaccessibility for microorganisms after matrix flow while site specific properties did not significantly affect stabilisation. Instead, a more fine-textured site promotes the vertical transport of DOC due to a higher abundance of preferential flow paths.

### Keywords

Forest subsoils; Cascade model; Incubation experiment;  $^{13}\text{C}$ ; Field experiment

### Introduction

Subsoils have been recognised as an overlooked key component of the terrestrial carbon pool, containing between 27 and 77% of soil organic carbon (SOC) in mineral soils (Harrison et al. 2011; Rumpel and Kogel-Knabner 2011). Especially forest soils represent an important component of the global C cycle, due to their higher C stocks as compared to arable soils (Poeplau et al. 2011). Organic C in subsoils is characterised by generally high mean residence times and thus high mean apparent  $^{14}\text{C}$  ages (Rumpel et al. 2002; Voort et al. 2016; Wang et al. 1996). Beside roots, dissolved organic carbon (DOC) is a major source of fresh carbon (C) that enters subsoils (Kaiser and Guggenberger 2000). Nevertheless, quantitative data on the contribution and turnover of different compounds such as DOC entering subsoils are scarce (Kögel-Knabner 2017). The results from two synthesis papers showed that the input of DOC into forest subsoils is much higher than the output via leaching which means that a considerable portion of DOC is retained or mineralised in the subsoil (Kindler et al. 2011; Michalzik et al. 2001). Kalbitz and Kaiser (2008) estimated the contribution of DOC to the subsoil C stock of a Podzol to be in the range of 25 – 66% for the B and C horizon. Consequent questions are inter alia: what is the origin of this DOC, how does it reach subsoils and what drives its stability if it is stable at all?

In general there are different pathways how DOC can reach subsoil horizons. One way is the direct transport to subsoils via preferential flow paths (Hagedorn et al. 2015), which is particularly taking place at heavy rainfall events (Kaiser and Guggenberger 2005). Another possibility is the “*continuous sorption and precipitation, combined with microbial processing and subsequent desorption and dissolution*” as it was described by Kaiser and Kalbitz (2012) and is referred to as the cascade model. This model can explain higher  $^{14}\text{C}$  ages of organic C and of DOC in subsoils and has been confirmed in a laboratory flow experiment by Leinemann et al. (2018), where the mobilisation and replacement of mineral-associated organic matter by percolating DOC was quantified. Accordingly in a laboratory experiment Hagedorn et al. (2015) tested the importance of DOC from fresh litter along a soil chronosequence. They found that DOC was retained in the uppermost centimetres of the mineral soil, whereas non litter derived soil organic matter is leached. Conversely Rothstein et al. (2018) showed in a field experiment that the organic horizon and the subsoil of a Podzol are directly linked. In their study around 80% of the C entering the subsoil derived from the organic layer while the rest derived from DOC that was produced during the passage of water through the topsoil. Until now there are no field experiments, testing the effect of different substrates and textural differences on the transport of DOC in topsoils and subsoils. Since the saturated water conductivity strongly depends on the texture of a soil (Saxton and Rawls 2006) one should expect large differences in the DOC transport between a clayey and a sandy soil.

Furthermore, not the fresh litter as it was used by Hagedorn et al. (2015), but the humified organic layer (Oa horizon) is recognised as the main source for DOC reaching partly also deeper soil horizons

## Study II

---

(Qualls and Haines 1992; Rothstein et al. 2018; Schulze et al. 2011). It has been shown that DOC from Oa horizons has a higher stability than that from fresh litter, both in solution and associated with the mineral phase (Don and Kalbitz 2005; Kalbitz et al. 2005). This is due to the different composition of DOC released from the differently degraded forest floor horizons (Klotzbücher et al. 2013). Dissolved organic carbon from Oa horizons is characterised by a much greater aromaticity, complexity of molecules and smaller content of carbohydrates compared to DOC from fresh litter, leading to stronger sorption and higher intrinsic stability (Kalbitz et al. 2005). DOC from fresh beech litter for example, can be mineralised by 65% within 90 days while DOC from degraded and humified beech litter could be mineralised by 9.1% only within the same time in a liquid incubation experiment from Kalbitz et al. (2003). The amount of organic carbon (OC) that is dissolved from the different organic layers and in the mineral topsoil thereby depends on seasonal, pedological, vegetational and microbial characteristics (Don and Schulze 2008; Guggenberger et al. 1994; Kögel-Knabner 2002; Lee et al. 2018). Consequently it should behave in a different way compared to DOC from fresh litter during its passage through the soil. To the best of our knowledge there are no field experiments testing the behaviour of DOC derived from humified organic layers within a soil profile and also if different soil and environmental conditions play a role. But this would be important to know, since subsoils underlie different environmental conditions than topsoils which influence organic matter decomposability and stabilisation. This is, e.g., due to lower SOC contents (Don et al. 2013; Rumpel and Kögel-Knabner 2011), different microbial communities (Agnelli et al. 2004), different water and oxygen availabilities (Schneider et al. 2017), temperature dependent effects (Tückmantel et al. 2017), or the availability of fresh organic matter inputs (Fontaine et al. 2007). Most studies indicate, that rather physical protection mechanisms than inherent recalcitrance are responsible for long-term stabilisation of SOC (Marschner et al. 2008; Schöning and Kögel-Knabner 2006; von Lützow et al. 2008) and that SOC turnover is governed by microbial accessibility (Dungait et al. 2012). As DOC reaches the subsoil it gets sorbed to the mineral phase and is part of SOC. Thereby sorption of DOC in subsoils is related to the amount of clay sized particles like phyllosilicates (Barré et al. 2014) or iron- and aluminium (hydr)oxides (Kaiser and Zech 1996; Kindler et al. 2011). In acidic subsoils, especially poorly crystalline minerals have been considered to exert a large impact on organic matter stabilization (Mikutta et al. 2006). In a sorption experiment, Kaiser and Guggenberger (2000) have shown that on the other hand a high coverage of mineral surfaces with organic matter reduces the availability of these surfaces to adsorb DOC. Consequently, subsoils should be more capable for DOC sorption and stabilisation compared to topsoils and fine textured soils with higher capacities of free sorption sites should be more capable than coarse textured soils. A critical step to test these assumptions under field conditions is to detect the source of DOC and its fate in top- and subsoils, because in all parts of the soil DOC is produced by solubilisation of SOC or root litter and influenced by sorption/desorption processes, transport and microbial consumption. Even though DOC fluxes reaching the subsoil are small, their contribution to build up



## Study II

---

stabilised SOC in subsoils may be large (Hagedorn et al. 2012; Kalbitz et al. 2007). Isotopic labelling techniques are useful tools to follow the fate of DOC (Fröberg et al. 2009; Hagedorn et al. 2015; Kammer and Hagedorn 2011). Furthermore, laboratory experiments may be useful to identify distinct processes participating in the DOC turnover, but the combined effect of microbial turnover and flux conditions on the role and fate of DOC in subsoils can be only realistically quantified under field conditions. To the best of our knowledge, there is only the field study from Rothstein et al. (2018), that assesses the DOC contribution to subsoils. And this study is restricted to one soil type and the authors could not distinguish between roots and SOC from O horizons as source for DOC.

Thus, the goal of this study was to assess the stability of DOC in topsoils and subsoils under beech forest from different soil parent materials. Our approach was to inject  $^{13}\text{C}$ -labelled DOC from decomposed beech litter into topsoil, upper subsoil and deeper subsoil horizons of different beech forest sites. The soils include two Cambisols and a Luvisol. This allowed us to directly assess the stability of DOC under field conditions as it was proposed by Schmidt et al. (2011) and Campbell and Paustian (2015). The stability of indigenous SOC and of SOC derived from DOC sorption was assessed by a laboratory incubation experiment. We tested the hypotheses that (i) more injected DOC is retained in subsoils than in topsoils and in fine textured soils compared to coarse textured soils, due to higher capacity of free sorption sites, (ii) coarse textured soils facilitate a more homogeneous and deeper translocation of injected DOC than fine textured soils, and (iii) retained DOC is more stable in subsoils than in topsoils.

### Material and methods

#### Site description

The field experiments were conducted at three sites under beech forest (*Fagus sylvatica*) with soils derived from different parent material (sand, red sandstone and loess). The soil at the first experimental site (near Nienburg (Weser), 51°34'41.34" N, 10°3'54.6192 E) was classified as a Dystric Cambisol developed on Pleistocene fluvial and aeolian sandy deposits and will be referred to as "Sand" in the following. The mean annual temperature at this site is 9.7 °C and the annual precipitation amounts to 762 mm (Leinemann et al. 2016). The soil at the second site (near Ebergötzen, 51°34'41.34" N, 10°3'54.6192 E) was a Dystric Cambisol, developed on Triassic upper red sandstone and therefore will be referred to as "Red Sandstone" in the following. Mean annual temperature and precipitation at this site are 8.3 °C and 794 mm respectively. The soil at the third site (near Rüdershausen, 51°34'47.532" N, 10°14'33.8424 E) was a Luvisol developed on loess deposits. This site will be referred to as "Loess" and has a mean annual temperature of 8.5 °C and an average annual precipitation of 733 mm. For further details about the three sites see Kirfel et al. (2019). Selected soil properties are summarised in Table 1.

### Injection experiment

To trace the fate of DOC from decomposed litter in different soil layers, a  $^{13}\text{C}$ -labelled DOC solution derived from  $^{13}\text{C}$ -labelled beech litter was directly injected into three different depths increments at the three experimental sites from 7 May to 6 June 2017. We use the term DOC even though it is organic matter that comprises also other elements than carbon. The depths chosen for injection were 10, 50 and 100 cm. Due to the shallower soil development at the Red Sandstone, the injection there was set to 10, 30 and 60 cm depth. In the following, the depth increments are referred to as “Topsoil”, “Upper Subsoil” and “Deeper Subsoil”, respectively. To prepare the injection into the Upper and Deeper Subsoil, three pits per site were excavated down to 150 cm depth. These pits were located approximately 50 m apart from each other (Fig. 1). One horizontal shaft was cut into the profile wall for Upper Subsoil injection and one on the opposite site of the soil pit for the Deeper Subsoil injection. For the Topsoil injection, the upper 10 cm of the mineral soil was removed as an intact soil block, directly adjacent to the respective pit for the Upper and Deeper Subsoil. The DOC solution was produced by mixing decomposed  $^{13}\text{C}$ -labelled beech litter ( $\delta^{13}\text{C}$  of  $\sim 468$  ‰) with de-ionised water in a 1:10 ratio for 12 hours in a 250 l barrel with an electric stirrer. The decomposed beech litter consisted of a mixture of highly labelled beech litter (10 atom-%, IsoLife, Wageningen, The Netherlands) and unlabelled beech litter. This mixture was used in a field experiment for 22 months (Liebmann et al. 2020) before it was removed and used as  $\text{DO}^{13}\text{C}$  source in this experiment. The obtained solution was pre-filtered to 2 mm via a tissue and finally filtered via cross-flow filtration (CMB 090, Microdyn-Nadir, Wuppertal, Germany) to  $< 0.2$   $\mu\text{m}$ . In total, 150 l of  $^{13}\text{C}$ -labelled DOC solution was produced. The DOC concentration of the solution was  $200 \text{ mg l}^{-1}$  with a  $\delta^{13}\text{C}$  value of 286 ‰. The DOC solution was injected with three field replicates (plots) per site. Additionally, one control plot per site was prepared with a 1 mmol  $\text{CaCl}_2$  solution being injected to test for disturbance and injection effects. Immediately before this solution was injected, one DOC sample per site was taken and frozen for further analyses. A qualitative analysis revealed a similar composition for all injected DOC samples. Further details are provided in the supplement (Table A1).

The injection was conducted with syringes which were filled with the DOC solution. Syringes were connected to 25 needles and combined at regular grid with on  $20 \times 20$  cm plates. Plates were horizontally placed into the shafts and for the topsoil onto the excavated soil and the solution was slowly injected into the profile (Fig. 2). In total 1.8 l of the DOC solution was injected into an area of  $400 \text{ cm}^2$  corresponding to an added amount of  $9 \text{ g DOC m}^{-2}$  and thus resembling a precipitation event of 45 mm. Three plates with syringes were injected adjacent to each other per shaft to enable three samplings and to reduce side effects. Especially at the Loess, former root channels were detected at some the profile walls. During injection, parts of the injected DOC flowed out of some of these channels, indicating preferential flow. After injection, plates were removed and the shafts as well as the profiles were carefully filled with soil

## Study II

---

from the same depth and compacted to original bulk density. At the Topsoil injection spots the removed soil block was carefully returned to the same location where it came from. The respective injection areas were marked with iron bars on top of the restored soil profiles.

### Sampling

In August 2017 and October 2018 (3 and 17 months after injection), three soil cores per site and injection depth, plus three adjacent control cores per site, were taken via a machine-driven percussion coring system (Nordmeyer Geotool, Berlin, Germany) (Fig. 1, plot 1-3). Additionally, three soil cores per site and injection depth from the CaCl<sub>2</sub>-control injection were sampled three months after injection (Fig. 1, plot 4). The amount of rainfall between injection and sampling after three months was as high as between 3 and 17 months after the injection due to a very dry summer period between the two sampling dates. In both periods of time precipitation amounted to ~ 300 mm at all three sites. Soil cores had a diameter of 6 cm and drilling depth was 100 cm below the respective injection depth, thus 200 cm deep for the Deep Subsoil injection. For the Red Sandstone, maximum drilling depth was 120 cm due to the shallow soil depth. Material above the injection depth was discarded. Material below the injection depth was separated into increments following defined depth Sects. (0-5, 5-10, 10-20, 20-30, 30-40, 40-50, 50-60, 60-80 and 80-100 cm below injection depth) resulting in 9 samples per core if possible and 934 samples in total for both samplings. For the Deeper Subsoil of the Red Sandstone, the deepest depth section consequently was 50-60 cm below injection depth. The respective control cores were separated into the same increments as the cores at the injection plots. Samples were filled into plastic bags and stored at 6°C until further processing.

**Table 1** Soil properties for the top 20 cm below the different injection depths. Values represent means and standard deviations of the DOC injection plots for a 20 cm depth increment (n = 9). Fe<sub>o</sub> and Al<sub>o</sub> represents the amount of poorly crystalline aluminosilicates and Fe hydroxides, Fe<sub>D</sub> the amount of poorly crystalline as well as crystalline iron oxides and BD is the bulk density of the fine soil.

Material	Horizon	Depth (cm)	SOC (mg g <sup>-1</sup> )	pH	C/N ratio	Clay (%)	Sand (%)	Fe <sub>o</sub> (mg g <sup>-1</sup> )	Al <sub>o</sub> (mg g <sup>-1</sup> )	Fe <sub>D</sub> (mg g <sup>-1</sup> )	BD (g cm <sup>-3</sup> )
Loess	Topsoil	10 - 30	6.7 (2.1)	3.6 (0.1)	10.5 (3.4)	11 (2)	2 (2)	3.0 (0.4)	1.3 (0.1)	6.1 (0.4)	1.10 (0.2)
	Upper Subsoil	50 - 70	1.3 (0.5)	3.7 (0.1)	5.8 (1.3)	9 (1)	2 (2)	2.8 (0.7)	1.2 (0.1)	9.0 (1.7)	1.32 (0.1)
	Deeper Subsoil	100 - 120	1.2 (0.3)	4.0 (0.1)	8.1 (3.3)	9 (1)	3 (3)	2.2 (0.5)	1.0 (0.2)	8.4 (0.9)	1.43 (0.2)
Red Sandstone	Topsoil	10 - 30	6.5 (2.3)	3.9 (0.3)	17.1 (2.4)	11 (2)	43 (8)	1.7 (0.1)	1.1 (0.1)	3.4 (0.2)	1.13 (0.1)
	Upper Subsoil	30 - 50	1.7 (0.8)	3.8 (0.3)	9.6 (3.2)	11 (3)	39 (12)	1.5 (0.8)	0.9 (0.6)	3.1 (1.1)	1.47 (0.2)
	Deeper Subsoil	60 - 80	0.9 (0.4)	3.7 (0.3)	6.2 (2.8)	9 (2)	30 (13)	1.3 (0.7)	0.7 (0.3)	2.9 (1.1)	1.17 (0.2)
Sand	Topsoil	10 - 30	9.9 (2.8)	3.8 (0.4)	25.9 (2.8)	3 (1)	64 (12)	1.3 (0.3)	0.9 (0.4)	2.7 (0.5)	1.19 (0.2)
	Upper Subsoil	50 - 70	2.2 (1.4)	4.2 (0.2)	15.4 (3.9)	3 (2)	73 (12)	0.6 (0.3)	1.0 (0.5)	1.7 (0.4)	1.54 (0.2)
	Deeper Subsoil	100 - 120	1.1 (1.3)	3.9 (0.2)	16.5 (20.3)	2 (1)	88 (8)	0.4 (0.4)	0.6 (0.6)	1.4 (0.6)	1.49 (0.2)

## Study II



**Fig. 1** Injection of DOC at 10 cm depth at the Red Sandstone site (left) and in 50 and 100 cm depth at the Loess site (right). Note that on the right site, the injection at 100 cm depth is shown. The injection at 50 cm depth was conducted on the opposite site. The injection area was designed for three possible samplings.

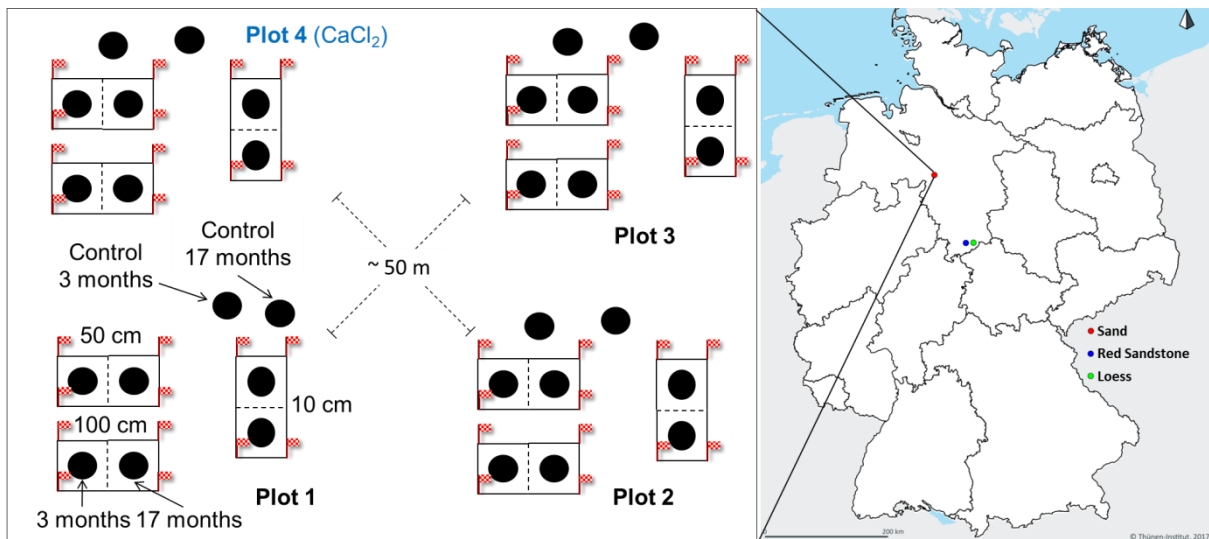


**Fig. 2** Concept of the sampling design for each of the three sites. The plots were approximately 50 m apart from each other. First sampling was conducted in August 2017, resulting in nine cores from the injection sites plus three respective control cores. Second sampling was conducted in October 2018. The water control ( $\text{CaCl}_2$ ) was completely sampled after 3 months.

### Chemical analyses and calculations

All soil samples were oven dried at  $60^\circ\text{C}$  and sieved to 2 mm. Subsamples were homogenised, ground in a ball mill, and analysed for inorganic C, total C and nitrogen by dry combustion in an elemental analyser (LECO TruMac, St. Joseph, MI, USA). Organic C content was calculated by the difference between total and inorganic C. Carbonate was present in only very few samples and in very low concentrations ( $< 0.025$

## Study II

---

weight %). Respective values for bulk density, pH and stone content were obtained from a formerly conducted regional site grid sampling at the same sites (Heinze et al. 2018). Oxalate extractions were conducted according to Schwertmann (1964) and McKeague and Day (1966) by using a 0.2 M ammonium oxalate solution (pH 3) to dissolve poorly crystalline aluminosilicates and Fe hydroxides like ferrihydrite as well as organic complexes (Fe<sub>o</sub>, Al<sub>o</sub>). Dithionite extractions were conducted according to Mehra and Jackson (2013), modified by Sheldrick and McKeague (1975), to extract poorly crystalline as well as crystalline iron oxides (Fe<sub>d</sub>, Al<sub>d</sub>).

Total SOC stocks (Mg ha<sup>-1</sup>) in each depth increment were calculated according Eq. 1,

$$\text{SOC stock} = \text{SOC} \cdot \text{BD} \cdot (1 - \text{stone content}) \cdot \text{depth} \cdot 0.1 \quad (1)$$

where *SOC* is the soil organic carbon content in the fine soil < 2-mm fraction (mg g<sup>-1</sup>), *BD* is the bulk density of the fine soil (g cm<sup>-3</sup>), the *stone content* is the volume based proportion of stones (cm<sup>3</sup> cm<sup>-3</sup>) and *depth* is the thickness of the depth increment (cm).

Homogenised samples were analysed for δ<sup>13</sup>C values in an isotope ratio mass spectrometer (Delta Plus, Thermo Fisher, Waltham, MA, USA) coupled to an elemental analyser (FLASH EA 1122 NA 1500; Wigan, United Kingdom). Because carbonate contents were so low and in the same range for a specific depth, we further measured δ<sup>13</sup>C without removing them to calculate the proportion of retained DOC. Resulting δ<sup>13</sup>C values (‰) were expressed relative to the international standard of Vienna Pee Dee Belemnite (V-PDB). δ<sup>13</sup>C values values from the labelled plots were compared with the upper quantile of a 90%-confidence interval from respective control samples calculated by Eq. 2:

$$x(Q_{95}) = \bar{x} + (s \cdot t_{\phi, \alpha}) \quad (2)$$

Thereby the upper 90%-quantile ( $x(Q_{95})$ ) is calculated by the mean ( $\bar{x}$ ) and standard deviation ( $s$ ) of the respective control samples from the same depth and both sampling dates ( $n = 6$ ) and the value from the Student t-distribution ( $t_{\phi, \alpha}$ ). Only when the δ<sup>13</sup>C value of the labelled soil sample was higher than  $x(Q_{95})$ , its value was taken into account for the calculation of a labelled DOC-derived SOC fraction. The fraction of labelled DOC-derived SOC in the bulk soil ( $f_{13C}$ ) was calculated with a two pool mixing model (Eq. 3) used by Cerri et al. (1985):

$$f_{13C} = \frac{\delta_{inject} - \delta_{control}}{\delta_{solution} - \delta_{control}} \quad (3)$$

where  $\delta_{inject}$  is the δ<sup>13</sup>C value (‰) of the labelled soil sample,  $\delta_{solution}$  is the δ<sup>13</sup>C value of the injected DOC solution and  $\delta_{control}$  is the mean δ<sup>13</sup>C value of the corresponding control samples.

## Study II

---

With this fraction of labelled DOC-derived SOC the amount of retained DOC per depth increment (%) was calculated by Eq. 4:

$$\text{retained DOC} = \frac{f_{13C} \cdot \text{SOC stock} \cdot 100}{\text{injected DOC}} \quad (4)$$

where *injected DOC* is the amount of injected DOC in Mg ha<sup>-1</sup>. For both sampling dates, the amount of retained DOC per plot and injection depth was summed up over the whole sampling depth respectively. The final amount of retained DOC per injection depth and time was obtained by averaging values from the three plots.

### Incubation experiment

To assess the potential stability of retained DOC against microbial decay a laboratory incubation experiment was conducted for 103 days at 20 °C. From each substrate, injection depth and plot we used three samples from within the top 20 cm below the respective injection depth (depth increments 0-5, 5-10 and 10- 20 cm) taken from the sampling three months after injection. Samples were taken from the three plots per site plus respective samples from the same depth of the control soils. The samples were filled into 250 ml glass bottles (between 26 and 156 g for equivalent SOC ranges) and adjusted to 60% of their water holding capacity. As a control, four additional blank samples with burned quartz sand and four samples with ambient air were incubated, resulting in a total of 170 samples. Before starting the incubation, samples were pre-incubated for 1 week at 7 °C and for 2 weeks at 20 °C.

The potential C mineralisation was determined by measuring the CO<sub>2</sub> production on five dates (after 1, 13, 27, 48, 103 days). At each sampling date incubation vessels were flushed with ambient air to reach a CO<sub>2</sub> starting concentration near 400 ppm. Then, incubation vessels were closed gas-tight and four gas samples per soil sample and date were taken. The first two samples were taken directly after the bottles were closed. The lids contained a septum composed of a fluorelastomer material to keep them air-tight after sampling with a syringe needle. The other two gas samples were taken after a determined time interval (between 1 and 3 days) to ensure a sufficient accumulation of CO<sub>2</sub>. Samples were filled into evacuated gas vials (Labco Exetainer, Labco Limited, Lampeter, UK). One sample from the start and one sample after the time interval were analysed for CO<sub>2</sub> concentrations by gas chromatography (Agilent 7890A, GC, Agilent Technologies, Santa Clara, USA) to account for the amount of accumulated CO<sub>2</sub>. The other two samples were analysed with an isotope ratio mass spectrometer (Delta Plus XP, Thermo Fisher Scientific, Bremen, Germany) to account for the development of δ<sup>13</sup>C of CO<sub>2</sub> during the respiration, leading to a total amount of 3400 analysed gas samples.

The amount of respired CO<sub>2</sub>-C (mg CO<sub>2</sub>-C d<sup>-1</sup>) was calculated with Eq 5,

## Study II

---

$$\text{CO}_2\text{-C} = \frac{0.1 \cdot p \cdot x_i \cdot M \cdot V}{R \cdot T \cdot t} \quad (5)$$

where  $p$  is the pressure (mbar),  $x_i$  is the difference of the  $\text{CO}_2$  concentration between the samplings (ppm),  $M$  is the molar mass of C ( $\text{g mol}^{-1}$ ),  $V$  the air volume of the sample ( $\text{m}^3$ ),  $R$  is the molar gas constant ( $\text{J kmol}^{-1} \text{K}^{-1}$ ),  $T$  is the temperature (K) and  $t$  is the elapsed time (d) between the samplings. This respiration rate was referred to the SOC content (called “SOC-normalised respiration”) by dividing it by the total amount of SOC in g in the sample. Since the content of inorganic carbon in the soil samples was extremely low we assumed that it has no considerable effect on the  $\text{CO}_2$  production (Bertrand et al. 2007).

To determine the amount of respired labelled material (called “labelled SOC-normalised respiration”) we also used the two pool mixing model (Eq. 2). For  $\delta_{control}$  we used median  $\delta^{13}\text{C}$  values of the respired  $\text{CO}_2$  from control samples from the three sites (Loess, Red Sandstone and Sand), injection depth (Top-, Upper and Deeper Subsoil), and sampling time (1, 13, 27, 48, 103) resulting in 9 observations per sampling date. The median was taken to reduce the influence of outliers on calculated labelled SOC-normalised respiration. In some cases only a small number of repetitions were obtained due to the fact that only samples from the labelled plots with significant amounts of retained DOC were taken into account. To account for natural fluctuations of the  $\delta^{13}\text{CO}_2$  values from the labelled samples we also included  $\delta^{13}\text{CO}_2$  values that showed more negative values than the control median.

### Statistics

Statistical analyses were conducted using R Core Team (2018), including the packages *glmmLasso* (Groll and Tutz 2014) to perform generalised linear mixed effect analyses and *ggplot2* (Wickham 2016) for graphical presentation. Significant differences of cumulative respiration normalised to SOC and labelled SOC after 103 days of incubation between the different sites and depths were tested with a Kruskal-Wallis test including a Wilcoxon posthoc analysis. The generalised linear mixed effect analysis was used to test for influencing parameters on the amount of retained DOC 3 months after injection. We only used the amount of retained DOC in the first depth increment below injection (0 – 5 cm). The mixed effect analysis was performed using SOC,  $\text{Al}_\text{O}$ ,  $\text{Fe}_\text{O}$ ,  $\text{Fe}_\text{D}$ , substrate and horizon as fixed effects and the field replicates (plots) as a random effect. All numerical variables were standardized to a mean of 0 and a standard deviation of 1. Models were tested for deviations from homoscedasticity, normality of residuals and absence of collinearity. We did not allow for random slopes since we assumed that the effects of the included soil parameters were not variable across the plots. The fitted linear model did not have normally distributed residuals and were strongly heteroscedastic when we also included retained values of zero for modelling. Therefore we used only depth increments with significant amounts of retained DOC. This was



also the reason why we could not perform a linear mixed effect analysis for the amount of retained DOC after 17 months, since the remaining samples did not contained enough data to provide reliable results.

### Results

#### Amount of retained DOC

The average amounts of retained DOC in the first meter below injection after three months were  $34 \pm 11\%$  for the Loess,  $23 \pm 9\%$  for the Red Sandstone and  $23 \pm 7\%$  for the Sand. Three months after injection more DOC was retained in the Topsoils ( $43 \pm 35\%$ ) compared to the Subsoils ( $21 \pm 17\%$  in Upper Subsoils and  $16 \pm 14\%$  in Deeper Subsoils) (Fig. 3). The amount of retained DOC accounted for only little OC in relation to the bulk SOC in the Topsoil (max. 0.5% of bulk SOC 3 months after injection) but quite high amounts in the Subsoils (max. 1.4% of bulk SOC in the Upper Subsoils and max. 4.8% of bulk SOC in the Deeper Subsoils) (Supplementary material, Fig. A2). For the Topsoil the maximum portion of 0.5% corresponds to  $0.013 \text{ mg SOC g}^{-1} \text{ soil}$ . The highest value of 4.8% was obtained at the Deeper Subsoil of the Sand and corresponds to  $0.053 \text{ mg SOC g}^{-1} \text{ soil}$ . Comparing the different sites, there was a decreasing trend of retained DOC from Loess to Red Sandstone and to Sand in Topsoils, whereas the retention in the Upper and Deeper Subsoil was similar for all sites. Due to the high within-group variability the differences between substrates and horizons were not statistical significant (Kruskal-Wallis rank sum test,  $p = 0.33$ ).

The bulk SOC content was found to be the best predictor for the retained amounts of DOC after 3 months within the first 5 cm below injection depth increasing it by  $3.2 \pm 0.8\%$  ( $p < 0.001$ ) as revealed by the linear mixed effect model. Thus, topsoils retained more DOC than subsoils due to their higher SOC content. More DOC retention in SOC-rich soil was also found when Topsoils were excluded from the model, increasing the amount of retained DOC by  $3.1 \pm 0.9\%$  ( $p < 0.001$ ) per  $\text{mg SOC g}^{-1} \text{ soil}$ . Thus, three months after injection more labelled DOC was retained in subsoils with high SOC contents compared to SOC poor subsoils.

Seventeen months after injection, the pattern of the retained labelled DOC changed. Highest amounts of retained DOC were found in the Deeper Subsoil of the Loess ( $41 \pm 52\%$ ) and lowest in the Topsoil of the Sand ( $3 \pm 5\%$ ). However, due to the small indigenous SOC contents, the retained amount after 17 months for the Deeper Subsoil of the Sand still represents  $6.1 \pm 10.6\%$  of bulk SOC. Corresponding mean values averaged over all sites range from  $11 \pm 12\%$  in Topsoils to  $19 \pm 20\%$  in Upper Subsoils and  $21 \pm 32\%$  in Deeper Subsoils. Thus, there was a change towards highest amounts of retained DOC in the Subsoils compared to the sampling after 3 months. The observed trends however, were not significant (Kruskal-Wallis rank sum test,  $p = 0.61$ ). We partly found a higher amount of retained

## Study II

DOC after 17 months than after 3 months, especially for the Deeper Subsoil of the Loess, which we attribute to a high small-scale variability of the soils in terms of flow paths. The amount of retained DOC per plot reveals a high variation in the data (Table 2). Thus the average amounts of retained DOC per site and depth obtained extremely disparate values resulting in high standard deviations.

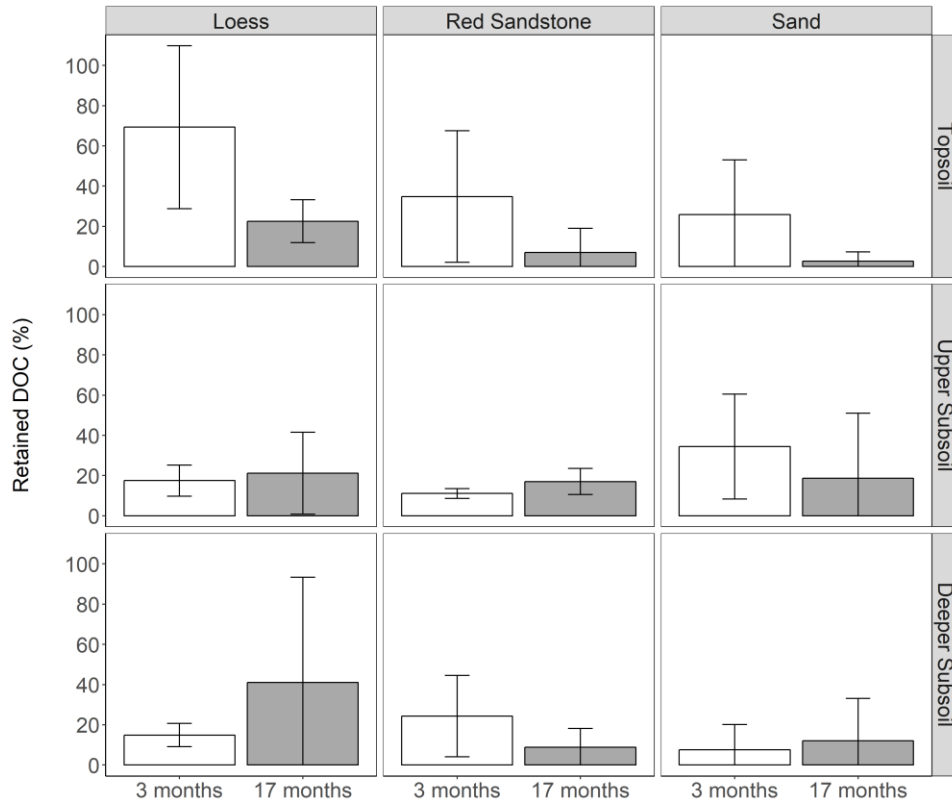


**Fig. 3** Summarised recovered labelled material over the first meter below injection depth after 3 (white boxes) and 17 months (grey boxes). Columns represent mean values from the three plots. Error bars represent standard errors.

## Study II

**Table 2** Recovered C from the injected DOC over the first meter below injection depth for all plots at the three sites.

Site	Sampling time (months)	Retained DOC (%)								
		Topsoil			Upper Subsoil			Deeper Subsoil		
		Plot 1	Plot 2	Plot 3	Plot 1	Plot 2	Plot 3	Plot 1	Plot 2	Plot 3
Loess	3	23	87	98	26	11	15	21	13	11
	17	33	11	24	23	0	41	100	0	23
Red	3	4	69	32	10	14	9	1	39	33
Sandstone	17	0	0	21	10	17	23	0	8	19
Sand	3	56	3	18	7	58	38	22	0	1
	17	0	0	8	0	0	56	36	0	0

### Translocation of DOC below the injection depths

We traced the  $^{13}\text{C}$  label within 100 cm below each injection depth to clarify as to which extent DOC was translocated downwards before adsorption to minerals, remobilisation from minerals or microbial immobilisation occurred. After 3 months, DOC injected into the Upper and Deeper Subsoils of all sites was largely restricted to the top 10 cm or even 5 cm below the injection depth (Fig. 4). In contrast, DOC injected into the Topsoil showed a comparatively deep translocation in particular at the Loess and Sand site. Especially the Topsoil of the Loess site showed a significant movement of DOC to 50 - 60 cm below injection.

Looking at the depth distribution 17 months after injection, the portion of DOC retained in the Topsoils decreased as compared to that after three months (Fig. 4). In the top 5 cm below the injection depth, no retained DOC was found any more after 17 months at the Loess and the Sand site. In the subsoils, we partly found a higher amount of retained DOC after 17 months than after three months, especially for the Upper Subsoil of the Loess with a strong translocation of injected DOC down to 70 cm below injection depth, which we attribute to a high small-scale variability of the soils in terms of flow paths (Fig. 4, lower panels). In general, there was only a decrease of retained DOC at the Red Sandstone and Sand suggesting no translocation but mainly decomposition.

### Incubation results

After 103 days of laboratory incubation, in the Topsoil of the Loess, SOC-normalised respiration added up to  $3.3 \pm 0.6\%$  within 103 days, which was significantly higher than respiration in the Upper and Deeper Subsoil with  $1.2 \pm 0.5$  and  $1.9 \pm 0.7\%$  (Fig. 5, Table 3). In contrast to the Loess, SOC-normalised respiration at the Sand and Red Sandstone showed no significant differences in potential respiration per SOC for different soil depths at all. Noteworthy, the more fine textured Loess did not show lower SOC-

## Study II

normalised respiration than the more sandy soils, and was even highest for the Topsoil. Averaged over all injection depths, the Sand showed the lowest respiration rates. When comparing the cumulative respiration normalized to bulk SOC with that from labelled SOC, eight out of nine samples tended to have higher values, except of the Topsoil samples from the Loess indicating a preferential respiration of labelled DOC than bulk SOC (Table 3). Due to the high variability of the labelled SOC-normalised respiration, these differences were not significant ( $p > 0.05$ , Kruskal-Wallis Test).

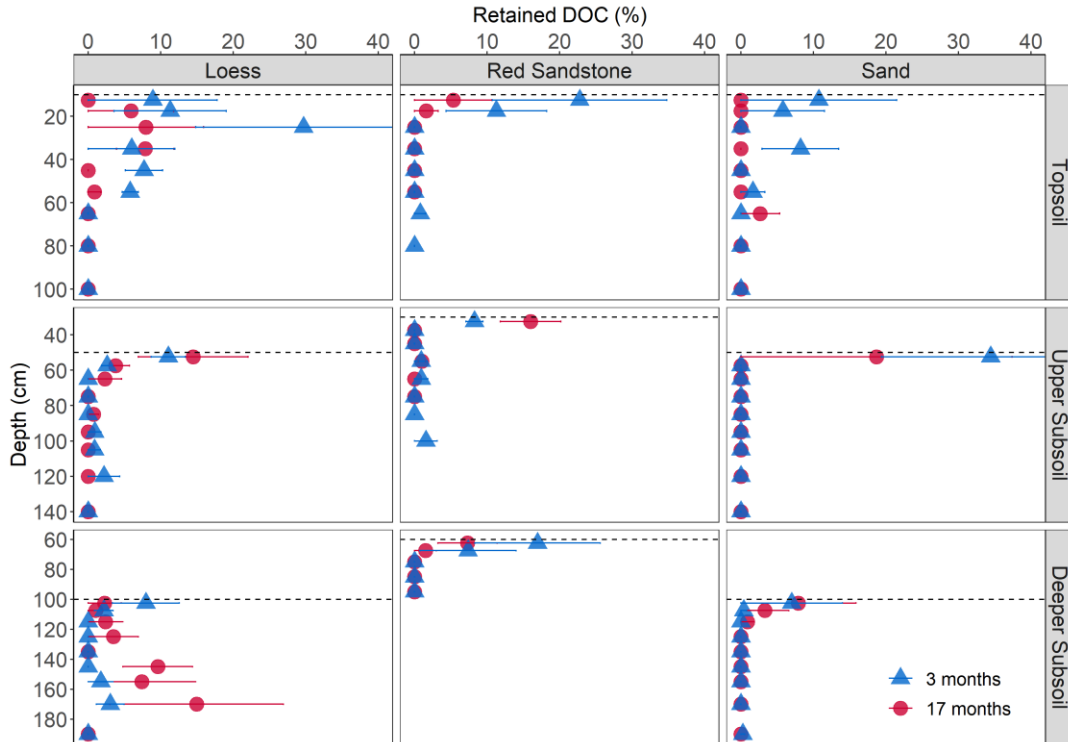


**Fig. 4** Depth distribution of retained DOC after three and after seventeen months. Values represent mean values of retained DOC ( $n = 3$ ) and their respective standard errors. Dashed lines represent respective injection depths.

## Study II

**Table 3** Cumulative respiration after 103 days of incubation normalised to bulk SOC and to the retained amount of injected DOC with standard errors.

Site	Injection Depth	SOC-normalised respiration (%)	SO <sup>13</sup> C-normalised respiration (%)	Field loss (%)*
Loess	Topsoil	3.3 (0.3)	1.9 (1.2)	16.3 (7.1)
	Upper Subsoil	1.2 (0.3)	2.1 (0.3)	0.0 (3.1)
	Deeper Subsoil	1.9 (0.4)	2.5 (1.9)	0.0 (32.8)
Red Sandstone	Topsoil	1.6 (0.3)	7.1 (1.7)	19.4 (22.1)
	Upper Subsoil	2.2 (0.7)	2.6 (1.5)	0.0 (3.3)
	Deeper Subsoil	1.7 (0.3)	4.9 (0.4)	15.4 (12.0)
Sand	Topsoil	1.2 (0.2)	5.0 (0.1)	21.7 (25.4)
	Upper Subsoil	0.9 (0.2)	2.8 (2.9)	11.0 (12.1)
	Deeper Subsoil	2.1 (0.7)	5.6 (0.8)	0 (19.5)

\* Field loss represents the difference between 3 and 17 months and has been converted to the duration of the incubation experiment (103 days). To include displaced DOC all samples have been included for the calculation instead just the top 20 cm below injection that were used for the incubation.

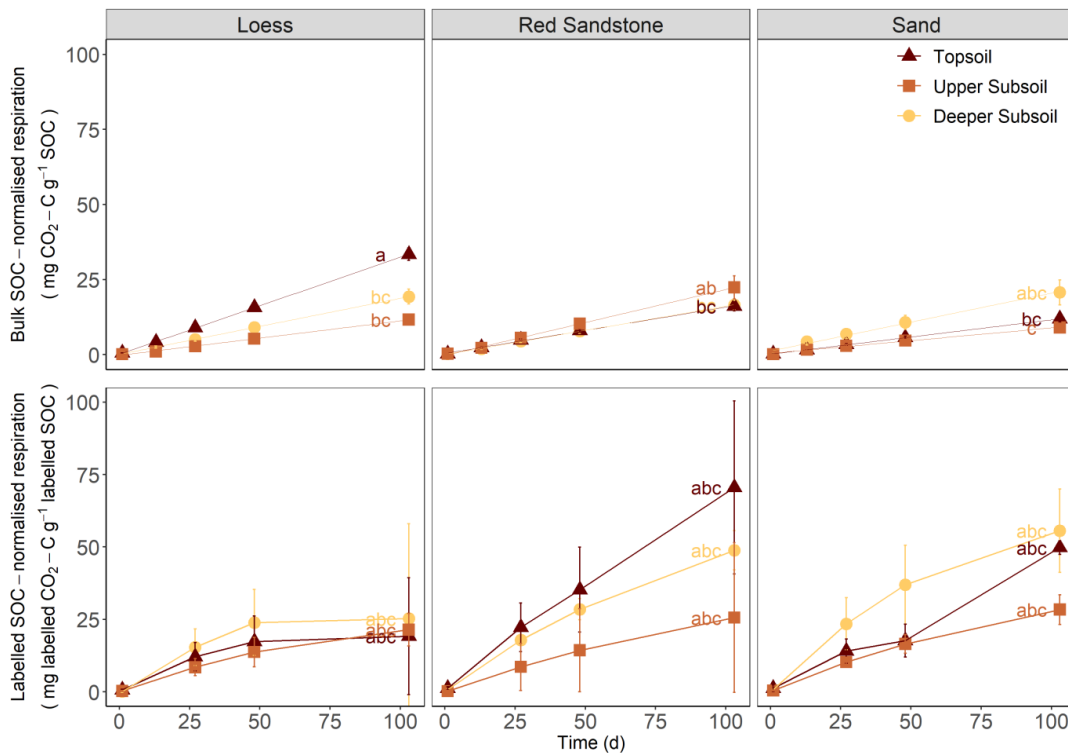


**Fig. 5** Cumulative bulk SOC-normalised (upper panel) and labelled SOC-normalised (lower panel) respiration in a 103 days laboratory incubation experiment. Values for SOC and labelled SOC-normalised respiration represent mean values from samples 0-5, 5-10 and 10-20 cm depth below injection with three repetitions per substrate ( $n = 9$ ). Error bars represent standard errors. Different letters indicate significant differences ( $P < 0.05$ ) for cumulative respiration after 103 days of incubation. Because only samples with positive recovery values were taken into account for labelled SOC-normalised respiration, number of observations strongly differs (loess: 5-6, red sandstone: 3-5, sand: 2-3).

### Behaviour of retained DOC in the field

The comparison of the amount of retained DOC after 17 months with that after three months allows assessing its stability under field conditions. Due to the depth distribution of retained DOC we exclude a translocation of retained DOC between three and 17 months to be responsible for the observed losses. Resulting losses, when existing, are therefore assigned to respiration processes. The loss of retained DOC in Topsoils was even higher between the two sampling dates (~ 19%) compared to the cumulative potential respiration during the incubation experiment, extrapolated to the same time period (~ 5%) (Table 3). This highlights the method dependency of estimated respiration rates and the importance of field studies to study DOC and SOC turnover. With regard to the amount of retained DOC at the Subsoils, four out of six field plots showed a lower loss compared to the incubation results. For the Deeper Subsoil of the Loess e.g. this was caused by a more pronounced retention of DOC after 17 months in greater depths, while the first 20 cm below injection showed a decreasing trend. We assume that this more pronounced retention after 17 months for the Deeper Subsoil of the Loess was due to a translocation directly after injection because of the increasing amounts with increasing depth (Fig. 4). Even though the estimation of field losses have to be handled with caution due to the mentioned problems, these values in general show the trend of more material being retained in the Upper and Deeper Subsoil (mean values of all samples:  $19 \pm 18$  and  $21 \pm 31\%$ ) compared to the Topsoil ( $11 \pm 12\%$ ). Additionally, a considerable amount of DOC being injected into the Topsoil was directly transferred to greater depths and thus became in fact part of the subsoil SOC (Fig. 4). The retained DOC within the top 40 cm below the topsoil injection at the Sand completely disappeared between 3 and 17 months after injection. Also the retained material at the first cm below injection at the topsoil injection at the Loess and Red Sandstone showed a strong decline.

### Discussion

In contrast to laboratory experiments under controlled conditions, field experiments impose more challenges in terms of effort and data interpretation. This has also become evident in the results of our experiment. In four out of nine cases, mean retained material after 17 months was higher than after 3 months. This can be due to the observed lateral flow or because of an unequal distribution of injected DOC in the soil matrix. Nevertheless, due to the fact that a direct injection of DOC to topsoils and subsoils in the field was never done before, this study provides first information on the fate of DOC under real environmental conditions compared to laboratory incubation experiments.

### Amount and distribution of injected DOC

Despite a partly deeper translocation, the amount of retained DOC in the first 10 cm below injection depth was comparatively high at the Topsoil increments for all sites after 3 months. This is contrary to our hypothesis that more DOC will be retained in Subsoils compared to Topsoils due to the higher availability of free sorption sites in the subsoil (Guggenberger and Kaiser 2003). According to Kaiser and Guggenberger (2000) a coverage of reactive mineral surfaces with organic matter should reduce the sorptive capacity. This was not the case for the Topsoils with their comparatively high amounts of SOC. Instead, the linear mixed effect model revealed that for the Topsoils, the SOC content was the best predictor for the amount of retained DOC after 3 months, confirming the findings of Vogel et al. (2014) in a mesocosm experiment. They have shown that new organic matter is preferentially attached to already present organo-mineral clusters. Injected DOC was therefore preferentially sorbed to already present organo-mineral clusters, while the amount of aluminium- or iron(hydr-)oxides was not crucial for the retention. These are partially unexpected field observations which stress the importance of studies in undisturbed soils, if possible under field conditions. Since these organo-mineral clusters represent microbial hotspots in the soil (Nannipieri et al. 2003), this would subsequently lead to a lower stabilisation of this retained DOC. This will be discussed in the stabilisation section later on.

Unlike expected, the more coarse sized Red Sandstone and Sand with their comparatively high water conductivity (Saxton and Rawls 2006) did not show a faster transport of the injected DOC compared to the fine textured Loess site. Furthermore, the Topsoil of the Loess and the Sand site showed a general deeper translocation of injected DOC after 3 months compared to the Subsoils. There are two explanations for the different translocations between the sites and the injection depths. One factor for a deeper distribution of injected DOC in Topsoils compared to Subsoils could be the decreasing water conductivity with increasing soil depth due to a higher bulk density (Table 1), leading to a longer contact time between DOC and the mineral phase and thus more efficient sorption and retention. The bulk density increased from 1.10 to 1.19 g cm<sup>-3</sup> in the Topsoils to 1.32 – 1.54 g cm<sup>-3</sup> in the Upper Subsoils. For a pure sand, Assouline (2006) has modelled a decrease of the saturated water conductivity from 236 mm h<sup>-1</sup> at a bulk density of 1.25 g cm<sup>-3</sup> to 112 mm h<sup>-1</sup> at a bulk density of 1.48 g cm<sup>-3</sup>. Thus it can be assumed that the high water conductivity in the Topsoils led to a deeper infiltration of DOC before it was sorbed due to a short contact time (Don and Schulze 2008). Besides that, the Topsoil of the Loess with its lower water conductivity even showed a deeper infiltration of injected DOC after three months. Therefore the other explanation that appears to be even more important for the depth distribution of injected DOC might be the abundance and stability of preferential flow paths. In general, macropores are recognised as the most important factor controlling preferential flow (Guo and Lin 2018). They are considered as possible pathways for DOC to reach deeper soil horizons Don and Schulze (2008). Indications for more

macropores at the Loess were the higher abundance of earthworm and root channels visible in soil profile. Such channels are less stable and abundant in more sandy soils such as at the Red Sandstone and Sand sites (Schneider and Don 2019). Nevertheless, to some extent preferential flow might be also important for the Sand and the Red Sandstone, since small amounts of retained DOC could also be found in greater depths. The deeper translocation of injected DOC at the Loess could therefore be a result of preferential flow directly after the injection. This is in agreement with the increasing amount of retained DOC with increasing depth in the deeper subsoil 17 months after injection (Fig. 4). A matrix flow between the sampling times seems unlikely since this would lead to a decreasing amount of retained material with increasing depth.

Despite this infiltration to greater depth due to preferential flow, the retention after three months was generally highest for all sites within the first centimetres below injection. This indicates a fast sorption even at the more sandy sites during the matrix flow. It is likely that there was enough time for the injected DOC to be retained within the first 10 cm below the injection depth, since even a structureless sandy soil can have very low infiltration rates as it was shown by Flury et al. (1994) with a dye infiltration experiment. This high retention potential of our investigated Sand is in agreement with studies from (Kalbitz et al. 2004; Nielsen et al. 1999) and was also apparent within field observations of Leinemann et al. (2016). The latter authors could observe a strong decline of transported DOC of 94 % within 150 cm soil depth. Further it must be considered that injected DOC concentrations of  $9 \text{ g m}^{-2}$  present the upper limit of DOC concentrations that can reach forest subsoils within one year (Fröberg et al. 2007; Kindler et al. 2011; Rothstein et al. 2018). In our experiment this concentration was injected within hours. Nevertheless, injected DOC was retained within the first cm below injection depth. This indicates that the retention of DOC in subsoils is mainly due to the presence of free sorption sites (Kindler et al. 2011) which are by far not exhausted in our investigated soils independent of their texture.

### Stability of topsoil and subsoil SOC

A bulk SOC-normalised respiration of 107 to  $320 \mu\text{g CO}_2\text{-C g}^{-1} \text{ C d}^{-1}$  is within the range of comparable incubation experiments (Agnelli et al. 2004; Salome et al. 2010; Schrumpf et al. 2013; Soucemarianadin et al. 2018; Wordell-Dietrich et al. 2017). Significantly higher respiration rates for the Topsoil of the Loess compared to the Subsoil samples and a clear trend of higher SOC-normalised respiration at the Deeper Subsoil of the Sand compared to the Topsoil samples revealed relevant site dependent effects. Although confounding, these different courses for the Loess and the Sand can be explained by their substrate driven impacts on the mineralisation as follows: The higher SOC-normalised respiration of Deeper Subsoil compared to the Topsoil for the Sand in our incubation experiment could also be observed by Wordell-Dietrich et al. (2017) and Heitkötter et al. (2017), who conducted incubation experiments with soil from the same Sand site as in our experiment. A possible disturbance effect due to the destruction of stabilising



aggregates (Salome et al. 2010) can be excluded here, since Vormstein (2017) also conducted incubation experiments with soil from the same site with undisturbed and sieved samples and could not find significant different respiration rates. An explanation could be a higher amount of particular organic matter (POM) compared to mineral associated organic matter (MOM) in the Deeper Subsoil of the Sand as a more easily degradable carbon source (Yakovchenko et al. 1998). This is indicated by a higher content of fine roots for the subsoil of the Sand site compared to the topsoil, shown by Kirfel et al. (2019) for samples from the same site. Despite this, stabilisation of SOC in acidic forest is mostly driven by poorly crystalline minerals (Kleber et al. 2015; Mikutta et al. 2006). This is due to their crystallinity, exhibiting a higher surface reactivity and thus a better protective capacity towards SOC (Mikutta et al. 2005). Hence, the higher amount of poorly crystalline minerals in the Upper Subsoil than in the Deeper Subsoil could be a factor for the differences between these both (Table 1). Interestingly, the comparatively high amounts of an easier degradable SOC source, indicated by a higher content of fine roots in the subsoil (Kirfel et al. 2019), and a lower content of stabilising poorly crystalline minerals did not lead to a higher SOC-normalised respiration of the Sand samples compared to the Loess and Red Sandstone. The Topsoil of the Loess with its highest SOC-normalised respiration even shows the highest amounts of SOC in the heavy fraction compared to the Topsoil of the Red Sandstone and the Sand (Vormstein 2017). This could be a hint for the physical effect of textural differences on the SOC-normalised respiration. As it was shown by Preusser et al. (2019) for sand samples from the same site, a reduced bacterial utilisation of SOC is due to a spatial separation from C sources and low soil moisture in the highly sandy subsoil environment. Also the physiology of different microbial communities could be responsible for the different stability of SOC between the sites (Kallenbach et al. 2016). However, this was not investigated here.

### Stability of injected DOC

The hypothesis of a higher stabilisation of injected DOC in Subsoils compared to Topsoils could be confirmed in our study, but with contrasting results regarding the incubation experiment and the loss between the two sampling dates. Our incubation results revealed no differences of potential labelled SOC-normalised respiration between Topsoil and Subsoils. A lack of significant differences between the labelled SOC-normalised respiration of Topsoil and Subsoil samples can be due to the high standard deviations of the incubations and the comparison of 9 groups which contained partly only two observations. Nevertheless, this was surprising, since the comparison of the amounts of DOC retained after 3 and 17 months revealed a strong decline in DOC retained in Topsoils and a stabilisation in Subsoils (Fig. 3). This may point to the fact that stabilisation effects in subsoils are largely driven by environmental factors that were not included in our incubation experiment, namely less temperature variation, a different moisture regime and an input of fresh bioavailable OC. The relatively strong decrease of injected DOC at

## Study II

---

the Topsoils after 17 months might be the result of a higher microbial activity, shown by the significantly higher respiration normalised to the bulk soil (Supplementary material, Fig. 4). Due to the fact that available energy sources in Topsoils are rather high compared to Subsoils, and injected DOC represents only a small amount of bulk SOC (Supplementary material, Fig. 1) it was likely less important as C and energy source for microorganisms in the Topsoils. In contrast, Subsoils are C poor and an addition of fresh organic substrate may immediately result in an increased microbial activity (Vogel et al. 2015) and higher mineralisation of added labile C (Kramer et al. 2013; Tian et al. 2016). Nevertheless, long-term stabilisation of SOC in Topsoils is rather hampered due to the probable accumulation of injected DOC to already present organo-mineral surfaces. This would explain the comparatively high amounts of retained DOC after 3 months in the Topsoils and the nearly complete mineralisation of this retained DOC within 14 months.

Contrary to our hypothesis, the more fine textured soils did not show higher amounts of stabilised DOC injected to the subsoils in the field. Per depth increment, there were no differences in the amounts of retained DOC after 17 months for the different sites. For the first cm below injection we can assume matrix flow conditions of injected DOC before it was sorbed to the mineral phase. Despite this, a considerable amount, especially at the Loess site, was translocated to greater depth via preferential flow paths before retention occurred. However, these rhizosphere habitats also represent the microbial hotspots in subsoil horizons (Bundt et al. 2001; Marschner et al. 2012), with higher specific enzyme activities compared to topsoil bulk SOC (Kramer et al. 2013). For the Sand site Wordell-Dietrich et al. (2019) showed that roots and root exudates in the Subsoil regions are the primary source of produced CO<sub>2</sub>. Injected DOC that was retained within these microbial hotspots might therefore be mineralised comparatively fast. In contrast, injected and retained DOC that has entered the soil via matrix flow might be spatially separated from these microbial hotspots and stabilised by poorly crystalline minerals. In conclusion the high stabilisation of injected DOC between the two sampling dates compared to the incubation results might be a result of its matrix flow and spatial separation from potential decomposers. The textural differences between the sites were rather responsible for a faster vertical movement, especially at the fine textured Loess, due to a higher abundance of preferential flow paths. Differences between the Upper and Deeper Subsoil were not substantial, pointing out to similar processes for subsoil OC stabilisation right from the spatial beginning of the subsoil.

Since retention of injected DOC with comparatively high concentrations occurred within the first 10 cm, it can be assumed that, for reaching deeper subsoils, this retained DOC requires permanent microbial degradation and translocation processes as described in the cascade model. Furthermore, as it was shown by Wordell-Dietrich et al. (in discussion), respired CO<sub>2</sub> from subsoils primarily derives from roots and root exudates. Organic carbon bound to the mineral surfaces in the Subsoils of the bulk soil should

therefore be relatively stable, not only because of the stabilising effect of organo-mineral complexes but also because it is not part of microbial hotspots.

### **Conclusion**

Our results point out the importance of field experiments with regards to questions about the fate and stability of DOC in different soil depths and substrates. Due to the combination of stable isotope techniques with field experiments at multiple sites we were able to obtain two important findings: First, stabilisation of injected DOC in acidic forest subsoils might not be preferentially driven by the sorptive capacity, like the amount of poorly crystalline minerals of the soil, but by its spatial inaccessibility, i.e. the distance to microbial decomposers. Second, the direct transport of DOC from Oa layers to subsoils seems to be higher in fine-textured soils than in coarse textured soils due to their higher abundance of preferential flow paths. These flow paths also represent biological hotspots in subsoils. Thus, our results point to the importance of microbially-degraded and subsequently displaced OC through the soil matrix for the build-up of possibly stable SOC in subsoils. Unexpectedly, SOC itself facilitated the retention of DOC in the short term with more DOC retention in the topsoil than in the subsoil; but in the long-term DOC stabilisation on accessible mineral surfaces is required.

### **Acknowledgement**

Open Access funding provided by Projekt DEAL. This study was funded by the Deutsche Forschungsgemeinschaft (DFG) (DO1734/4-2) within the framework of the research unit SUBSOM (FOR1806)—“The Forgotten Part of Carbon Cycling: Organic Matter Storage and Turnover in Subsoils”. We would like to thank Frank Hegewald and the student assistants for their support in the field and in the laboratory, Roland Fuß for his detailed help regarding the application of a generalised linear mixed effect model and Jens Dyckmanns and Lars Szwec from the Centre for Stable Isotope Research and Analysis at the University of Göttingen for  $^{13}\text{CO}_2$  measurements. We would also like to thank the AK laboratory team for their support and patience with a disorder inducing experiment.

### **Open Access**

This article is licensed under a Creative Commons Attribution 4.0 International License, which permits use, sharing, adaptation, distribution and reproduction in any medium or format, as long as you give appropriate credit to the original author(s) and the source, provide a link to the Creative Commons licence, and indicate if changes were made. The images or other third party material in this article are included in the article's Creative Commons licence, unless indicated otherwise in a credit line to the material. If material is not included in the article's Creative Commons licence and your intended use is not permitted

## Study II

---

by statutory regulation or exceeds the permitted use, you will need to obtain permission directly from the copyright holder. To view a copy of this licence, visit <http://creativecommons.org/licenses/by/4.0/>.

### References

Agnelli A, Ascher J, Corti G, Ceccherini MT, Nannipieri P, Pietramellara G (2004) Distribution of microbial communities in a forest soil profile investigated by microbial biomass, soil respiration and DGGE of total and extracellular DNA. *Soil Biology and Biochemistry* 36(5): 859-868

Assouline S (2006) Modeling the relationship between soil bulk density and the hydraulic conductivity function. *Vadose Zone Journal* 5(2): 697-705

Barré P, Fernandez-Ugalde O, Virto I, Velde B, Chenu C (2014) Impact of phyllosilicate mineralogy on organic carbon stabilization in soils: Incomplete knowledge and exciting prospects. *Geoderma* 235: 382-395

Bertrand I, Delfosse O, Mary B (2007) Carbon and nitrogen mineralization in acidic, limed and calcareous agricultural soils: Apparent and actual effects. *Soil Biology and Biochemistry* 39(1): 276-288

Bundt M, Widmer F, Pesaro M, Zeyer J, Blaser P (2001) Preferential flow paths: Biological 'hot spots' in soils. *Soil Biology Biochemistry* 33(6): 729-738

Campbell EE, Paustian K (2015) Current developments in soil organic matter modeling and the expansion of model applications: A review. *Environmental Research Letters* 10(12): 123004

Core Team R (2018) R: a language and environment for statistical computing. R Foundation for Statistical Computing, Austria

Don A, Kalbitz K (2005) Amounts and degradability of dissolved organic carbon from foliar litter at different decomposition stages. *Soil Biol Biochem* 37(12): 2171-2179

Don A, Schulze ED (2008) Controls on fluxes and export of dissolved organic carbon in grasslands with contrasting soil types. *Biogeochemistry* 91(2-3): 117-131

Don A, Rodenbeck C, Gleixner G (2013) Unexpected control of soil carbon turnover by soil carbon concentration. *Environ Chem Lett* 11(4): 407-413

Dungait JA, Hopkins DW, Gregory AS, Whitmore AP (2012) Soil organic matter turnover is governed by accessibility not recalcitrance. *Global Change Biology* 18(6): 1781-1796

Flury M, Flühler H, Jury WA, Leuenberger J (1994) Susceptibility of soils to preferential flow of water: A field study. *Water resources research* 30(7): 1945-1954

Fontaine S, Barot S, Barre P, Bdioui N, Mary B, Rumpel C (2007) Stability of organic carbon in deep soil layers controlled by fresh carbon supply. *Nature* 450(7167): 277-U210

Fröberg M, Jardine PM, Hanson PJ, Swanston C, Todd D, Tarver J, Garten C (2007) Low dissolved organic carbon input from fresh litter to deep mineral soils. *Soil Science Society of America Journal* 71(2): 347-354

Fröberg M, Hanson PJ, Trumbore SE, Swanston CW, Todd DE (2009) Flux of carbon from <sup>14</sup>C-enriched leaf litter throughout a forest soil mesocosm. *Geoderma* 149(3-4): 181-188

## Study II

---

- Groll A, Tutz G (2014) Variable selection for generalized linear mixed models by L<sub>1</sub>-penalized estimation. *Statistics Computing* 24(2): 137-154
- Guggenberger G, Kaiser K (2003) Dissolved organic matter in soil: Challenging the paradigm of sorptive preservation. *Geoderma* 113(3-4): 293-310
- Guggenberger G, Zech W, Schulten H-R (1994) Formation and mobilization pathways of dissolved organic matter: Evidence from chemical structural studies of organic matter fractions in acid forest floor solutions. *Org Geochem* 21(1): 51-66
- Guo L, Lin H (2018) Addressing two bottlenecks to advance the understanding of preferential flow in soils. In: *Advances in Agronomy*. Elsevier. p 61-117
- Hagedorn F, Kammer A, Schmidt MW, Goodale CL (2012) Nitrogen addition alters mineralization dynamics of <sup>13</sup>C-depleted leaf and twig litter and reduces leaching of older DOC from mineral soil. *Global Change Biology* 18(4): 1412-1427
- Hagedorn F, Bruderhofer N, Ferrari A, Niklaus PA (2015) Tracking litter-derived dissolved organic matter along a soil chronosequence using <sup>14</sup>C imaging: Biodegradation, physico-chemical retention or preferential flow? *Soil Biology and Biochemistry* 88: 333-343
- Harrison RB, Footen PW, Strahm BDJFS (2011) Deep soil horizons: Contribution and importance to soil carbon pools and in assessing whole-ecosystem response to management and global change. *57(1): 67-76*
- Heinze S, Ludwig B, Piepho HP, Mikutta R, Don A, Wordell-Dietrich P, Helfrich M, Hertel D, Leuschner C, Kirfel K, Kandeler E, Preusser S, Guggenberger G, Leinemann T, Marschner B (2018) Factors controlling the variability of organic matter in the top- and subsoil of a sandy Dystric Cambisol under beech forest. *Geoderma* 311: 37-44
- Heitkötter J, Heinze S, Marschner B (2017) Relevance of substrate quality and nutrients for microbial C-turnover in top-and subsoil of a Dystric Cambisol. *Geoderma* 302: 89-99
- Kaiser K, Guggenberger G (2000) The role of DOM sorption to mineral surfaces in the preservation of organic matter in soils. *Org Geochem* 31(7-8): 711-725
- Kaiser K, Guggenberger GJG (2005) Storm flow flushing in a structured soil changes the composition of dissolved organic matter leached into the subsoil. *127(3-4): 177-187*
- Kaiser K, Kalbitz K (2012) Cycling downwards - dissolved organic matter in soils. *Soil Biol Biochem* 52: 29-32
- Kaiser K, Zech W (1996) Nitrate, sulfate, and biphosphate retention in acid forest soils affected by natural dissolved organic carbon. *Journal of Environmental Quality* 25(6): 1325-1331
- Kalbitz K, Kaiser K (2008) Contribution of dissolved organic matter to carbon storage in forest mineral soils. *Journal of Plant Nutrition and Soil Science* 171(1): 52-60
- Kalbitz K, Schmerwitz J, Schwesig D, Matzner E (2003) Biodegradation of soil-derived dissolved organic matter as related to its properties. *Geoderma* 113(3-4): 273-291
- Kalbitz K, Glaser B, Bol R (2004) Clear-cutting of a Norway spruce stand: Implications for controls on the dynamics of dissolved organic matter in the forest floor. *Eur J Soil Sci* 55(2): 401-413
- Kalbitz K, Schwesig D, Rethemeyer J, Matzner E (2005) Stabilization of dissolved organic matter by sorption to the mineral soil. *Soil Biol Biochem* 37(7): 1319-1331

## Study II

---

Kalbitz K, Meyer A, Yang R, Gerstberger P (2007) Response of dissolved organic matter in the forest floor to long-term manipulation of litter and throughfall inputs. *Biogeochemistry* 86(3): 301-318

Kallenbach CM, Frey SD, Grandy AS (2016) Direct evidence for microbial-derived soil organic matter formation and its ecophysiological controls. *Nature communications* 7: 13630

Kammer A, Hagedorn F (2011) Mineralisation, leaching and stabilisation of <sup>13</sup>C-labelled leaf and twig litter in a beech forest soil. *Biogeosciences* 8(8): 2195-2208

Kindler R, Siemens J, Kaiser K, Walmsley DC, Bernhofer C, Buchmann N, Cellier P, Eugster W, Gleixner G, Grunwald T, Heim A, Ibrom A, Jones SK, Jones M, Klumpp K, Kutsch W, Larsen KS, Lehuger S, Loubet B, McKenzie R, Moors E, Osborne B, Pilegaard K, Reibmann C, Saunders M, Schmidt MWI, Schrumpp M, Seyfferth J, Skiba U, Soussana JF, Sutton MA, Tefs C, Vowinckel B, Zeeman MJ, Kaupenjohann M (2011) Dissolved carbon leaching from soil is a crucial component of the net ecosystem carbon balance. *Global Change Biology* 17(2): 1167-1185

Kirfel K, Heinze S, Hertel D, Leuschner C (2019) Effects of bedrock type and soil chemistry on the fine roots of European beech—A study on the belowground plasticity of trees. *Forest Ecology Management* 444: 256-268

Kleber M, Eusterhues K, Keiluweit M, Mikutta C, Mikutta R, Nico PS (2015) Mineral–organic associations: Formation, properties, and relevance in soil environments. In: *Advances in agronomy*. Elsevier. p 1-140

Klotzbücher T, Kaiser K, Filley TR, Kalbitz K (2013) Processes controlling the production of aromatic water-soluble organic matter during litter decomposition. *Soil Biol Biochem* 67: 133-139

Kögel-Knabner I (2002) The macromolecular organic composition of plant and microbial residues as inputs to soil organic matter. *Soil Biology and Biochemistry* 34(2): 139-162

Kögel-Knabner I (2017) The macromolecular organic composition of plant and microbial residues as inputs to soil organic matter: Fourteen years on. *Soil Biology Biochemistry* 105: A3-A8

Kramer S, Marhan S, Haslwimmer H, Ruess L, Kandeler E (2013) Temporal variation in surface and subsoil abundance and function of the soil microbial community in an arable soil. *Soil Biology and Biochemistry* 61: 76-85

Lee MH, Park JH, Matzner E (2018) Sustained production of dissolved organic carbon and nitrogen in forest floors during continuous leaching. *Geoderma* 310: 163-169

Leinemann T, Mikutta R, Kalbitz K, Schaarschmidt F, Guggenberger G (2016) Small scale variability of vertical water and dissolved organic matter fluxes in sandy Cambisol subsoils as revealed by segmented suction plates. *Biogeochemistry* 131(1-2): 1-15

Leinemann T, Preusser S, Mikutta R, Kalbitz K, Cerli C, Hoschen C, Mueller CW, Kandeler E, Guggenberger G (2018) Multiple exchange processes on mineral surfaces control the transport of dissolved organic matter through soil profiles. *Soil Biol Biochem* 118: 79-90

Liebmann P, Wordell-Dietrich P, Kalbitz K, Mikutta R, Kalks F, Don A, Woche SK, Dsilva LR, Guggenberger G (2020) Relevance of aboveground litter for soil organic matter formation – a soil profile perspective. *Biogeosci Discuss* 2020:1–29

Marschner B, Brodowski S, Dreves A, Gleixner G, Gude A, Grootes PM, Hamer U, Heim A, Jandl G, Ji R, Kaiser K, Kalbitz K, Kramer C, Leinweber P, Rethemeyer J, Schaeffer A, Schmidt MWI, Schwark L,

## Study II

---

- Wiesenberg GLB (2008) How relevant is recalcitrance for the stabilization of organic matter in soils? *Journal of Plant Nutrition and Soil Science* 171(1): 91-110
- Marschner P, Marhan S, Kandeler E (2012) Microscale distribution and function of soil microorganisms in the interface between rhizosphere and detritusphere. *Soil Biology Biochemistry* 49: 174-183
- McKeague J, Day J (1966) Dithionite-and oxalate-extractable Fe and Al as aids in differentiating various classes of soils. *Canadian journal of soil science* 46(1): 13-22
- Mehra O, Jackson M (2013) Iron oxide removal from soils and clays by a dithionite–citrate system buffered with sodium bicarbonate. *Clays and clay minerals*. Elsevier, Amsterdam, pp 317–327
- Michalzik B, Kalbitz K, Park J-H, Solinger S, Matzner E (2001) Fluxes and concentrations of dissolved organic carbon and nitrogen—a synthesis for temperate forests. *Biogeochemistry* 52(2): 173-205
- Mikutta R, Kleber M, Jahn RJG (2005) Poorly crystalline minerals protect organic carbon in clay subfractions from acid subsoil horizons. *128(1-2)*: 106-115
- Mikutta R, Kleber M, Torn MS, Jahn R (2006) Stabilization of soil organic matter: Association with minerals or chemical recalcitrance? *Biogeochemistry* 77(1): 25-56
- Nannipieri P, Ascher J, Ceccherini M, Landi L, Pietramellara G, Renella G (2003) Microbial diversity and soil functions. *Eur J Soil Sci* 54(4): 655-670
- Nielsen KE, Ladekar UL, Nørnberg P (1999) Dynamic soil processes on heathland due to changes in vegetation to oak and Sitka spruce. *Forest Ecology Management* 114(1): 107-116
- Poeplau C, Don A, Vesterdal L, Leifeld J, Van Wesemael B, Schumacher J, Gensior AJGcb (2011) Temporal dynamics of soil organic carbon after land-use change in the temperate zone—carbon response functions as a model approach. *Global change biology* 17(7): 2415-2427
- Preusser S, Poll C, Marhan S, Angst G, Mueller CW, Bachmann J, Kandeler E (2019) Fungi and bacteria respond differently to changing environmental conditions within a soil profile. *Soil Biology and Biochemistry* 137: 107543
- Qualls RG, Haines BLJSSSoAJ (1992) Biodegradability of dissolved organic matter in forest throughfall, soil solution, and stream water. *56(2)*: 578-586
- Rothstein DE, Toosi ER, Schaetzl RJ, Grandy AS (2018) Translocation of carbon from surface organic horizons to the subsoil in coarse-textured Spodosols: Implications for deep soil C dynamics. *Soil Science Society of America Journal* 82(4): 969-982
- Rumpel C, Kogel-Knabner I (2011) Deep soil organic matter—a key but poorly understood component of terrestrial C cycle. *Plant Soil* 338(1-2): 143-158
- Rumpel C, Kögel-Knabner I, Bruhn F (2002) Vertical distribution, age, and chemical composition of organic carbon in two forest soils of different pedogenesis. *Org Geochem* 33(10): 1131-1142
- Salome C, Nunan N, Pouteau V, Lerch TZ, Chenu C (2010) Carbon dynamics in topsoil and in subsoil may be controlled by different regulatory mechanisms. *Global Change Biology* 16(1): 416-426
- Saxton KE, Rawls WJ (2006) Soil water characteristic estimates by texture and organic matter for hydrologic solutions. *Soil Science Society of America Journal* 70(5): 1569-1578

## Study II

---

Schmidt MWI, Torn MS, Abiven S, Dittmar T, Guggenberger G, Janssens IA, Kleber M, Kögel-Knabner I, Lehmann J, Manning DAC, Nannipieri P, Rasse DP, Weiner S, Trumbore SE (2011) Persistence of soil organic matter as an ecosystem property. *Nature* 478(7367): 49-56

Schneider F, Don A, Hennings I, Schmittmann O, Seidel SJ (2017) The effect of deep tillage on crop yield - What do we really know? *Soil & Tillage Research* 174: 193-204

Schneider F, Don AJP, Soil (2019) Root-restricting layers in German agricultural soils. Part II: Adaptation and melioration strategies. *442(1-2)*: 419-432

Schöning I, Kögel-Knabner I (2006) Chemical composition of young and old carbon pools throughout Cambisol and Luvisol profiles under forests. *Soil Biology and Biochemistry* 38(8): 2411-2424

Schrumpf M, Kaiser K, Guggenberger G, Persson T, Kögel-Knabner I, Schulze E-D (2013) Storage and stability of organic carbon in soils as related to depth, occlusion within aggregates, and attachment to minerals. *Biogeosciences* 10: 1675-1691

Schulze K, Borken W, Matzner E (2011) Dynamics of dissolved organic  $^{14}\text{C}$  in throughfall and soil solution of a Norway spruce forest. *Biogeochemistry* 106(3): 461-473

Schwertmann U (1964) Differenzierung der Eisenoxide des Bodens durch Extraktion mit Ammoniumoxalat-Lösung. *Zeitschrift für Pflanzenernährung, Düngung, Bodenkunde* 105(3): 194-202

Sheldrick B, McKeague J (1975) A comparison of extractable Fe and Al data using methods followed in the USA and Canada. *Canadian journal of soil science* 55(1): 77-78

Soucemarianadin LN, Cecillon L, Guenet B, Chenu C, Baudin F, Nicolas M, Girardin C, Barre P (2018) Environmental factors controlling soil organic carbon stability in French forest soils. *Plant Soil* 426(1-2): 267-286

Tian Q, Yang X, Wang X, Liao C, Li Q, Wang M, Wu Y, Liu F (2016) Microbial community mediated response of organic carbon mineralization to labile carbon and nitrogen addition in topsoil and subsoil. *Biogeochemistry* 128(1): 125-139

Tückmantel T, Leuschner C, Preusser S, Kandeler E, Angst G, Mueller CW, Meier IC (2017) Root exudation patterns in a beech forest: Dependence on soil depth, root morphology, and environment. *Soil Biology Biochemistry* 107: 188-197

Vogel C, Mueller CW, Höschel C, Buegger F, Heister K, Schulz S, Schloter M, Kögel-Knabner I (2014) Submicron structures provide preferential spots for carbon and nitrogen sequestration in soils. *Nature Communications* 5: 2947

Vogel C, Heister K, Buegger F, Tanuwidjaja I, Haug S, Schloter M, Kögel-Knabner I (2015) Clay mineral composition modifies decomposition and sequestration of organic carbon and nitrogen in fine soil fractions. *Biology and fertility of soils* 51(4): 427-442

von Lützw M, Kögel-Knabner I, Ludwig B, Matzner E, Flessa H, Ekschmitt K, Guggenberger G, Marschner B, Kalbitz K (2008) Stabilization mechanisms of organic matter in four temperate soils: Development and application of a conceptual model. *Journal of Plant Nutrition and Soil Science* 171(1): 111-124

Voort TSvd, Hagedorn F, McIntyre C, Zell C, Walthert L, Schleppei P, Feng X, Eglinton TI (2016) Variability in  $^{14}\text{C}$  contents of soil organic matter at the plot and regional scale across climatic and geologic gradients. *Biogeosciences* 13(11): 3427-3439



## Study II

---

Vormstein S (2017) Amount, composition and turnover of organic matter in topsoils and subsoils under mature beech forest. Faculty of Organic Agricultural Sciences University of Kassel, Witzenhausen, p 92

Wang Y, Amundson R, Trumbore S (1996) Radiocarbon dating of soil organic matter. *Quaternary Research* 45(3): 282-288

Wickham H (2016) *ggplot2: elegant graphics for data analysis*. Springer,

Wordell-Dietrich P, Don A, Helfrich M (2017) Controlling factors for the stability of subsoil carbon in a Dystric Cambisol. *Geoderma* 304: 40-48

Wordell-Dietrich P, Don A, Wotte A, Rethemeyer J, Bachmann J, Helfrich M, Kirfel K, Leuschner C (2019) Vertical partitioning of CO<sub>2</sub> production in a Dystric Cambisol. *Biogeosci Discuss* 2019:1 27

Yakovchenko V, Sikora L, Millner P (1998) Carbon and nitrogen mineralization of added particulate and macroorganic matter. *Soil Biology Biochemistry* 30(14): 2139-2146

## Study II – Supplementary material

### Figures

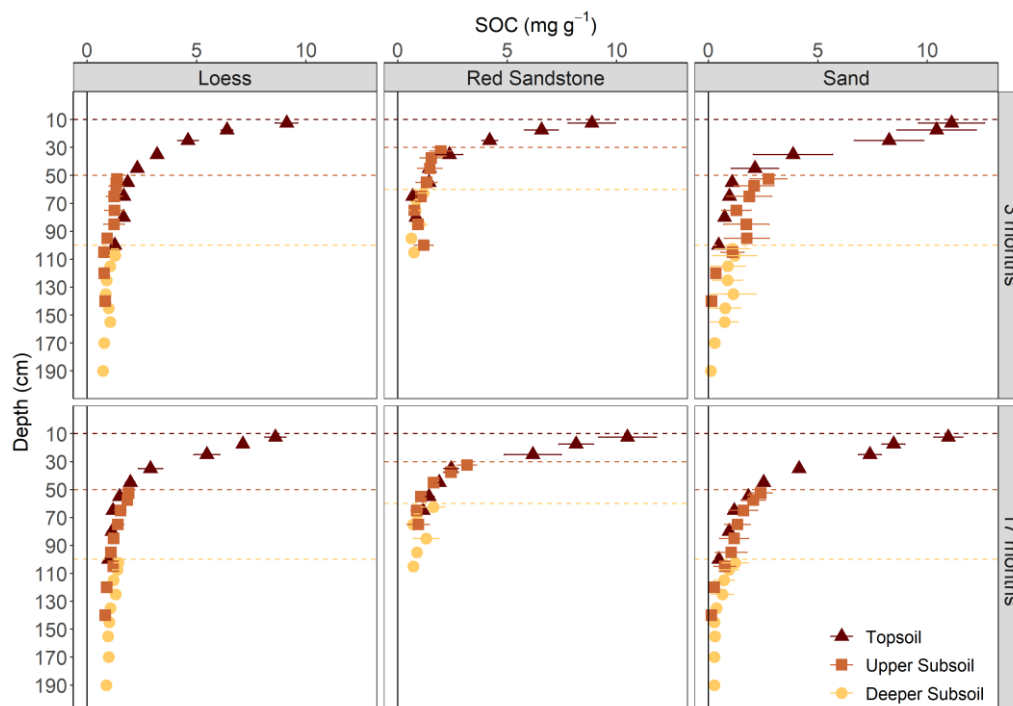


**Fig. A1** Bulk SOC content after 3 (upper panels) and 17 months (lower panels) of injection. Values represent mean values derived from the different plots (n = 3) and the respective standard deviations

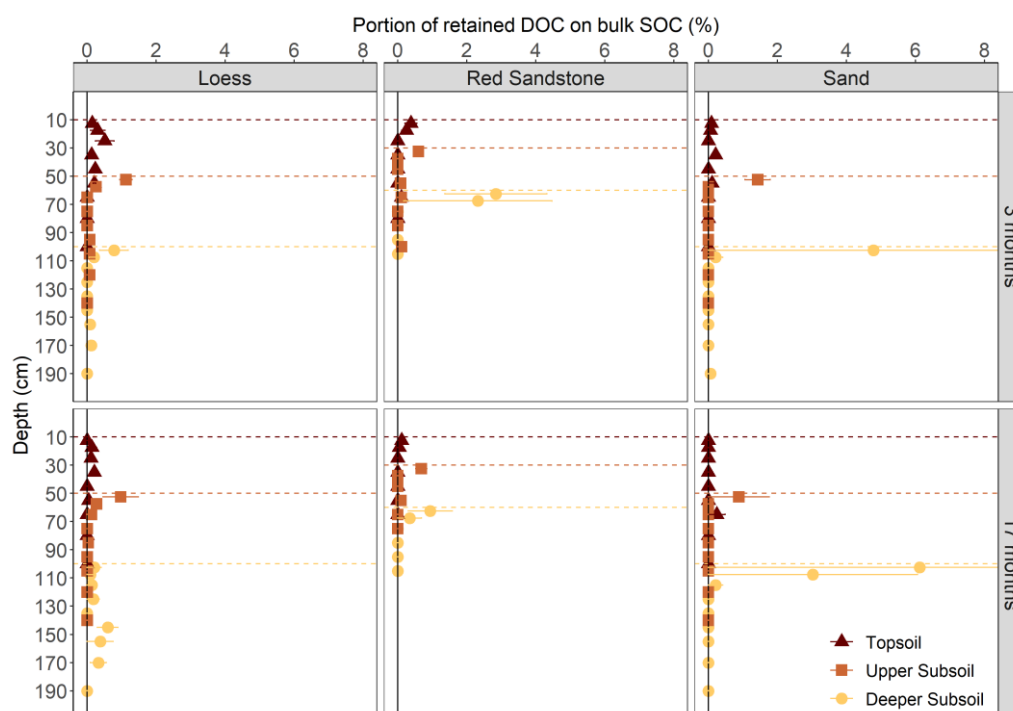


**Fig. A2** Amount of retained DOC after 3 (upper panels) and 17 months (lower panels) in relation to bulk SOC content. Values represent mean values derived from the different plots (n = 3) and the respective standard deviations.

## Study II – Supplementary material

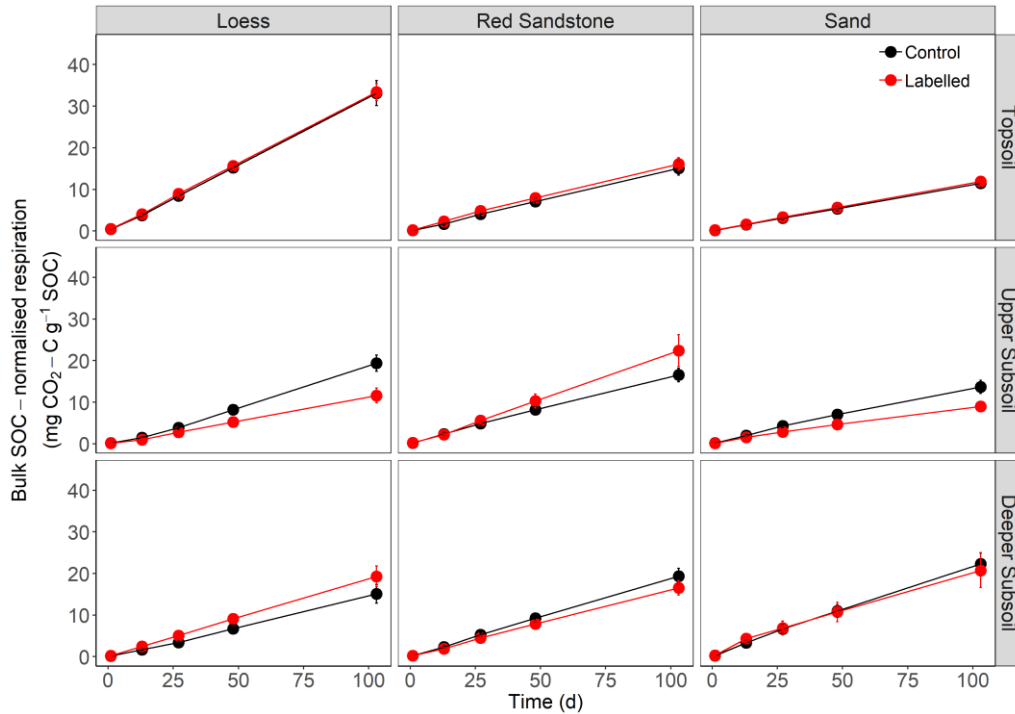


**Fig. A3** Comparison of cumulative respiration normalised to bulk SOC respiration for the samples with labelled substrate and control samples. Values represent mean values derived from the different plots and injection depths (n = 9) and the respective standard deviations.

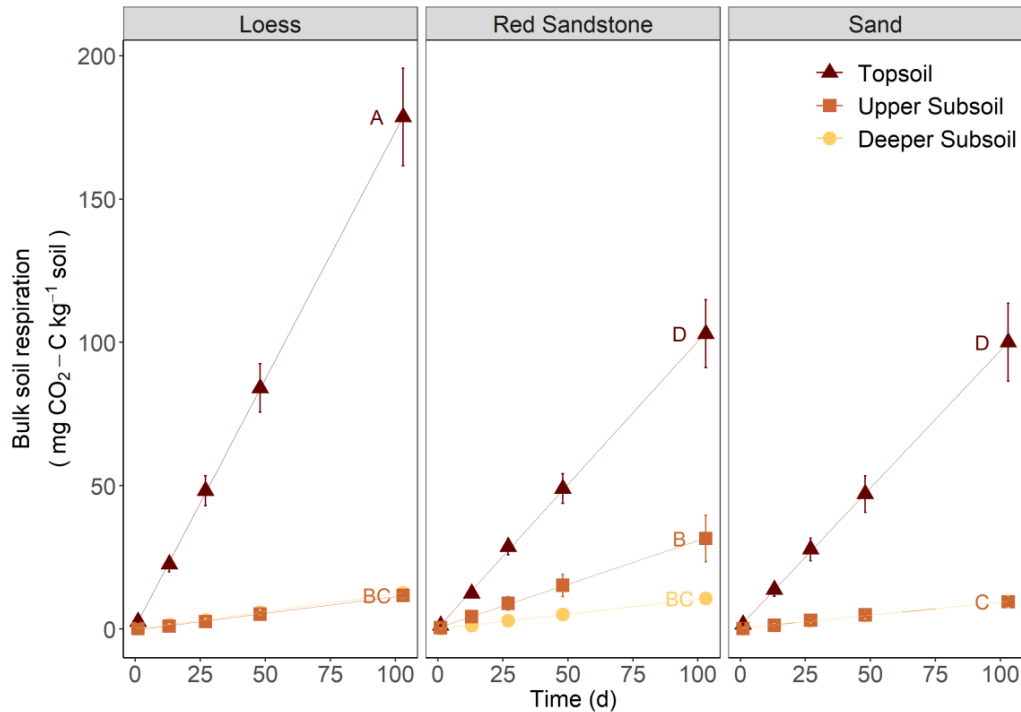


**Fig. A4** Cumulative respiration normalised to the bulk soil. Values represent mean values from samples 0-5, 5-10 and 10-20 cm depth below injection with three repetitions per substrate (n = 9). Error bars represent standard errors. Different letters indicate significant differences ( $p < 0.05$ ) for cumulative respiration after 103 days of incubation.

## Study II – Supplementary material

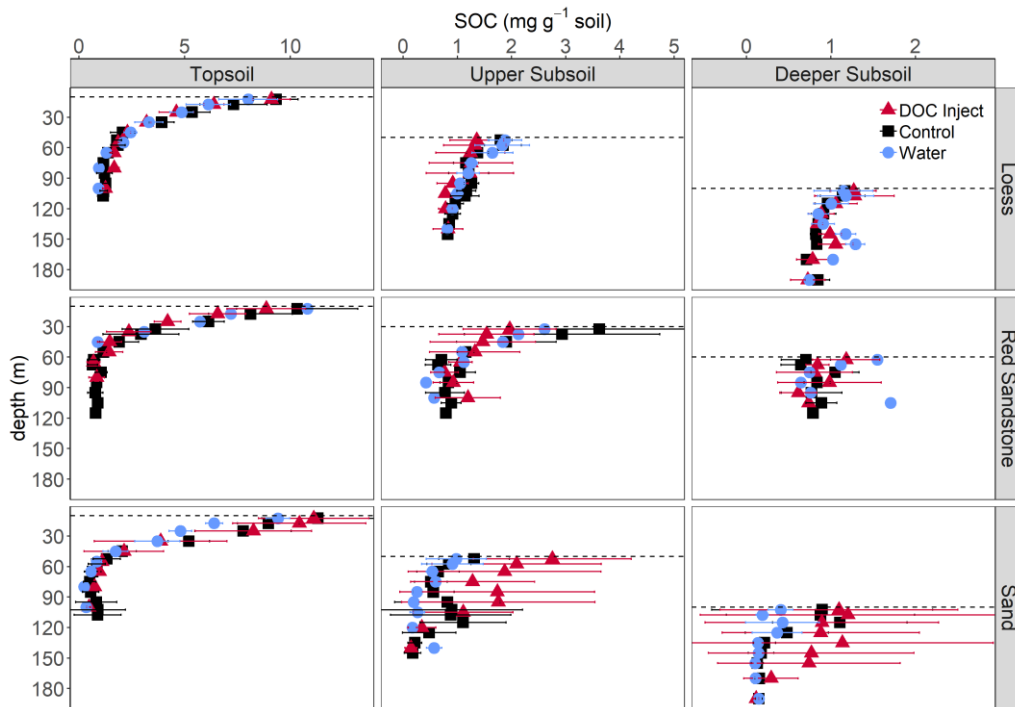


**Fig. A5** Possible influence of the water added with the DOC injection on bulk SOC investigated with the injection of water ( $\text{CaCl}_2$  solution). Values represent mean values for samples 3 months after injection. For the Red Sandstone site only one sample per injection depth was taken.

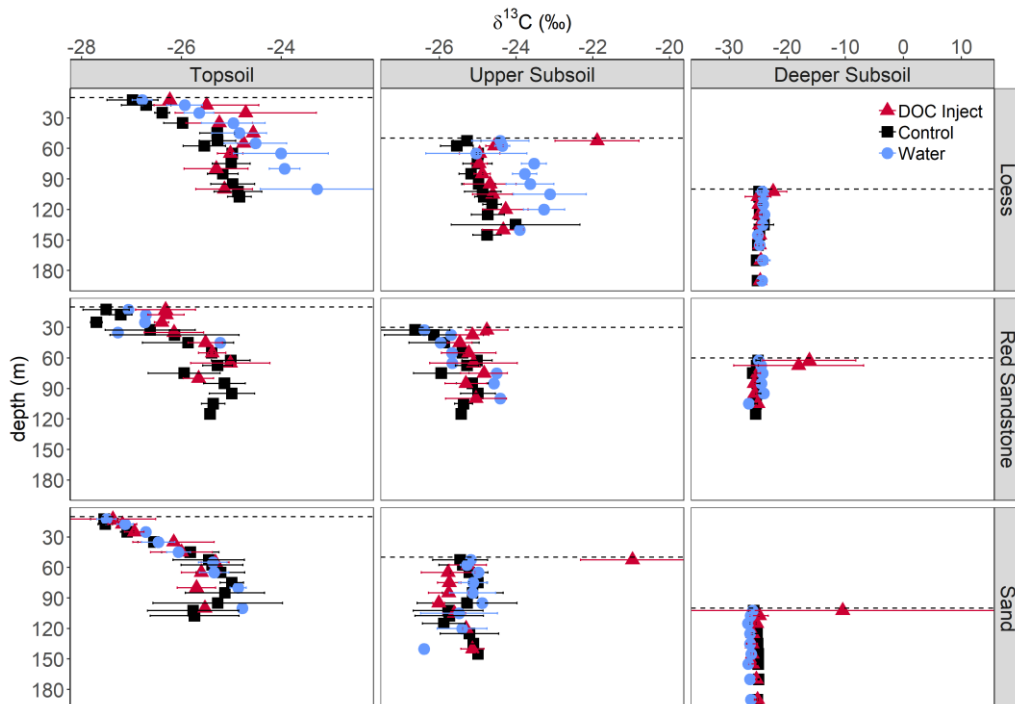


**Fig. A6** Possible influence of the water added with the DOC injection on  $\delta^{13}\text{C}$  values investigated with the injection of water ( $\text{CaCl}_2$  solution). Values represent mean values for samples 3 months after injection. For the Red Sandstone site only one sample per injection depth was taken.

## Study II – Supplementary material

### Tables

**Table A1** Qualitative results from a GCMS pyrolysis for the freeze-dried DOC samples. The samples (approx. 300 µg) were pyrolyzed at 600°C for 6 s using a Multi-Shot Pyrolyzer EGA/PY-3030D (Frontier Laboratories Ltd.; Fukushima, Japan) connected to an Agilent 7890B gas chromatograph (Agilent Technologies, Inc.; Santa Clara, CA, USA). The pyrolysis products were separated on a HP-5 ms column (30 m length, 0.25 mm inner diameter, 0.25 µm film thickness) with 5.0 He as carrier gas. Inlet temperature of the GC was set to 320°C. A split ratio of 1:20 was applied. The GC column was connected to an Agilent 5977 MSD (Agilent Technologies, Inc.; Santa Clara, CA, USA) and scanned from 50 to 600 m/z. The raw data files were exported from the proprietary instrument software (Agilent Masshunter GC MS Acquisition B.07.00) and processed in MassLab version 1.2.7 using the NIST library.

Group	Compound	mass- to charge ratio (m/z)	Formula
Polysaccharides	Acetic acid	60	C <sub>2</sub> H <sub>4</sub> O <sub>2</sub>
Polysaccharides	Furan, 2-methyl-	81+82	C <sub>5</sub> H <sub>6</sub> O
Benzenesenes	Benzene	78	C <sub>6</sub> H <sub>6</sub>
Polysaccharides	C2-Furan	95+96	C <sub>6</sub> H <sub>8</sub> O
Polysaccharides	C2-Furan	95+96	C <sub>6</sub> H <sub>8</sub> O
N-containing compounds	1H-Pyrrole, 1-methyl-	80+81	C <sub>5</sub> H <sub>7</sub> N
N-containing compounds	Pyridine	52+79	C <sub>5</sub> H <sub>5</sub> N
N-containing compounds	Pyrrole	67	C <sub>4</sub> H <sub>5</sub> N
Benzenesenes	Toluene	91+92	C <sub>7</sub> H <sub>8</sub>
Polysaccharides	(2H)-Furan-3-one	54+84	C <sub>4</sub> H <sub>4</sub> O <sub>2</sub>
Polysaccharides	3-Furaldehyde	95+96	C <sub>5</sub> H <sub>4</sub> O <sub>2</sub>
N-containing compounds	Pyridine, 2-methyl-	66+93	C <sub>6</sub> H <sub>7</sub> N
N-containing compounds	Pyrazine, methyl-	67+94	C <sub>5</sub> H <sub>6</sub> N <sub>2</sub>
Polysaccharides	2-Furaldehyde	95+96	C <sub>5</sub> H <sub>4</sub> O <sub>2</sub>
N-containing compounds	C1-Pyrrole (Pyrrole, ethyl-)	80+81	C <sub>6</sub> H <sub>9</sub> N
N-containing compounds	C1-Pyrrole (Pyrrole, methyl-)	80+81	C <sub>6</sub> H <sub>9</sub> N
Polysaccharides	2-Furanmethanol	81+98	C <sub>5</sub> H <sub>6</sub> O <sub>2</sub>
Benzenesenes	C2 benzene (Benzene, ethyl-)	91+106	C <sub>8</sub> H <sub>10</sub>
Polysaccharides	Cyclopent-4-ene-1,3-dione	68+96	C <sub>5</sub> H <sub>4</sub> O <sub>2</sub>
Benzenes	Styrene	103+104	C <sub>8</sub> H <sub>8</sub>
Polysaccharides	2-Cyclopenten-1-one, 2-methyl-	67+96	C <sub>6</sub> H <sub>8</sub> O
Polysaccharides	2-Cyclopenten-1-one, 2-hydroxy-	55+98	C <sub>5</sub> H <sub>6</sub> O <sub>2</sub>
Polysaccharides	2-Furaldehyde, 5-methyl-	109+110	C <sub>6</sub> H <sub>6</sub> O <sub>2</sub>
Polysaccharides	2-Cyclopenten-1-one, 3-methyl-	67+96	C <sub>6</sub> H <sub>8</sub> O
Phenols	Phenol	66+94	C <sub>6</sub> H <sub>6</sub> O
Polysaccharides, Lg	Resorcinol	68+110	C <sub>6</sub> H <sub>6</sub> O <sub>2</sub>
Benzenes	C3-Benzene	105+120	C <sub>9</sub> H <sub>12</sub>
Benzenes	C3-Benzene	105+120	C <sub>9</sub> H <sub>12</sub>
Polysaccharides	2-Cyclopenten-1-one, 2-hydroxy-3-methyl-	69+112	C <sub>6</sub> H <sub>8</sub> O <sub>2</sub>
Polysaccharides	2-Cyclopenten-1-one, 2,3-dimethyl-	67+110	C <sub>7</sub> H <sub>10</sub> O
Phenols	C1-Phenol (Phenol, methyl-)	107+108	C <sub>7</sub> H <sub>8</sub> O
Lignin-derived compounds	Guaiacol	109+124	C <sub>7</sub> H <sub>8</sub> O <sub>2</sub>

## Study II – Supplementary material

---

Polysaccharides	4H-Pyran-4-one, 3-hydroxy-2-methyl- (Maltol)	71+126	C <sub>6</sub> H <sub>6</sub> O <sub>3</sub>
Benzenes	Benzoxazole, 2-methyl-	64+133	C <sub>8</sub> H <sub>7</sub> NO
N-containing compounds	unidentified N-compound	81+82	
Phenols	C2-Phenol	107+122	C <sub>8</sub> H <sub>10</sub> O
Phenols	C2-Phenol (Phenol, dimethyl-)	107+122	C <sub>8</sub> H <sub>10</sub> O
Phenols	C2-Phenol (Phenol, dimethyl-)	107+122	C <sub>8</sub> H <sub>10</sub> O
Lignin-derived compounds	4-Vinylphenol	91+120	C <sub>8</sub> H <sub>8</sub> O
N-containing compounds	3-Acetamidofuran	83+125	C <sub>6</sub> H <sub>7</sub> NO <sub>2</sub>
N-containing compounds	1H-Pyrrole-2,5-dione, 3-ethyl-4-methyl-	67+139	C <sub>7</sub> H <sub>9</sub> NO <sub>2</sub>
Lignin-derived compounds	2-Coumaranone	78+134	C <sub>8</sub> H <sub>6</sub> O <sub>2</sub>
N-containing compounds	Quinoline	102+129	C <sub>9</sub> H <sub>7</sub> N
N-containing compounds	1H-Pyrrole-2,5-dione, 3-ethenyl-4-methyl	66+137	C <sub>7</sub> H <sub>7</sub> NO <sub>2</sub>
Indenes	1H-Indene, 1,1-dimethyl-	129+144	C <sub>11</sub> H <sub>12</sub>
Indenes	1H-Inden-1-one, 2,3-dihydro-	104+132	C <sub>9</sub> H <sub>8</sub> O
N-containing compounds	Indole	90+117	C <sub>8</sub> H <sub>7</sub> N
Polycyclic aromatic hydrocarbons	C1-Naphtalene (Naphthalene, methyl-)	141+142	C <sub>11</sub> H <sub>10</sub>
Lignin-derived compounds	4-Vinylguaiacol	135+150	C <sub>9</sub> H <sub>10</sub> O <sub>2</sub>
Polycyclic aromatic hydrocarbons	C1-Naphtalene (Naphthalene, methyl-)	141+142	C <sub>11</sub> H <sub>10</sub>
Phenols	Phenol, 2,6-dimethoxy-	139+154	C <sub>8</sub> H <sub>10</sub> O <sub>3</sub>
N-containing compounds	C1-Indole	130+131	C <sub>9</sub> H <sub>9</sub> NO
Lignin-derived compounds	Dimethoxy benzaldehyde	151+152	C <sub>9</sub> H <sub>10</sub> O <sub>3</sub>
Polycyclic aromatic hydrocarbons	Naphthalene, 2,7-dimethyl-	141+156	C <sub>12</sub> H <sub>12</sub>
Lignin-derived compounds	C3-Guaiacol	164	C <sub>10</sub> H <sub>14</sub> O <sub>2</sub>
Phenols	Phenol, 4-butyl-	107+150	C <sub>10</sub> H <sub>14</sub> O
Lignin-derived compounds	Guaiacylacetone	137+180	C <sub>10</sub> H <sub>12</sub> O <sub>3</sub>
Lignin-derived compounds	4-Vinylsyringol	165+180	C <sub>10</sub> H <sub>12</sub> O <sub>3</sub>
N-containing compounds	Diketodipyrrole	93+186	C <sub>10</sub> H <sub>6</sub> O <sub>2</sub> N <sub>2</sub>

## 4. Study III

### **Biogeochemical constraints limit carbon storage in forest subsoils**

**Contribution:** I was equally involved in the field sampling campaigns, designed the laboratory sorption experiments and carried out about half of the analysis in the lab. I collected and evaluated the data, compiled the tables and figures, and wrote the manuscript.

**Submitted to:** *Nature Communications*, 08.12.2020

**Accepted for Peer Review:** For *Nature Communications*, 15.12.2020

**Manuscript tracking number:** NCOMMS-20-48745-T

**Data repository:** [doi.org/10.20387/bonares-rmtx-ttaj](https://doi.org/10.20387/bonares-rmtx-ttaj)

# Biogeochemical constraints limit carbon storage in forest

## subsoils

*Patrick Liebmann<sup>1\*</sup>, Robert Mikutta<sup>2</sup>, Karsten Kalbitz<sup>3</sup>, Patrick Wordell-Dietrich<sup>3,4</sup>, Timo Leinemann<sup>1</sup>, Sebastian Preusser<sup>5</sup>, Jörg Bachmann<sup>1</sup>, Axel Don<sup>4</sup>, Ellen Kandeler<sup>5</sup>, Bernd Marschner<sup>6</sup>, Frank Schaarschmidt<sup>7</sup> and Georg Guggenberger<sup>1</sup>*

<sup>1</sup> Institute of Soil Science, Leibniz Universität Hannover, Herrenhäuser Straße 2, 30419, Hannover, Germany

<sup>2</sup> Soil Science and Soil Protection, Martin Luther University Halle-Wittenberg, Von-Seckendorff-Platz 3, 06210 Halle (Saale), Germany

<sup>3</sup> Institute of Soil Science and Site Ecology, Technische Universität Dresden, Piener Straße 19, 01737 Tharandt, Germany

<sup>4</sup> Thünen Institute of Climate-Smart Agriculture, Bundesallee 65, 38116 Braunschweig, Germany

<sup>5</sup> Institute of Soil Science and Land Evaluation, Soil Biology, University of Hohenheim, Emil-Wolff-Straße 27, 70599 Stuttgart, Germany

<sup>6</sup> Department of Soil Science/Soil Ecology, Institute of Geography, Ruhr-University Bochum, Universitätsstraße 150, 44801 Bochum, Germany

<sup>7</sup> Institute of Cell Biology and Biophysics, Leibniz Universität Hannover, Herrenhäuser Straße 2, 30419, Hannover, Germany

\*Correspondence to Patrick Liebmann (liebmann@ifbk.uni-hannover.de)

### Keywords

Soil, subsoil, cascade model, <sup>13</sup>C, carbon cycling, carbon stabilization, dissolved organic carbon, microbial community composition, mineral-associated organic carbon, temperate forest



### **Abstract**

Soils are important carbon sinks or sources and thus of great importance for the global carbon cycling. Especially subsoils are considered to have high potential for additional carbon accumulation, likely mitigating further increase in atmospheric carbon dioxide. Based on a multiple-method approach including a field labelling experiment with  $^{13}\text{C}$ -enriched litter, we show for temperate forest soils that the laboratory-based carbon sink capacity of subsoils cannot be reached in reality. Surface carbon inputs via litter leachates are little conducive to the subsoil carbon pool. Only 0.5 % of litter-derived C entered the subsoil as dissolved organic matter within nearly two years and most of the translocated organic matter is prone to fast microbial mineralisation. Sorption of fresh organic matter to mineral surfaces only resulted in a short-term storage of carbon. Desorption to the soil solution and an adapted microbial community re-mobilises organic matter in subsoils faster than considered so far. We conclude that under current conditions forest subsoils cannot be considered as additional C sink, which is in contrast to their widely debated C sink potential.

### **Main**

Globally, 50 % of soil organic carbon (SOC) is stored in the subsoil below 30 cm depth, making subsoils one of the largest terrestrial C reservoirs<sup>1,2</sup>. Recently fixed carbon can be transferred to subsoils via dissolved organic matter (DOM) or inputs of roots<sup>3</sup>. A paramount relevance of the downward solute transport followed by sorption to minerals is advocated by the oftentimes negligible contents of plant residues and high <sup>14</sup>C ages of organic matter in subsoils<sup>4</sup>. The extent to which soils can accumulate organic C (OC) thus largely depends on available sorption sites at reactive minerals, e.g. pedogenic metal (oxyhydr)oxides<sup>5-7</sup> and clay minerals<sup>7</sup>, and is limited by their sorption capacity<sup>8</sup> or by reaching steady-state equilibrium<sup>9</sup>. While most aboveground C inputs are retained in topsoil horizons<sup>10</sup>, subsoils contain considerable amounts of uncovered mineral surfaces<sup>8</sup>. Hence, especially mineral subsoils are considered to have high potential to preserve additional C<sup>11,12</sup> and particularly forest ecosystems are thought to act as future C sinks if managed accordingly<sup>13-15</sup>. Based on sorption experiments in the laboratory<sup>16</sup> or on models<sup>17</sup>, forest subsoils are assumed to have an enormous capability to retain additional C<sup>3,12,16</sup>. Many forests, including widespread temperate forests, are located in high sensitivity biomes<sup>5</sup>, which can vastly react to climate change. Since the 1980s, a human-induced greening of the vegetation has been observed globally<sup>18</sup> and of the northern hemisphere in particular<sup>19</sup>, predominantly connected to forest management, nitrogen deposition, CO<sub>2</sub> fertilisation, and climate change<sup>18-20</sup>. This greening is particularly related to the growth of young forests <140 yrs<sup>21</sup> and enhanced net primary production<sup>22</sup> and thus litter-C inputs to soils<sup>23</sup>. Disturbances as droughts and windthrow events additionally contribute to enhanced C inputs to soil by dead biomass<sup>21,24</sup>.

Field experiments, however, suggest that increased aboveground litter inputs have little or no effect on soil C stocks<sup>25</sup>. Not only that most of this additional input is rapidly mineralised<sup>25</sup>, it is also thought to foster C mobilisation in mineral topsoils and its translocation towards deeper subsoils and aquifers<sup>8,26</sup>. In fact, browning of lakes and rivers in Northern Europe and temperate North America due to the increasing input of dissolved organic C (DOC) from soils<sup>27,28</sup> indicate a limited capability of subsoils to retain C mobilised in the topsoils. It remains an intriguing paradox that, although laboratory experiments suggest a vast capacity of forest subsoils to store more C<sup>16,29</sup>, this potential has not been exploited under natural conditions. This “staying-below-capacity” effect could substantially reduce the value of forest subsoils for additional C sequestration. Here, we challenge the perception that forest subsoils can retain more C than they currently do and investigate the biogeochemical factors that interfere in exploiting their C storage potential. We assessed C retention and underlying processes in a forest subsoil down to 150 cm soil depth based on a 20-m<sup>2</sup> field labelling experiment with <sup>13</sup>C-enriched litter<sup>30</sup> with a unique long-term DO<sup>13</sup>C and <sup>13</sup>CO<sub>2</sub> monitoring<sup>31,32</sup>, an *in-situ* C exchange field experiment with C-coated minerals, and batch sorption experiments.

### **Translocation of litter-derived carbon towards forest subsoils**

The application of  $^{13}\text{C}$ -enriched litter on the surface of subsoil observatories<sup>30</sup> allowed us to trace fluxes of litter-derived C into different C pools and to create a 22-month C balance at various soil depths. Soil solutions were collected with segmented suction plates, covering for the first time both, DOC fluxes through matrix and preferential flow path domains<sup>31</sup> (see method section). We were able to recover about 85 % of the initially applied tracer. More than one-third of the litter-C was directly mineralised and lost to the atmosphere while another third remained in the surface litter layer after nearly two years (Fig. 1, Supplementary Fig. S1). Only 1.5 % of the litter-C was mobilised as DOC and immobilised as mineral-associated organic carbon (MAOC) in the topsoil horizon (0-10 cm soil depth), and another 0.5 % of the  $^{13}\text{C}$ -labelled litter-C entered the upper subsoil in a depth >10 cm via the DOC pathway (Fig. 1). This shows that most of the litter inputs are retained in the topsoil<sup>33</sup>, while the majority of the DOC in the mineral top- and subsoil originate from native SOC<sup>33</sup> (Supplementary Fig. S2). It took about one year after  $^{13}\text{C}$ -litter application, before small amounts of litter-derived DOC showed up in the subsoil solution (Supplementary Fig. S3), indicating a significant lag-phase due to multiple sorption-decomposition-desorption cycles through the soil matrix<sup>26</sup>. About 0.7 % of the applied litter-C was found as MAOC in the upper part of the subsoil (10-50 cm depth) after 22 months (Fig. 1), which matches the range of litter-derived  $\text{DO}^{13}\text{C}$  inputs into the upper subsoil. The ratio of litter-derived  $\text{CO}_2$  production in the upper subsoil (0.25 % of the added litter-C) and retained C (0.25 + 0.7 = 0.95 %) shows that about one-fourth of the litter layer inputs entering the upper subsoil were respired within less than two years (Fig. 1). In the deep subsoil, this ratio remained constant, indicating that substantial parts of fresh C inputs are not stabilised over longer periods<sup>30</sup>, but rather represent a labile C source<sup>34</sup>. In fact, litter-derived  $\text{CO}_2$  was observed in all soil depths right from the start of the experiment (Supplementary Fig. S4), suggesting rapid mineralisation of recent organic compounds without or with only very short temporal immobilisation by the mineral phase<sup>26</sup>. In accordance, high apparent  $^{14}\text{C}$  ages of subsoil SOC indicates that rejuvenation by fresh inputs is negligible<sup>3</sup>. The microbial utilisation of fresh DOC inputs is also reflected by the overall high contribution of microbial-derived carbohydrates in subsoil soil solution<sup>26,35,36</sup> (Supplementary Table S1 and Fig. S5). We conclude that recent litter-derived DOC facilitates predominantly MAOC formation in the topsoil, with only limited supply of rather labile C to subsoils.

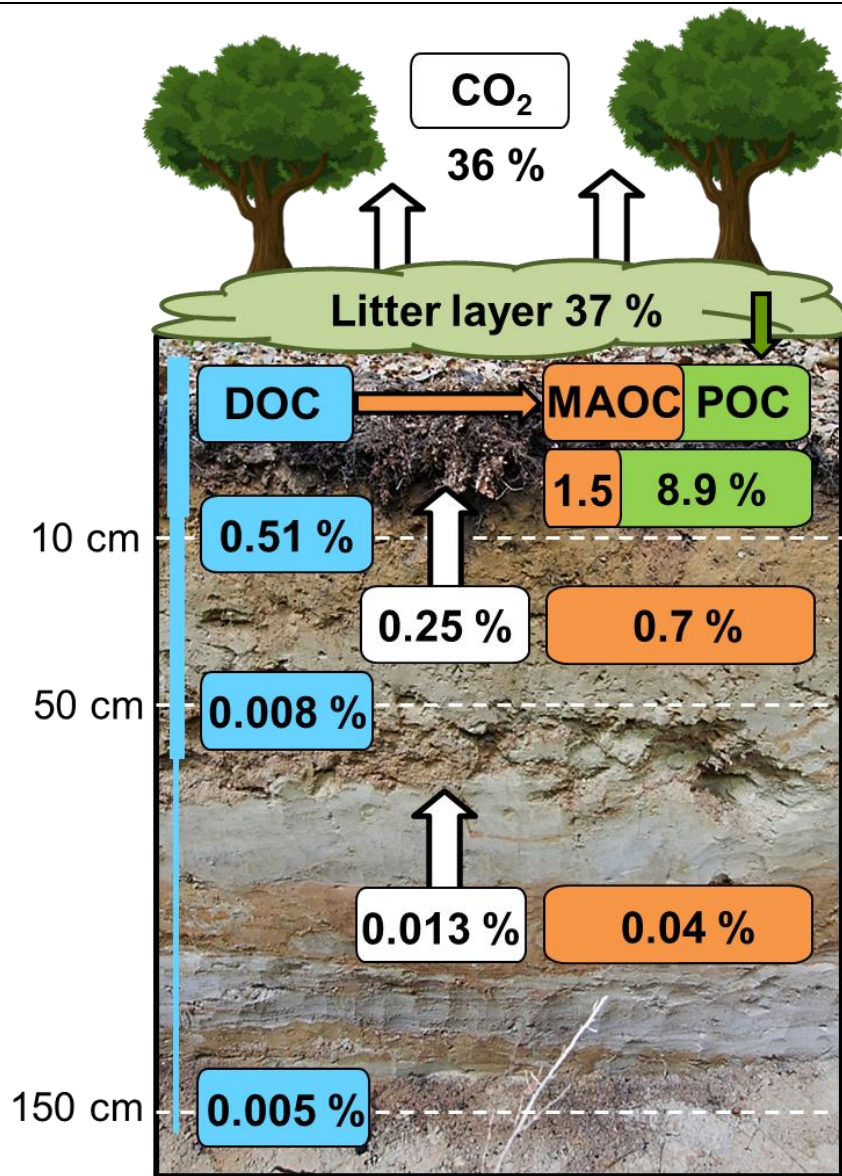


**Fig. 1** Recovery of litter-derived C into different C pools in topsoil (10 cm), upper subsoil (50 cm), and deeper subsoil (150 cm) over the course of 22 months in a Dystric Cambisol located in a temperate European beech forest in Germany. Values are given in percent of the initially applied labelled litter. Evaluated C pools included the CO<sub>2</sub> production at the soil surface and in the depth increments 10-50 and 50-90 cm (white), leachates of dissolved organic C (DOC) in 10, 50, and 150 cm soil depth (blue), and incorporation of litter material in the depth increments 0-10, 10-50, and 50-150 cm, due to bioturbations as C in particulate organic matter (POC; green) and due to sorption to mineral surfaces thereby forming mineral-associated organic C (MAOC; brown). Residual litter after the field exposure was quantified and is given in the litter layer. The complete C balance revealed a recovery of initially applied litter of about 85 %. CO<sub>2</sub> data were adapted from Wordell-Dietrich et al.<sup>32</sup>, and MAOC/POC differentiation was adapted from Liebmann et al.<sup>30</sup>. The latter authors did not analyse the MAOC in the depth increment 50-100 cm, but reported an interpolation of 0.03 % which we added here.

### **Subsoil capacities for additional carbon uptake**

Even though recent litter contributes little to soil DOC fluxes, considerable amounts of DOC are percolating through forest soil profiles<sup>10,31</sup> (Fig. 2, Supplementary Table S1). Therefore, we explored the sorption capacities of forest top- and subsoils and the vulnerability of sorbed <sup>13</sup>C-labelled organic matter towards desorption in batch experiments. To assess the sorption capacity, we used three temperate European beech forest soils with a typical clay mineral assemblage (dominated by vermiculite, chlorite, illitic clay, and kaolinite; Supplementary Fig. S7), but varying in soil texture (silty to sandy). Sorption isotherms showed that typical topsoil DOC concentrations of 50-100 mg L<sup>-1</sup> (Supplementary Table S1)<sup>31</sup> induced desorption of native SOC from topsoils (Fig. 2), supporting that topsoils already reached their steady state<sup>37</sup>. Unexpectedly, typical subsoil DOC concentrations of <10 mg L<sup>-1</sup> (Fig. 2, Supplementary Table S1)<sup>10,31</sup> resulted either in no additional net C uptake or in a net release of native SOC from subsoils at 50 and 150 cm depth (Fig. 2, Supplementary Fig. S8). Like observed under field conditions<sup>29,31</sup>, a decrease in specific UV absorption at 280 nm with soil depth indicates preferential sorption of aromatic compounds and mobilisation of native organic matter of lower aromaticity<sup>26</sup> (Supplementary Fig. S9). Only at substantially higher DOC concentrations of >>10 mg L<sup>-1</sup>, subsoils retained additional C, suggesting further C uptake only for highly sorptive DOM and DOC concentrations considerably higher than under present natural conditions. But typical subsoil solutions are much less reactive, containing a high share of carbohydrates<sup>26</sup> (Supplementary Fig. S5). We infer that a disadvantage of the past and current adsorption experiments is the use of highly reactive litter-derived DOM as standard, whereas the inherent DOM composition of solutions entering a particular soil depth would be more representative for field situations. It must be further noted that, unlike in laboratory sorption experiments, the accessibility of sorption sites in natural subsoils is reduced as DOM percolates also along preferential flow paths<sup>31</sup>, thus bypassing possible sorption sites.

Another key factor in the subsoil C sequestration is the stability of recently retained C<sup>30,38,39</sup>. Previous studies with C-free pedogenic minerals showed a strong sorption-desorption hysteresis of freshly retained C and a subsequent decrease in mineralisation rates<sup>40,41</sup>. Our batch desorption experiment with natural soils indicates that newly sorbed litter-derived C was held in weaker associations and thus a significant part remained mobilisable (20-39 % of sorbed C,  $p < 0.05$ ) in the deeper subsoil samples, whereas older, native C was more strongly bound (Supplementary Fig. S10 and S11). Recent investigations into *in-situ* mineral-organic associations of various soil depths likewise revealed short retention times of newly sorbed C<sup>30</sup>. As sorption-desorption processes are governed by the *in-situ* solution equilibrium state and sorption site availability differs between field and laboratory conditions, the laboratory-based sorption capacity of forest subsoils remains an unsuitable predictor for further C sequestration.

## Study III

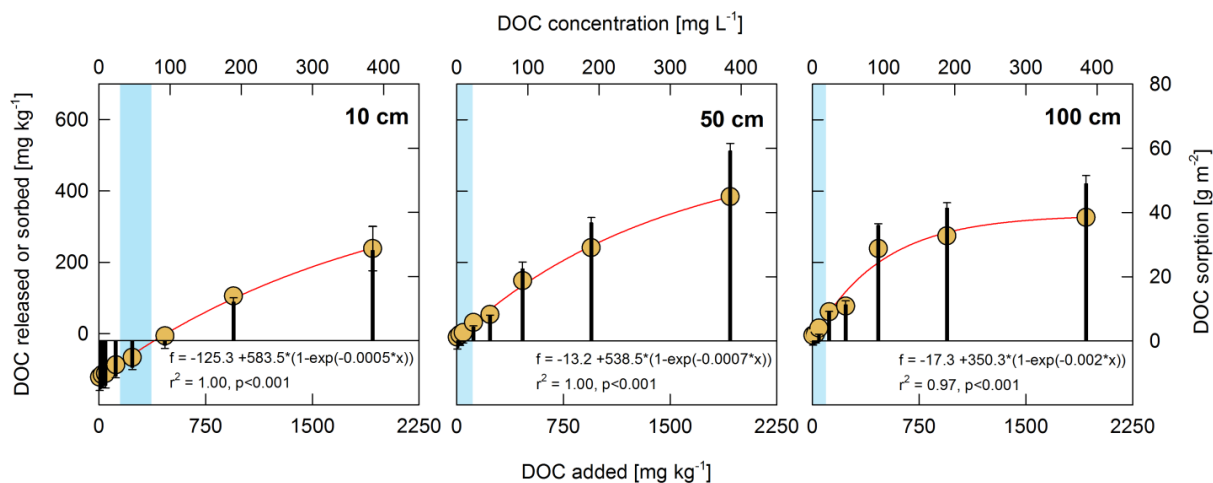


**Fig. 2** Dissolved organic C (DOC) sorption isotherms of soil from 10, 50, and 150 cm soil depth of a Dystric Cambisol located in a temperate European beech forest in Germany. Both x-axes show the DOC added to the soil, on the bottom x-axis normalised to soil mass, on the top x-axis as concentration. Sorption isotherms (yellow circles and red line) show the released or sorbed DOC after the experiment (left y-axis,  $n = 3$ ) as a function of added DOC. Black bars show the quantified DOC sorption (right y-axis,  $n = 3$ ), estimated for one m<sup>2</sup> and a soil thickness of 10 cm (since soil samples for the sorption experiments were taken as composite samples of a 10-cm increment; 10-20, 50-60, 100-110 cm). The blue-marked areas represent typical DOC concentrations (top x-axis) in the respective soil depths measured at this study site (see Supplementary Table S1). Concentrations were calculated as the mean of all samples taken during the timeframe February 2015 to November 2016, and amounted to  $51.5 \pm 22.0$  mg L<sup>-1</sup> in 10 cm ( $n = 112$ ),  $13.0 \pm 9.0$  in 50 cm ( $n = 60$ ), and  $8.6 \pm 11.2$  in 150 cm ( $n = 88$ ). The DOC concentration in 150 cm soil depth was used for the 100-cm variant in this figure.

### Soil minerals and carbon sequestration

Given the fact that considerable DOC fluxes and available sorption sites in forest subsoils contrast low C stocks, we further tested the persistence of subsoil MAOC under *in-situ* field conditions. Native soil minerals (goethite and vermiculite) coated with a <sup>13</sup>C-enriched organic matter, with C contents similar to those of the subsoil clay fraction<sup>42</sup>, were buried in the soil profile. As a prerequisite for further C sequestration, we expected a slow *in-situ* C cycling. After a two-year exposure period, however, the gross C balance revealed an unexpected high exchange rate of C (Fig. 3, Supplementary Table S2). While goethite acted as net C sink in the topsoil as its sorption capacity was still not reached<sup>43</sup>, both minerals were net C sources in the subsoil. Carbon exchange as well as microbial driven C cycling on minerals in the topsoil support the assumption that mineral surfaces in topsoils are the place of pronounced C cycling<sup>26</sup>. Minerals buried in the subsoil showed a net release of C without concomitant retention of fresh C from the soil solution, although being exposed to subsoil DOC (Fig. 2, Supplementary Table S1). A mobilisation of 30-40 % of native C from both minerals (Fig. 3) suggests a mobilisation process independent from the mineral composition. The high rate of mobilisation is consistent with our field findings, showing a loss of about two-third of fresh mineral-bound C within 18 months<sup>30</sup>. Similarly, our

batch sorption and desorption experiments with native soil samples and DO<sup>13</sup>C solution revealed that there is a frequent exchange of DOC with native SOC and a preferential desorption of recently retained C, irrespective of the mineral composition and being more pronounced in subsoils compared to topsoils (Supplementary Fig. S11). The minerals loaded with litter-derived C represent microbial hotspots<sup>44,45</sup>, thus promoting the growth of bacteria compared to the surrounding bulk soil, especially of copiotrophic *Betaproteobacteria*<sup>46</sup> (Supplementary Fig. S12). Their activity might be further fueled by the carbohydrate-rich DOM, as with increasing soil depth, the soil solution comprises an increasing proportion of carbohydrates (Supplementary Fig. S5) with a low affinity to form bonds to mineral surfaces<sup>47</sup>. Additional C input may thus promote the growth of copiotrophic microorganisms, which benefit most from easy available C sources<sup>46</sup>. Overall, the *in-situ* field exposure experiment suggests that C storage ability in subsoil environments is limited and depends more on the composition of organic matter and an active and adapted microbial community associated with such pedogenic minerals<sup>46</sup> (Supplementary Fig. S12 and S13) than on mineral properties, such as surface area and sorption capacity.

### **Implications for forest subsoils as future carbon sink**

Subsoils are highly discussed regarding their potential to sequester C, thereby helping to counteract the globally increasing atmospheric CO<sub>2</sub> concentrations. Our integrative approach of field labelling with flux monitoring, laboratory sorption experiments, and *in-situ* exposure of C-coated minerals provides several lines of evidence that under the current conditions, subsoils in temperate forests should not be considered as additional C sinks. These insights mainly derive from a beech forest with a stand age of >100 years. But since site-specific properties are likely of subordinate importance for DOC stabilisation among temperate beech forests<sup>39</sup>, we consider our results applicable also to other locations within the temperate forest biome and beyond. We identified the following factors for the “staying-below-capacity” state of subsoils, which likely prevent future C sequestration in temperate subsoils and are contradictory to the yet proposed role of subsoils as additional C sinks: (1) Forest subsoils are in a steady-state equilibrium between inputs and outputs of C, facilitated by exchange and mineralisation of temporarily retained C; (2) C inputs into subsoils, which potentially bind to mineral surfaces, are limited, rather dominated by less sorptive carbohydrates<sup>26</sup>, and are further channeled along preferential flow paths<sup>31</sup>. The resulting associations are weaker than those with highly sorptive plant-derived DOM in the topsoil and can result in a fast C turnover even in the subsoil; (3) An increased C input into subsoils rather promotes the mineralisation and mobilisation of fresh inputs as well as older native organic matter<sup>48</sup>, thus making it unlikely that the remaining available sorption sites will be effectively used under natural conditions. This probably also applies when increasing the input of root-derived C into subsoils by changing tree species composition towards more deep-rooting trees. In conclusion, although forest subsoils do have high capacities for



## Study III

further C sequestration, such potentials are unlikely to be exploitable. Constraints such as low and spatially variable DOC inputs, sorptive fractionation, mobilisation of sorbed OC into soil solution, and its mineralisation maintain the current input-output equilibrium. Enhancing C storage in subsoils would require substantially increased inputs of highly sorptive plant-derived OM. Yet, additional inputs of labile and more bioavailable C sources may unlock the stabilisation of the old native carbon pool by co-metabolic decomposition<sup>48</sup>, going along with an increased desorption of C, and consequently contributing to C losses from soil and browning of surface and ground waters.

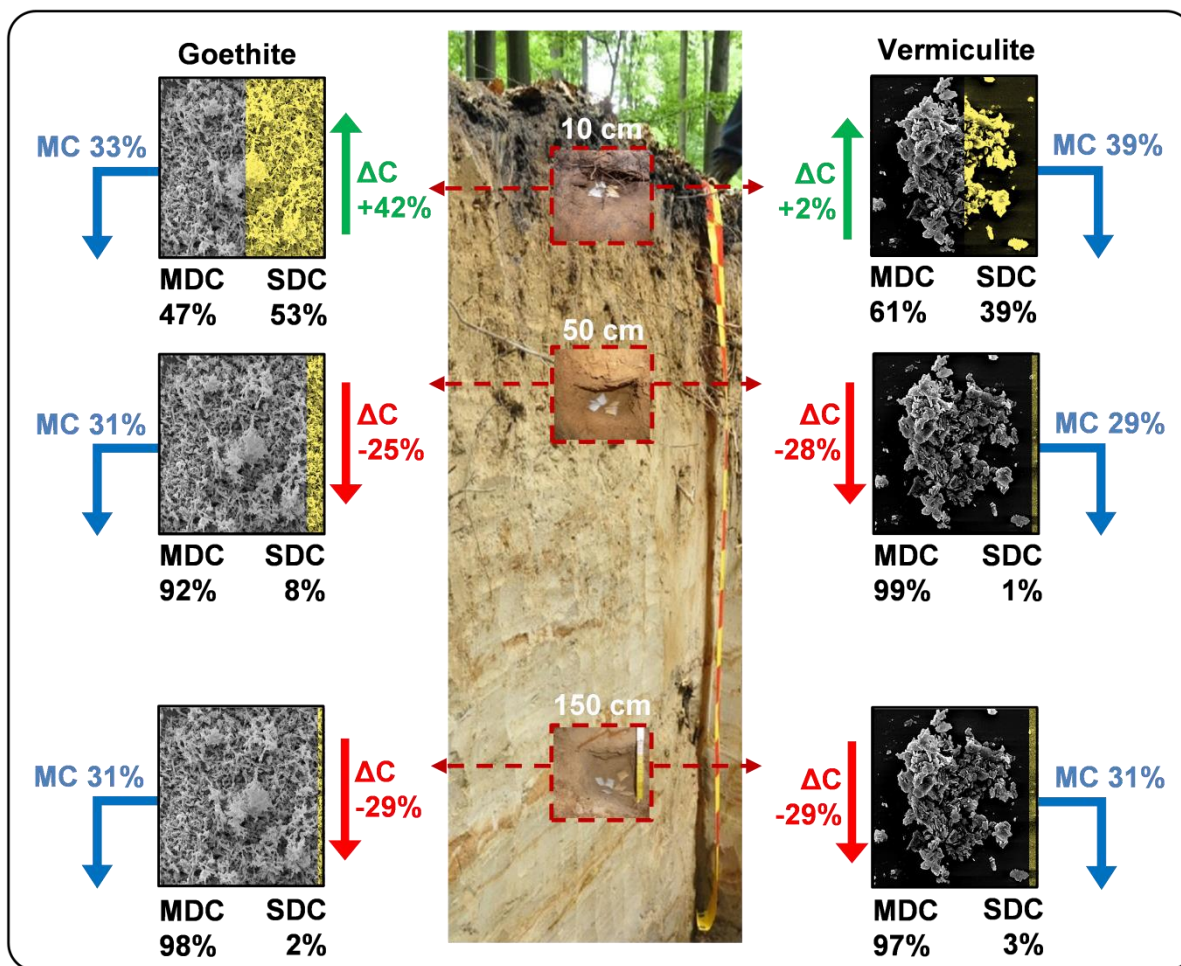


**Fig. 3** Depth-dependent gross C exchange of <sup>13</sup>C-labelled mineral-associated organic C (MAOC) after two-years of field exposure in a Dystric Cambisol located in a temperate European beech forest in Germany. Goethite was chosen as a representative pedogenic Fe oxyhydroxide (left side) and vermiculite as representative 2:1 clay mineral (right side). The net difference in C content before and after the field exposure is given in percent of the initial MAOC content ( $\Delta C$ ). The amount of mobilizable C (MC) during the field exposure is given in percent of initial MAOC as well. The final C content after field exposure was differentiated in pre-existent <sup>13</sup>C-labelled mineral-derived C (MDC) and fresh unlabelled solution-derived C (SDC; yellow color). The soil profile in the center representatively shows a Dystric Cambisol in the Grindewald forest (Germany); left and right figures show scanning electron microscope (SEM) images of the respective C-loaded minerals.



### **Methods**

Three subsoil monitoring observatories (distance about 60 m) are located in a European beech (*Fagus sylvatica* L.) forest on sandy glacio-fluvial deposits in Lower Saxony, Germany (Grinderwald). They are equipped with suction plates for soil solution sampling installed at 10, 50, 150 cm soil depth<sup>31</sup>, suction cups and CO<sub>2</sub> sensors at 10, 30, 50, 90 cm soil depth for analysis of soil CO<sub>2</sub> concentration profiles in combination with closed chambers for measurement of total soil CO<sub>2</sub> efflux<sup>32</sup> (Supplementary Fig. S14a). A field labelling approach was performed on the circular areas of the monitoring observatories by replacing the natural litter layer on 50 % of the area with <sup>13</sup>C-enriched litter (Supplementary Fig. S14b), the other 50 % remained unlabelled. Sampling of soil solution and soil air was done on a weekly basis between January 2015 and November 2016, and DOC and CO<sub>2</sub>, and their δ<sup>13</sup>C values were determined. After 22 months, the remaining labelled litter was removed and soil cores down to 200 cm soil depth were taken to account for the incorporation of labelled litter-derived C in SOC<sup>30</sup> (more details are provided in the Supplementary Methods).

Batch sorption and desorption experiments were conducted with soil samples from three beech (*Fagus sylvatica*) forest sites (Grinderwald, Rüdershausen, Ebergötzen) in Lower Saxony (Germany) and three soil depths following the experimental design of Kalks et al.<sup>39</sup>. Soils developed on different parent materials, including sandy glacio-fluvial and loess deposits, and red sandstone. Sorption isotherms were recorded with bulk soil samples and DOC extracts from local beech litter in eight different concentrations up to 400 mg C L<sup>-1</sup>. Gross OC sorption and exchange with native OC was quantified with a DOC extract from <sup>13</sup>C-enriched beech litter at the highest DOC concentration of the sorption isotherm. Subsequent desorption experiments were carried out by using an ionic background solution (more details are provided in the Supplementary Methods).

The field experiment for the *in-situ* C exchange on mineral surfaces was conducted on an adjacent plot of the soil monitoring study site Grinderwald, following a previous laboratory approach<sup>46</sup>. Goethite and vermiculite, representative for two groups of pedogenic minerals responsible for the majority of reactive surfaces in temperate soils, were coated with DOM extracted from <sup>13</sup>C-enriched beech litter. The minerals had C loadings of 4-9 mg C g<sup>-1</sup> mineral and were buried in meshbags in triplicates in 10, 50, and 150 cm soil depth. After 24 months of field exposure, meshbags were removed and analysed for bulk C, δ<sup>13</sup>C, and the microbial community composition (more details are provided in the Supplementary Methods).

For the three study sites, we refer to a soil depth between 0-10 cm as topsoil, 10-50 cm as upper subsoil, and 50-150 cm as deeper subsoil based on recent publications describing these sites<sup>30,31,39</sup>.

### **Acknowledgements**

We thank Martin Volkmann, Hanna Böhme, and Frank Hegewald for their help in the field, and Heike Steffen and Anne Kathrin Herwig for sample preparations. We thank Manuela Unger for the DO<sup>13</sup>C measurements and Heike Haslwimmer for molecular analyses (qPCR data). Ole Mewes and Eike Perrin are acknowledged for their work on the laboratory batch experiments and Carsten Beyer for analysis of the DOM composition. Financial support for this work was provided by the Deutsche Forschungsgemeinschaft (DFG) within the framework of the DFG Research Unit 1806 “The forgotten Part of Carbon Cycling: Organic Matter Storage and Turnover in Subsoils (SUBSOM)” and the individual grants GU 406/28-1,2, KA 1737/15-2, MI 1377/10-2, DO 1734/4-2, KA 1590/11-2, BA1359/13-2, BA1359/14-2, and MA 1830/14-2.

### **Author contributions**

AD, BM, EK, GG, KK, and RM designed the field experiments, PL designed the laboratory experiments. PL, PWD, SP, and TL conducted the samplings and analysis in the lab. JB provided additional data and FS conducted the statistical analysis of the monitoring data. PL performed the data analysis and drafted the figures. GG, KK, PL, and RM wrote the manuscript with contributions from all co-authors.

### **Competing interests statement**

The authors declare no competing interests.

### **Data availability**

The datasets created during the current study are published in figures and tables of the paper and the supplementary information. Detailed primary data are stored and published in the BonaRes repository and are accessible at: <https://doi.org/10.20387/bonares-rmtx-ttaj>.

### **References**

1. Schimel, D. S. Terrestrial ecosystems and the carbon cycle. *Glob. Change Biol.* **1**, 77–91 (1995).
2. Ciais, P., Sabine, C., Bala, G. & Peters, W. Carbon and other biogeochemical cycles. in *Climate Change 2013: The Physical Science Basis. Contribution of Working Group I to the Fifth Assessment Report of the Intergovernmental Panel on Climate Change* 465–570 (Cambridge University Press, 2013).
3. Rumpel, C., Chabbi, A. & Marschner, B. Carbon storage and sequestration in subsoil horizons: Knowledge, gaps and potentials. in *Recarbonization of the Biosphere* (eds. Lal, R., Lorenz, K., Hüttl, R. F., Schneider, B. U. & von Braun, J.) 445–464 (Springer Netherlands, 2012).

## Study III

---

4. Torn, M. S., Trumbore, S. E., Chadwick, O. A., Vitousek, P. M. & Hendricks, D. M. Mineral control of soil organic carbon storage and turnover. *Nature* **389**, 170–173 (1997).
5. Kramer, M. G. & Chadwick, O. A. Climate-driven thresholds in reactive mineral retention of soil carbon at the global scale. *Nat. Clim. Change* **8**, 1104–1108 (2018).
6. Hagedorn, F., Bruderhofer, N., Ferrari, A. & Niklaus, P. A. Tracking litter-derived dissolved organic matter along a soil chronosequence using  $^{14}\text{C}$  imaging: Biodegradation, physico-chemical retention or preferential flow? *Soil Biol. Biochem.* **88**, 333–343 (2015).
7. Rasmussen, C. *et al.* Beyond clay: Towards an improved set of variables for predicting soil organic matter content. *Biogeochemistry* **137**, 297–306 (2018).
8. Guggenberger, G. & Kaiser, K. Dissolved organic matter in soil: Challenging the paradigm of sorptive preservation. *Geoderma* **113**, 293–310 (2003).
9. Sommer, R. & Bossio, D. Dynamics and climate change mitigation potential of soil organic carbon sequestration. *J. Environ. Manage.* **144**, 83–87 (2014).
10. Fröberg, M. *et al.* Low dissolved organic carbon input from fresh litter to deep mineral soils. *Soil Sci. Soc. Am. J.* **71**, 347 (2007).
11. Lavania, U. C. & Lavania, S. Sequestration of atmospheric carbon into subsoil horizons through deep-rooted grasses - vetiver grass model. *Curr. Sci.* **97**, 618–619 (2009).
12. Lorenz, K., Lal, R. & Shipitalo, M. J. Stabilized soil organic carbon pools in subsoils under forest are potential sinks for atmospheric  $\text{CO}_2$ . *For. Sci.* **57**, 19–25 (2011).
13. Kaipainen, T., Liski, J., Pussinen, A. & Karjalainen, T. Managing carbon sinks by changing rotation length in European forests. *Environ. Sci. Policy* **7**, 205–219 (2004).
14. Lal, R. Soil carbon sequestration to mitigate climate change. *Geoderma* **123**, 1–22 (2004).
15. Luysaert, S. *et al.* Old-growth forests as global carbon sinks. *Nature* **455**, 213–215 (2008).
16. Mayes, M. A., Heal, K. R., Brandt, C. C., Phillips, J. R. & Jardine, P. M. Relation between soil order and sorption of dissolved organic carbon in temperate subsoils. *Soil Sci. Soc. Am. J.* **76**, 1027–1037 (2012).
17. Robertson, A. D. *et al.* Unifying soil organic matter formation and persistence frameworks: The MEMS model. *Biogeosciences* **16**, 1225–1248 (2019).
18. Zhu, Z. *et al.* Greening of the Earth and its drivers. *Nat. Clim. Change* **6**, 791–795 (2016).
19. Mao, J. *et al.* Human-induced greening of the northern extratropical land surface. *Nat. Clim. Change* **6**, 959–963 (2016).
20. Magnani, F. *et al.* The human footprint in the carbon cycle of temperate and boreal forests. *Nature* **447**, 849–851 (2007).
21. McDowell, N. G. *et al.* Pervasive shifts in forest dynamics in a changing world. *Science* **368**, (2020).

### Study III

---

22. Liu, Y. Y. *et al.* Recent reversal in loss of global terrestrial biomass. *Nat. Clim. Change* **5**, 470–474 (2015).
23. Pan, Y. *et al.* A Large and Persistent Carbon Sink in the World's Forests. *Science* **333**, 988–993 (2011).
24. Anderegg, W. R. L. *et al.* Climate-driven risks to the climate mitigation potential of forests. *Science* **368**, (2020).
25. Lajtha, K. *et al.* The detrital input and removal treatment (DIRT) network: Insights into soil carbon stabilization. *Sci. Total Environ.* **640–641**, 1112–1120 (2018).
26. Kaiser, K. & Kalbitz, K. Cycling downwards – dissolved organic matter in soils. *Soil Biol. Biochem.* **52**, 29–32 (2012).
27. Finstad, A. G. *et al.* From greening to browning: Catchment vegetation development and reduced S-deposition promote organic carbon load on decadal time scales in Nordic lakes. *Sci. Rep.* **6**, 1–8 (2016).
28. Meyer-Jacob, C. *et al.* The browning and re-browning of lakes: Divergent lake-water organic carbon trends linked to acid deposition and climate change. *Sci. Rep.* **9**, 1–10 (2019).
29. Kaiser, K., Guggenberger, G. & Zech, W. Sorption of DOM and DOM fractions to forest soils. *Geoderma* **74**, 281–303 (1996).
30. Liebmann, P. *et al.* Relevance of aboveground litter for soil organic matter formation – a soil profile perspective. *Biogeosciences* **17**, 3099–3113 (2020).
31. Leinemann, T., Mikutta, R., Kalbitz, K., Schaarschmidt, F. & Guggenberger, G. Small scale variability of vertical water and dissolved organic matter fluxes in sandy Cambisol subsoils as revealed by segmented suction plates. *Biogeochemistry* **131**, 1–15 (2016).
32. Wordell-Dietrich, P. *et al.* Vertical partitioning of CO<sub>2</sub> production in a Dystric Cambisol. *Biogeosciences Discuss.* 1–27 (2019) doi:<https://doi.org/10.5194/bg-2019-143>.
33. Fröberg, M., Hanson, P. J., Trumbore, S. E., Swanston, C. W. & Todd, D. E. Flux of carbon from <sup>14</sup>C-enriched leaf litter throughout a forest soil mesocosm. *Geoderma* **149**, 181–188 (2009).
34. Schrumpf, M. *et al.* Storage and stability of organic carbon in soils as related to depth, occlusion within aggregates, and attachment to minerals. *Biogeosciences* **10**, 1675–1691 (2013).
35. Gunina, A. & Kuzyakov, Y. Sugars in soil and sweets for microorganisms: Review of origin, content, composition and fate. *Soil Biol. Biochem.* **90**, 87–100 (2015).
36. Roth, V.-N. *et al.* Persistence of dissolved organic matter explained by molecular changes during its passage through soil. *Nat. Geosci.* **12**, 755–761 (2019).
37. Mikutta, R. *et al.* Microbial and abiotic controls on mineral-associated organic matter in soil profiles along an ecosystem gradient. *Sci. Rep.* **9**, 1–9 (2019).
38. Chabbi, A., Kögel-Knabner, I. & Rumpel, C. Stabilised carbon in subsoil horizons is located in spatially distinct parts of the soil profile. *Soil Biol. Biochem.* **41**, 256–261 (2009).

## Study III

---

39. Kalks, F. *et al.* Fate and stability of dissolved organic carbon in topsoils and subsoils under beech forests. *Biogeochemistry* (2020) doi:10.1007/s10533-020-00649-8.
40. Mikutta, R. *et al.* Biodegradation of forest floor organic matter bound to minerals via different binding mechanisms. *Geochim. Cosmochim. Acta* **71**, 2569–2590 (2007).
41. Saidy, A. R., Smernik, R. J., Baldock, J. A., Kaiser, K. & Sanderman, J. The sorption of organic carbon onto differing clay minerals in the presence and absence of hydrous iron oxide. *Geoderma* **209–210**, 15–21 (2013).
42. Angst, G., Kögel-Knabner, I., Kirfel, K., Hertel, D. & Mueller, C. W. Spatial distribution and chemical composition of soil organic matter fractions in rhizosphere and non-rhizosphere soil under European beech (*Fagus sylvatica* L.). *Geoderma* **264**, 179–187 (2016).
43. Kaiser, K. & Guggenberger, G. Sorptive stabilization of organic matter by microporous goethite: sorption into small pores vs. surface complexation. *Eur. J. Soil Sci.* **58**, 45–59 (2007).
44. Kuzyakov, Y. & Blagodatskaya, E. Microbial hotspots and hot moments in soil: Concept & review. *Soil Biol. Biochem.* **83**, 184–199 (2015).
45. Kandeler, E. *et al.* The mineralosphere – Succession and physiology of bacteria and fungi colonising pristine minerals in grassland soils under different land-use intensities. *Soil Biol. Biochem.* **136**, 107534 (2019).
46. Leinemann, T. *et al.* Multiple exchange processes on mineral surfaces control the transport of dissolved organic matter through soil profiles. *Soil Biol. Biochem.* **118**, 79–90 (2018).
47. Kalbitz, K., Schwesig, D., Rethemeyer, J. & Matzner, E. Stabilization of dissolved organic matter by sorption to the mineral soil. *Soil Biol. Biochem.* **37**, 1319–1331 (2005).
48. Fontaine, S. *et al.* Stability of organic carbon in deep soil layers controlled by fresh carbon supply. *Nature* **450**, 277 (2007).
49. Liebmann, P. *et al.* Basic information of three beech forest sites in Lower Saxony (GER), part of the research unit SubSOM. BonaRes Data Centre (ZALF), Version 1.0. <https://doi.org/10.20387/bonares-rmtx-ttaj> (2020).

### Study III – Supplementary material

#### Supplementary Methods

##### Field approaches

###### Study sites

###### *Grinderwald*

The monitoring and main labelling experiments were carried out in the Grinderwald beech forest (*Fagus sylvatica* L.) 40 km north-west of Hanover, Germany (52°34'22'' N, 9°18'49'' E), hereafter referred to as “Grinderwald site”. The beech forest was established in 1916 and replaced a former pine forest. Mean annual temperature is 9.7°C, and mean annual precipitation accounts to 762 mm (Deutscher Wetterdienst, period 1981-2010). Soils are primarily Dystric Cambisols, which developed on Pleistocene glacio-fluvial sandy deposits<sup>1</sup>. Soil texture is dominated by sand-sized particles. For a more detailed site description, please refer to Bachmann et al.<sup>2</sup> and Angst et al.<sup>3</sup>.

The laboratory sorption experiments included the Ebergötzen and Rüdershausen sites, as did the related DOC injection experiment from Kalks et al.<sup>4</sup>.

###### *Rüdershausen*

The site Rüdershausen comprises a European beech forest (*Fagus sylvatica* L.) located north of Göttingen, Germany (51°34'48'' N, 10°14'34'' E) and is hereafter referred to as “Rüdershausen site”. Soils are mostly Haplic Luvisols, which developed on silty loess deposits of late Weichselian origin<sup>1</sup>. Mean annual temperature is about 8.5°C and the mean annual precipitation amounts to 733 mm<sup>4</sup> (Deutscher Wetterdienst, period 1981-2010). Detailed site descriptions were previously published by Kalks et al.<sup>4</sup>.

###### *Ebergötzen*

The site Ebergötzen comprises a European beech forest (*Fagus sylvatica* L.) located north of Göttingen, Germany (51°34'41'' N, 10°3'55'' E) and is hereafter referred to as “Ebergötzen site”. Soils are primarily Dystric Cambisols, which developed on Triassic upper red sandstone and are characterised by sandy texture<sup>1</sup>. Mean annual temperature is about 8.3°C and the mean annual precipitation amounts to 794 mm<sup>4</sup> (Deutscher Wetterdienst, period 1981-2010). Detailed site descriptions were previously published by Kalks et al.<sup>4</sup>.

### Soil monitoring and <sup>13</sup>C-litter manipulation experiment in the field

#### *Setup of field experiment*

In 2013, the Grinderwald site was equipped with three subsoil observatories for monitoring water and dissolved organic carbon (DOC) fluxes as well as CO<sub>2</sub> fluxes<sup>5,6</sup> (Supplementary Fig. S14a). The relevant spherical catchment area per observatory was about 13.2 m<sup>2</sup> (Supplementary Fig. S14b). Briefly, in each of the three soil depths 10, 50, 150 cm three multi-segment suction plates (25×25 cm, ecoTech Umwelt-Meßsysteme GmbH, Bonn, Germany), with 16 squared segments (36 cm<sup>2</sup>) each, were installed per observatory. Plates were installed horizontally and covered by polyamide filter membranes. Fixation and a tight contact with the soil matrix were ensured by adding a mixture of silt-sized quartz and 2 mm-sieved soil from the observatories. All plates per observatory were connected to a vacuum pump and a pressure of 50 mbar was applied in order to collect the free percolating soil solution<sup>7</sup>. Each segment was connected to a collection vessel (250 mL). A detailed description of the installed equipment at the Grinderwald has been published elsewhere<sup>5,6</sup>. Selected soil parameters from the subsoil observatories were adapted from Leinemann et al.<sup>5</sup> and are given in Supplementary Table S3. Further, soil temperature and volumetric water content was monitored every 15 minutes in 10, 30, 50, 90, and 150 cm depth in each subsoil observatory by combined temperature and moisture sensors (UMP-1, Umwelt-Geräte-Technik GmbH, Müncheberg, Germany). Sensors were installed with a horizontal distance of 100 cm from the wall of the subsoil observatories. The vertical CO<sub>2</sub> profile in the soil was monitored by solid-state infrared gas sensors (GMP221, Vaisala Oyi, Helsinki, Finland)<sup>6</sup>. Measurements were taken every three hours from August 2014 to November 2016. Next to the CO<sub>2</sub> sensors, PTFE suction cups (25 mm diameter, 60 mm length) (ecoTech Umwelt-Meßsysteme GmbH, Bonn, Germany) with steel tubing (2 mm diameter) were installed for soil air sampling. The horizontal distance of CO<sub>2</sub> sensors and gas samplers from the subsoil observatory wall increased from 40 cm to 100 cm with increasing soil depth (Supplementary Fig. S14a).

Soil CO<sub>2</sub> efflux was measured at the soil surface as described by Wordell-Dietrich et al.<sup>6</sup>. In brief, 15 polyvinyl chloride collars (diameter 10.4 cm) were installed to a depth of 5 cm in the soil around the subsoil observatories.

#### *<sup>13</sup>C labelling*

The experimental approach was designed to trace litter-derived organic matter on its way down the soil profile in order to investigate into C fluxes from a recent litter layer down to the deep mineral subsoil and to create a complete <sup>13</sup>C budget. To accomplish that, the natural litter layer on the catchment areas of the subsoil observatories was removed manually in January 2015. Half of the area (6.57 m<sup>2</sup>) was replaced by <sup>13</sup>C-enriched beech litter, the other half by natural beech litter as control (Supplementary Fig. 14b). The labelled litter was prepared by mixing 237 g of uniformly <sup>13</sup>C-enriched beech litter (10 to 14 at%)

purchased from IsoLife (Wageningen, The Netherlands) with 1575 g of un-labelled beech litter from plants of similar age. The mixture was placed on the 6.57 m<sup>2</sup> area, corresponding to a total litter input of about 275 g m<sup>-2</sup>, representing mean annual litterfall in central German beech forests<sup>8</sup>. The final  $\delta^{13}\text{C}$ -enrichment was about 1241 ‰ for observatory 1 (OB1) and 1880 ‰ for observatories 2 (OB2) and 3 (OB3) due to delivery of more <sup>13</sup>C-enriched labelled litter batch for the latter two. The label was applied on the half of the observatory equipped with the suction plates and gas samplers, suction cups were installed on the control side to collect soil solution for  $\delta^{13}\text{C}$  values of the control in 25, 50, and 150 cm soil depth (Supplementary Fig. S14a). Further, two polyvinyl chloride collars (30 cm diameter, height 30 cm) for <sup>13</sup>CO<sub>2</sub> measurements on the surface were inserted down to a depth of 15 cm in the area where the labelled litter was applied. Afterwards, a net with a mesh size of 2 cm was installed on top of the litter layer to exclude dilution by freshly fallen leaves and to prevent translocation of the label, e.g. by wind. In autumn, fresh litterfall on the mesh was removed. The continuous leaching of <sup>13</sup>C-labelled dissolved organic matter (DOM) was maintained until November 2016, which adds up to a label duration of 22 months. Then, <sup>13</sup>C input was stopped by removing the labelled litter and restoring the natural litter layer with material from the surrounding area. Afterwards, the amount of removed litter was dried, quantified, and measured for the remaining <sup>13</sup>C-enrichment. Removed litter amounted to an average of 405 g m<sup>-2</sup>, due to incorporation of small leaf debris and beechnut shells. Consequently, mean residual  $\delta^{13}\text{C}$  amounted to 384±183 ‰. During the 22 months of the field experiment, a total of 946 mm throughfall was recorded by a weather station located in the research forest.

### *Sampling and analyses*

Monitoring of the soil solution via suction plates started in August 2014<sup>5</sup> and is still ongoing. Sampling of the soil solutions was realised on a weekly basis during this time. In total, 57 samplings were done during the <sup>13</sup>C labelling from February 2015 to November 2016 (Supplementary Table S4). Soil water flow varied with seasonal weather conditions. Correspondingly, dry periods (especially from late spring to late summer) prevented sampling of 60 % of the theoretical maximum of samples (Supplementary Table S4). In contrast, extremely wet conditions induced a water flux which exceeded the capacities of 9 % of the actually taken samples (Supplementary Table S4).

Volumes of collected samples were immediately determined in the laboratory for water flux calculations. Thereafter, samples were passed through 0.45- $\mu\text{m}$  polyethersulfone filters (VWR International GmbH, Darmstadt, Germany) and stored at 4°C for a maximum of 30 days until analysis. Dissolved OC concentrations were measured by high temperature combustion with a limit of quantification of 1 mg L<sup>-1</sup> via a varioTOC cube (Elementar Analysensysteme GmbH, Langenselbold, Germany). The UV absorbance at 280 nm was analyzed by a Varian Cary 50 UV-Vis spectrophotometer (Agilent Technologies, Santa Clara, CA, USA) and the specific UV absorbance at 280 nm (SUVA<sub>280</sub>)<sup>9,10</sup>



was calculated as the ratio of the UV absorbance and DOC concentration. Soil solutions from twelve sampling campaigns were chosen for  $\text{DO}^{13}\text{C}$  measurements and stored frozen until measured by an isoTOC cube coupled to an isotope ratio mass spectrometer (IRMS) vision<sup>11</sup> (Elementar Analysensysteme GmbH, Langenselbold, Germany).

Soil respiration was measured with soil respiration chambers EGM-3 SRC-1 (PP-Systems, Amesbury, MA, USA) and the LI-6400-09 (LI-COR Inc., Lincoln, NE, USA) at the soil collars around the subsoil observatories from March 2014 to March 2016 from once a month to once a week. Further, the chamber method was used for sampling  $\text{CO}_2$  from the headspace of the installed collars on the labelled area for measurement of the  $\delta^{13}\text{C}$  value of  $\text{CO}_2$ . For that, a lid with an inlet and outlet connection was placed on the collars. Thereafter, the air inside the chamber was circulated at a flow rate of  $2 \text{ L min}^{-1}$  for 30 min over a column filled with soda lime. Then, the air flow was turned off and the soda lime was removed. Chambers were closed for an additional time of 15 to 40 min for  $\text{CO}_2$  accumulation and finally gas samples were taken with a syringe and filled to 12 mL evacuated gas vials. The vertical  $^{13}\text{CO}_2$  profile data were adapted from Wordell-Dietrich et al.<sup>6</sup>. Briefly, two gas samples per depth and subsoil observatory were taken at the end of the stainless steel tubing from the suction cups with a syringe and filled into 12-mL evacuated gas vials (Labco Exetainer, Labco Limited, Lampeter UK). Gas samples were taken from once a month to once a week from May 2014 to November 2016. The  $\delta^{13}\text{C}$  values of  $\text{CO}_2$  in the collected gas samples were determined by an isotope ratio mass spectrometer (Delta Plus with GP interface and GC-Box (Thermo Fisher Scientific, Bremen, Germany) connected to a PAL autosampler (CTC Analytics AG, Zwingen, Switzerland).

Soil OC data and the incorporation of labelled litter-derived C in different functional organic matter fractions were adapted from Liebmann et al.<sup>12</sup>. In short, soil samples from the subsoil observatories were taken by drilling soil cores down to 200 cm depth at the time of label removal (November 2016). Three replicate cores were taken from both sides per observatory, in total 18 soil cores. Cores were divided into 15 depth increments, oven dried at  $60^\circ\text{C}$ , and sieved to  $<2 \text{ mm}$ . Composite samples were prepared by mixing the replicate soil samples of each depth increment on a mass-equivalent basis. Total C and N along with the  $\delta^{13}\text{C}$  values were measured by a vario ISOPRIME cube elemental analyzer (Elementar Analysensysteme GmbH, Langenselbold, Germany) coupled with an IsoPrime100 IRMS (IsoPrime Ltd, Cheadle Hulme, UK) (EA-IRMS). Since the soil pH was  $< 4.2$  (Supplementary Table S3), total C was considered to represent OC.

### *Dissolved organic matter composition analysis*

Soil solution taken during the weekly sampling at the subsoil observatories was analysed for different organic components on four sample sets from samplings between January 2015 and April 2015. Solutions were sampled from the installed suction plates and covered the three sampling depths 10, 50, and 150 cm.

After sampling, soil solutions were filtered through 0.45-um polyethersulfone filters (VWR International GmbH, Darmstadt, Germany) and stored frozen at -20°C until analysis. Stored solutions were thawed at room temperature. Quantitative analysis of the five main DOM components hexoses, pentoses, amino acids, proteins, and phenols was done according to Chantigny et al.<sup>13</sup>. Briefly, component-specific reagents (anthrone-sulfuric acid, orcinol in ethanol, ninhydrin, Bradford protein reagent, and Foli-Ciocalteu's reagent) were added separately to soil solution aliquots and the UV absorbance was measured by using a UV-Vis spectrometer (Specord 210 Plus, Analytik Jena, Jena, Germany). Each DOM component was measured individually by using different standards and wavelengths.

### *Calculations and statistics*

Based on the recent publications describing the three sites under study<sup>4,5,12</sup>, we refer to a soil depth between 0-10 cm as topsoil, 10-50 cm as upper subsoil, and 50-150 cm as deeper subsoil.

Sampled solution volumes were set against the segment area (36 cm<sup>2</sup>) of the plate lysimeter and given in mm for weekly water fluxes. Dissolved OC fluxes were calculated based on the weekly water fluxes multiplied by the DOC concentration and given in g m<sup>-2</sup> week<sup>-1</sup>. Dissolved OC fluxes ( $F_{\text{DOC}}$ , in g m<sup>-2</sup>) and  $\delta^{13}\text{C}$  values ( $\delta^{13}\text{C}$ , in ‰) from all segments per suction plate were used to calculate average and DOC flux-normalised  $\delta^{13}\text{C}$  values per suction plate (in ‰), following Eq. (1):

$$\text{average } \delta^{13}\text{C} = \frac{\sum(F_{\text{DOC}} \times \delta^{13}\text{C})}{\sum F_{\text{DOC}}} . \quad \text{Eq. (1)}$$

From February 2015 until November 2016, 57 sampling campaigns were performed but  $\text{DO}^{13}\text{C}$  data are available for twelve time points only. In addition, those twelve sampling campaigns did not all provide full sample sets due to dry soils. For that reason, it was necessary to interpolate  $^{13}\text{C}$  data for the samplings which were not measured. We chose linear interpolations between two samplings with  $\text{DO}^{13}\text{C}$  data, based on the time (d) between both samplings. By fitting a linear regression, we calculated the potential  $\text{DO}^{13}\text{C}$  values for all samplings.

In a preliminary analysis, the control samples of the twelve  $\text{DO}^{13}\text{C}$  sampling campaigns were considered for significantly different  $^{13}\text{C}$  background values between plots, depths, and sampling dates. Since locations and setup of the observatories were similar, no differences were assumed between the plots. The depth, and spatial and seasonal effects and the three two-way-interactions between these factors on the background  $\delta^{13}\text{C}$  values were evaluated by variance components analysis<sup>14</sup> and revealed a minor impact of the latter two factors and all interactions, thus providing no evidence against using mean background values of  $\delta^{13}\text{C}$  values of the soil solutions per soil depth. In addition, we observed clear differences between the three depths for multiple parameters, including DOC concentration, DOC flux,  $\text{SUVA}_{280}$ , and the contribution of recent litter-derived C. Consequently we considered the background  $\delta^{13}\text{C}$  values to be significantly different between 10, 50, and 150 cm soil depth. In consequence, recovery

calculations were based on mean background values (sites and dates) per depth. Data sets for the three depths were checked for normal distribution by applying the Shapiro-Wilk test.

All measured and interpolated DO<sup>13</sup>C data were tested for significant enrichments compared to the background values using a comparison with the prediction interval<sup>15</sup> ( $\Phi = n-1$ ,  $\alpha = 0.1$ ) given in Eq. (2):

$$^{13}\text{C}_L > \bar{X}_{uL} + \left( t_{\Phi; 1-\alpha} \times \text{SD}_{uL} \times \sqrt{1 + \frac{1}{n}} \right). \quad \text{Eq. (2)}$$

Only significantly enriched samples were included into recovery calculations. Proportions of native DOC (DOC<sub>nat</sub>) and labelled litter-derived DOC (DOC<sub>L</sub>) were determined by Eq. (3) and (4) in percent:

$$\text{DOC}_{\text{nat}} (\%) = \frac{^{13}\text{C}_L - ^{13}\text{C}_{\text{in}}}{^{13}\text{C}_{uL} - ^{13}\text{C}_{\text{in}}} \times 100, \quad \text{Eq. (3)}$$

$$\text{DOC}_L (\%) = 100 \% - \text{DOC}_{\text{nat}}, \quad \text{Eq. (4)}$$

with <sup>13</sup>C<sub>L</sub> as the δ<sup>13</sup>C value of the labelled sample, <sup>13</sup>C<sub>uL</sub> as the δ<sup>13</sup>C value of the un-labelled control, and <sup>13</sup>C<sub>in</sub> as the δ<sup>13</sup>C value of the initial labelled litter. The proportion of DOC<sub>L</sub> was further multiplied with the DOC flux to calculate the absolute amount of litter-derived DOC (in mg) flowing in each sampling interval.

The soil respiration at the surface was modeled by fitting an Arrhenius-type model<sup>16</sup> (Eq. 5), using soil temperature in 10 cm depth and the measured CO<sub>2</sub> fluxes.

$$F_0 = a \times e^{\left( \frac{E_0}{T + 273.2 - T_0} \times \frac{T - 10}{283.2 - T_0} \right)}, \quad \text{Eq. (5)}$$

where F<sub>0</sub> is the soil respiration (μmol m<sup>-2</sup> s<sup>-1</sup>), a, E<sub>0</sub>, and T<sub>0</sub> are fitted model parameters, and T is the soil temperature (°C) at 10 cm depths. The contribution of litter-derived CO<sub>2</sub> was calculated analogously as described in Eq. (3) and Eq. (4) with <sup>13</sup>C<sub>L</sub> as the measured δ<sup>13</sup>C value of the labelled sample, the δ<sup>13</sup>C value of the control (<sup>13</sup>C<sub>uL</sub>) was estimated with -27 ‰ and <sup>13</sup>C<sub>in</sub> as the δ<sup>13</sup>C enrichment of the initial labelled litter. The amount of litter-derived CO<sub>2</sub> (Eq. 4) was multiplied with the daily mean CO<sub>2</sub> flux (F<sub>0</sub>) for each sampling day.

The CO<sub>2</sub> production data and the amount of litter-derived CO<sub>2</sub> in the subsoil observatories were derived from Wordell-Dietrich et al.<sup>6</sup>, who provide a detailed description of the calculations. In short, the CO<sub>2</sub> flux of a soil layer was calculated using Fick's first law (Eq. 6):

$$F = -D_s \times \frac{dC}{dz}, \quad \text{Eq. (6)}$$

where F is the diffusive CO<sub>2</sub> flux across a horizontal plane at each soil depth [μmol m<sup>-2</sup> s<sup>-1</sup>], dC is the difference in CO<sub>2</sub> concentration in the between the lower and upper boundary of the respective soil layer, dz is the height of the soil layer [m], D<sub>s</sub> is the effective diffusivity in the soil atmosphere [m<sup>2</sup> s<sup>-1</sup>]. The effective diffusivity (D<sub>s</sub>) was determined using Eq. (7):

$$D_s = D_0 \times \tau, \quad \text{Eq. (7)}$$

where  $D_0$  is the  $\text{CO}_2$  diffusivity in free air at the soil temperature and air pressure and  $\tau$  is the dimensionless tortuosity factor. The tortuosity factor was modeled as a function of the air-filled pore space for each soil depth and observatory. Therefore, undisturbed soil cores (5.7 cm diameter, 4 cm height) were taken during the excavation of the subsoil observatories for each depth (10, 30, 50, 90, and 150 cm) with five replicates. The soil cores were adjusted in the laboratory at different matrix potentials (-30 hPa, -60 hPa, -300 hPa) and then attached to a diffusion chamber<sup>17</sup>. Thereafter, the chamber was flushed with  $\text{N}_2$  to create a gradient between the top of the sample and the chamber. The oxygen concentration in the chamber was monitored with an oxygen dipping probe DP-PSt3-L2.5-St10-YOP (PreSens Precision Sensing GmbH, Regensburg, Germany). An inverse diffusion model was used to calculate diffusivity and  $\tau$ <sup>18</sup>.

The  $\text{CO}_2$  production ( $P_i$ ) in a soil layer was calculated as the difference between the flux ( $F_i$ ) leaving the soil layer at the top and the flux ( $F_{i+1}$ ) entering the soil layer at the bottom (Eq. 8):

$$P_i = F_i - F_{i+1} \quad \text{Eq. (8)}$$

To determine the proportion of litter-derived C to the  $\text{CO}_2$  production in a soil layer and accounting for diffusion effects, the isotopic signature of  $\text{CO}_2$  production ( $\delta^{13}\text{P-CO}_2$ ) in each soil layer was calculated with Eq. (9):

$$\delta^{13}\text{P-CO}_2 = \left( \frac{^{13}\text{P-CO}_2}{R_{\text{st}} \times ^{12}\text{P-CO}_2} - 1 \right) \times 1000, \quad \text{Eq. (9)}$$

where  $^{12}\text{P-CO}_2$  and  $^{13}\text{P-CO}_2$  are the  $\text{CO}_2$  production for each isotopologue ( $^{12}\text{CO}_2$  and  $^{13}\text{CO}_2$ ) and  $R_{\text{st}}$  is the isotopic ratio of the Vienna-PDB reference standard. Thereafter, the percentage contribution of litter-derived C to  $\text{CO}_2$  production in a soil layer was calculated using the isotopic mixing equations (Eq. (3) and Eq. (4)), where  $^{13}\text{C}_{\text{ul}}$  is the average isotopic signature of  $\text{CO}_2$  production before the labelling,  $^{13}\text{C}_L$  is the isotopic signature of  $\text{CO}_2$  production after the labelling and  $^{13}\text{C}_{\text{in}}$  is the  $\delta^{13}\text{C}$  enrichment of the initial labelled litter. Litter-derived  $\text{CO}_2$  production was estimated by multiplying the amount of litter-derived C with the  $\text{CO}_2$  production of the respective soil layer. Linear interpolation was used to estimate the cumulative litter-derived  $\text{CO}_2$  production.

Soil OC data and calculations were adapted from Liebmann et al.<sup>12</sup>. Briefly, soil samples from all increments were used to determine C stocks from 0–180 cm depth. Stocks were calculated for each core individually. Data showing C stocks per observatory represent the mean of the three replicate cores, while stocks of the entire location represent the mean of all nine cores.

Label recovery was determined similarly as for the DOC calculations. Eq. (3) and Eq. (4) were used to calculate the litter-derived SOC proportion for the significantly enriched samples ( $\alpha = 0.1$ ).

All fluxes and incorporation rates were calculated for the total duration of the labeling experiment (22 months) and afterwards recalculated to fluxes and rates per year.

### Artificial mineral-associated organic matter (MAOM)

#### *Preparations*

Two minerals commonly found in soils were used to prepare MAOM: goethite ( $\alpha$ -FeOOH) representing the group of iron oxides and vermiculite representing 2:1 layered expandable clay minerals. Goethite was provided by Lanxess (Cologne, Germany; Bayferrox 920 Z) and the manufacturer information included a nominal density of  $4.0 \text{ g cm}^{-3}$ . A specific surface area (SSA) of  $11.8$  to  $12.0 \text{ m}^2 \text{ g}^{-1}$  was determined with the Brunauer-Emmett-Teller (BET) method on a Quantasorb (Quantachrome, Oedelzhausen, Germany) and a mean particle size of  $475.5 \text{ nm}$  was measured by dynamic light scattering measurements (ZetaPALS, Brookhaven Instruments Corp., Holtsville, NY, USA) (supplementary information in Carstens et al.<sup>19</sup>). Vermiculite was purchased from União Brasileira de Mineração S/a (Sao Paulo, SP, Brazil)<sup>20</sup>, grinded in a ball mill and the clay-sized particles were separated by sedimentation. The clay fraction was conditioned with  $\text{CaCl}_2$  and freeze-dried. The SSA amounted to  $38.6 \text{ m}^2 \text{ g}^{-1}$ .

Preparation of the  $^{13}\text{C}$ -enriched DOM solution was done according to Leinemann et al.<sup>11</sup> by mixing  $10 \text{ g}$  of highly and homogeneously enriched beech litter ( $12.6 \text{ at}\%$ ; IsoLife, Wageningen, The Netherlands) with  $240 \text{ g}$  of naturally grown beech litter. Litter material ground to a size  $<3 \text{ cm}$  was mixed with  $2500 \text{ mL}$  ultra-pure water ( $1/10$ , w/v), and allowed to rest for  $16 \text{ h}$  at room temperature. The solution was first pressure-filtered through  $0.7\text{-}\mu\text{m}$  glass fiber filters (GF 92, Whatman GmbH, Dassel, Germany) and afterwards filtered through  $0.45\text{-}\mu\text{m}$  cellulose-nitrate filters (Sartorius, Göttingen, Germany). Extracts had DOC concentrations of about  $1000 \text{ mg C L}^{-1}$ , and were diluted to  $500 \text{ mg L}^{-1}$  for the mineral coating procedure. Minerals were coated by adding  $1000 \text{ mL}$  DOM solution to  $10 \text{ g}$  of the respective mineral. The suspension was shaken for  $24 \text{ h}$  in the dark on an end-over-end shaker and afterwards centrifuged for  $20 \text{ min}$  at  $2000 \text{ g}$ . The supernatant was discarded and the remaining mineral was washed two times for  $10 \text{ min}$  with ultra-pure water and subsequently separated by centrifugation for  $10 \text{ min}$  at  $2000 \text{ g}$ . The C-coated minerals were freeze-dried and stored in the dark until further use. Organic carbon concentrations were  $3.96 \text{ mg g}^{-1}$  for C-coated goethite (G0) and  $9.21 \text{ mg g}^{-1}$  for C-coated vermiculite (V0). The  $\delta^{13}\text{C}$ -values of the organic matter coating were about  $1014 \text{ ‰}$  for goethite and  $731 \text{ ‰}$  for vermiculite, respectively. The SSA decreased considerably due to the sorption of the organic matter (Supplementary Table S2).

#### *Set up of field experiment and sampling*

Two  $\text{g}$  C-coated goethite and  $1.6 \text{ g}$  C-coated vermiculite, respectively, were filled into meshbags with a size of  $3\text{-}4 \text{ cm}$  in diameter and consisting of a polyamide mesh with a pore size of  $20 \mu\text{m}$  and a fiber thickness of  $34 \mu\text{m}$  (Polyamide Fabrics reference: PA-20/14). In May 2016, meshbags of both minerals were buried in  $10$ ,  $50$ , and  $150 \text{ cm}$  soil depth in triplicates in the Dystric Cambisol of the Grinderwald site.

## Study III – Supplementary material

---

In each depth, a soil volume of about 20×20×10 cm (L×W×H) was excavated and refilled with the excavated soil after the meshbag placement. Due to this, the natural water flow through the soil was least disturbed.

After 24 months of field incubation, bags were removed in May 2018. Besides the meshbags also soil 1 cm above and below each bag was sampled to trace organic matter translocation originating from the mineral coating and to compare the composition of the microbial community. Translocation of mineral-associated organic C (MAOC) to the soil above the meshbags was found to be on average <0.01 % of the total MAOC, while translocation to the soil below amounted to about 0.5 % of the total MAOC. Bulk soil samples were taken from an adjacent plot in the respective depths. Immediately after sampling, the meshbags were shock frozen in liquid nitrogen in the field. Subsamples of the meshbag-derived minerals and adjacent soil were separated in the laboratory at the same day. One aliquot of fresh minerals and soil was kept frozen for microbial analysis. The remaining mineral material was freeze dried for bulk and surface analyses, while the remaining soil was oven dried at 60°C<sup>12</sup> and sieved to <2 mm for further treatments.

### *Analyses*

Dried C-coated minerals and soil samples were analysed on OC, total N ( $N_{\text{tot}}$ ) and  $\delta^{13}\text{C}$  using an EA-IRMS. The SSA and pore volumes of mineral samples were derived from 40-point  $\text{N}_2$  gas adsorption isotherms recorded at 77 K with a Quantachrome Autosorb iQ instrument (Quantachrome, Boynton Beach, Florida, USA). Up to about 0.5 g of each sampled field replicate ( $n = 3$ ) were weighed into the sample cell and degassed at 333 K for at least 12 hours. The SSA derived from 7-10 adsorption points in the  $P/P_0$  range of 0.05-0.3 using the linear BET plot<sup>21,22</sup>.

Analysis of the microbial community was done by extracting the DNA from 0.3 g of each of the buried mineral samples and soil samples above and underneath the mineral meshbags with a FastDNA SPIN Kit for soil (BIO101, MP Biomedicals, Irvine, CA, USA) and quantified with a Nanodrop ND-2000 spectrophotometer (Thermo Scientific, Waltham, MA, USA) followed by dilution of the samples with ultra-pure water to a target concentration of 5 ng DNA  $\mu\text{l}^{-1}$ . The quantification of the abundances of total bacteria, fungi and archaea<sup>23-26</sup> and the abundances of the bacterial taxa  *$\beta$ -Proteobacteria*, *Actinobacteria*, *Acidobacteria*, *Bacteroidetes*, *Firmicutes*, *Verrucomicrobia* and *Gemmatimonadetes*<sup>27-29</sup> via quantitative PCR (qPCR) was carried out with an ABI prism 7500 Fast System (Applied Biosystems, USA). For each qPCR assay a cocktail of 0.75  $\mu\text{l}$  of each forward and reverse primer, 0.375  $\mu\text{l}$  T4gp32, 7.5  $\mu\text{l}$  SYBR Green, 4.125  $\mu\text{l}$  ultra-pure water and 1.5  $\mu\text{l}$  DNA template (for total bacteria and archaea only 1.0  $\mu\text{l}$ ) was dispensed. Standard curves were generated in triplicate with serial dilutions of a known amount of the

respective isolated plasmid DNA. Each qPCR run included two no template controls showing no or negligible values. Supplementary Table S5 lists the primers, thermal cycling conditions, and efficiencies.

### *Calculations and statistics*

Bulk EA-IRMS data were used to calculate elemental and isotopic changes before and after the experiment, according to Leinemann et al.<sup>11</sup>. The proportion of mineral-bound organic C after the experiment, which derived from the solution (solution-derived C, SDC) was calculated relative to the  $\delta^{13}\text{C}$  ratio of the inflow soil solution ( $\delta^{13}\text{C}_{\text{in}}$ ) according to Eq. (10). Since the field setup did not allow us to sample the exact soil solution flowing into the meshbags, the two-year-mean  $\delta^{13}\text{C}$  values of the soil solution in the respective depths from the adjacent subsoil observatories<sup>5</sup> were used here;  $\delta^{13}\text{C}_{\text{Ma}}$  represents the  $\delta^{13}\text{C}$  ratio of the MAOC after the experiment, while  $\delta^{13}\text{C}_{\text{Mb}}$  represents the  $\delta^{13}\text{C}$  ratio of the MAOC before the experiment.

$$\text{SDC (\%)} = \frac{(\delta^{13}\text{C}_{\text{Ma}} - \delta^{13}\text{C}_{\text{Mb}})}{(\delta^{13}\text{C}_{\text{in}} - \delta^{13}\text{C}_{\text{Mb}})} \times 100 . \quad \text{Eq. (10)}$$

Since the remaining proportion of labelled organic C on the mineral surface after the experiment still derived from the coating before the experiment, the pre-existent  $^{13}\text{C}$ -labelled mineral-derived organic C (MDC) was calculated as the difference between the total mineral-bound C after the experiment ( $C_{\text{tot}} = 100\%$ ) minus the proportion of SDC using Eq. (11).

$$\text{MDC (\%)} = 100\% - \text{SDC} . \quad \text{Eq. (11)}$$

The relative change in organic C concentration ( $\Delta\text{C}$ ) of the C-coated minerals before ( $C_{\text{before}}$ ) and after the experiment ( $C_{\text{after}}$ ) was calculated with equation Eq. (12):

$$\Delta\text{C (\%)} = \frac{(C_{\text{after}} - C_{\text{before}})}{C_{\text{before}}} \times 100 . \quad \text{Eq. (12)}$$

The C fraction, which was previously bound to the mineral surfaces, and got mobilised during the experiment (MC) was calculated according to Eq. (13). Thereby, the difference in the absolute amount of SDC and the change in mineral-bound C before and after the experiment is relative to the C content before the experiment.

$$\text{MC (\%)} = \frac{\left(\frac{\text{SDC(\%)} \times C_{\text{after}}}{100} - (C_{\text{after}} - C_{\text{before}})\right)}{C_{\text{before}}} \times 100 . \quad \text{Eq. (13)}$$

## **Laboratory approaches**

### Sorption isotherms

#### *Preparations*

Preparation of DOM solution followed the descriptions of Kaiser and Guggenberger<sup>30</sup> by mixing 200 g dried and shredded (<30 mm) beech litter with 2 L ultra-pure water (18.2 M $\Omega$ ). After 16 h resting time at

## Study III – Supplementary material

---

room temperature, mixtures were pre-filtered (0.7  $\mu\text{m}$  glassfibre filters; GF 92, Whatman GmbH, Dassel, Germany) followed by filtration down to  $<0.45 \mu\text{m}$  (cellulose-nitrate filters; G, Sartorius AG, Göttingen, Deutschland) using a pressure filtration system. The stock solution was analysed for its DOC concentrations by a varioTOC cube (Elementar Analysensysteme GmbH, Langenselbold, Germany) and diluted to the following concentrations: 1, 5, 10, 25, 50, 100, 200, 400  $\text{mg C L}^{-1}$ . Prepared solutions were again analysed for DOC concentrations, as well as for pH and UV absorbance (SPECTROstar Nano, BMG LABTECH, Ortenberg, Germany) (Supplementary Table S6).

### *Batch sorption experiments*

Sorption isotherms of DOC (representing sorption of DOM in general) were determined for all three sites, Grinderwald, Rüdershausen, and Ebergötzen. Composite soil samples were taken at three depths (10-20 cm representing the topsoil, 50-60 cm representing the upper subsoil, and 100-110 cm representing the deeper subsoil<sup>12</sup>), consistent with the DOC injection depths discussed in Kalks et al.<sup>4</sup>. Soils were oven-dried at 60°C for 48 h and sieved to  $<2 \text{ mm}$ . Basic soil parameters are given in Supplementary Table S7. The mineralogical composition of the clay fractions from each site and soil depth was assessed by X-ray diffraction (X'Pert Pro-MPD; PANalytical, Almelo, The Netherlands). Clay samples were prepared by removing organic matter with 35 % hydrogen peroxide and Fe (oxyhydr)oxides by extraction with dithionite-citrate-bicarbonate<sup>31</sup>. Oriented clay samples saturated with  $\text{K}^+$  (with and without heating to 550°C) and  $\text{Mg}^{2+}$  (with and without ethylene glycol solvation) were measured in the range of 3-30° 2 $\theta$  with  $\text{CuK}\alpha$  radiation (45 kV, 40 mA), and a step size of 0.01° (Supplementary Fig. S7). Sorption experiments were carried out in triplicates according to Kaiser et al.<sup>32</sup> by adding 40 mL of the DOM solution with the respective DOC concentration between 1 and 400  $\text{mg L}^{-1}$  to 8 g of soil. Mixtures were shaken on a horizontal shaker for 24 h at room temperature and a frequency of 1.7  $\text{s}^{-1}$ . Thereafter, the samples were centrifuged at 3000 g for 10 min, and the supernatant was decanted and filtered (0.45  $\mu\text{m}$  PES filters, VWR International GmbH, Darmstadt, Germany).

### *Measurements and calculations*

The pH and the UV absorbance (SPECTROstar Nano, BMG LABTECH, Ortenberg, Germany) of the filtrates were determined directly after filtration. Filtrates were stored at 4°C and the DOC concentrations were measured within 24 h (varioTOC cube; Elementar Analysensysteme GmbH, Langenselbold, Germany). Sorption isotherms were calculated according to the initial mass approach<sup>33</sup>.



### Gross sorption and desorption (exchange) experiments

#### *Preparations*

Two types of DOM solutions were prepared (adjusted method from Kaiser and Guggenberger<sup>30</sup>). The first one was produced by mixing 200 g undecomposed (“fresh”), dried, and shredded (<30 mm) un-labelled and recently fallen beech litter with 2 L ultra-pure water (18.2 MΩ). The second solution contained 200 g of <sup>13</sup>C-enriched beech litter (sieved to <5 mm) instead, which was previously exposed in the field for 22 months (“altered”). After 16 h resting time at room temperature, mixtures were pre-filtered (0.7 μm glass fibre filters; GF 92, Whatman GmbH, Dassel, Germany) and then filtered to <0.45 μm (cellulose-nitrate filters; G, Sartorius AG, Göttingen, Deutschland) using a pressure filtration system. Stock solutions were analysed for DOC concentrations (varioTOC cube; Elementar Analysensysteme GmbH, Langenselbold, Germany), δ<sup>13</sup>C values (isoTOC cube coupled to an IRMS vision; Elementar Analysensysteme GmbH, Langenselbold, Germany), and the ionic background (IB) composition by ion chromatography (30 Compact IC Flex, Metrohm, Filderstadt, Germany). The δ<sup>13</sup>C values were at -28.1 ‰ for the un-labelled solution and 169.7 ‰ for the labelled solution with a pH of 6.04 and 4.94, respectively. Stock solutions were diluted to a final DOC concentration of 400 mg L<sup>-1</sup> and stored frozen until use. An artificial IB solution was prepared on the basis of the IB of the DOM solutions, including the following anions and cations: Cl<sup>-</sup>, NO<sub>3</sub><sup>-</sup>, SO<sub>4</sub><sup>2-</sup>, PO<sub>4</sub><sup>3-</sup>, Na<sup>+</sup>, K<sup>+</sup>, Mg<sup>2+</sup>, and Ca<sup>2+</sup>.

#### *Experimental setup*

Batch sorption and desorption experiments were carried out with soil from all the study sites, Grinderwald, Rüdershausen, and Ebergötzen, using the same depth increments as described above. Sorption experiments were carried out in triplicates as mentioned above, adding 40 mL of the respective 400 mg L<sup>-1</sup> DOC solution to eight g of soil. While the <sup>13</sup>C-labelled approach was in the focus, an un-labelled DOM solution was used and needed as a control for calculations. Another aspect was the evaluation of two DOM solutions of different origin (altered vs. fresh litter), which turned out to be not of major importance in our sorption experiments (Supplementary Fig. S10). After 24 hours, samples were centrifuged (3000 g for 10 min) and the supernatant filtered through <0.45 μm PES membranes (VWR International GmbH, Darmstadt, Germany). Sixteen mL of the IB solution was added to the soil pellets in order to remove remnants of the DOM solution<sup>34</sup>, manually shaken, and immediately centrifuged again. Supernatants were discarded and the soil pellets were separated. Four grams of soil were removed and freeze-dried for bulk analysis of the soil after the sorption experiment. The other four g were used to carry out the desorption experiment under the same conditions as the sorption experiments, according to Saïdy et al.<sup>34</sup>. Mean differences in soil weight after separation were <2 %. The four g of soil were mixed with 20 mL of the IB solution, shaken for 24 h on a horizontal shaker, centrifuged at 3000 g for 15 min, and the

supernatant was filtered to <0.45 µm (PES filters, VWR International GmbH, Darmstadt, Germany). Soils were freeze-dried after the desorption experiment. Overall mass recovery after both experiments amounted to 99 %.

### *Measurements*

All filtrates were directly analyzed for UV absorbance at 280 nm (SPECTROstar Nano, BMG LABTECH, Ortenberg, Deutschland) and pH, and stored at 4°C for further analysis of DOC concentrations (varioTOC cube; Elementar Analysensysteme GmbH, Langenselbold, Germany) within 24 h. Freeze-dried soils were measured for organic C, total N, and  $\delta^{13}\text{C}$  by EA-IRMS (vario ISOPRIME cube elemental analyzer (Elementar Analysensysteme GmbH, Langenselbold, Germany) coupled to an IsoPrime100 IRMS (IsoPrime Ltd, Cheadle Hulme, UK)).

### *Definitions and calculations*

Mobilisable C (MC) represents the C released into the IB solution after the respective treatment. Mobilisable C before the sorption experiments ( $\text{MC}_B$ ) and mobilisable C after the desorption experiment ( $\text{MC}_D$ ) represents the IB-mobilisable C, which was directly measured in the extracts. We observed that after the sorption experiment, there was always a decrease of the DOC content in the solution, but not always a corresponding increase of SOC in the soil. This discrepancy originated from the washing step with the IB solution between the sorption and desorption experiment directly before separating the soil. To account for both, the increase in SOC contents for some soils and the overall decrease in DOC contents during sorption, mobilisable C after the sorption experiment ( $\text{MC}_S$ ) was calculated with Eq. (14):

$$\text{MC}_S = (\text{DOC}_{\text{in}} - \text{DOC}_a) - (\text{SOC}_S - \text{SOC}_B), \quad \text{Eq. (14)}$$

with the difference of the initial DOC content in the DOM solution ( $\text{DOC}_{\text{in}}$ ) and the DOC content after the sorption experiment ( $\text{DOC}_a$ ) subtracted by the net increase of the SOC content as the difference of the SOC content after the sorption experiment ( $\text{SOC}_S$ ) and the SOC content before the sorption experiment ( $\text{SOC}_B$ ).

Distribution of native and label-derived SOC in the samples was calculated according to mixing Eq. (3) and Eq. (4). Label-derived SOC contents before and after the desorption experiment were further tested for significant differences using a Student t-test ( $p < 0.05$ ). Prior, normality was assured by using the Shapiro-Wilk test.

**Supplementary Tables**

**Supplementary Table S1** Mean dissolved organic carbon (DOC) concentrations, annual water and DOC and fluxes and mean specific UV absorbance at 280 nm (SUVA<sub>280</sub>) values during the experiment runtime February 2015 – November 2016. Values in brackets represent the standard deviation. This table is an extension to the data published by Leinemann et al.<sup>5</sup>.

Depth [cm]	Water flux [mm yr <sup>-1</sup> ]	DOC [mg L <sup>-1</sup> ]	DOC flux [g m <sup>-2</sup> yr <sup>-1</sup> ]	SUVA <sub>280</sub> [L mg C <sup>-1</sup> cm <sup>-1</sup> ]
Observatory 1				
10	162	57.1 (30.2)	8.7	0.029 (0.019)
50	205	12.1 (7.2)	2.1	0.007 (0.004)
150	427	9.2 (13.4)	2.4	0.006 (0.003)
Observatory 2				
10	329	53.5 (20.6)	17.1	0.034 (0.020)
50	77	22.3 (10.7)	1.3	0.005 (0.003)
150	114	11.9 (15.5)	0.8	0.004 (0.002)
Observatory 3				
10	284	44.4 (11.9)	12.6	0.029 (0.006)
50	117	8.3 (4.2)	0.8	0.003 (0.002)
150	447	6.0 (3.0)	2.1	0.005 (0.009)

## Study III – Supplementary material

**Supplementary Table S2** Basic parameters of the C-coated goethite and vermiculite (G0, V0) and the buried goethite and vermiculite in the respective depths (G/V-10, 50, 150 cm). Data of the buried mineral samples are given as the mean of three replicates with the standard deviation in brackets, while the other samples show single values.

Sample	OC <sup>1</sup> [mg g <sup>-1</sup> ]	TN <sup>2</sup> [mg g <sup>-1</sup> ]	C/N	ΔC <sup>3</sup> [%]	<sup>13</sup> C [‰]	MDC <sup>4</sup> [%]	SDC <sup>5</sup> [%]	MC <sup>6</sup> [%]	SSA <sup>7</sup> [m <sup>2</sup> g <sup>-1</sup> ]
G0	3.96	0.53	7.49	-	1013.52	100.00	0.00	-	9.41
G-10	5.63 (0.27)	0.40 (0.03)	14.22 (0.67)	41.98 (6.86)	464.19 (34.63)	47.28 (3.32)	52.72 (3.32)	33.02 (1.55)	11.82 (1.51)
G-50	2.97 (0.06)	0.37 (0.04)	8.16 (1.12)	-25.03 (1.45)	926.54 (19.75)	91.65 (1.90)	8.35 (1.90)	31.27 (2.75)	12.18 (2.54)
G-150	2.80 (0.02)	0.30 (0.04)	9.45 (1.33)	-29.32 (0.50)	992.10 (8.86)	97.94 (0.85)	2.06 (0.85)	30.77 (0.64)	12.44 (2.43)
V0	9.21	0.98	9.41	-	731.23	100.00	0.00	-	21.87
V-10	9.40 (1.03)	0.63 (0.10)	15.05 (0.88)	2.07 (11.20)	433.14 (77.09)	60.76 (10.15)	39.24 (10.15)	38.74 (4.05)	36.06 (9.79)
V-50	6.65 (0.30)	0.46 (0.08)	14.62 (1.74)	-27.78 (3.24)	723.53 (18.64)	98.99 (2.46)	1.01 (2.46)	28.56 (1.86)	31.17 (10.96)
V-150	6.55 (0.21)	0.43 (0.01)	15.07 (0.16)	-28.90 (2.23)	711.87 (6.44)	97.45 (0.85)	2.55 (0.85)	30.72 (2.08)	33.95 (8.81)

<sup>1</sup> Organic carbon (OC)

<sup>2</sup> Total nitrogen (TN)

<sup>3</sup> Net carbon accrual/loss (ΔC)

<sup>4</sup> Mineral-derived C (MDC)

<sup>5</sup> Solution-derived C (SDC)

<sup>6</sup> Mobilised C (MC)

<sup>7</sup> Specific surface area (SSA)

## Study III – Supplementary material

**Supplementary Table S3** Selected soil parameters as the mean of the three subsoil observatories with the standard deviation in brackets (adopted from Liebmann et al.<sup>12</sup>).

Horizon	Depth	OC <sup>2</sup>	TN <sup>3</sup>	pH	Clay	Silt	Sand
WRB <sup>1</sup>	[cm]	[mg g <sup>-1</sup> ]	[mg g <sup>-1</sup> ]	[CaCl <sub>2</sub> ]	-----	[mg g <sup>-1</sup> ]	-----
AE	0-10	15.18 (1.72)	0.59 (0.06)	3.2 (0.2)	19 (3)	282 (56)	699 (57)
Bsw	10-23	9.59 (2.52)	0.41 (0.09)	3.5 (0.4)	27 (11)	307 (81)	666 (90)
Bw	23-67	4.65 (1.96)	0.26 (0.04)	3.9 (0.1)	26 (4)	332 (99)	642 (103)
C	67-99	1.07 (0.46)	0.08 (0.02)	3.9 (0.2)	29 (8)	255 (41)	716 (47)
2C	99-138	0.34 (0.11)	0.07 (0.09)	4.1 (0.1)	21 (14)	87 (55)	891 (66)
3C	138-175	1.05 (0.11)	0.10 (0.11)	4.0 (0.3)	32 (44)	268 (422)	700 (466)
4C	175+	0.29 (0.14)	0.03 (0.04)	3.9 (0.2)	19 (6)	58 (8)	923 (14)

<sup>1</sup> according to IUSS Working Group WRB<sup>1</sup>

<sup>2</sup> Organic carbon (OC)

<sup>3</sup> Total nitrogen (TN)

## Study III – Supplementary material

---

**Supplementary Table S4** Number of soil solutions sampled and their proportion of the theoretical possible number per observatory and depth.

Depth [cm]	Quantity	Proportion [% of samples <sub>real</sub> ]
Observatory 1		
10	401	12.5
50	277	8.6
150	386	12.0
Observatory 2		
10	659	20.6
50	126	3.9
150	226	7.1
Observatory 3		
10	546	17.0
50	178	5.6
150	407	12.7
<hr style="border-top: 1px dashed black;"/>		
Samples <sub>real</sub> (theoretical = 8151) <sup>1</sup>	3206	
Samples > 250 mL	290	9.1

<sup>1</sup> 57 samplings à 143 samples max.

## Study III – Supplementary material

**Supplementary Table S5** qPCR primers and conditions.

Gene	Primer <sup>1</sup>	Thermal profile <sup>2</sup>	No. of cycles	Efficiency mean [%]	Reference
16S rRNA genes	341F	95°C – 10 m	1	99	López-Gutiérrez et al. <sup>23</sup>
	515R	95°C – 15 s, 60°C – 30 s, 72°C – 30 s, 75°C – 30 s	35		
Fungal ITS fragment	ITS3F	95°C – 10 m	1	93	White et al. <sup>24</sup> , Manerkar et al. <sup>25</sup>
	ITS4R	95°C – 15 s, 55°C – 30 s, 72°C – 30 s, 76°C – 30 s	35		
16S Archaea	Ar912R	95°C – 10 m	1	92	Lueders and Friedrich <sup>26</sup>
	Ar109F	95°C – 30 s, 52°C – 60 s, 72°C – 60 s, 75°C – 30 s	40		
<i>Acidobacteria</i>	Acid31	95°C – 10 m	1	92	Fierer et al. <sup>27</sup>
	Eub518	95°C – 15 s, 55°C – 30 s, 72°C – 30 s, 81°C – 30 s	35		
<i>Actinobacteria</i>	Act920F3	95°C – 10 m	1	92	Bacchetti De Gregoris et al. <sup>29</sup>
	Act1200R	95°C – 15 s, 61.5°C – 30 s, 72°C – 30 s, 78°C – 30 s	35		
<i>β-Proteobacteria</i>	Eub338	95°C – 10 m	1	92	Fierer et al. <sup>27</sup>
	Bet680	95°C – 15 s, 55°C – 30 s, 72°C – 30 s, 80°C – 30 s	35		
<i>Firmicutes</i>	Lgc353	95°C – 10 m	1	97	Fierer et al. <sup>27</sup>
	Eub518	95°C – 15 s, 60°C – 30 s, 72°C – 30 s, 79°C – 30 s	35		
<i>Verrucomicrobia</i>	Verr 349	95°C – 10 m	1	90	Philippot et al. <sup>28</sup>
	Eub 518	95°C – 15 s, 60°C – 30 s, 72°C – 30 s, 77°C – 30 s	35		
<i>Gemmatimonadetes</i>	Gem440	95°C – 10 m	1	95	Philippot et al. <sup>28</sup>
	Eub518	95°C – 15 s, 58°C – 30 s, 72°C – 30 s, 78°C – 30 s	35		
<i>Bacteroidetes</i>	Cfb798F	95°C – 10 m	1	96	Bacchetti De Gregoris et al. <sup>29</sup>
	Cfb967R	95°C – 15 s, 61.5°C – 30 s, 72°C – 30 s, 75°C – 30 s	35		

<sup>1</sup> Primer concentration was 10 pmol μl<sup>-1</sup>

<sup>2</sup> Additionally, a 60°C to 95°C step was added to each run to obtain the denaturation curve specific for each amplified sequence.

## Study III – Supplementary material

---

**Supplementary Table S6** Parameters of the sorption isotherm solutions and the stock solution, including the target dissolved organic carbon (DOC) level, the actual DOC concentration, dissolved total nitrogen (DTN), pH, and the specific UV absorbance at 280 nm (SUVA<sub>280</sub>).

Target DOC level [mg L <sup>-1</sup> ]	DOC [mg L <sup>-1</sup> ]	DTN [mg L <sup>-1</sup> ]	pH [H <sub>2</sub> O]	SUVA <sub>280</sub> [L mg C <sup>-1</sup> cm <sup>-1</sup> ]
Stock solution	862	95.9	6.06	0.0076
1	1.00	0.16	6.84	0.0035 <sup>1</sup>
5	4.69	0.71	6.49	0.0079
10	9.26	1.24	6.17	0.0083
25	23.6	3.04	6.02	0.0082
50	46.8	6.42	6.08	0.0112
100	92.7	12.2	6.09	0.0078
200	189	24.9	6.12	0.0079
400	385	51.4	6.13	0.0079

<sup>1</sup> Value was at detection limit



## Study III – Supplementary material

**Supplementary Table S7** Basic parameters of soils used for the sorption isotherms, and sorption and desorption experiments.

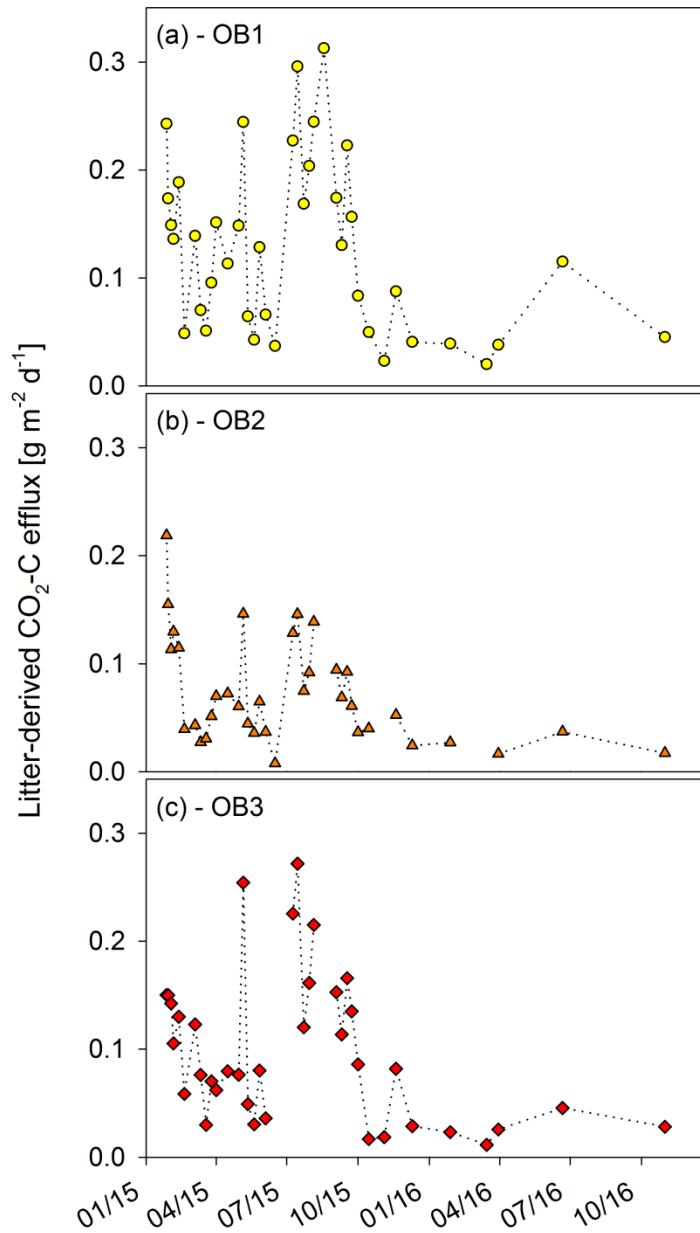
Site	Depth [cm]	OC <sup>1</sup>	TN <sup>2</sup>	$\delta^{13}\text{C}$	pH	Clay	Silt	Sand	Fe <sub>d</sub> <sup>3</sup>	Fe <sub>o</sub> <sup>4</sup>	Al <sub>o</sub> <sup>4</sup>	Mn <sub>o</sub> <sup>4</sup>
		--- [mg g <sup>-1</sup> ] ---		[%o]	[H <sub>2</sub> O]				----- [mg g <sup>-1</sup> ] -----			
Grinderwald	10	8.03	0.34	-27.08	5.2	9	121	870	1.99	1.04	1.32	0.15
	50	0.77	0.10	-24.58	5.2	7	128	865	0.64	0.09	0.67	0.04
	100	0.22	0.04	-23.20	5.5	4	9	987	0.50	0.00	0.19	0.03
Rüdershausen	10	5.38	0.50	-26.18	4.9	159	767	74	2.76	1.27	1.12	0.58
	50	2.23	0.32	-25.18	4.7	137	795	68	2.38	0.96	0.85	0.55
	100	1.05	0.26	-24.63	5.2	177	655	168	2.71	0.96	0.95	0.63
Ebergötzen	10	4.03	0.40	-26.32	5.2	96	183	721	4.62	2.64	1.37	0.91
	30	1.68	0.27	-25.12	4.8	85	175	740	4.77	2.96	1.37	1.01
	60	1.29	0.25	-23.79	4.6	102	184	714	6.87	1.78	1.09	0.31

<sup>1</sup> Organic carbon (OC)

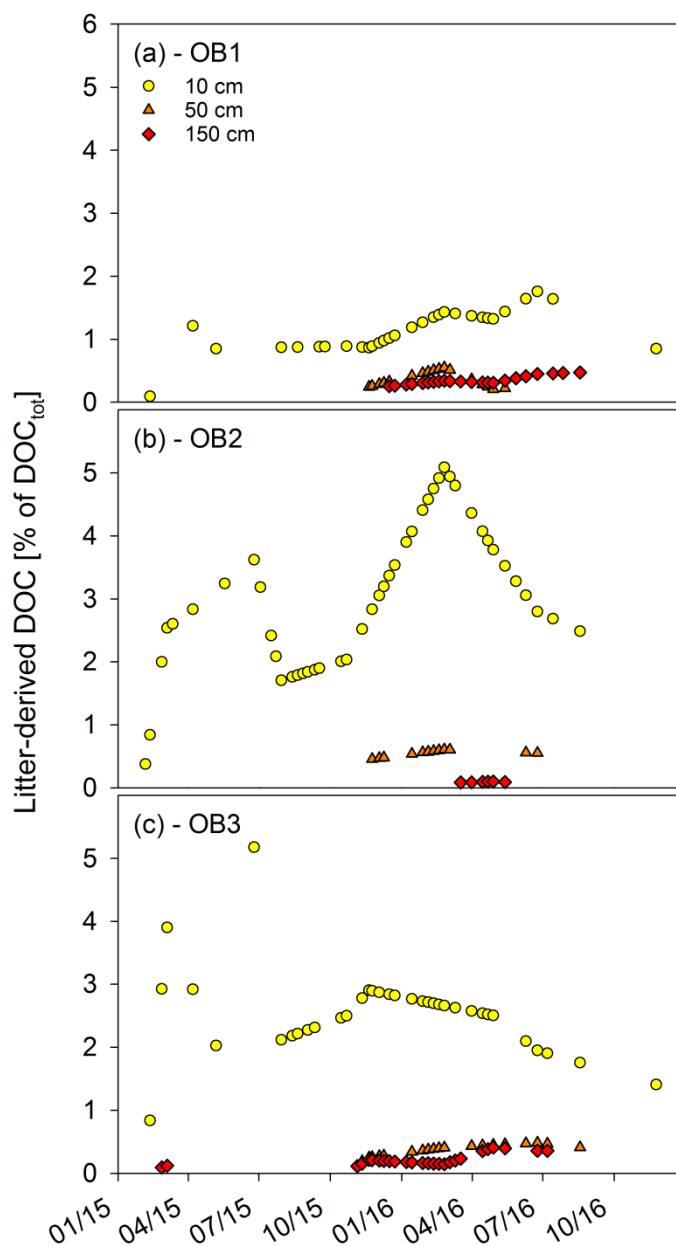
<sup>2</sup> Total nitrogen (TN)

<sup>3</sup> Dithionite-extractable Fe (Fe<sub>d</sub>)

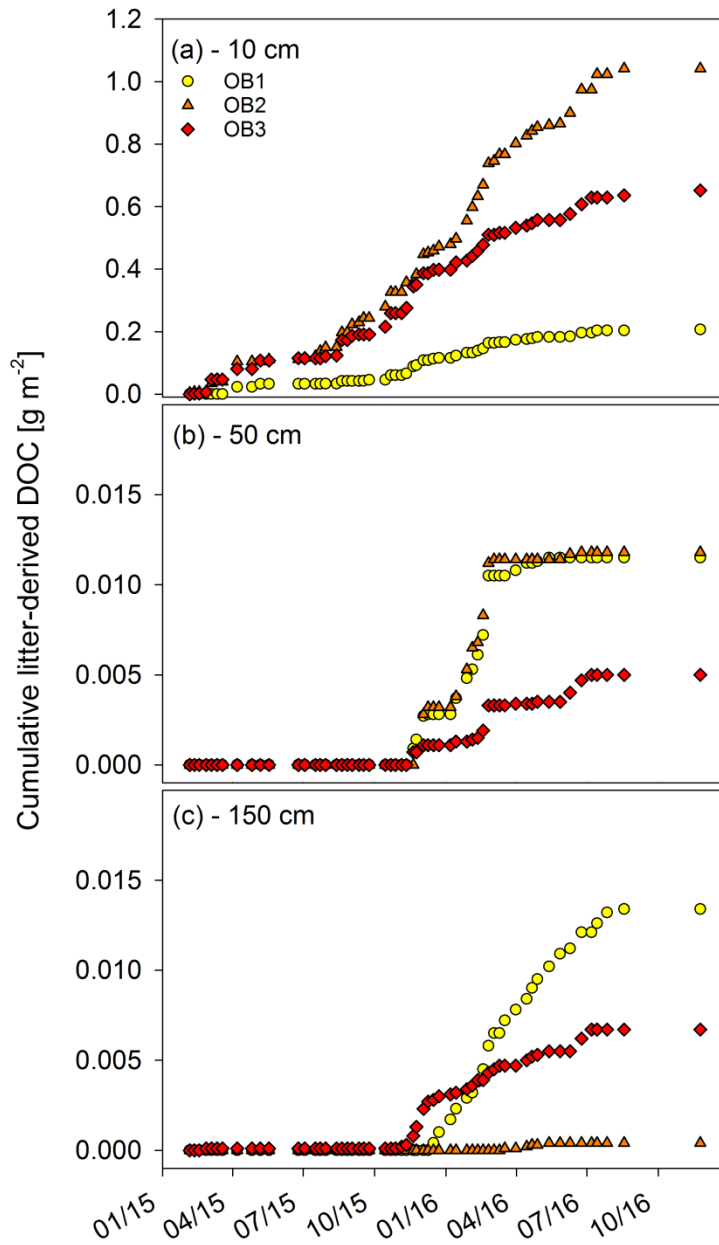
<sup>4</sup> Oxalate-extractable Fe, Al, and Mn (Fe<sub>o</sub>, Al<sub>o</sub>, Mn<sub>o</sub>)

**Supplementary Figures**

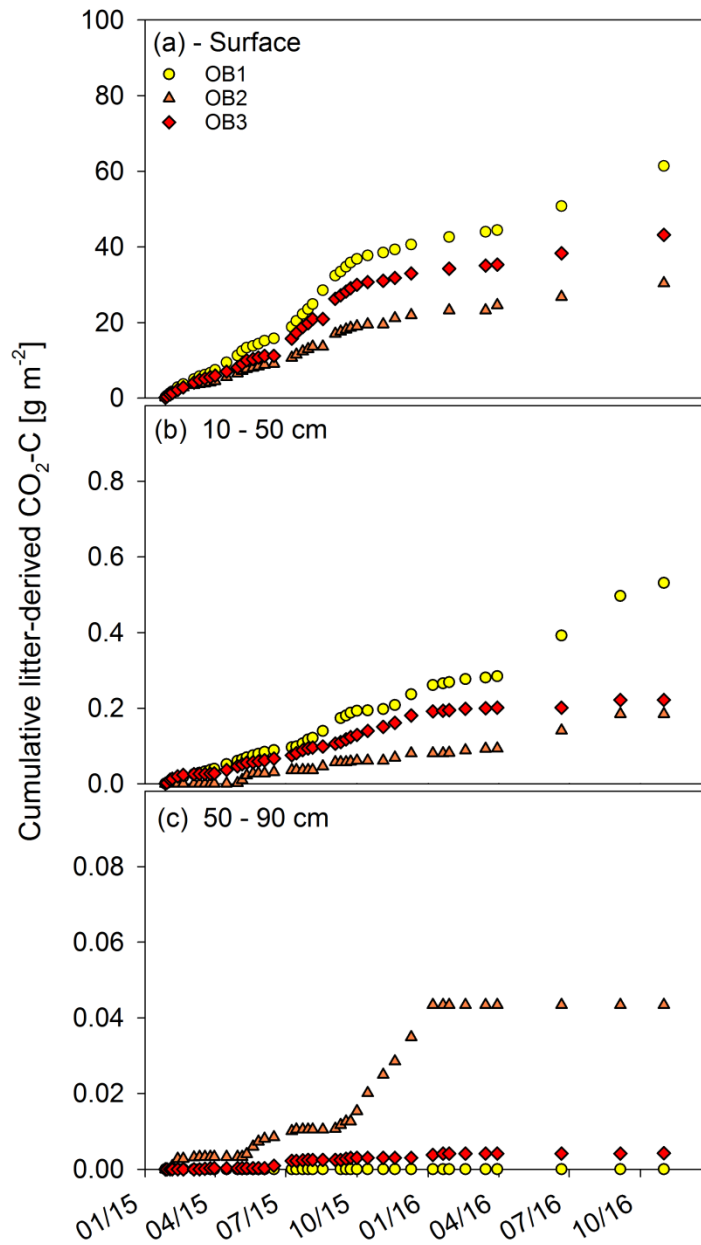
**Supplementary Fig. S1** Rates of the litter-derived CO<sub>2</sub> efflux at the soil surface during the 22 months of the labelling at observatory 1 (a), observatory 2 (b), and observatory 3 (c), calculated with the Lloyd-Taylor model<sup>16</sup> in g per m<sup>2</sup> and day. For a better visibility, data points are connected by dotted lines, but do not represent functions or regressions. Data adapted from Wordell-Dietrich et al.<sup>6</sup>



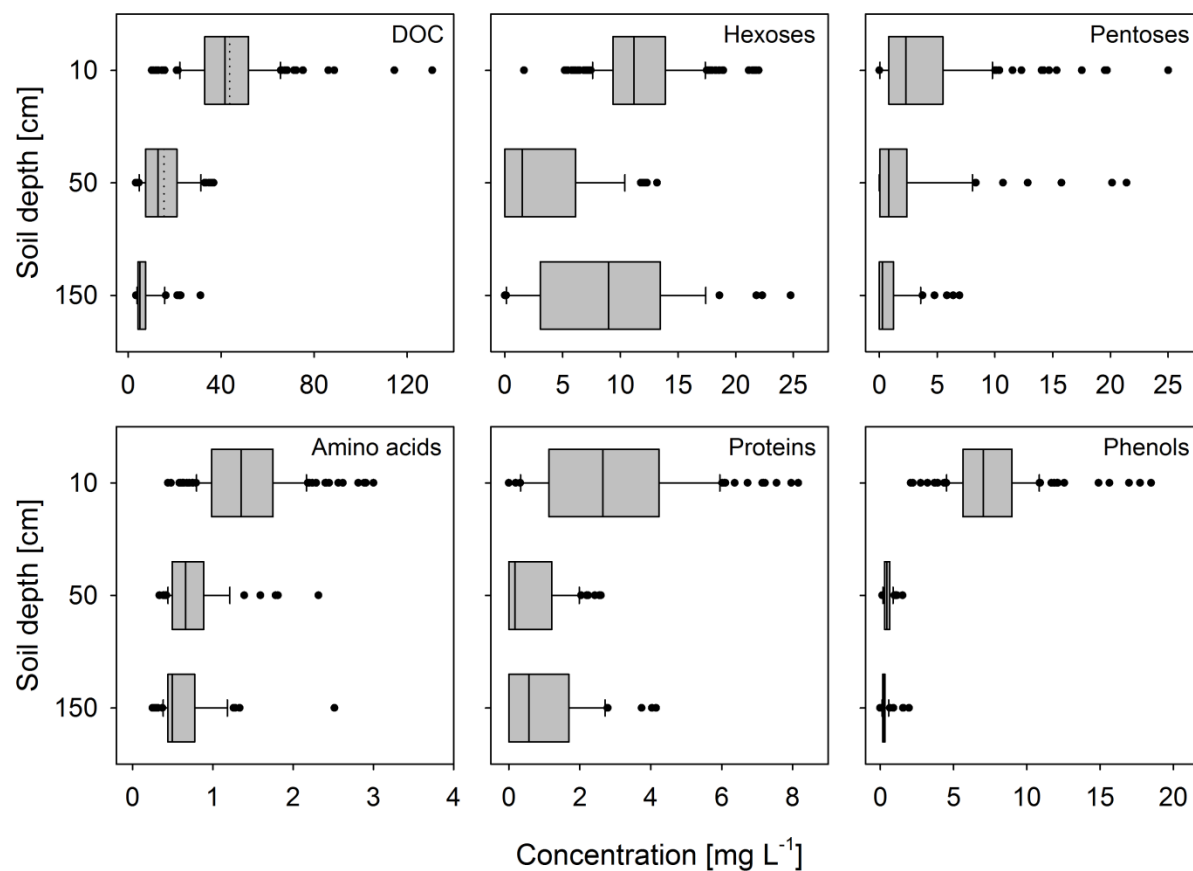
**Supplementary Fig. S2** Contribution of labelled litter-derived DOC to the total DOC flux ( $\text{DOC}_{\text{tot}}$ ) during the 22 months of the labelling per depth (10, 50, 150 cm) in observatory 1 (a), observatory 2 (b), and observatory 3 (c). Variations in the data quantities and gaps at some time points are the results of insufficient water flow or insignificant  $\text{DO}^{13}\text{C}$  enrichment. Please note that only twelve out of 57 sampling campaigns were analysed for  $\text{DO}^{13}\text{C}$ , thus the data points in between were calculated by linear interpolations as stated in the supplementary methods section.



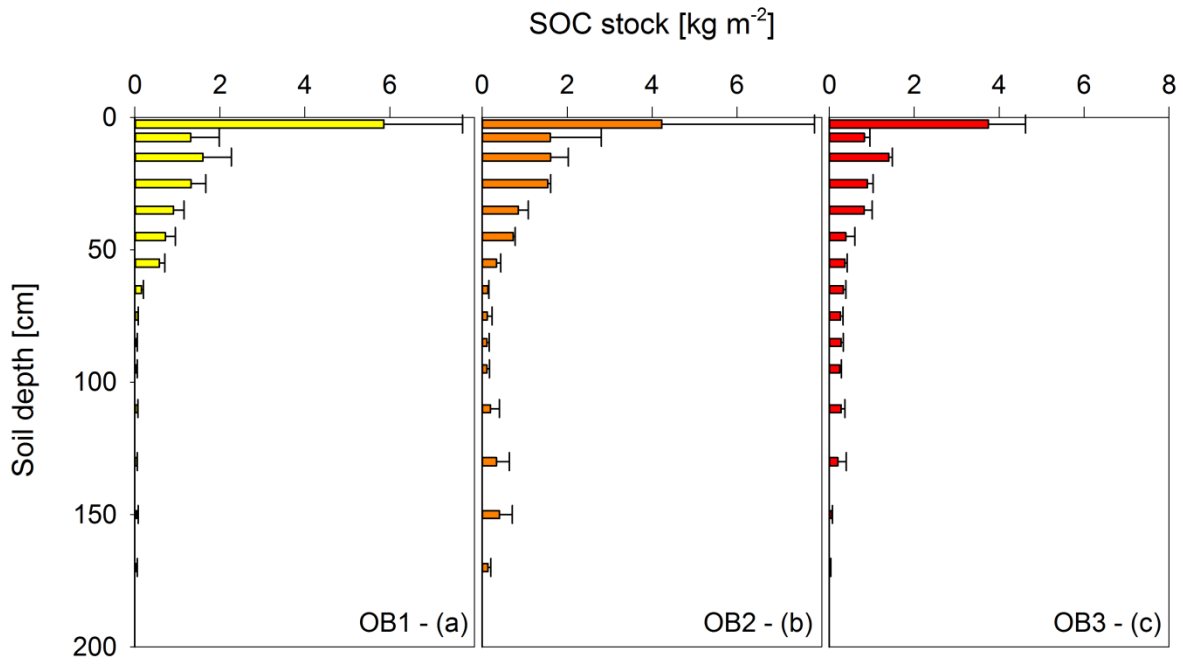
**Supplementary Fig. S3** Cumulative litter-derived DOC fluxes during the 22 months of the labelling in  $\text{g DO}^{13}\text{C}$  per  $\text{m}^2$ . Graph (a) shows the 10 cm data of each observatory, (b) data from 50 cm, and (c) data from 150 cm. Please note the different scales for the y-axes.



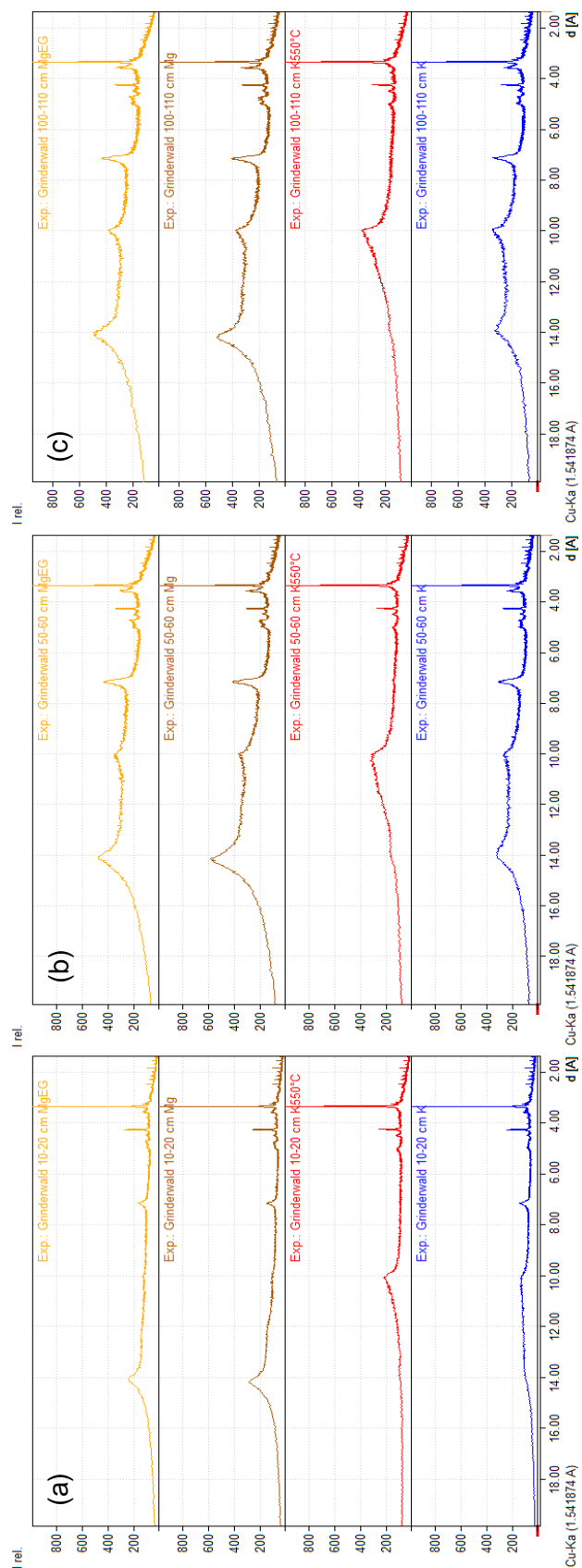
**Supplementary Fig. S4** Cumulated litter-derived CO<sub>2</sub> flux during the 22 months of the labelling at the soil surface (a), in a soil depth of 10 to 50 cm (b), and in a soil depth of 50 to 90 cm (c) during the label experiment for the three observatories, calculated with the Lloyd-Taylor model<sup>16</sup>. Data were generated by multiplying the rates per day with the interval between two sampling dates. Please note the different scales for the y-axes.



**Supplementary Fig. S5** Concentrations of individual compounds (hexoses, pentoses, amino acids, proteins, phenols) and the total DOC concentration in the soil solution at different soil depths. Boxplots show the data of four samplings between January and April 2015, with a total sample size of  $n = 133$  for 10 cm,  $n = 69$  for 50 cm, and  $n = 58$  for 150 cm. Boxes represent 50 % of the concentrations, the solid line shows the median. Dotted lines represent the mean and error bars depict the 10 % and 90 % quantiles with black circles as outliers. Please note that the x-axes have different scales.



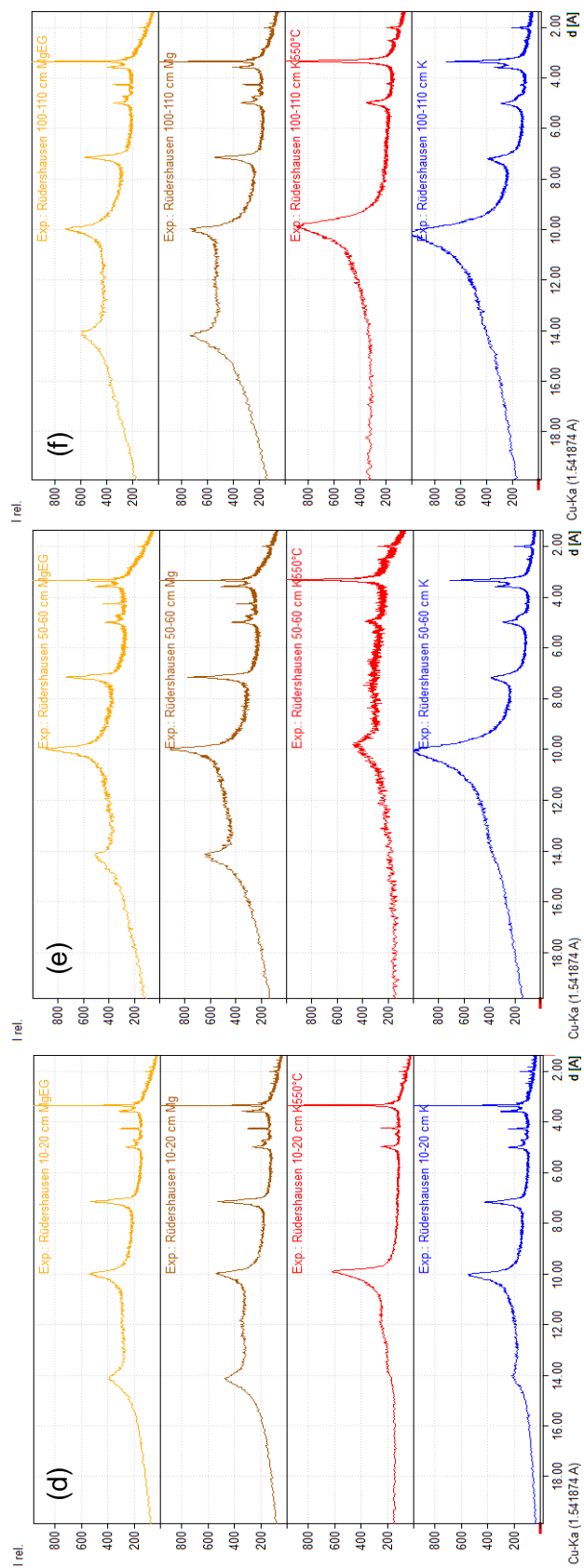
**Supplementary Fig. S6** Mean SOC stocks per depth increment at observatory 1 (a), observatory 2 (b), and observatory 3 (c). Data show the mean of three replicate soil cores, error bars represent the standard deviation. Only soil cores from the labelled plots were used for the analyses. Data were adopted from Liebmann et al.<sup>12</sup>.

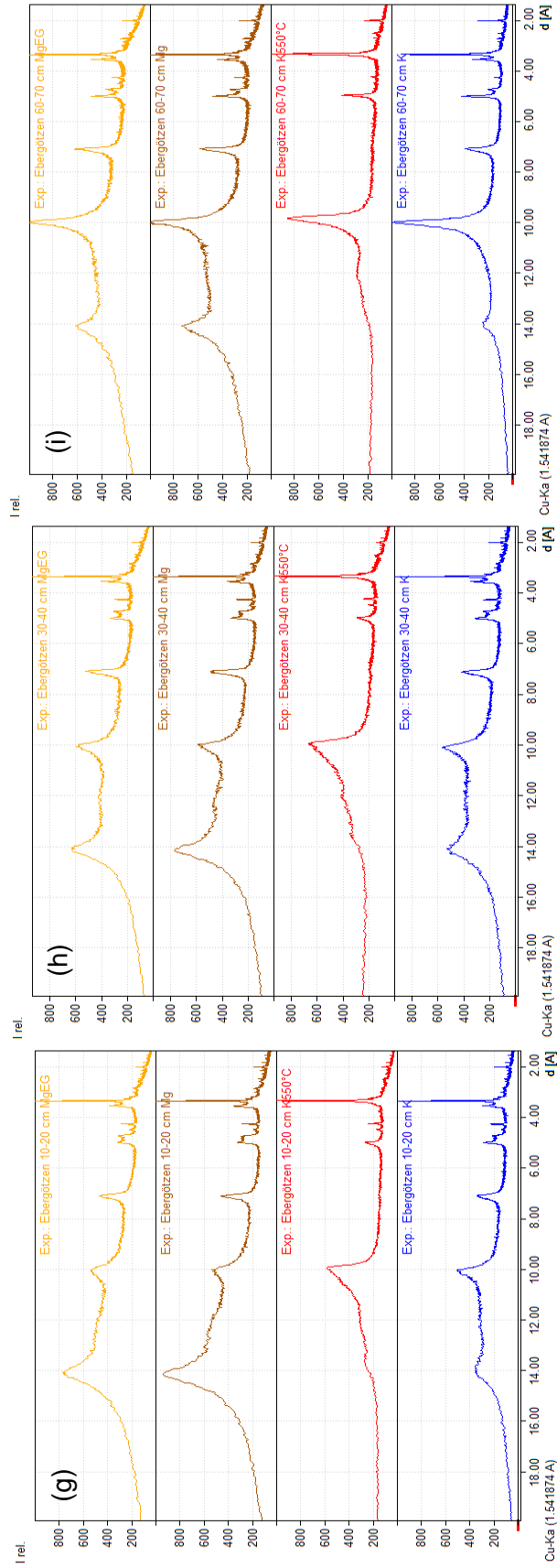


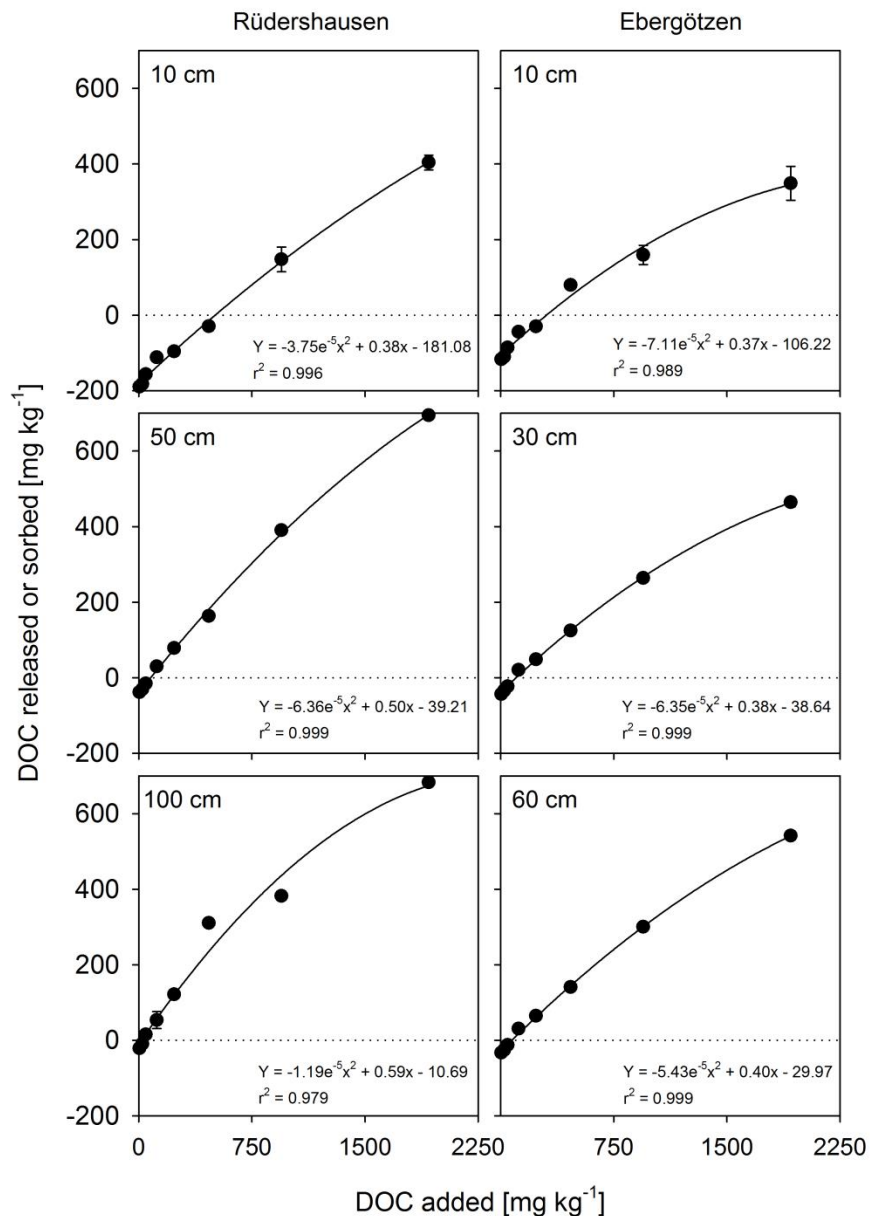
**Supplementary Fig. S7** X-ray diffraction patterns of oriented clay specimens from three study sites (a–c) Grinderwald, (d–f) Rüdershausen, and (g–i) Ebergötzen and the depth increments 10–20 cm (left), 30–40/50–60 cm (center), and 60–70/100–110 cm (right). Each sample was analysed in the following four depicted treatments (from top to bottom): Mg-saturated and solvated in ethylene glycol (MgEG), magnesium-saturated (Mg), potassium-saturated and heated to 550°C (K550°C), and potassium-saturated (K). Peaks at 14 Å in the K treatment indicate d(001) reflections of pedogenic chlorite together with a d(003) reflection at 4.7 Å; peaks at 7 Å and 3.5 Å reveal d(001) and d(002) reflections of kaolinite (both signals vanish in the K550°C treatment). The presence of illitic clay is indicated by a d(001) peak at 10 Å in the Mg/MgEG treatments. Increasing intensities at ~14 Å in the Mg/MgEG treatments relative to the K treatment indicate the presence of expandable vermiculite. Broad unresolved signals between ~10–14 Å in the K treatments suggest the presence of hydroxy-interlayered vermiculites with varying degrees of Al hydroxide incorporation.



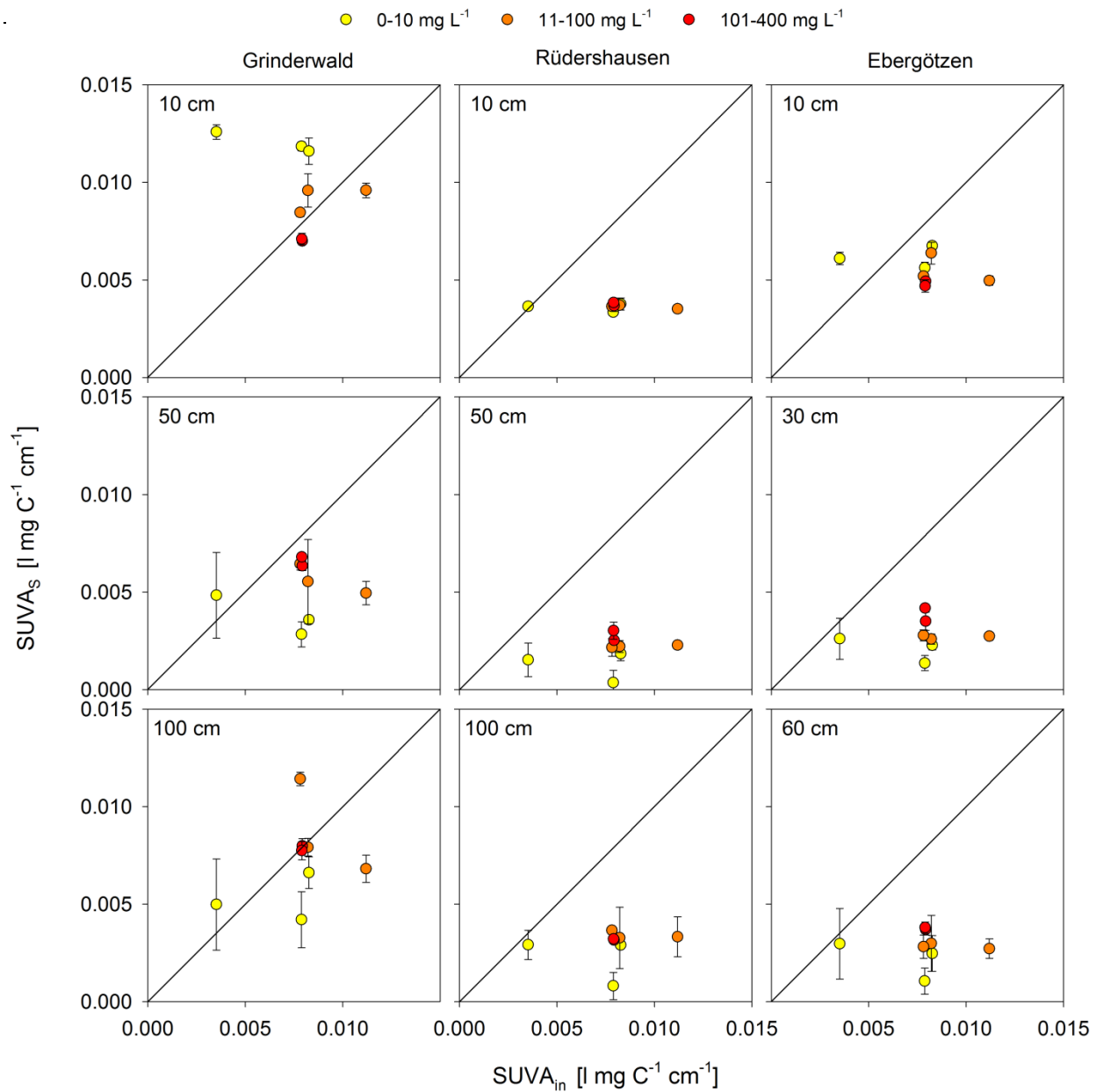
Supplementary Fig. S7: *continued.*



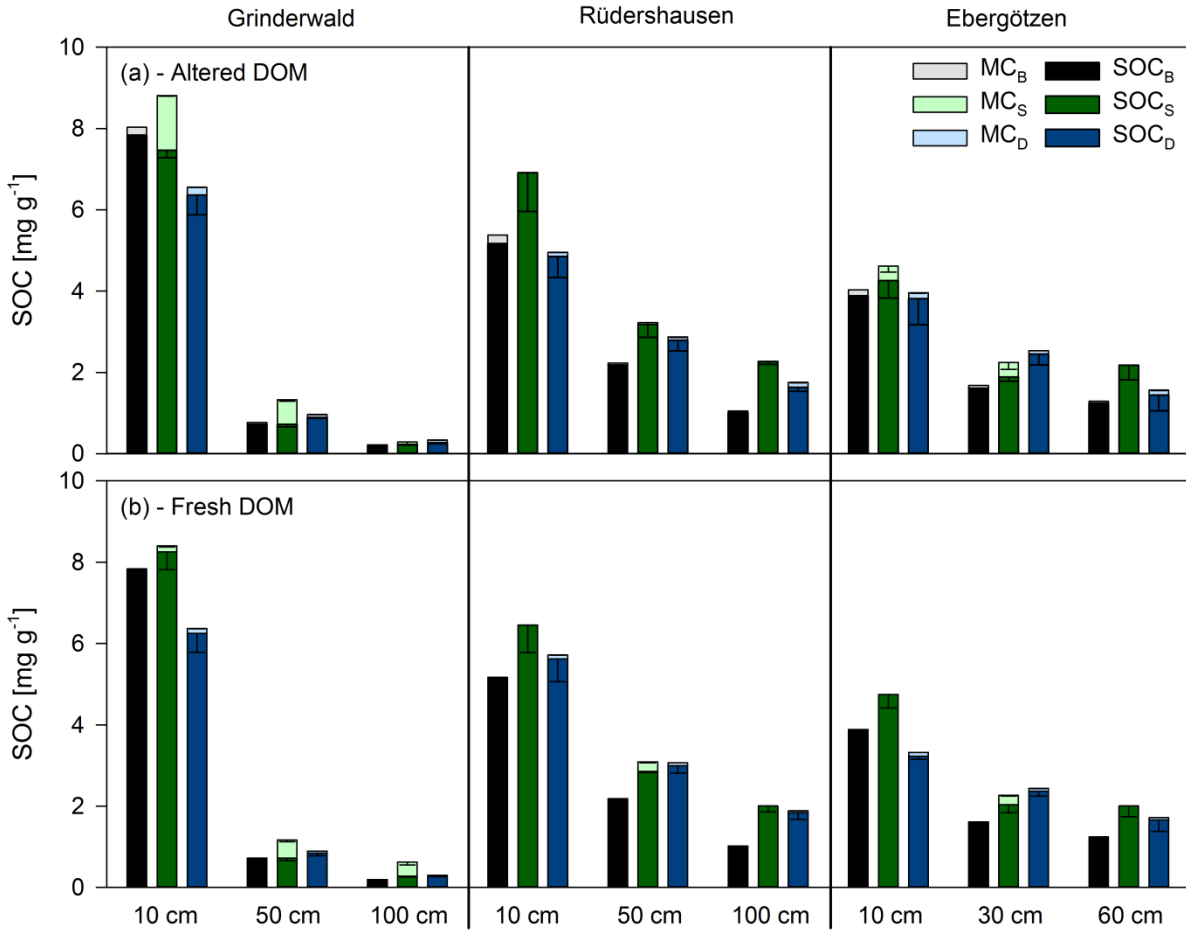




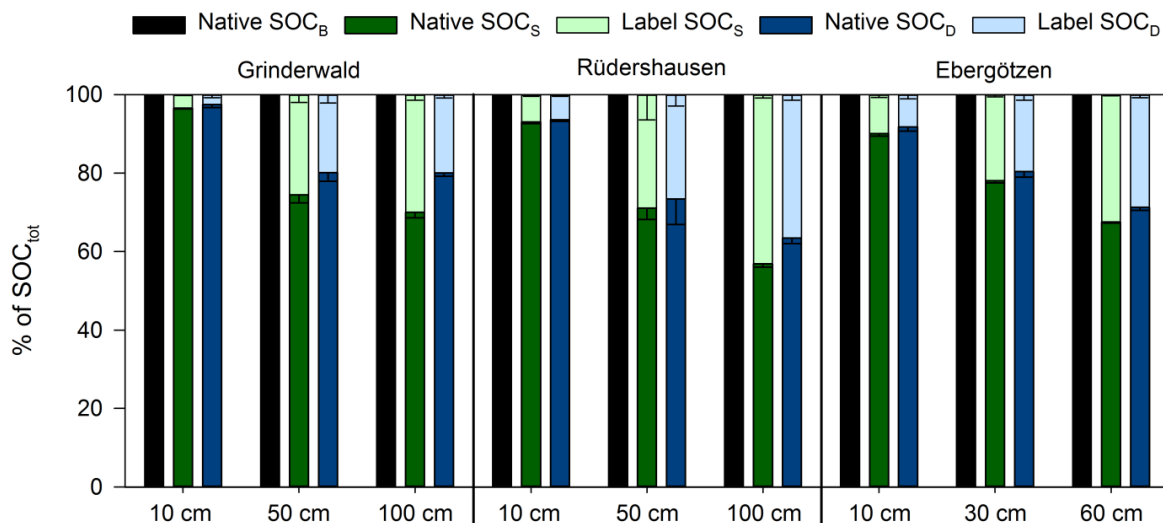
**Supplementary Fig. S8** Sorption isotherms of the Rüdershausen site (left) and Ebergötzen site (right), including three depths according to the initial mass approach by Nodvin et al.<sup>33</sup>. Numbers represent the soil depth. Data show the mean of three replicates and the error bars represent the standard deviation.



**Supplementary Fig. S9** Specific UV absorbance (SUVA) at 280 nm of the initial DOC solution before the sorption experiment (SUVA<sub>in</sub>, x-axis) and in the solution after the experiment (SUVA<sub>s</sub>, y-axis). The Grinderwald site is on the left, the Rüdershausen site in the middle, and the Ebergötzen site on the right. Numbers represent the soil depth. Data are given as the mean (n = 3) with error bars representing the standard deviation. Values above the 1:1 line indicate a net release of aromatic DOM components, while values below indicate a net retention. Colors depict the different DOC concentrations of the sorption experiments. Yellow show the concentrations between 0-10 mg L<sup>-1</sup> (1, 5, 10 mg L<sup>-1</sup>), orange show the concentrations between 11-100 mg L<sup>-1</sup> (25, 50, 100 mg L<sup>-1</sup>), and red show the concentrations between 101-400 mg L<sup>-1</sup> (200 and 400 mg L<sup>-1</sup>).

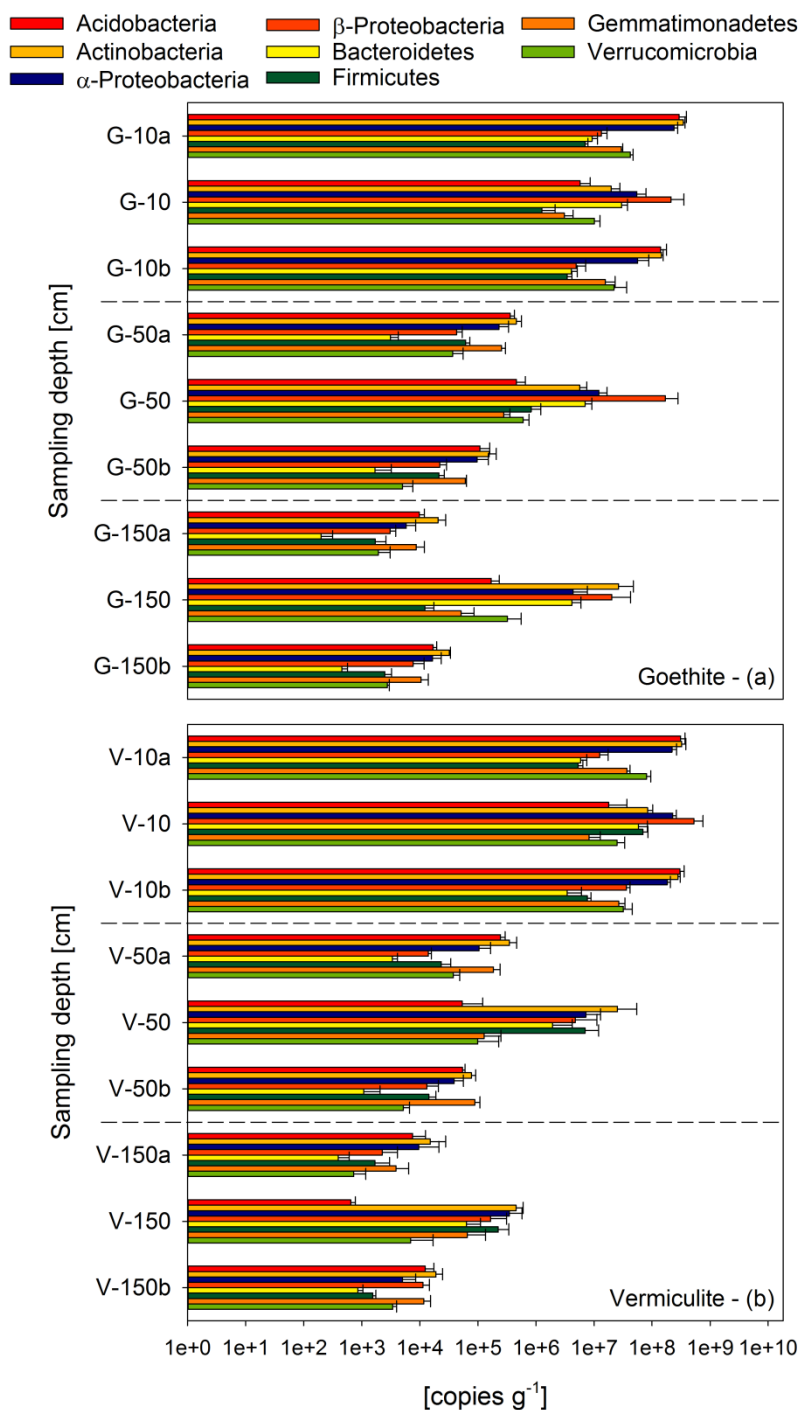


**Supplementary Fig. S10** Soil organic C (SOC) and mobilisable C (MC) in the 9 different soil samples determined before and after batch sorption experiments with (a) “altered” DOM extracted from the field exposed labelled beech litter and with (b) “fresh” DOM extracted from recently fallen un-labelled beech litter. Data show the mean of three replicates and the error bars represent the standard deviation. The Grinderwald site is on the left, the Rüdershausen site in the middle, and the Ebergötzen site on the right. On the x-axis, numbers represent the soil depth. Black and grey bars show the data before the experiment (B), green bars show the data after the DOC sorption experiment (S), and blue bars show the data after the desorption experiment (D).



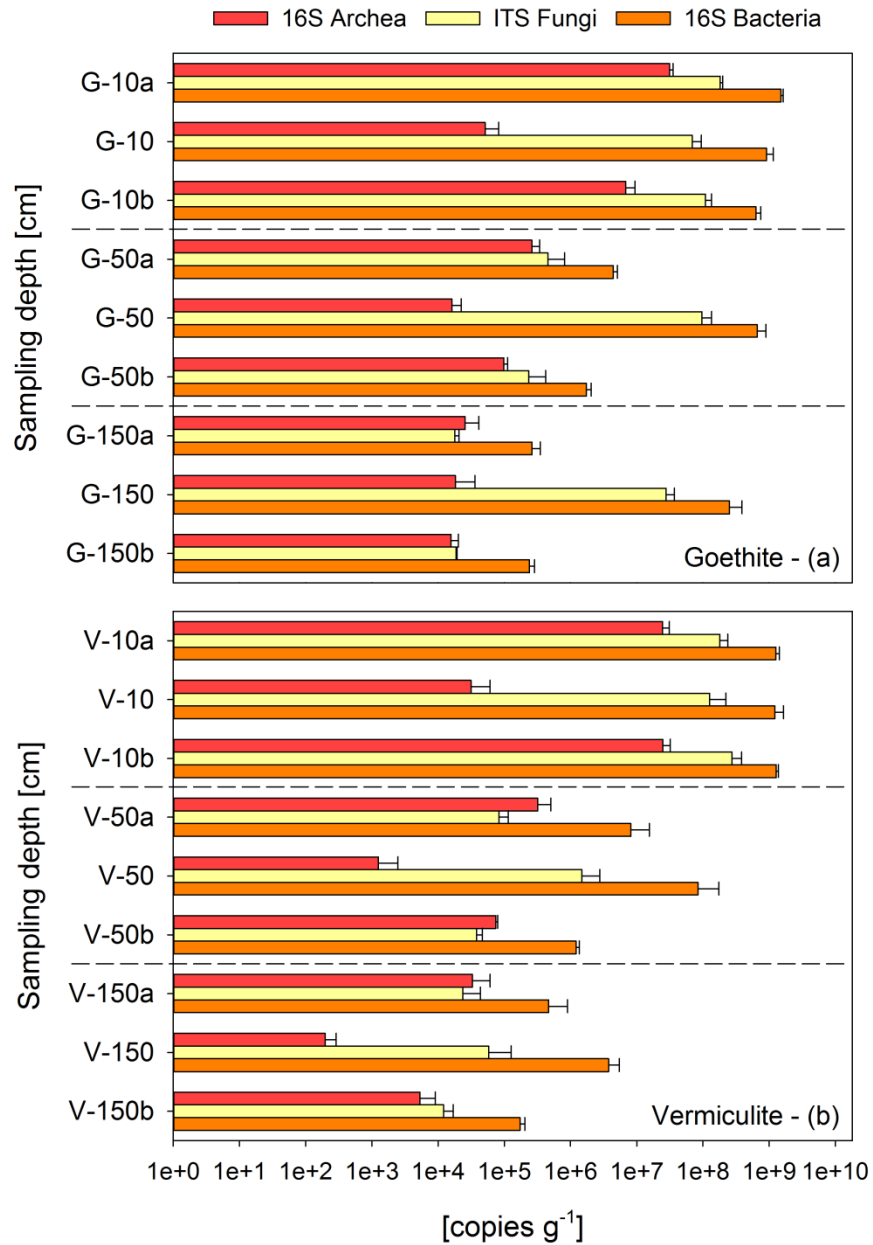
**Supplementary Fig. S11** Distribution of native soil organic C (SOC) and label-derived SOC in topsoil, upper subsoil, and deeper subsoil samples of the three sites in percent of the total SOC (SOC<sub>tot</sub>). Bars show the results of the “altered” DOM approach and include the distribution in the bulk soil (black), which is naturally 100 % native, after the sorption experiment (green), and after the desorption experiment (blue). Bright colored bars represent the label-derived SOC, while dark colored bars depict the native SOC. Bars show the mean of three replicates, error bars show the standard deviation. The Grinderwald site (sandy deposits) is on the left, the Rüdershausen site (loess deposits) in the middle, and the Ebergötzen site (red sandstone) on the right. On the x-axis, numbers represent the soil depth.

## Study III – Supplementary material



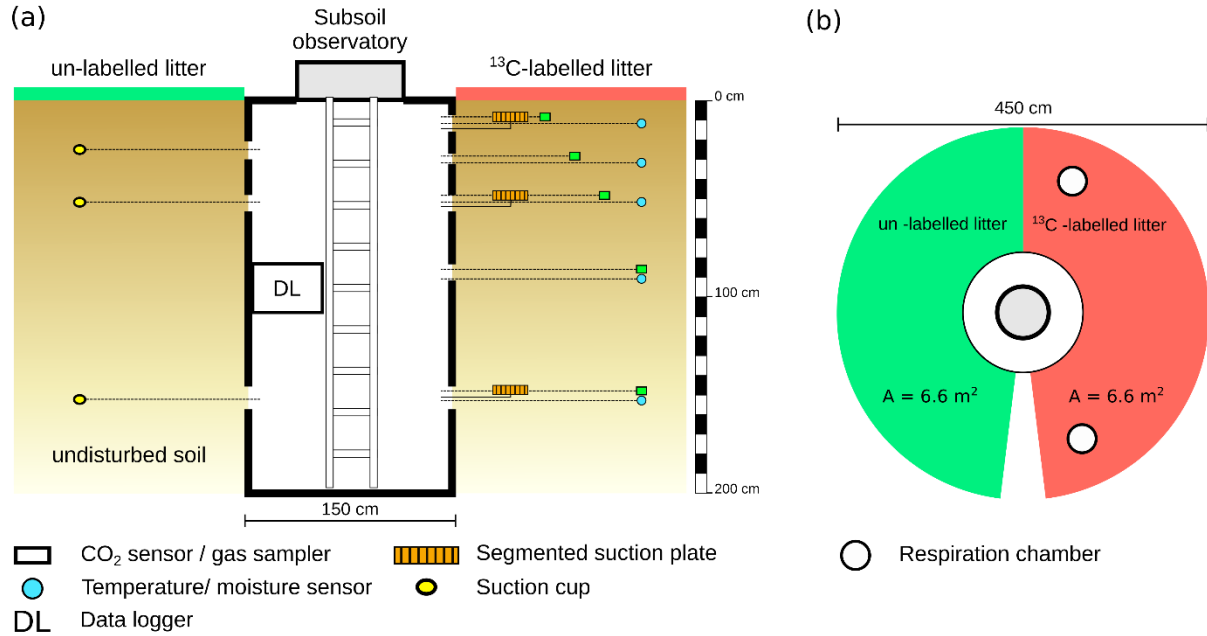
**Supplementary Fig. S12** Bacterial community composition of the goethite (a) and vermiculite (b), respectively, after 24 months of *in-situ* field exposure in combination with the bulk soil samples taken above and below each mineral meshbag. Sample names on the y-axes are a combination of the mineral types goethite (G) or vermiculite (V), the soil depth (10, 50, 150 cm), and in case of the bulk samples the suffix above (a) or below (b) the meshbag. Data show the mean of three replicates and the error bars represent the standard deviation.

## Study III – Supplementary material



**Supplementary Fig. S13** Microbial community composition of the goethite (a) and vermiculite (b), respectively, after 24 months of *in-situ* field exposure in combination with the bulk soil samples taken above and below each mineral meshbag. Sample names on the y-axes are a combination of the mineral types goethite (G) or vermiculite (V), the soil depth (10, 50, 150 cm), and in case of the bulk samples the suffix above (a) or below (b) the meshbag. Data show the mean of three replicates and the error bars represent the standard deviation.





**Supplementary Fig. S14** Schematic illustration of the installations in the Grinderwald subsoil observatories (a) and a top view of the catchment area divided into a  $^{13}\text{C}$ -labelled and un-labelled side (b). Illustrations were adapted and modified from Wordell-Dietrich et al.<sup>6</sup>. Please note that the suction plates were not installed below each other in the soil profile as pictured in this 2D scheme (a). To avoid mutual influences of the plates, they were installed with a horizontal offset.

### Supplementary References

1. IUSS Working Group WRB. *World reference base for soil resources 2014, update 2015: International soil classification system for naming soils and creating legends for soil maps*. vol. World Soil Resources Reports No. 106 (FAO, 2015).
2. Bachmann, J., Krueger, J., Goebel, M.-O. & Heinze, S. Occurrence and spatial pattern of water repellency in a beech forest subsoil. *J. Hydrol. Hydromech.* **64**, (2016).
3. Angst, G., Kögel-Knabner, I., Kirfel, K., Hertel, D. & Mueller, C. W. Spatial distribution and chemical composition of soil organic matter fractions in rhizosphere and non-rhizosphere soil under European beech (*Fagus sylvatica* L.). *Geoderma* **264**, 179–187 (2016).
4. Kalks, F. *et al.* Fate and stability of dissolved organic carbon in topsoils and subsoils under beech forests. *Biogeochemistry* (2020) doi:10.1007/s10533-020-00649-8.
5. Leinemann, T., Mikutta, R., Kalbitz, K., Schaarschmidt, F. & Guggenberger, G. Small scale variability of vertical water and dissolved organic matter fluxes in sandy Cambisol subsoils as revealed by segmented suction plates. *Biogeochemistry* **131**, 1–15 (2016).
6. Wordell-Dietrich, P. *et al.* Vertical partitioning of CO<sub>2</sub> production in a Dystric Cambisol. *Biogeosciences Discuss.* 1–27 (2019) doi:https://doi.org/10.5194/bg-2019-143.
7. Zsolnay, A. Chapter 4 - Dissolved humus in soil waters. in *Humic Substances in Terrestrial Ecosystems* (ed. Piccolo, A.) 171–223 (Elsevier Science B.V., 1996).
8. Meier, I. C., Leuschner, C. & Hertel, D. Nutrient return with leaf litter fall in *Fagus sylvatica* forests across a soil fertility gradient. *Plant Ecol.* **177**, 99–112 (2005).
9. Chin, Y.-P., Aiken, G. & O’Loughlin, E. Molecular weight, polydispersity, and spectroscopic properties of aquatic humic substances. *Environ. Sci. Technol.* **28**, 1853–1858 (1994).
10. McKnight, D. M., Harnish, R., Wershaw, R. L., Baron, J. S. & Schiff, S. Chemical characteristics of particulate, colloidal, and dissolved organic material in Loch Vale Watershed, Rocky Mountain National Park. *Biogeochemistry* **36**, 99–124 (1997).
11. Leinemann, T. *et al.* Multiple exchange processes on mineral surfaces control the transport of dissolved organic matter through soil profiles. *Soil Biol. Biochem.* **118**, 79–90 (2018).
12. Liebmann, P. *et al.* Relevance of aboveground litter for soil organic matter formation – a soil profile perspective. *Biogeosciences* **17**, 3099–3113 (2020).
13. Chantigny, M. H., Angers, D. A., Kaiser, K. & Kalbitz, K. Extraction and characterization of dissolved organic matter. in *Soil Sampling and Methods of Analysis* (eds. Carter, M.R., Gregorich, E.G.) 617–635 (Canadian Society of Soil Science, 2008).
14. Rao, P. S. R. S. Variance components estimation. in *Monographs on Statistics and Applied Probability* vol. Vol. 78 93–106 (Chapman and Hall, 1997).
15. Hedderich, J. & Sachs, L. *Angewandte Statistik: Methodensammlung mit R*. (Springer Spektrum, 2016).

16. Lloyd, J. & Taylor, J. A. On the temperature dependence of soil respiration. *Funct. Ecol.* **8**, 315–323 (1994).
17. Böttcher, J. *et al.* Emission of groundwater-derived nitrous oxide into the atmosphere: Model simulations based on a <sup>15</sup>N field experiment. *Eur. J. Soil Sci.* **62**, 216–225 (2011).
18. Schwen, A. & Böttcher, J. A simple tool for the inverse estimation of soil gas diffusion coefficients. *Soil Sci. Soc. Am. J.* **77**, 759–764 (2013).
19. Carstens, J. F., Bachmann, J. & Neuweiler, I. Effects of organic matter coatings on the mobility of goethite colloids in model sand and undisturbed soil. *Eur. J. Soil Sci.* **69**, 360–369 (2018).
20. Mikutta, R. *et al.* Biodegradation of forest floor organic matter bound to minerals via different binding mechanisms. *Geochim. Cosmochim. Acta* **71**, 2569–2590 (2007).
21. Brunauer, S., Emmett, P. H. & Teller, E. Adsorption of gases in multimolecular layers. *J. Am. Chem. Soc.* **60**, 309–319 (1938).
22. Mayer, L. M. Extent of coverage of mineral surfaces by organic matter in marine sediments. *Geochim. Cosmochim. Acta* **63**, 207–215 (1999).
23. López-Gutiérrez, J. C. *et al.* Quantification of a novel group of nitrate-reducing bacteria in the environment by real-time PCR. *J. Microbiol. Methods* **57**, 399–407 (2004).
24. White, T. a *et al.* ‘Amplification and direct sequencing of fungal ribosomal RNA genes for phylogenetics,’ in. (1990) doi:10.1016/b978-0-12-372180-8.50042-1.
25. Manerkar, M. A., Seena, S. & Bärlocher, F. Q-RT-PCR for assessing archaea, bacteria, and fungi during leaf decomposition in a stream. *Microb. Ecol.* **56**, 467–473 (2008).
26. Lueders, T. & Friedrich, M. Archaeal population dynamics during sequential reduction processes in rice field soil. *Appl. Environ. Microbiol.* **66**, 2732–2742 (2000).
27. Fierer, N., Jackson, J. A., Vilgalys, R. & Jackson, R. B. Assessment of soil microbial community structure by use of taxon-specific quantitative PCR Assays. *Appl. Environ. Microbiol.* **71**, 4117–4120 (2005).
28. Philippot, L. *et al.* Spatial patterns of bacterial taxa in nature reflect ecological traits of deep branches of the 16S rRNA bacterial tree. *Environ. Microbiol.* **11**, 3096–3104 (2009).
29. Bacchetti De Gregoris, T., Aldred, N., Clare, A. S. & Burgess, J. G. Improvement of phylum- and class-specific primers for real-time PCR quantification of bacterial taxa. *J. Microbiol. Methods* **86**, 351–356 (2011).
30. Kaiser, K. & Guggenberger, G. The role of DOM sorption to mineral surfaces in the preservation of organic matter in soils. *Org. Geochem.* **31**, 711–725 (2000).
31. Schlichting, E. & Blume, H.-P. *Bodenkundliches Praktikum; Eine Einführung in pedologisches Arbeiten für Ökologen, insbesondere Land- und Forstwirte, und für Geowissenschaftler.* (1966).
32. Kaiser, K., Guggenberger, G. & Zech, W. Sorption of DOM and DOM fractions to forest soils. *Geoderma* **74**, 281–303 (1996).

### Study III – Supplementary material

---

33. Nodvin, S. C., Driscoll, C. T. & Likens, G. E. Simple partitioning of anions and dissolved organic carbon in a forest soil. *Soil Sci.* **142**, 27–35 (1986).
34. Saidy, A. R., Smernik, R. J., Baldock, J. A., Kaiser, K. & Sanderman, J. The sorption of organic carbon onto differing clay minerals in the presence and absence of hydrous iron oxide. *Geoderma* **209–210**, 15–21 (2013).

## 5. Synthesis

The thesis aimed at providing field evidence for quantitative and structural changes of OM during migration down the soil profile, hereby passing through consecutive sorption/microbial processing/desorption cycles versus fast translocation by preferential flow. Here, the first and second parts of the synthesis address the fate of litter layer inputs and their translocation pathways through the mineral soil down to 180 cm soil depth. Since it is generally assumed that subsoils are an OM stabilizing environment, the stability of such inputs in the subsoil was a major subject of this thesis. The third and fourth parts of the synthesis focus on the discrepancies between potential retention (determined in laboratory) and the actual retention (observed in the field) of forest top- and subsoils as well as on the stability of newly formed SOC deriving from recent litter inputs in the timeframe of years.

### 5.1. Aboveground litter translocation

Aboveground litter represents a major C source in forest ecosystems, and the translocation of litter C into the soil via bioturbation and leaching can have a significant contribution to SOC stocks. Thus, investigating the fate of litter layer inputs is a prerequisite for understanding the C dynamics in forest soils.

The use of the field setup in the Grindewald research forest allowed detailed tracking of recent litter derived C inputs into different OM fractions of various soil depths down to the deep mineral subsoil in addition to their stability. In the course of 22 months after  $^{13}\text{C}$ -labelled litter application, in total about 0.52 % of the applied litter C was translocated as DOC into the mineral soil below 10 cm soil depth, while about 0.26 % was mineralized to  $\text{CO}_2$  (Study III, Fig. 1). After 22 months, 11.1 % of the litter C was found in the whole soil profile down to 150 cm (Study I, Fig. 6a), while 36 % were directly released to the atmosphere as  $\text{CO}_2$  and another 37 % remained in the litter layer after 22 months (Study III, Fig. 1). Litter-derived C in the mineral soil decreased strongly with increasing soil depth. While about 10.4 % were found in the upper 10 cm of soil (= topsoil), it was only 0.7 % in the upper subsoil of 10-50 cm soil depth and minor contributions of 0.04 % in the deeper subsoil of 50-150 cm soil depth after 22 months of labelled litter application (Study I, Fig. 6a; Study III, Fig. 1).

The structure of litter-derived C in the mineral soil was differentiated between C in POM (termed  $\text{C}_{\text{POM}}$  in Study I, POC in Study III) and C in MAOM (termed  $\text{C}_{\text{MAOM}}$  in Study I, MAOC in Study III) in order to distinguish between input pathways like C migration via DOC movement ( $\text{C}_{\text{MAOM}}/\text{MAOC}$ ) and C migration via bioturbation of litter debris ( $\text{C}_{\text{POM}}/\text{POC}$ ). The majority of litter inputs (8.9 %) entered as POM, but was restricted to the topsoil (< 10 cm soil depth; Study I, Fig. 6a; Study III, Fig. 1), with a steep decrease from the surface to 10 cm soil depth, likely as a result of faunal activity (e.g. active mice and dorbeetle populations were observed at the Grindewald site). Below the topsoil, there were no significant

contributions of fresh litter-derived C detectable in the POM fraction. A smaller proportion of litter inputs in the topsoil (1.5 %) was found in association with the mineral matrix, which requires prior leaching of organic particles (= DOM), from recent leaf litter in the organic layer or litter-derived POM in the topsoil, and migration in the soil solution until retention at mineral surfaces.

Contrary to litter-derived C in POM, litter-derived C in MAOM reached deeper soil depths, as it depends on OM transport in dissolved stage, and contributed statistically significant, albeit only to a minor degree, to the subsoil OM pool down to a depth of at least 140 cm. However, there was a distinct decline in the quantity of recent litter-derived MAOM from 1.5 % in the topsoil to 0.04 % for the deep mineral subsoil in 50-140 cm soil depth (Study III, Fig. 1). Tipping et al. (2012) concluded from a modelling approach that most of the DOM transported by percolating soil solution is adsorbed on mineral surfaces followed by microbial respiration in large extents. These model assumptions fit to our finding on the small contribution of litter-derived OM to MAOM. Also long-term litter manipulation experiments likewise suggest that increasing litter layer C inputs to the mineral soil does not result in a concomitant increase in subsoil SOC (Bowden et al., 2014; Lajtha et al., 2014). Results of the current study thus confirms hypothesis **H1** that the majority of aboveground inputs do not reach the subsoil.

### *Retention of litter-derived C inputs*

The depth gradient of mineral-associated aboveground litter inputs is hypothesized in **H1** to depend on its retention and microbial processing in the above laying horizon, e.g. the topsoil. Previously, Fröberg et al. (2009) stated that a large part of litter-derived DOC is retained in the topsoil horizon. Thus, the 1.5 % litter-derived C in MAOM retained in the Grindewald topsoil likely represent the majority of litter-derived DOC inputs from the organic layer, in addition to DOC mobilized from litter-derived POM in the topsoil. Dissolved OC monitoring started below the topsoil in 10 cm soil depth and quantification yielded an input of litter-derived DOC into the upper subsoil of about 0.5 % of the initially applied litter C during the 22 months, whereas 0.7 % litter-derived C was found as MAOM between 10 cm and 50 cm soil depth (Study III, Fig. 1). Since inputs and retention in the upper subsoil are in the same range, the hypothesis that retention at mineral surfaces is a controlling process in downward migration of litter-derived DOM is supported (**H1**). This trend observed in the upper subsoil shifts slightly in the deep mineral subsoil. Here, the 0.01 % of litter-derived DOC input in 50 cm soil depth contrasts the 0.04 % of litter-derived C found in the MAOM fraction (Study III, Fig. 1), because DOM inputs are assumed to be the prerequisite for MAOM formation. There are two possible explanations for the observed difference. (i) Actual measurements of litter-derived MAOC were done for the depth increment 100-140 cm, which resulted in about 0.01 %, i.e. the proportion quantified as DOC input to soil below 50 cm depth, whereas the other 0.03 % of MAOC was interpolated for the depth increment 50-100 cm, which was not analyzed. Interpolation in combination with overall small values likely has a larger uncertainty. Additionally, (ii)

suction plate monitoring faced the phenomenon that considerably fewer samples could be taken from 50 cm soil depth compared to 10 cm and 150 cm (Study III, Supplementary Table S4), which makes the litter-derived DOC value in 50 cm the least reliable of all depths.

Despite these two methodological aspects, potentially affecting the litter-derived DOC/MAOC differences, the data of recovered litter-derived DOC and MAOC in the respective subsoil depth increments clearly demonstrate that retention at mineral surfaces is a controlling process of C cycling in the subsoil, as it was previously reported by Hagedorn et al. (2015) and Rothstein et al. (2018). In addition, the output of litter-derived DOC in 150 cm (0.005 %) is much smaller than the calculated MAOC in the soil directly above (0.04 %; Study III, Fig. 1), which shows an overall large retention of litter-derived DOC inputs in top- and subsoil, largely by the formation of MAOC, and thus supporting **H1**.

### *Microbial mobilization and decomposition*

Next to retention at mineral surfaces, microbial decomposition is hypothesized to be responsible for the decreasing share of litter-derived inputs with increasing soil depth (**H1**). Microbial utilization of recent litter-derived OM in all soil increments was evaluated by monitoring the production of litter-derived CO<sub>2</sub>. Quantifying the litter-derived CO<sub>2</sub> released during the runtime of 22 months revealed that a depth independent proportion of about one fourth of the litter-derived C reaching the respective depth increment was lost due to microbial utilization (Study III, Fig. 1). It cannot be differentiated whether this CO<sub>2</sub> originates from microbial consumption of litter-derived DOC or shortly after retention at mineral surfaces, but it nevertheless implies that considerable amounts of the respective litter-derived inputs are microbially processed in each soil depth. Further evidence for large losses of OM by microorganisms comes from the MAOM burial experiment using goethite and vermiculite coated with <sup>13</sup>C-enriched OM extracted from beech litter (Study III). The artificial goethite and vermiculite MAOM was incubated for two years in the Grindelwald soil in the same depths as the segmented suction plates from the subsoil observatories (10, 50, 150 cm). After two years, about 30 % of the initial C coating was mobilized from the mineral surfaces, irrespective of the mineral type and the soil depth (Study III, Fig. 3). Microbial community analysis of MAOM revealed that the associations in both subsoil depths constituted microbial hotspots (Kuzyakov and Blagodatskaya, 2015), as the size of the microbial community was larger compared to the surrounding bulk soil (Study III, Supplementary Fig. S13). This finding applied to bacteria and fungi but it was not transferable to archaea, potentially due to unfavorably wide C/N ratios and competitive interactions with bacteria groups (Bates et al., 2011). In soil, fungi make use of substrate rich minerals by a fast colonization due to hyphal network (Kandeler et al., 2019). The bacterial community appeared to be already adapted to the utilization of substrate rich MAOM, where copiotrophic *β-Proteobacteria* were benefitting most in such environment (Study III, Supplementary Fig. S12; Leinemann et al. (2018)), while oligotrophic bacteria (e.g. *Acidobacteria*) were largely outcompeted and increased only on the goethite

surfaces in the deep subsoil samples, as they are supposed to be able to process more recalcitrant C sources like microbial necromass (Fierer et al., 2007). Both, the size and compositional adaptation indicate that microbial processing was an important factor in the mobilization of C from mineral surfaces. Combining the results of both field experiments it seems evident that, next to retention at mineral surfaces, also microbial processing is responsible for the small share of litter layer C reaching the mineral subsoil during a two year timeframe. Thus, hypothesis **H1** can be confirmed in this respect.

### *Temporal resolution of C inputs*

What is overlooked in the total C budget at the end of the 22 months labelling period discussed above is the resolution of the temporal progress of the downward migration during the labelling period, which is an important aspect of the proposed sequential cycling of C inputs through the soil profile (Kaiser and Kalbitz, 2012). Monitoring of DOC movement showed that litter-derived DOC was entering the subsoil at 10 cm depth rather continuously from the start of the labelling until the end (Study III, Supplementary Fig. S3a). In both subsoil depths of 50 cm and 150 cm, however, first significant inputs via DOC were detectable about ten months (around November 2015) after label application in February 2015 (Study III, Supplementary Fig. S3b,c). The delay in translocation likely resulted from the retention and microbial processing in the horizon above (topsoil cycling), which in consequence releases smaller amounts of litter-derived C to the subsoil. The production of litter-derived CO<sub>2</sub> in the soil increment of 10 cm to 50 cm began, similarly to litter-derived DOC, shortly after the litter application (Study III, Supplementary Fig. S4b), which confirms an early rapid microbial consumption of fresh litter inputs in the upper subsoil. This suggests that fresh litter inputs represent the actively cycling C pool in subsoils. A direct comparison of litter-derived DOC inputs in 10 cm soil depth and the production of litter-derived CO<sub>2</sub> in the 40 cm thick soil compartment below (10-50 cm) revealed that the majority of litter-derived DOC inputs were microbially respired in the first months of the experiment (data are close to the 1:1 line until the marked data point in Fig. 5.1). This is likely related to a higher bioavailability of OM in soil solution than in association with minerals (Kalbitz and Kaiser, 2008). The close relation of litter-derived DOC and CO<sub>2</sub> changes at the marked time point in Fig. 5.1, at which more litter-derived DOC entered the upper subsoil in 10 cm than was microbially respired in the depth increment of 10-50 cm. The marked time point belongs to the sampling at 20.11.15, which is likewise the date of the DOC monitoring, where the first significant litter-derived DOC fluxes were recorded in 50 cm soil depth (Study III, Supplementary Fig. S3b). This confirms that as soon as litter-derived DOC inputs are not rapidly microbially processed, they can be translocated to greater soil depth, which represents the movement of the translocation front from inputs reaching the topsoil during the first months towards inputs reaching the subsoil ten months after litter application. At the Grinderwald study site, this movement in November was likely promoted by a high microbial activity during the summer months (largest litter-derived CO<sub>2</sub> efflux at the soil surface



between July and October 2015; Study III, Supplementary Fig. S1) and enhanced exchange of soil solution and mineral surfaces due to an increased water flux in autumn. The data further indicate the beginning of the next cycle in the cascade-like downward migration of aboveground C inputs (Kaiser and Kalbitz, 2012). However, pathways of litter-derived DOC cannot be differentiated any further, since DOC entering the deeper subsoil after a certain time offset, could have originated from (i) microbially processed litter-derived OM, from (ii) litter-derived MAOM desorbed from the mineral soil above, or (iii) directly by preferential flow from the litter layer. Given the fact that litter-derived DOC was detected in 50 cm and 150 cm about the same time and in comparable amounts (Study III, Supplementary Fig. S3b,c) suggests that there is no temporal offset in translocation as it was found between 10 cm and 50 cm. This likewise reflects the similar DOC concentrations and fluxes as well as SUVA<sub>280</sub> values in the soil solution of these depths (Study III, Supplementary Table S1) and indicates that the upper and the deeper subsoil in the Grindewald are closely coupled via downward-oriented soil solution fluxes.

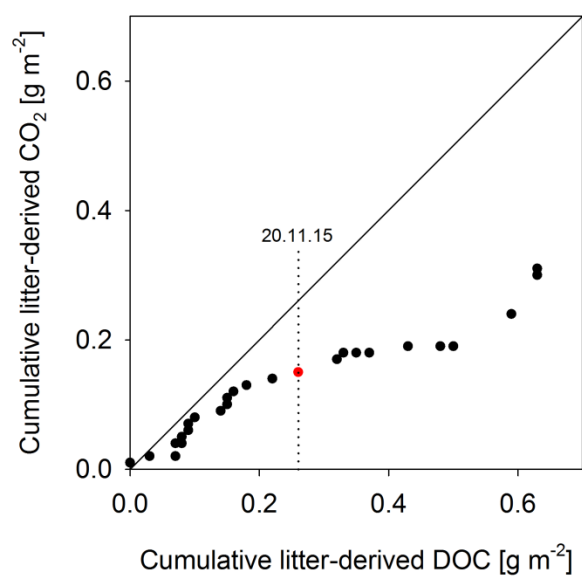


**Fig. 5.1** Correlation of mean litter-derived DOC in 10 cm ( $n = 3$ ) and mean litter-derived CO<sub>2</sub> production in the soil increment of 10-50 cm ( $n = 3$ , data from Study III). The red point and the dotted line mark the value from the 20.11.15. The solid line represents the 1:1 line. Due to a better visibility of the general trend, the error bars were excluded in this figure.

The temporal progress of microbial consumption (via CO<sub>2</sub> production) and translocation of litter-derived DOC to the subsoil resulted in a time offset until litter-derived DOC reached greater soil depth, which is in accordance to the conceptual model by Kaiser and Kalbitz (2012). Taken together, the monitoring data show a clear temporal offset of about ten months before litter layer C entered the subsoil in 50 cm soil depth as proposed in **H1**.

### *Composition of SOM and DOM*

Another aspect of OM passing through several cascade cycles involves a compositional change of SOM and DOM with increasing soil depth, as it is hypothesized in **H1**. A change in SOM composition with increasing soil depth is widely known and frequently reported in studies from various regions (e.g. Guggenberger and Zech, 1994; Kramer et al., 2017; Mikutta et al., 2019). Soil OM close to the surface typically displays a vegetation type signature with a small  $\delta^{13}\text{C}$  value and a wide C/N ratio (Kaiser and Kalbitz, 2012). For example,  $\delta^{13}\text{C}$  values of fresh beech litter are in the range of -29 ‰ (Steffens et al., 2015) to -33 ‰ (litter measurements at University of Hohenheim) and C/N ratios of the soils in this thesis decreased from 11-26 in the topsoil to 6-17 in the deep subsoil (Study II, Table 1). Microbial processing of plant-derived OM changes both parameters. The C/N ratio gets narrower since C-rich compounds like carbohydrates are used as an energy source by the microorganisms (Gunina and Kuzyakov, 2015), while the  $\delta^{13}\text{C}$  value increases due to the discrimination of the heavier  $^{13}\text{C}$  isotope during microbial metabolism (Balesdent et al., 1993; Nadelhoffer and Fry, 1988; Šantrůčková et al., 2000). A  $^{13}\text{C}$  enrichment with depth may also be related to a change in the microbial community (Kohl et al., 2015). A narrowing of the C/N ratio was observed with increasing soil depth in the bulk soil (Study I, Supplementary Fig. S1) and in the MAOM fraction (Study I, Fig. 3b), with a C/N ratio of > 20 in the topsoil, between 10-15 in the upper subsoil, and < 10 in the deeper subsoil (albeit N concentrations in the deep subsoil were below the detection limit, hence ratios are potentially not reliable). Moreover, an increase in  $\delta^{13}\text{C}$  values of up to 3 ‰ from topsoil down to the deep subsoil was detected in both, bulk soil and MAOM (Study I, Fig. 5a,b), which is in the range of isotope discrimination reported elsewhere (e.g. Balesdent et al., 1993; Bird et al., 2003; Wynn, 2007). Accordingly, comparison of both parameters revealed a close and, in large parts, linear relationship (Study I, Supplementary Fig. S4). Since DOM and SOM are interconnected (Kalbitz and Kaiser, 2008; Kaiser and Kalbitz, 2012), microbial alteration consequently affects the composition of both OM pools. The increase of  $^{13}\text{C}$  in DOM was not as pronounced as in the solid phase, but a significant increase by 1 ‰ was detected from topsoil to upper subsoil (data not shown). Additionally, hexoses in soil were reported to originate rather from microorganisms over plants (Gunina and Kuzyakov, 2015), thus a change in DOM composition towards a larger concentration of hexoses in the deep subsoil DOM (Study III, Supplementary Fig. S5) supports the assumption that subsoil OM is increasingly of microbial origin. Overall, several parameters, including composition, concentration, and C isotopy, indicate a change of OM source as a function of soil depth, which is in line with the hypothesized signature change in **H1**.

Combining results from the overall distribution of litter-derived C in the soil profile, retention of litter-derived DOC, microbial processing of recent inputs, and the compositional change of OM with depth, thus provided comprehensive mechanistic insights for a cascade-like downward cycling of OM in forest soils.

## 5.2. Pathways of dissolved organic matter within the mineral soil

There are several pathways of OM to enter the different soil horizons from aboveground and belowground sources. Particulate OM, including litter and roots, represented less than 1 % of soil mass below 30 cm soil depth (Study I, Supplementary Fig. S2) and its contribution to the total SOC decreases with increasing soil depth, down to 22 % below 100 cm depth (Study I, Fig. 2). Input of fresh litter-derived POM was restricted to the top 10 cm of the mineral soil and also the relevance of root-derived C is assumed to be rather small in the Grunderwald as well, since root density (Heinze et al., 2018; Wordell-Dietrich et al., 2020) and root exudation (Tückmantel et al., 2017) are low in the subsoil. Consequently, DOM flux, governed by the amount of leaching water, appeared to be a controlling factor of OM migration in the Grunderwald soil. Soil solution monitoring showed that there is a strong decline in DOC concentration and flux with soil depth, e.g. DOC fluxes of about  $12.8 \pm 4.2 \text{ g m}^{-2} \text{ yr}^{-1}$  in 10 cm soil depth,  $1.4 \pm 0.7 \text{ g m}^{-2} \text{ yr}^{-1}$  in 50 cm soil depth, and  $1.8 \pm 0.9 \text{ g m}^{-2} \text{ yr}^{-1}$  in 150 cm soil depth (Study III, Supplementary Table S1; Leinemann et al. (2016)). However, 2-fold to 3-fold larger water fluxes in the deeper subsoil compared to the upper subsoil did not involve an increase in the DOC flux of the same magnitude (Fig. 5.2c,d), attributable to the decreasing DOC concentrations (Study III, Supplementary Table S1). The litter manipulation experiment in the Grunderwald further allowed the evaluation of the DOM origin. Migration of litter-derived DOC through the mineral soil was overall low (Study III, Supplementary Fig. S3). Stable isotope tracing further revealed that recent litter-derived DOC fluxes decline similarly to the recent litter-derived MAOC with increasing soil depth (Study III, Fig. 1). In addition, the overall contribution of recent litter-derived DOC to the total DOC flux below the topsoil horizon was less than 5 % for all observatories and depths (Study III, Supplementary Fig. S2), showing that the majority of DOC flowing through the soil profile originates from older C sources of above-lying horizons. These results are in good agreement with findings from Hagedorn et al. (2012), who reported that DOC fluxes from the upper 10 cm of mineral soil consist about 5.5 % of litter-derived DOC. Sources of DOC were, for example, evaluated by Fröberg et al. (2007), who conducted a litter manipulation experiment and reported that < 4 % of DOC leaching from the organic layer was litter-derived while the vast majority derived from the Oe and Oa horizons themselves. A mesocosm study from Fröberg et al. (2009) further showed that a large part of the DOC leaching from the A horizon originated in the A horizon itself, suggest that A horizons can be sources of DOC inputs into subsoil.

The overall flow of DOM through the soil profile and the good consensus of the current study with previous findings support the assumption of a high relevance of DOM for the translocation of OM (**H2**). However, Study III did not take the small-scale heterogeneity of soil solution fluxes into account. But the unique setup of segmented suction plates and  $^{13}\text{C}$  labelling would have allowed a more detailed view on the flow paths. Leinemann et al. (2016) evaluated DOM flow paths with the segmented suction plates and

reported that the small scale spatial heterogeneity increases with soil depth, indicating that preferential flow paths are increasingly important for the subsoil DOM fluxes and potential retention and accumulation of OM. A closer look on the temporal dynamic of soil solution fluxes reveals that both water and DOC migrate through the subsoil in pathways which persist for years (Fig. 5.2) and potentially decades (Hagedorn and Bundt, 2002). The increasing difference between smallest and largest water flux from the upper subsoil (Fig. 5.2a) towards the deeper subsoil (Fig. 5.2b) further highlights the increasing importance of these stable preferential flow paths, thus supporting hypothesis **H2**.

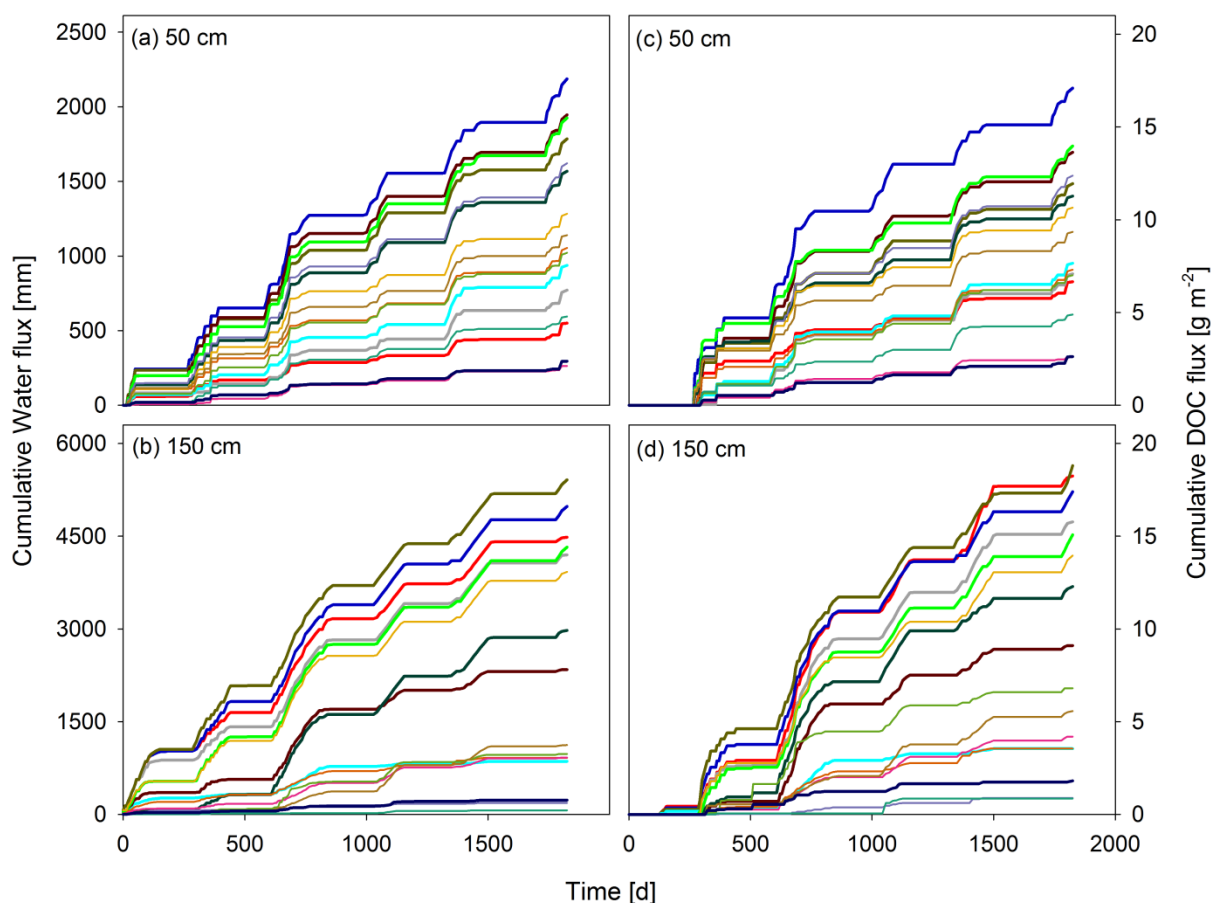


**Fig. 5.2** Cumulative water flux in 50 cm (a) and 150 cm (b) cm soil depth collected by the segmented suction plates installed in the Grindewald Observatory 1, next to the cumulative DOC flux in 50 cm (c) and 150 cm (d) from the same installations (Liebmann, unpublished). Colors depict each of the 16 segments per suction plate. Graphs include data from the 10.04.2014 ( $t = 0$  d) until 09.04.2019 ( $t = 1825$  d), covering 5 years of monitoring.

The impact of soil texture on the translocation of DOC in topsoils and subsoils was evaluated in Study II. At three sites, ranging from fine textured loess to coarse textured sand dominated soil profiles, DO<sup>13</sup>C solutions were injected to trace its downward migration at two time points down to 100 cm below the injection depth. It was assumed that the larger pores of the sand dominated sites (Grindewald and Ebergötzen, in Study II termed “Sand” and “Red sandstone”) will result in a faster and deeper

translocation of DOC. In contrast, it appeared that the fine textured, silt dominated site (Rüdershausen, in Study II termed “Loess”) facilitated the deepest translocation of injected DOC, both 3 and 17 months after injection (Study II, Fig. 4). This was ascribed to a higher abundance of preferential flow paths (e.g. in old root channels which were visible in the soil profile) and further supports the assumption that preferential flow paths are a major factor for DOM translocation. The special features (here old root channels) in soils with fine texture did enhance DOM translocation, but this was not observed in the coarse textured soil matrices which was hypothesized to allow a continuous downward migration. Instead, the fine textured soil positively affected the formation of preferential flow paths and consequently DOM translocation, thus supporting hypothesis **H2**.

### **5.3. Retention of organic matter in subsoils**

Retention of OM in the subsoils involves to a large extent sorption of DOM to mineral surfaces, where POM constitutes a minor fraction (Study I, Supplementary Fig. S2). Conversely, the presence and availability of sorption sites on mineral surfaces is considered as controlling factor for OM retention in subsoils (Rumpel et al., 2012). Sorption isotherms provide insights into the potential sorption capacities under ideal laboratory conditions. Comparing sorption isotherms of topsoil and subsoil samples from the three study sites Grödenwald, Rüdershausen, and Ebergötzen, it became evident that the same DOC input resulted in a larger retention in subsoils than in topsoils (Study III, Fig. 2, Supplementary Fig. S8). Likewise, Abramoff et al. (2021) attested a larger potential for retention of additional C to subsoils than to topsoils based on compiling > 400 laboratory sorption experiments.

Typically, main acceptors for DOC in soil are pedogenic oxides (Hagedorn et al., 2015; Kramer and Chadwick, 2018), clay minerals (Rasmussen et al., 2018), and organic matter itself (Vogel et al., 2014). Oxalate and dithionite extractions showed that pedogenic oxides change only minor with soil depth or, contrary to the sorption isotherm observations, had largest concentrations in the topsoil (Study III, Supplementary Table S7). The same holds true for the clay and silt fraction (Study III, Supplementary Table S7) as well as the overall mineral assemblage (Study III, Supplementary Fig. S7). This implies that the amount of sorption site rich minerals cannot explain the differences of topsoil and subsoil sorption isotherms. Besides, SOC contents in the topsoil was 2-10 fold larger compared to the upper subsoil and even 3-38 fold compared to the deeper subsoil (Study III, Supplementary Table S7). Considering the rather similar mineralogical situation in top-and subsoils, much larger SOC contents in the topsoil suggest a larger surface coverage of the mineral matrix by OM, and consequently a larger C saturation. Thus, it can be concluded that not the presence but rather the availability (i.e. occupancy) of mineral sorption sites is important for sorption processes in soil. Moreover, topsoils, due to the large and continuous leaching of DOM from the organic layer, exhibit a large degree of C saturation (Guggenberger and Kaiser, 2003;

Wiesmeier et al., 2014; Mikutta et al., 2019), which reduces the retention of additional C (Wiesmeier et al., 2014) and is in line with hypothesis **H3**. But the small soil to solution ratio and the constant motion of the samples during the laboratory sorption experiments are far away from natural conditions in the field. In the laboratory approach, interaction between solution and mineral surfaces were limited to sorption/desorption along the concentration gradient, thereby neglecting other factors like microbial consumption, in laboratory experiments with a runtime only some hours, and the actual probability of contact between mineral surface and solution via natural flow paths.

The question remains, whether results from sorption experiments could be transferred to field conditions. This was tested in Study II by injecting a  $\text{DO}^{13}\text{C}$  solution into the intact soil matrix at the same three study sites (Grinderwald, Rüdershausen, and Ebergötzen) in the same soil depths (10, 30/50, 60/100 cm). Sampling the soil below the injection depth 3 months later allowed the evaluation of the *in-situ* retention of DOC. Unexpectedly, a higher share of injected DOC was retained in the first 10 cm below the topsoil injection depth (10-20 cm soil depth) compared to the subsoil injections (Study II, Fig. 4). Considering similar conditions in mineralogical composition as discussed above, these findings imply that the retention of injected DOC was less dependent on available mineral sorption sites, but occurred likely at pre-existent SOM, as it was previously shown in a mesocosm experiment by Vogel et al. (2014). Also, the MAOM burial experiment from Study III supports this assumption because NanoSIMS measurements revealed that after two years of field incubation, only a few fresh (un-labelled) OM patches were formed (Fig. 5.3).

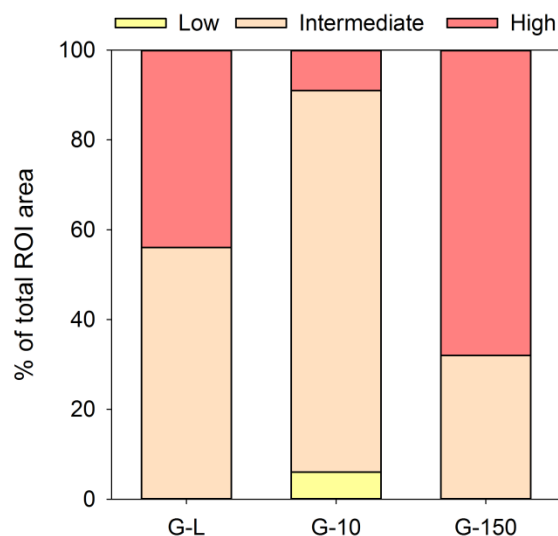


**Fig. 5.3** Classification of the C-coated goethite (G-L), the 10 cm buried goethite MAOM (G-10), and the 150 cm buried goethite MAOM (G-150) regions of interest (ROIs) classified according to their  $^{13}\text{C}$  values [at%] measured with the low energy deposit method (Liebmann, unpublished). The classification was done according to Leinemann et al. (2018) by defining three classes, including a low [ $< 1.4$  at%], intermediate [ $> 1.4$  &  $< 2.2$  at%], and high [ $> 2.2$  at%]  $^{13}\text{C}$  enrichment. The  $^{13}\text{C}$  value of each ROI was normalized to the area of all identified ROIs and is given in percent of the total ROI area.

Instead, the highly  $^{13}\text{C}$ -enriched OM patches visualized by the NanoSIMS (sorbed onto the minerals prior to burial) decreased while the intermediate fraction increased due to sorption of fresh solution-derived OM to existing patches, thereby diluting the  $^{13}\text{C}$  tracer (Leinemann et al., 2018). Taken together, the availability of free mineral sorption sites determines the potential retention under ideal conditions and supporting **H3**. Albeit this is not controlling retention under natural conditions where blockage of sorption sites by OM can have the opposing effect and attract more OM, thus contrasting **H3**.

Findings from Studies II and III demonstrate that laboratory results cannot be transferred to the field without further ado. The laboratory-based sorption isotherms showed that a larger number of available sorption sites in the subsoil resulted in a larger retention of DOM. This was, however, not observed for injected DOM into intact soil profiles, which reduces the transferability of the laboratory results. It has to be noted that the injection experiment was indeed conducted under field conditions, but the DOC concentration of the injected solution was much larger than natural concentrations in soil solution (10 fold larger compared to concentrations in the Grindelwald subsoil (Study III, Supplementary Table S1)) and the total DOC ( $9 \text{ g m}^{-2}$ ) injected over a period of hours correspond to a natural DOC flux of a whole year or more (Study III, Supplementary Table S1). Further considering that there was a three months offset between injection and first sampling, both large DOC input and time offset emphasize that in the field, the stability of retained C is more important than the potential retention itself.

### **5.4. Stability of organic matter in subsoils**

Stability of OM in soil is a key aspect for long-term storage of C, thereby reducing C release to the atmosphere and consequently mitigating global climate change (Lorenz et al., 2011; Kramer et al., 2012).  $^{14}\text{C}$  dating of SOM frequently shows an increasing SOM age with increasing soil depth, up to millennia in subsoils (Rumpel et al., 2012), thus emphasizing the outstanding role of subsoils to remove C from the biogeochemical cycle (Fig. 1.1) for long periods of time. Being able to take advantage of the apparent potentials would allow a better defining of mitigation strategies to global climate change. But since the origin of old subsoil OM and the processes behind its stabilization are not fully understood (Abramoff et al., 2021), it remains unclear if the current situation in soils can be leveraged. To account for the importance of the topic, all studies included the time aspect, e.g. repeated sampling (Study I, II), continuous monitoring (Study III), or field incubation (Study III).

#### *Current carbon stabilization*

Dissolved OM leached from the litter layer to the subsoil in the first months after litter application were to a large part directly consumed by the microbial community before retention and stabilization came into play (Fig. 5.1; Study III, Supplementary Fig. S3, S4). The C budget after the complete 22 months of litter

application further revealed that about 25 % of the total litter-derived DOC inputs to the subsoil were not or only short-term retained and microbially processed thereafter (Study III, Fig. 1). A second evaluation of the stabilization of the actually retained litter-derived C in the whole soil profile 18 months later showed that mineral-associated litter inputs as well as litter inputs in other functional OM fractions were neither in the topsoil nor in the subsoil effectively stabilized (Study I, Fig. 6). Instead, litter-derived C in the subsoil below 20 cm soil depth was almost gone, thereby not confirming hypothesis **H4** with respect to aboveground inputs. However, summing up litter-derived C per functional OM fraction (at both samplings 22 and 40 months) at least highlights the processes which generally favor stabilization of OM in the mineral soil. While the fPOM fraction lost nearly 90 % of its litter-derived C in 18 months, it was about 77 % in the oPOM fraction (Study I, Table 3), a reduction likely attributable to a lower bioavailability of OM occluded in soil aggregates (von Lützwow et al., 2006). Losses in the MAOM fraction amounted to 66 %, illustrating that also sorption to minerals cannot ensure comprehensive protection, but the inhibition of microbial processing is more effective than in other soil OM fractions (Schrumpf et al., 2013). Although the predicted pronounced stabilization of aboveground litter inputs was not detected in the subsoil (nor in the topsoil), it was possible to principally assign partial stabilization to interactions with mineral surfaces, thereby supporting that mineral interactions reduce the availability of OM for microbial consumption (**H4**).

A closer look at the MAOM burial experiment, i.e. the fate of OM sorbed to the surfaces of oxides and clay minerals, reveals consensus with observations from the litter manipulation experiment. About 30 % of MAOC was mobilized during two years of field incubation in top- and subsoil samples and regardless of the mineral type (Study III, Fig. 3, Supplementary Table S2). However, the interplay of processes differed between topsoil and subsoil minerals. Interactions in the topsoil were dominated by exchange of MAOC with DOC from bypassing soil solution, which rendered these minerals to C sinks. Subsoil minerals showed only little OC uptake but to a greater degree release of OC through microbial processing and desorption, thereby serving as a C source in both subsoil depths (50 cm, 150 cm). Considering that initial OC loadings resembled natural OC contents of the subsoil clay fraction at the Grinderwald site (Angst et al., 2016), these findings do not provide evidence for a high stabilization of subsoil C (**H4**).

### *Carbon stabilization under changing environmental conditions*

The litter manipulation experiment and the MAOM burial experiment tested the OC translocation to and stabilization in the subsoil under current natural conditions. Both approaches suggest that the present situation in temperate forests does not allow extensive retention of additional OC in subsoils. But this raised the question of whether a future change in conditions would increase OC stabilization in subsoils. Injection of a 200 ppm DOC solution, which was extracted from altered beech litter, can be considered as



a simulation of an extensive leaching of DOM from the organic layer into top- and subsoils, potentially occurring in a scenario of climate change induced increase in forest growth (McDowell et al., 2020), net primary production (Liu et al., 2015), and consequently more litter C inputs to the soil (Pan et al., 2011). But even under these favorable conditions, retention of DOC was larger in topsoils than in subsoils three months after injection (Study II, Fig. 3, Table 2). Fourteen months later, however, a notable decline of retained DOC in the topsoil was observed, while retained DOC showed a comparatively less pronounced decline in the subsoil, which suggests a better preservation respectively stabilization (Study II, Fig. 3, Table 2), which is in accordance with hypothesis **H4**. Contrasting, laboratory incubations yielded no significant differences in microbial respiration of retained DOC between topsoils and subsoils (Study II, Table 3), implying that retained DOC in subsoils is not per se better protected against microbial consumption compared to topsoils, but stabilization rather arises by a spatial separation from potential decomposers (Preusser et al., 2017; Wordell-Dietrich et al., 2017; Lehmann et al., 2020). But in a scenario where such large DOM inputs to top- and subsoils would be possible, inputs would not occur only once in 17 months as it was simulated in this field approach. More realistically, DOM inputs would be more frequent as observed in the Grindewald monitoring (Leinemann et al., 2016) and likely overcome the current stabilizing mechanisms, e.g. by unlocking the spatial separation, thus enhancing microbial activity, decomposition, and outputs as well.

Taken together, sorption to mineral surfaces and spatial inaccessibility for microorganisms both can have a stabilizing effect on OM in the mineral soil, likely pronounced in subsoils compared to topsoils. But at present, no additional OM retention and stabilization seems possible under natural conditions, hence hypothesis **H4** was not confirmed.

### 6. Conclusion and outlook

This thesis evaluated the role of aboveground litter inputs for the formation of stable subsoil OM and at providing comprehensive field evidence for the downward cycling OM.

An extensive litter manipulation experiment combined with long-term DOC and CO<sub>2</sub> monitoring, an injection of litter-derived DOM into undisturbed soil, and especially the inclusion of the deep mineral subsoil > 100 cm in the determination of OM dynamics constitute new field approaches in the assessment of C cycling in forest soils.

<sup>13</sup>C-labelled litter application revealed that the recent litter layer is not a major source of subsoil C, as the majority of litter-derived inputs is retained in the horizons above. The dynamic of C translocation with depth and with time follows a sequence of sorption, microbial processing, desorption cycles (Kaiser and Kalbitz, 2012). Several parameters show that also the quality of migrating OM changes, illustrating a shift from plant-derived to microbial-derived OM with increasing soil depth, which is also a consequence of passing through several sorption, microbial processing, desorption cycles. Ultimately, key processes for the limited translocation to subsoils involve retention in topsoils, microbial decomposition and associated partial remobilization of OM during downward migration. Preferential flow paths were found to be stable for years, thus controlling the percolation of DOM through the soil profile. Increasing heterogeneity of the small scale water fluxes with increasing soil depth further illustrates their relevance for the distribution of OM in subsoils, which in turn affects OC retention. Apparently, the stability of previously retained OC was more decisive for OC storage in subsoils than its potential retention alone. But under the current natural conditions, the potential capacities in subsoils are unlikely to be exploitable. The present equilibrium of inputs and outputs allows only a very limited retention of aboveground OM in subsoils, which, in fact, is not effectively stabilized. For example, changes in forest management (Magnani et al., 2007) may increase C inputs into forest soils with the aim to raise the input-output equilibrium to a higher level. But it is not assured that larger inputs will cause increasing stabilization at all. Even buried minerals in the subsoil with a C-coating similarly large as the surrounding native minerals can act as C sources rather than make use of their potential free capacities and take up additional C. It is likewise possible that existing natural barriers will be removed by additional inputs, thereby provoking decomposition and mobilization of old and allegedly stable SOM (Fontaine et al., 2007).

Classic laboratory experiments were not able to depict the situation in forest (sub)soils under natural conditions, hence methodological adjustment should be considered in upcoming approaches. Laboratory sorption experiments should include treatments with DOM compositions based on the native soil solution in the respective soil depth. This can be achieved for example by manually removing aromatic components from fresh litter extracts to resemble deep subsoil DOM solutions (Leinemann et al., 2016),

## Conclusion and outlook

or by imitating successive cycling in intact soil columns (Leinemann et al., 2018) or flow cells (Krüger et al., 2018). Considering that a major part of DOM originates from the soil directly above (Fröberg et al., 2007, 2009), it is also conceivable to sample the soil above the depth of interest and perform a water extraction. Water extractable OM can be considered as a surrogate for DOM (Chantigny et al., 2008), thus the use of water extracts instead of litter extracts may help to better simulate actual field conditions in laboratory sorption experiments.

In this thesis, the  $\text{DO}^{13}\text{C}$  fluxes were evaluated for the period of the litter manipulation experiment. But it is unknown what happened with the  $\text{DO}^{13}\text{C}$  fluxes after the labelled litter was removed and tracer inputs were stopped. Study I showed that  $\text{SO}^{13}\text{C}$  was lost throughout the soil profile 18 months later, but it is unclear where it has gone. Microbially processed or mobilized and translocated to greater soil depth would be two conceivable possibilities. The former likely dominates, but in case of the latter or a combination of both, it would be important to know for how long there will be significant fluxes detectable. Analyzing the  $\text{DO}^{13}\text{C}$  fluxes of the months and years after label removal and restoration of the natural litter layer will be of great help to answer these questions. In a preliminary analysis, a period of nearly three years after label removal was evaluated similar to Study III and proportions of  $\text{DO}^{13}\text{C}$  (Fig. 6.1) and cumulative  $\text{DO}^{13}\text{C}$  fluxes (Fig. 6.2) were added to the timeline to give a first impression of the progress in downward cycling of litter-derived OM during 5 years of observation.

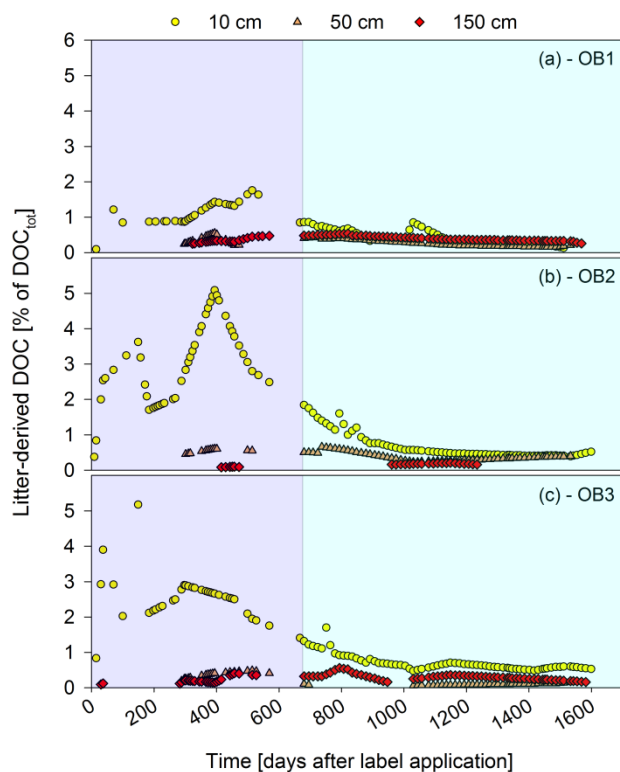


**Fig. 6.1** Proportions of litter-derived DOC averaged per suction plate in 10, 50, and 150 cm soil depth in OB1 (a), OB2 (b) and OB3 (c). The area marked in dark blue represent the time of labelled litter application from Mai 2015 until November 2016, which is given in Study III (Supplementary Fig. S2). The area marked in light blue represent a period of nearly three years after labelled litter application from November 2016 until June 2019.

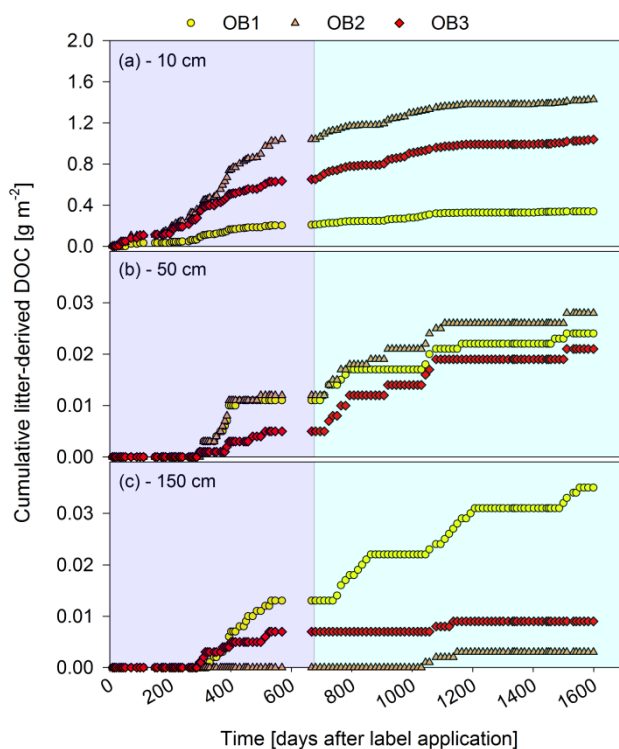


**Fig. 6.2** Cumulative litter-derived DOC in all three observatories (OB1-3) detected with the segmented suction plates in 10 cm (a), 50 cm (b) and 150 cm (c) soil depth. The area marked in dark blue represent the time of labelled litter application from Mai 2015 until November 2016, which is given in Study III (Supplementary Fig. S3). The area marked in light blue represent a period of nearly three years after labelled litter application from November 2016 until June 2019.

The use of segmented suction plates in the Grindelwald yielded novel results, but they were not used to their full potential yet. A more detailed look at the  $\text{DO}^{13}\text{C}$  flux of each segment would provide new insights of matrix and preferential flow paths and their relevance for litter leachate translocations, a perspective which is largely untouched until now.

In conclusion, it was surprising that the outstanding role of forest (sub)soils for C stabilization and climate change mitigation, as it is proposed mainly from laboratory experiments and modeling exercises, was not confirmed by the field approaches in this thesis. The  $^{13}\text{C}$  manipulation experiments yielded comprehensive field evidence that it is unlikely that forest (sub)soils will serve as potential future C-sinks. It became apparent that the performance of subsoils is controlled by their environment, as an intact soil matrix and an active microbial community were more decisive for C stabilization than potential sorption capacities. Thus laboratory approaches alone are not sufficient to evaluate the processes in natural forest soils. A combination with field experiments is needed to obtain a comprehensive picture of the potentials and shortcomings of forest subsoils for the preservation of C in the future.

### References Synthesis & Conclusion and outlook

Abramoff, R. Z., Georgiou, K., Guenet, B., Torn, M. S., Huang, Y., Zhang, H., Feng, W., Jagadamma, S., Kaiser, K., Kothawala, D., Mayes, M. A. and Ciais, P.: How much carbon can be added to soil by sorption?, *Biogeochemistry*, <https://doi.org/10.1007/s10533-021-00759-x>, 2021.

Angst, G., Kögel-Knabner, I., Kirfel, K., Hertel, D. and Mueller, C. W.: Spatial distribution and chemical composition of soil organic matter fractions in rhizosphere and non-rhizosphere soil under European beech (*Fagus sylvatica* L.), *Geoderma*, 264, 179–187, <https://doi.org/10.1016/j.geoderma.2015.10.016>, 2016.

Balesdent, J., Girardin, C. and Mariotti, A.: Site-related  $\delta^{13}\text{C}$  of tree leaves and soil organic matter in a temperate forest, *Ecology*, 74(6), 1713–1721, <https://doi.org/10.2307/1939930>, 1993.

Bates, S. T., Berg-Lyons, D., Caporaso, J. G., Walters, W. A., Knight, R. and Fierer, N.: Examining the global distribution of dominant archaeal populations in soil, *ISME J.*, 5(5), 908–917, <https://doi.org/10.1038/ismej.2010.171>, 2011.

Bird, M., Kracht, O., Derrien, D. and Zhou, Y.: The effect of soil texture and roots on the stable carbon isotope composition of soil organic carbon, *Soil Res.*, 41(1), 77–94, 2003.

Bowden, R. D., Deem, L., Plante, A. F., Peltre, C., Nadelhoffer, K. and Lajtha, K.: Litter input controls on soil carbon in a temperate deciduous forest, *Soil Sci. Soc. Am. J.*, 78(S1), S66–S75, <https://doi.org/10.2136/sssaj2013.09.0413nafsc>, 2014.

Chantigny, M. H., Angers, D. A., Kaiser, K. and Kalbitz, K.: Extraction and characterization of dissolved organic matter, in *Soil Sampling and Methods of Analysis* (eds. Carter, M.R., Gregorich, E.G.), pp. 617–635, Canadian Society of Soil Science, Taylor & Francis Group, LLC, Boca Raton, USA, last access: 26 March 2020, 2008.

Fierer, N., Bradford, M. A. and Jackson, R. B.: Toward an ecological classification of soil bacteria, *Ecology*, 88(6), 1354–1364, <https://doi.org/https://doi.org/10.1890/05-1839>, 2007.

Fontaine, S., Barot, S., Barré, P., Bdioui, N., Mary, B. and Rumpel, C.: Stability of organic carbon in deep soil layers controlled by fresh carbon supply, *Nature*, 450(7167), 277, <https://doi.org/10.1038/nature06275>, 2007.

Fröberg, M., Berggren Kleja, D. and Hagedorn, F.: The contribution of fresh litter to dissolved organic carbon leached from a coniferous forest floor, *Eur. J. Soil Sci.*, 58(1), 108–114, <https://doi.org/10.1111/j.1365-2389.2006.00812.x>, 2007.

Fröberg, M., Hanson, P. J., Trumbore, S. E., Swanston, C. W. and Todd, D. E.: Flux of carbon from  $^{14}\text{C}$ -enriched leaf litter throughout a forest soil mesocosm, *Geoderma*, 149(3–4), 181–188, <https://doi.org/10.1016/j.geoderma.2008.11.029>, 2009.

Guggenberger, G. and Kaiser, K.: Dissolved organic matter in soil: Challenging the paradigm of sorptive preservation, *Geoderma*, 113(3), 293–310, [https://doi.org/10.1016/S0016-7061\(02\)00366-X](https://doi.org/10.1016/S0016-7061(02)00366-X), 2003.

Guggenberger, G. and Zech, W.: Composition and dynamics of dissolved carbohydrates and lignin-degradation products in two coniferous forests, N.E. Bavaria, Germany, *Soil Biol. Biochem.*, 26(1), 19–27, 1994.

## References

---

- Gunina, A. and Kuzyakov, Y.: Sugars in soil and sweets for microorganisms: Review of origin, content, composition and fate, *Soil Biol. Biochem.*, 90, 87–100, <https://doi.org/10.1016/j.soilbio.2015.07.021>, 2015.
- Hagedorn, F. and Bundt, M.: The age of preferential flow paths, *Geoderma*, 108(1), 119–132, [https://doi.org/10.1016/S0016-7061\(02\)00129-5](https://doi.org/10.1016/S0016-7061(02)00129-5), 2002.
- Hagedorn, F., Kammer, A., Schmidt, M. W. I. and Goodale, C. L.: Nitrogen addition alters mineralization dynamics of  $^{13}\text{C}$ -depleted leaf and twig litter and reduces leaching of older DOC from mineral soil, *Glob. Change Biol.*, 18(4), 1412–1427, <https://doi.org/10.1111/j.1365-2486.2011.02603.x>, 2012.
- Hagedorn, F., Bruderhofer, N., Ferrari, A. and Niklaus, P. A.: Tracking litter-derived dissolved organic matter along a soil chronosequence using  $^{14}\text{C}$  imaging: Biodegradation, physico-chemical retention or preferential flow?, *Soil Biol. Biochem.*, 88, 333–343, <https://doi.org/10.1016/j.soilbio.2015.06.014>, 2015.
- Heinze, S., Ludwig, B., Piepho, H.-P., Mikutta, R., Don, A., Wordell-Dietrich, P., Helfrich, M., Hertel, D., Leuschner, C., Kirfel, K., Kandeler, E., Preusser, S., Guggenberger, G., Leinemann, T. and Marschner, B.: Factors controlling the variability of organic matter in the top- and subsoil of a sandy Dystric Cambisol under beech forest, *Geoderma*, 311, 37–44, <https://doi.org/10.1016/j.geoderma.2017.09.028>, 2018.
- Kaiser, K. and Kalbitz, K.: Cycling downwards – dissolved organic matter in soils, *Soil Biol. Biochem.*, 52, 29–32, <https://doi.org/10.1016/j.soilbio.2012.04.002>, 2012.
- Kalbitz, K. and Kaiser, K.: Contribution of dissolved organic matter to carbon storage in forest mineral soils, *J. Plant Nutr. Soil Sci.*, 171(1), 52–60, <https://doi.org/10.1002/jpln.200700043>, 2008.
- Kandeler, E., Gebala, A., Boeddinghaus, R. S., Müller, K., Rennert, T., Soares, M., Rousk, J. and Marhan, S.: The mineralosphere – Succession and physiology of bacteria and fungi colonising pristine minerals in grassland soils under different land-use intensities, *Soil Biol. Biochem.*, 136, 107534, <https://doi.org/10.1016/j.soilbio.2019.107534>, 2019.
- Kohl, L., Laganière, J., Edwards, K. A., Billings, S. A., Morrill, P. L., Van Biesen, G. and Ziegler, S. E.: Distinct fungal and bacterial  $\delta^{13}\text{C}$  signatures as potential drivers of increasing  $\delta^{13}\text{C}$  of soil organic matter with depth, *Biogeochemistry*, 124(1), 13–26, <https://doi.org/10.1007/s10533-015-0107-2>, 2015.
- Kramer, M. G. and Chadwick, O. A.: Climate-driven thresholds in reactive mineral retention of soil carbon at the global scale, *Nat. Clim. Change*, 8(12), 1104–1108, <https://doi.org/10.1038/s41558-018-0341-4>, 2018.
- Kramer, M. G., Sanderman, J., Chadwick, O. A., Chorover, J. and Vitousek, P. M.: Long-term carbon storage through retention of dissolved aromatic acids by reactive particles in soil, *Glob. Change Biol.*, 18(8), 2594–2605, <https://doi.org/10.1111/j.1365-2486.2012.02681.x>, 2012.
- Kramer, M. G., Lajtha, K. and Aufdenkampe, A. K.: Depth trends of soil organic matter C:N and  $^{15}\text{N}$  natural abundance controlled by association with minerals, *Biogeochemistry*, 136(3), 237–248, <https://doi.org/10.1007/s10533-017-0378-x>, 2017.
- Krüger, J., Heitkötter, J., Leue, M., Schlüter, S., Vogel, H.-J., Marschner, B. and Bachmann, J.: Coupling of interfacial soil properties and bio-hydrological processes: The flow cell concept, *Ecohydrology*, 11(6), e2024, <https://doi.org/https://doi.org/10.1002/eco.2024>, 2018.

## References

---

- Kuzyakov, Y. and Blagodatskaya, E.: Microbial hotspots and hot moments in soil: Concept & review, *Soil Biol. Biochem.*, 83, 184–199, <https://doi.org/10.1016/j.soilbio.2015.01.025>, 2015.
- Lajtha, K., Bowden, R. D. and Nadelhoffer, K.: Litter and root manipulations provide insights into soil organic matter dynamics and stability, *Soil Sci. Soc. Am. J.*, 78(S1), S261–S269, <https://doi.org/10.2136/sssaj2013.08.0370nafsc>, 2014.
- Lehmann, J., Hansel, C., Kaiser, C., Kleber, M., Maher, K., Manzoni, S., Nunan, N., Reichstein, M., Schimel, J., Torn, M., Wieder, W. and Kögel-Knabner, I.: Persistence of soil organic carbon caused by functional complexity, *Nat. Geosci.*, 1–6, <https://doi.org/10.1038/s41561-020-0612-3>, 2020.
- Leinemann, T., Mikutta, R., Kalbitz, K., Schaarschmidt, F. and Guggenberger, G.: Small scale variability of vertical water and dissolved organic matter fluxes in sandy Cambisol subsoils as revealed by segmented suction plates, *Biogeochemistry*, 131(1–2), 1–15, <https://doi.org/10.1007/s10533-016-0259-8>, 2016.
- Leinemann, T., Preusser, S., Mikutta, R., Kalbitz, K., Cerli, C., Höschen, C., Mueller, C. W., Kandeler, E. and Guggenberger, G.: Multiple exchange processes on mineral surfaces control the transport of dissolved organic matter through soil profiles, *Soil Biol. Biochem.*, 118, 79–90, 2018.
- Liu, Y. Y., van Dijk, A. I. J. M., de Jeu, R. A. M., Canadell, J. G., McCabe, M. F., Evans, J. P. and Wang, G.: Recent reversal in loss of global terrestrial biomass, *Nat. Clim. Change*, 5(5), 470–474, <https://doi.org/10.1038/nclimate2581>, 2015.
- Lorenz, K., Lal, R. and Shipitalo, M. J.: Stabilized soil organic carbon pools in subsoils under forest are potential sinks for atmospheric CO<sub>2</sub>, *For. Sci.*, 57(1), 19–25, <https://doi.org/10.1093/forestscience/57.1.19>, 2011.
- von Lütow, M., Kögel-Knabner, I., Ekschmitt, K., Matzner, E., Guggenberger, G., Marschner, B. and Flessa, H.: Stabilization of organic matter in temperate soils: mechanisms and their relevance under different soil conditions – a review, *Eur. J. Soil Sci.*, 57(4), 426–445, <https://doi.org/10.1111/j.1365-2389.2006.00809.x>, 2006.
- Magnani, F., Mencuccini, M., Borghetti, M., Berbigier, P., Berninger, F., Delzon, S., Grelle, A., Hari, P., Jarvis, P. G., Kolari, P., Kowalski, A. S., Lankreijer, H., Law, B. E., Lindroth, A., Loustau, D., Manca, G., Moncrieff, J. B., Rayment, M., Tedeschi, V., Valentini, R. and Grace, J.: The human footprint in the carbon cycle of temperate and boreal forests, *Nature*, 447(7146), 849–851, <https://doi.org/10.1038/nature05847>, 2007.
- McDowell, N. G., Allen, C. D., Anderson-Teixeira, K., Aukema, B. H., Bond-Lamberty, B., Chini, L., Clark, J. S., Dietze, M., Grossiord, C., Hanbury-Brown, A., Hurtt, G. C., Jackson, R. B., Johnson, D. J., Kueppers, L., Lichstein, J. W., Ogle, K., Poulter, B., Pugh, T. A. M., Seidl, R., Turner, M. G., Uriarte, M., Walker, A. P. and Xu, C.: Pervasive shifts in forest dynamics in a changing world, *Science*, 368(6494), <https://doi.org/10.1126/science.aaz9463>, 2020.
- Mikutta, R., Turner, S., Schippers, A., Gentsch, N., Meyer-Stüve, S., Condon, L. M., Peltzer, D. A., Richardson, S. J., Eger, A., Hempel, G., Kaiser, K., Klotzbücher, T. and Guggenberger, G.: Microbial and abiotic controls on mineral-associated organic matter in soil profiles along an ecosystem gradient, *Sci. Rep.*, 9(1), 1–9, <https://doi.org/10.1038/s41598-019-46501-4>, 2019.
- Nadelhoffer, K. J. and Fry, B.: Controls on natural nitrogen-15 and carbon-13 abundances in forest soil organic matter, *Soil Sci. Soc. Am. J.*, 52(6), 1633–1640, <https://doi.org/10.2136/sssaj1988.03615995005200060024x>, 1988.

## References

---

- Pan, Y., Birdsey, R. A., Fang, J., Houghton, R., Kauppi, P. E., Kurz, W. A., Phillips, O. L., Shvidenko, A., Lewis, S. L., Canadell, J. G., Ciais, P., Jackson, R. B., Pacala, S. W., McGuire, A. D., Piao, S., Rautiainen, A., Sitch, S. and Hayes, D.: A large and persistent carbon sink in the world's forests, *Science*, 333(6045), 988–993, <https://doi.org/10.1126/science.1201609>, 2011.
- Preusser, S., Marhan, S., Poll, C. and Kandeler, E.: Microbial community response to changes in substrate availability and habitat conditions in a reciprocal subsoil transfer experiment, *Soil Biol. Biochem.*, 105, 138–152, <https://doi.org/10.1016/j.soilbio.2016.11.021>, 2017.
- Rasmussen, C., Heckman, K., Wieder, W. R., Keiluweit, M., Lawrence, C. R., Berhe, A. A., Blankinship, J. C., Crow, S. E., Druhan, J. L., Hicks Pries, C. E., Marin-Spiotta, E., Plante, A. F., Schädel, C., Schimel, J. P., Sierra, C. A., Thompson, A. and Wagai, R.: Beyond clay: Towards an improved set of variables for predicting soil organic matter content, *Biogeochemistry*, 137(3), 297–306, <https://doi.org/10.1007/s10533-018-0424-3>, 2018.
- Rothstein, D. E., Toosi, E. R., Schaetzl, R. J. and Grandy, A. S.: Translocation of carbon from surface organic horizons to the subsoil in coarse-textured Spodosols: Implications for deep soil C dynamics, *Soil Sci. Soc. Am. J.*, 82(4), 969–982, doi:10.2136/sssaj2018.01.0033, 2018.
- Rumpel, C., Chabbi, A. and Marschner, B.: Carbon storage and sequestration in subsoil horizons: Knowledge, gaps and potentials, in *Recarbonization of the Biosphere*, edited by R. Lal, K. Lorenz, R. F. Hüttl, B. U. Schneider, and J. von Braun, pp. 445–464, Springer Netherlands, Dordrecht, [http://www.springerlink.com/index/10.1007/978-94-007-4159-1\\_20](http://www.springerlink.com/index/10.1007/978-94-007-4159-1_20), last access: 10 January 2018, 2012.
- Šantrůčková, H., Bird, M. I. and Lloyd, J.: Microbial processes and carbon-isotope fractionation in tropical and temperate grassland soils, *Funct. Ecol.*, 14(1), 108–114, 2000.
- Schrumpf, M., Kaiser, K., Guggenberger, G., Persson, T., Kögel-Knabner, I. and Schulze, E.-D.: Storage and stability of organic carbon in soils as related to depth, occlusion within aggregates, and attachment to minerals, *Biogeosciences*, 10(3), 1675–1691, <https://doi.org/https://doi.org/10.5194/bg-10-1675-2013>, 2013.
- Steffens, C., Helfrich, M., Joergensen, R. G., Eissfeller, V. and Flessa, H.: Translocation of <sup>13</sup>C-labeled leaf or root litter carbon of beech (*Fagus sylvatica* L.) and ash (*Fraxinus excelsior* L.) during decomposition – A laboratory incubation experiment, *Soil Biol. Biochem.*, 83, 125–137, <https://doi.org/10.1016/j.soilbio.2015.01.015>, 2015.
- Tipping, E., Chamberlain, P. M., Fröberg, M., Hanson, P. J. and Jardine, P. M.: Simulation of carbon cycling, including dissolved organic carbon transport, in forest soil locally enriched with <sup>14</sup>C, *Biogeochemistry*, 108(1–3), 91–107, <https://doi.org/10.1007/s10533-011-9575-1>, 2012.
- Tückmantel, T., Leuschner, C., Preusser, S., Kandeler, E., Angst, G., Mueller, C. W. and Meier, I. C.: Root exudation patterns in a beech forest: Dependence on soil depth, root morphology, and environment, *Soil Biol. Biochem.*, 107, 188–197, <https://doi.org/10.1016/j.soilbio.2017.01.006>, 2017.
- Vogel, C., Mueller, C. W., Höschel, C., Buegger, F., Heister, K., Schulz, S., Schloter, M. and Kögel-Knabner, I.: Submicron structures provide preferential spots for carbon and nitrogen sequestration in soils, *Nat. Commun.*, 5(1), 1–7, <https://doi.org/10.1038/ncomms3947>, 2014.
- Wiesmeier, M., Hübner, R., Spörlein, P., Geuß, U., Hangen, E., Reischl, A., Schilling, B., Lützw, M. von and Kögel-Knabner, I.: Carbon sequestration potential of soils in southeast Germany derived from stable



## References

---

soil organic carbon saturation, *Glob. Change Biol.*, 20(2), 653–665, <https://doi.org/10.1111/gcb.12384>, 2014.

Wordell-Dietrich, P., Don, A. and Helfrich, M.: Controlling factors for the stability of subsoil carbon in a Dystric Cambisol, *Geoderma*, 304, 40–48, <https://doi.org/10.1016/j.geoderma.2016.08.023>, 2017.

Wordell-Dietrich, P., Wotte, A., Rethemeyer, J., Bachmann, J., Helfrich, M., Kirfel, K., Leuschner, C. and Don, A.: Vertical partitioning of CO<sub>2</sub> production in a forest soil, *Biogeosciences*, 17(24), 6341–6356, <https://doi.org/https://doi.org/10.5194/bg-17-6341-2020>, 2020.

Wynn, J. G.: Carbon isotope fractionation during decomposition of organic matter in soils and paleosols: Implications for paleoecological interpretations of paleosols, *Palaeogeogr. Palaeoclimatol. Palaeoecol.*, 251(3), 437–448, <https://doi.org/10.1016/j.palaeo.2007.04.009>, 2007.

### **Acknowledgements**

First of all, I would like to thank Prof. Dr. Georg Guggenberger, whose support and advice during the PhD, but also during my Bachelor and Master, had considerable impact on me becoming a soil scientist.

I want to thank all my supervisors in the SubSOM Project, Prof. Dr. Georg Guggenberger, Prof. Dr. Karsten Kalbitz, and Prof. Dr. Robert Mikutta, for their time and patience, and the great teamwork, which made this a successful time.

My gratitude belongs to all colleagues from the Institute of Soil Science, in particular the lab crew and especially Dr. Poldi Sauheitl for not getting tired of explaining methods, measurements and evaluations to me, and Heike Steffen, Anne Kathrin Herwig, Michael Klatt, and Hanna Böhme for their help with processing thousands of samples. I am further indebted to Hanna Böhme and Moritz Rahlfs for the support in the Grunderwald.

I had great help from a number of students over the years, including Ciarán Fitzgerald, Eike Perrin, Ole Mewes, and Tristan Lohmeier.

I thank Patrick Wordell-Dietrich and Fabian Kalks for a good collaboration, long and fun days in the field and fruitful discussions.

I have to thank Manuela Unger for DO<sup>13</sup>C measurements in Dresden and Dr. Carmen Höschen for NanoSIMS measurements in Freising.

For many mood lifting talks, a great office atmosphere and proofreading, I am indebted to Dr. Stefan Dultz and Markus Koch.

I would like to thank Philipp, Ole, Jake, and Markus for extensive scientific exchange, but even more for the quality time apart from work.

Last but definitely most important, I want to highlight some very special persons, without whom none of these things would have been possible, my wife Miriam and my sons Leander and Mattheo. You gave me the support and the energy to keep up, although this meant less time together. Having you in my life is the best motivation I can imagine, thank you.

## CV

Patrick Liebmann

e-mail: liebmann@ifbk.uni-hannover.de

---

**Personal details**

Date of birth: 26.10.1990

Nationality: German

---

**Education/Higher education**

- 02/2017 – **PhD student at the Institute of Soil Science**  
Leibniz University Hannover  
Supervisor: Prof. Dr. Georg Guggenberger
- 10/2014 – 01/2017 **Master studies in Earth Sciences**  
Leibniz University Hannover, Graduation: Master of Science  
Master thesis in Soil Science
- 10/2011 – 09/2014 **Bachelor studies in Earth Sciences**  
Leibniz University Hannover, Graduation: Bachelor of Science  
Bachelor thesis in Soil Science
- 08/2010 – 04/2011 **Alternative civilian service**  
Diakoniezentrum Jägerallee Springe
- 08/2003 – 06/2010 **Secondary school**  
Otto-Hahn Gymnasium, Springe, Higher Education Entrance Qualification (Abitur)

---

**Work experience**

- 10/2020 – 09/2023 **Research assistant at the Institute of Soil Science**  
Leibniz University Hannover  
Project: CRYOVULCAN - Vulnerability of carbon in Cryosols – substrate-microorganisms-aggregate interactions
- 02/2017 – 09/2020 **Research assistant at the Institute of Soil Science**  
Leibniz University Hannover  
Project: Origin and fate of dissolved organic matter in the subsoil driven by dynamic exchange and remobilization processes (FOR1806: SUBSOM, P5)
- 10/2015 – 01/2017 **Student assistant at the Institute of Soil Science, Leibniz University Hannover (Timo Leinemann, Prof. Guggenberger)**  
Analyses of dissolved organic matter solutions on total organic carbon and carbon composition, working with <sup>13</sup>C labeled material (mineral and organic)
- 11/2015 – 02/2016 **Tutor at the Institute of Soil Science, Leibniz University Hannover (Prof. Guggenberger)**  
Tutorial to the lecture: Soils – Processes and Characteristics
- 11/2014 – 02/2015 **Tutor at the Institute of Soil Science, Leibniz University Hannover (Prof. Guggenberger)**  
Tutorial to the lecture: Soils – Processes and Characteristics

### Publications

**Liebmann, P.**, Wordell-Dietrich, P., Kalbitz, K., Mikutta, R., Kalks, F., Don, A., Woche, S. K., Dsilva, L. R. and Guggenberger, G.: Relevance of aboveground litter for soil organic matter formation – a soil profile perspective, *Biogeosciences*, 17(12), 3099–3113, <https://doi.org/https://doi.org/10.5194/bg-17-3099-2020>, 2020.

Kalks, F., **Liebmann, P.**, Wordell-Dietrich, P., Guggenberger, G., Kalbitz, K., Mikutta, R., Helfrich, M. and Don, A.: Fate and stability of dissolved organic carbon in topsoils and subsoils under beech forests, *Biogeochemistry*, <https://doi.org/10.1007/s10533-020-00649-8>, 2020.

**Liebmann, P.**, Mikutta, R., Kalbitz, K., Wordell-Dietrich, P., Leinemann, T., Preusser, S., Bachmann, J., Don, A., Kandeler, E., Marschner, B., Schaarschmidt, F. and Guggenberger, G.: Biogeochemical constraints limit carbon storage in forest subsoils, 2020.

*Under Review for Nature Communications*

Poggenburg, C., Mikutta, R., **Liebmann, P.**, Koch, M. and Guggenberger, G.: Siderophore-promoted dissolution of ferrihydrite associated with adsorbed and coprecipitated natural organic matter, *Org. Geochem.*, 125, 177–188, <https://doi.org/10.1016/j.orggeochem.2018.09.004>, 2018.